Antiplasmodial Neolignans from *Trema orientalis* – Identification, Synthesis and Analogue Generation

by

Pamisha Pillay

Thesis Presented for the Degree of

DOCTOR OF PHILOSOPHY

In the Department of Chemistry

Faculty of Science

UNIVERSITY OF CAPE TOWN

November 2011

ABSTRACT

Thesis Title: Antiplasmodial neolignans from *Trema orientalis* – Identification, synthesis and analogue generation
Author: Pamisha Pillay
Date of submission: 30 November 2011

In the continued search for new classes of antimalarial agents that are safe, affordable and effective against multi-drug resistant parasites, medicinal plants still provide a useful starting point. *Trema orientalis*, a widely distributed evergreen tree with various medicinal properties including the treatment of malaria, was investigated as a potential source of new antimalarial lead compounds. Organic extracts of the young growing twigs of *T. orientalis* were reproducibly shown to be active against the chloroquine-sensitive (D10) and chloroquine-resistant (K1) strains of *Plasmodium falciparum*. The 8-*O*-4' oxyneolignans, dadahols A and B, were identified as the major active compounds using two bioassay-guided fractionation approaches. The new accelerated "HPLC biogram" methodology allowed for early recognition of the active compounds in the complex plant extract, requiring considerably less time and material compared to the classical reiterative approach.

Although the natural products were shown to have promising antiplasmodial activity (IC_{50} < 1 µg/ml) and selectivity (SI > 100) *in vitro*, they lacked antimalarial activity *in vivo*. This could be attributed to the poor pharmacokinetic (pK) properties of the compounds, which was confirmed by an *in vivo* pK study.

Biomimetic oxidative coupling, ion exchange chromatography and carbonyldiimidazole (CDI) coupling were shown to be useful techniques in completing the diastereo-selective synthesis of dadahol B. The 8-*O*-4´ neolignan core of dadahol B, *i.e.* guaiacyglycerol *β*-*O*-4-coniferyl alcohol ether (GGCE), lacked antiplasmodial activity identifying the *p*-coumaroyl moieties as key pharmacophores of the natural product. A by-product of the oxidative coupling step, dehydrodiconiferyl alcohol (DHCA), showed better initial activity than GGCE and was subsequently also used as a scaffold for analogue generation. Using a selection of synthetic techniques and approaches, a range of GGCE and DHCA analogues were prepared, focusing on optimization of the ester and aromatic ring substituents. None of the precursors, by-products or analogues showed improved antiplasmodial activity relative to the natural products or chloroquine, and were therefore not considered as potential antimalarial lead compounds.

ACKNOWLEDGEMENTS

I would like to express my sincere gratitude to my superviser, Prof. Kelly Chibale, for his invaluable supervision and guidance throughout the duration of this work. In addition, I wish to thank my co-supervisor Dr Vinesh Maharaj, for his all encompassing technical input and support.

I gratefully acknowledge the National Research Foundation Innovation Fund Grant (Project 31313), EU AntiMal FP6 and the CSIR for funding and permission to present this work for degree purposes.

Special mention must be made of my CSIR colleagues Dr Chris Parkinson, Dr Chris van der Westhuyzen, Xolani Peters, Dr Paul Steenkamp, Nial Harding, Dr Gerda Fouche, Tasmiyah Khan, Michele Enslin and Prenitha Sewnarain for their technical advice, input and support. I also humbly acknowledge my UCT colleagues Prof Pete Smith, Carmen DeKock, Lubbe Wiesner, and Yassir Adam for their contribution to biological assay and analytical data.

Heartfelt thanks to my family and friends for their continuous inspiration and encouragement. I dedicate this thesis to my parents, my brothers, and my beloved Paul, for their unwavering love and support.

ABBREVIATIONS

^{1}H	Proton (^{1}H)
^{3}H	Tritium
2D	Two-dimensional
^{13}C	Carbon-13
[α]	Specific optical rotation
Acetone-d_6	Hexadeuterioacetone
ACT	Artemisinin based combination therapies
ADME	Absorption, distribution, metabolism and excretion
APAD	3-Acetylpyridine adenine dinucleotide
APADH	Reduced APAD
ATP	Adenosine triphosphate
BLQ	Below limit of quantification
BPI	Base Peak Intensity
BCE	Before Common Era
br	Broad resonance
br s	Broad singlet
^{o}C	Degrees Celcius
C	Carbon
c	Concentration
CAD	Cinnamyl alcohol dehydrogenase
CAD's	Cinnamic acid derivatives
calcd.	Calculated
CCoA-OMT	Caffeoyl-CoA 3-O-methyltransferase
$CDCl_3$	Deuterated chloroform
CDI	N,N'–carbonyldiimidazole
CCR	Cinnamoyl-CoA reductase
CE	Common Era
cf.	Consult
CHO	Chinese Hamster Ovarian cell line
cm	Centimetre
CNS	Central Nervous System
COSY	Correlated spectroscopy
conc.	Concentrated
CoA	Coenzyme A
COX	Cyclooxygenase

CSIR	Council for Scientific and Industrial Research
CQ	Chloroquine
CYP	Cytochrome P450
d	Doublet
dd	Doublet of doublets
ddd	Doublet of doublets of doublets
ddt	Doublet of doublets of triplets
DAD	Diode Array Detector
DCM	Dichloromethane
DCC	N, N'-dicyclohexylcarbodiimide
DHCA	Dehydrodiconiferyl alcohol
DIAD	Diisopropyl azodicarboxylate
DIBAL	Diisobutylaluminum hydride
dil.	Dilute
DP	Directing protein
DEPT	Distortionless Enhancement by Polarisation Transfer
DHA	dihydroartemisinin
DHFR	dihydrofolate reductase
DHPS	dihydropteroate synthetase
DIAD	diisopropyl azodicarboxylate
DMAP	4-dimethyaminopyridine
DMF	Dimethylformamide
DMSO	Dimethyl Sulfoxide
DMEM	Dulbecos Modified Eagles Medium
DNA	Deoxyribonucleic acid
DNP	Dictionary of Natural Products
dq	Doublet of quartets
dt	Doublet of triplets
E	East
equiv.	Equivalents
ES	Electrospray
ESI	Electrospray ionisation
FBS	Fetal bovine serum
FSA	Flora of Southern Africa
g	Gram
GGCE	Guaiacyglycerol *β-O*-4-coniferyl alcohol
g/L	Grams per litre
H	Proton

GPS	Global Positioning System
h	Hour
HEPES	N-[2-hydroxyethyl]-piperazine-N'-[2-ethansulphonic acid]
HIV	Human immunodeficiency virus
HDMS	High Definition Mass Spectrometry
HMBC	Heteronuclear Multiple Bond Correlation
HPLC	High-Performance Liquid Chromatography
H_3PO_4	Phosphoric acid
HRESI-MS	High-Resolution Electrospray Ionisation – Mass Spectrometry
HRMS	High-Resolution Mass Spectrometry
HRP	Horseradish peroxidase
HSQC	Heteronuclear Single Quantum Coherence
HR	High Resolution
Hz	Hertz
IC_{50}	Inhibitory concentration at which 50% inhibition is achieved
i.e.	That is
J	Spin-spin coupling constant
kD	Kilodalton
kg	Kilogram
K_b	Basicity constant
K_m	Concentration of substrate that leads to half-maximal velocity
kV	Kilovolt
L	Litre
LC	Liquid chromatography
LDH	Lactate dehydrogenase
linn.	Linnaeus
lit.	Literature
m	Metres
m	Multiplet
mm	Millimetre
m/z	Mass-to-charge ratio
Me	Methyl
mg	Milligrams
mg/L	Milligrams per litre
mg/kg	Milligrams per kilogram
$MgSO_4$	Magnesium sulfate
µCi	Microcurie
µg/mL	Micrograms per millilitre

ml	Millilitre
min	Minute
μM	Micro molar
mmol	Millimoles
MTT	3-(4,5-dimethylthiazol-2-yl)-2,5-diphenyltetrazolium bromide
MW	Molecular weight
NAD	Nicotinamide adenine dinucleotide
NADP	Nicotinamide adenine dinucleotide phosphate
NADPH	Reduced form of nicotinamide adenine dinucleotide phosphate
NBT	Nitroblue tetrazolium
nM	Nano molar
nm	Nano meter
NMR	Nuclear Magnetic Resonance Spectroscopy
NOESY	Nuclear Overhauser Effect Spectroscopy
OMT	*O*-methyltransferase
P.	Plasmodium
PAL	Phenylalanine ammonia-lyase
p	Para
PBS	Phosphate-buffered saline
PDA	Photodiode array detector
PES	Phenazine ethosulphate
PI	Post infection
pK	Pharmacokinetic
PLCγl	Phospholipase cystathionine γ lyase
pLDH	Parasite lactate dehydrogenase
ppm	Parts per million
PPTS	Pyridinium *para*-toluene sulfonate
prep	Preparative (HPLC)
pH	cLog of the activity of dissolved hydrogen ions
pfCRT	*Plasmodium falciparum* chloroquine-resistance transporter
pLDH	Parasite lactate dehydrogenase
PPh_3	Triphenylphosphine
q	Quartet (NMR)
QAE	Quaternary aminoethyl
QTOF	Quadrupole time-of-flight mass spectrometer
RBC	Red blood cells or erythrocytes
RI	Resistance Index
R_f	Retention factor

rt	Retention time
r.t.	Room temperature
rpm	Revolutions per minute
RPMI	Roswell Park Memorial Institute
RSA	Republic of South Africa
S	South
s	Singlet
SANBI	South African National Biodiversity Institute
SAR	Structure activity relationship
SI	Selectivity index
SiO_2	Silica gel
SOMO	Single-occupied molecular orbitals
SP	Pyrimethamine-sulfadoxine
SPE	Solid Phase Extraction
spp.	Species
St	Saint
STZ	Streptozotocin
subsp.	Subspecies
Swiss TPH	Swiss Tropical and Public Health Institute
T.	*Trema*
T.	*Trypanosoma*
t	Triplet
TBAF	tetra-*n*-butylammonium fluoride
TBS-Cl	*tert*-butyldimethylsilyl chloride
THF	Tetrahydrofuran
THP	Tetrahydropyranyl
TPP	Triphenylphosphine
TLC	Thin Layer Chromatography
TMS	Tetramethylsilane
TRIS	Tris(hydroxymethyl)aminomethane
UCT	University of Cape Town
UGT	UDP-glucuronosyltransferase
Umg^{-1}	Enzyme unit per milligram
UPLC	Ultra Performance Liquid Chromatography
UV_{max}	Maximum of the UV absorption
UV	Ultraviolet
V	Volume
v.	Version

var.	Variety
viz.	namely
v/v	Volume ratio
VLC	Vacuum Liquid Chromatography
V_{max}	Maximum initial velocity/rate that enzyme catalyses reaction
w/w	Weight ratio
WHO	World Health Organisation
δ_H	^1H chemical shift
δ_C	^{13}C chemical shift

TABLE OF CONTENTS

CHAPTER 1
Malaria and antimalarials from plants

1.1 History of Malaria

Malaria, a life-threatening disease that is transmitted by *Anopheles* mosquitoes, is probably one of the oldest diseases known to mankind. Mention of this disease can be found in ancient Chinese, Indian and Egyptian manuscripts. In the 5th century BCE Hippocrates, the Greek physician, was the first to describe the manifestations of the disease. In the 7th century CE, the Italians named the disease *mal'aria* meaning bad air, due to its association with ill-smelling vapors from the Roman swamps.

The first recorded treatment of malaria dates back to 1600 when the bark of the *Cinchona* tree was first used by the native Peruvian Indians to treat the intermittent fevers associated with this illness (Lee, 2002). It was not until 1889 that Alphonse Laveran discovered the protozoal (single celled parasite) cause of malaria and not until 1897 that Ronald Ross demonstrated that the *Anopheles* mosquito was the vector for the disease (Robert *et al*., 2001). His pioneering work on establishing the main features of the parasitic life cycle earned Ross the Nobel Prize in Medicine in 1902.

Over the next century significant advances were made towards attempts to eradicate malaria particularly with respect to controlling mosquitoes, understanding the parasite and developing drugs to treat the disease (Targett, 1991). But despite this, malaria has proven to be one of the biggest killers in the world. Between 300 and 500 million people have been infected annually and nine out of ten of these cases have occurred in sub-Saharan Africa (World Health Organisation, 2010). This is due to the majority of infections in Africa being caused by *Plasmodium falciparum*, the most dangerous of the human malaria parasites. It is also because the most effective and most difficult to control malaria vector - the mosquito *Anopheles gambiae* - is the most widespread in Africa. Climatic conditions over a large part of Africa favor malaria transmission and global warming together with changes in land use have extended the areas of

transmission. Moreover, many countries in Africa lacked the infrastructures and resources necessary to mount sustainable campaigns against malaria and, as a result few benefited from historical efforts to eradicate the disease. Also, methods aimed at eradicating the disease have been hindered by lack of governmental commitment, failure to use existing resources and poor health care facilities.

1.2 Malaria Today

Today approximately forty percent of the world's population, in more than 100 countries, is at risk to malaria. Malaria is endemic in Africa, much of South and Southeast Asia, Central America, and northern South America (Figure1.1). In 2008, there were an estimated 243 million cases that led to nearly 863 000 deaths (World Health Organisation, 2009). The introduction of long-lasting mosquito nets and artemisinin-combination therapy, a revival of support for indoor residual insecticide spraying, and increased funding for implementation of control strategies in endemic countries have provided evidence that treatment and prevention can alleviate the burden of disease. However, the ability of the parasite to quickly adapt and overcome eradication efforts remains a constant threat in global malaria control.

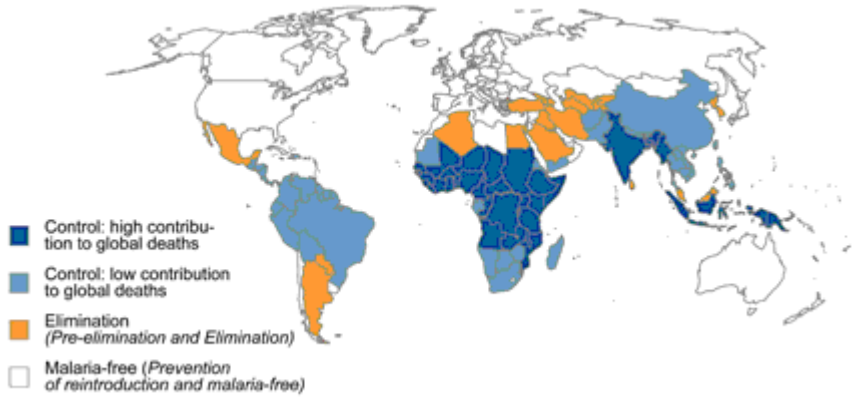

Figure 1.1 Malaria-endemic regions (Roll Back America, 2010)

In South Africa the malaria burden is relatively low. Malaria is mainly transmitted in the low altitude areas of the northeastern parts of southern Africa; this includes the

lowveld region of Mpumalanga, Limpopo Province and the northeastern parts of KwaZulu-Natal. Malaria transmission is seasonal with the greatest number of cases occurring between October and May with a significant inter-annual variation in the number of malaria cases (Department of Health, South Africa, 2003). In 2006 there were 12295 cases while in 2007 there were 3597 recorded cases (Department of Health, South Africa, 2008). This variation is mainly attributed to favorable climatic conditions, population migration and the emergence of drug resistant parasites.

An increased number of malaria cases were reported in Limpopo Province in December 2009 (International Society for Infectious Diseases, 2010). The South African government has increased efforts to control the spread of malaria, particularly due to its threat to the economy.

Annual economic growth in countries with high malaria transmission has historically been lower than in countries without malaria. The direct costs of malaria include a combination of personal and public expenditures on both prevention and treatment of the disease. The indirect costs of malaria include lost productivity or income associated with illness or death. Also, the prevalence of malaria in a country can lead to a decline in international trade and tourism and foreign investment, which are vital for economic growth.

1.3 The Malaria Parasite

The malaria parasite*, Plasmodium falciparum*, is a very small, single-cell blood organism, or 'protozoan'. There are three other parasite species (*P. malariae*, *P. vivax* and *P. ovale*) that also cause malaria but they are rare in sub-Saharan Africa. The parasite is transmitted to humans by a vector, namely the female *Anopheles* mosquito.

Knowledge of the life cycle of the malaria parasite is fundamental to understanding the methods of prevention and treatment. Interrupting the life cycle will prevent malaria, but this has proven more difficult than anticipated. The *Plasmodium* parasite

spends part of its life cycle in humans and partly in mosquitoes (Caniato and Puricelli, 2003; Taubes, 2000) (Figure 1.2).

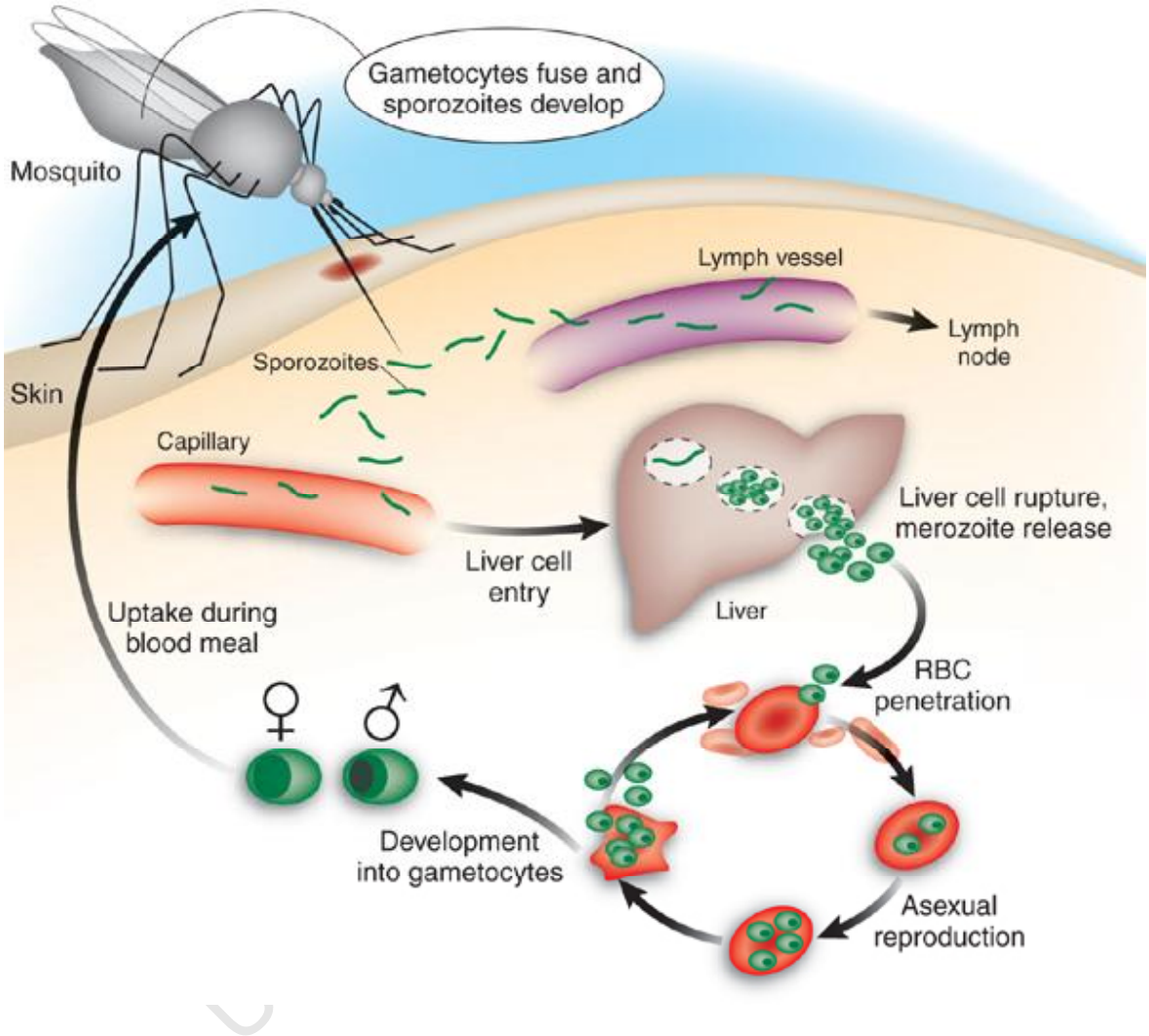

Figure 1.2 Life cycle of *Plasmodium* spp. (Jones and Good, 2006)

While ingesting a blood meal, sporozoites are injected into a human host through the bite of an infected *Anopheles* mosquito. After innoculation, sporozoites migrate to the liver and infect liver cells to establish the first intracellular replicative stage. Sporozoites reproduce by mitosis and develop into schizonts, which rupture and release merozoites into the bloodstream. Following the exoerythrocytic phase, the merozoites invade erythrocytes (RBCs), where they undergo asexual multiplication

(erythrocytic schizogony). The ring stage trophozoites mature into schizonts, which rupture releasing merozoites. Two out of every three red blood cells soon become infected. The periodic fever and chills associated with malaria occur when the red blood cells rupture and release the merozoites. This is the blood stage of the disease. A fraction of the merozoites differentiate into gamete producing cells, gametocytes.

The gametocytes, male (microgametocytes) and female (macrogametocytes), are ingested by an *Anopheles* mosquito during a blood meal. The parasites' multiplication in the mosquito is known as the sporogenic cycle. While in the mosquito's stomach, the male gametes fertilize the female gametes ultimately generating sporozoites, which make their way to the mosquito's salivary glands. Inoculation of the sporozoites into a new human host occurs and the cycle begins again.

Malaria symptoms appear about 9 to 14 days after the infectious mosquito bite, although this varies with different plasmodium species. Typically, malaria produces fever, headache, vomiting and other flu-like symptoms. If drugs are not available for treatment or the parasites are resistant to them, the infection can progress rapidly to become life threatening. Malaria can kill by infecting and destroying red blood cells (anemia) and by clogging the capillaries that carry blood to the brain (cerebral malaria) or other vital organs.

1.4 Malaria Prevention and Control

There are a number of approaches towards the prevention and control of malaria and the choice of intervention in a country or region is usually most dependant on cost-effectiveness.

The early diagnosis of malaria and prompt treatment with antimalarial drugs is essential in controlling the spread of the disease. By reducing the number of infected humans, the number of infected mosquitoes is effectively reduced. This type of control is especially important when outbreaks of malaria occur. When humans are treated the life cycle of the parasite is essentially interrupted. The malaria parasite

invades erythrocytes and feeds off the hemoglobin (oxygen transport protein) during growth and development in the red blood cell. Hemoglobin is digested in an acidic digestive vacuole of the parasite. Many of the current antimalarial agents, such as chloroquine, are thought to disrupt this digestive process one way or another.

Another approach is the use of personal protection. The first objective of this is to protect people from being bitten by an infected mosquito. Insecticide-treated mosquito nets, door and window screens, wearing protective clothing, using insect repellants, coils and vapourizers are all ways of doing this. The other objective of personal control is the use of preventative or prophylactic drug treatment. For instance, travelers to regions where malaria is present often take prophylactics which help prevent the development of the disease but not the initial infection. Cost and availability of drugs can be dictating factors in many countries.

A third approach is vector or mosquito control. Spraying of insecticides to kill the adult or larval mosquitoes can be quite effective. DDT (dichlorodiphenyltrichloroethane) was used successfully for years before environmental campaigns restricting its use resulted in a resurgence of malaria related deaths. More recently the WHO has made the move to bring back DDT declaring it relatively safe for use in indoor spraying and mosquito nets. Managing the environment by reducing mosquito breeding sites has also helped to eliminate malaria in some areas. Using natural biological controls such as mosquito predators are also promising. In the last few years there has been growing interest in bioengineering insects that are unable to transmit the malaria parasite (Kotler, 2003). This is referred to as vector manipulation.

The greatest challenge lies in the parasites ability to quickly adapt and overcome eradication efforts when these are fragmented and uncoordinated. Malaria quickly rebounded from the mass DDT spraying campaigns in the 1950s and 1960s. Since the 1980s parasite resistance to chloroquine, then the most commonly available antimalarial drug, has emerged as a major challenge.

Ideally, a protective vaccine would be the most effective approach to controlling malaria. Attempts to develop a vaccine, however, have been hindered by the great genetic diversity of the parasite, its multistage life cycle, as well as the complex and inefficient human immune response (Newton and White, 1999). Years of vaccine research have produced few hopeful candidates and although scientists are redoubling the search, an effective vaccine is at best years away.

In addition to destroying the parasite, health care providers are attentive to treating the multiple symptoms of malaria. These symptoms include fever, chills, headaches, malaise, weakness, hepatomegaly (enlarged liver), splenomegaly (enlarged spleen) and dehydration. Malaria can also cause anemia, anorexia, nausea, vomiting, abdominal pain and diarrhea. Deaths from malaria are normally caused by cerebral, renal or pulmonary fever, or a combination of the three (Strickland and Hunter, 1982).

1.5 Malaria Treatment

Drugs used for the treatment of malaria do not assist the natural healing processes of the body; instead they act chemically on the parasite as a controlled poison. In most cases antimalarial drugs target the asexual erythrocytic stage of the parasite. The parasite degrades hemoglobin in its acidic food vacuole, producing free heme able to react with molecular oxygen and thus generating reactive oxygen species as toxic by-products. A major pathway of detoxification of heme moieties is polymerization as malaria pigment. Most antimalarial drugs act by disturbing the polymerization of heme, thus killing the parasite with its own metabolic waste. Antimalarial drugs fall into several chemical groups. The first and most commonly used are the quinoline based antimalarials, which include quinine **(1)** and its derivatives chloroquine **(2)**, amodiaquine **(3)** and mefloquine **(4)** (Figure 1.3).

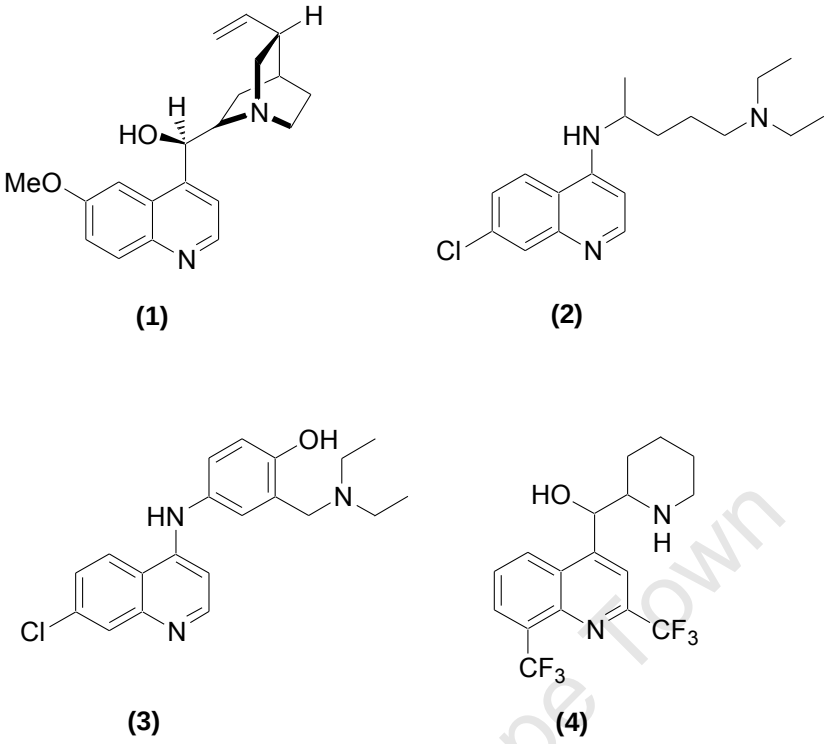

Figure 1.3 Quinoline based antimalarials

Quinine **(1)** has been used for more than three centuries and until the 1930s was the only effective agent for the treatment of malaria. Of the 36 alkaloids found in the bark of the *Cinchona* tree, only four possess antimalarial properties, with quinine being the most effective (Lee, 2002). It is able to bind strongly to blood proteins and forms complexes that are toxic to the malarial parasite. Due to its undesirable side effects it is now only used as an intravenous injection to treat severe malaria.

Chloroquine **(2)** was introduced in 1944 and soon became the mainstay of therapy and prevention, since this drug was cheap, non-toxic and effective against all strains of the parasite (Robert *et al*., 2001). It is capable of blocking the polymerisation of heme to hemozoin (malaria pigment) (Zhang *et al*., 1999). It is a chemically synthesized drug. Increased parasite resistance has virtually rendered chloroquine useless. Chloroquine's reduced efficacy led to the development of the synthetic

analogues amodiaquine **(3)** and mefloquine **(4)** that are used to treat cases of uncomplicated malaria in areas where chloroquine resistance is prevalent.

The second class of common antimalarials is the folate antagonists (Figure 1.4). These compounds inhibit the synthesis of parasitic pyrimidines and thus of parasitic DNA (Robert *et al*., 2001). There are two types of antifolates, the dihydrofolate reductase (DHFR) inhibitors pyrimethamine **(5)** and proguanil **(6)**, and the dihydropteroate synthetase (DHPS) inhibitors, which include the sulphonamide drugs, sulpha-doxine **(7)** and dapsone **(8)**. Due to a marked synergistic effect, a drug of the first group is usually used in combination with a drug of the second one. Pyrimethamine-sulfadoxine (SP), or Fansidar®, is the most widely used combination and has been used to replace chloroquine as a first line treatment of *P. falciparum* in many parts of Africa (Na-Bangchang and Karbwang, 2009).

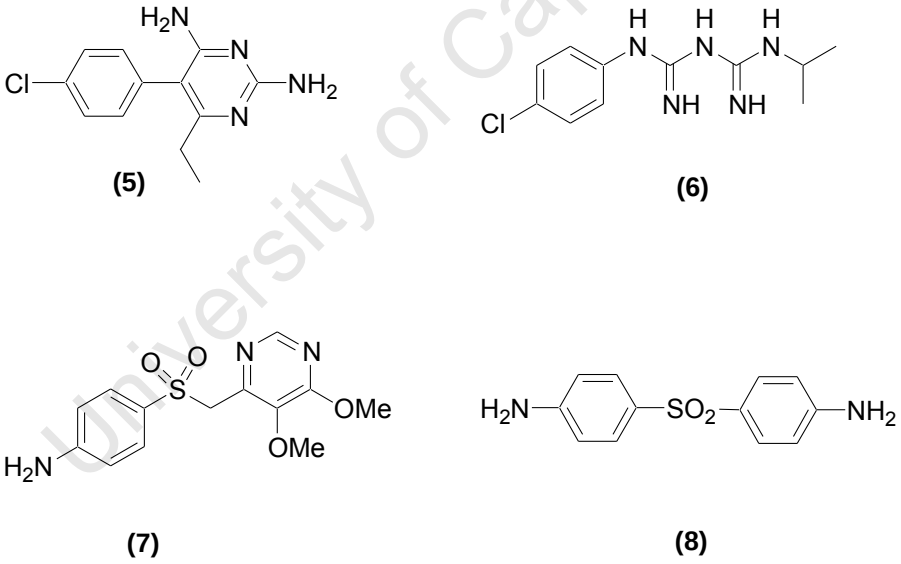

Figure 1.4 DHPS and DHFR inhibitors

The third class of antimalarials is based on the natural endoperoxide artemisinin **(9)** which was first extracted from the Chinese traditional medicine, *Artemisia annua*, in 1972 (Vroman *et al*., 1999). Artemisinin is not soluble in water or oil and because of this poor solubility; the drug absorption and its bioavailability are also poor. However,

since the peroxide bridge of the compound is stable under various chemical reaction conditions, several oil and water-soluble derivatives of artemisinin have since been synthesized (Lee, 2002). These include dihydroartemisinin (DHA) **(10)**, artemether **(11)**, arteether **(12)**, artesunate **(13)** and artelinic acid **(14)** (Figure 1.5) (Robert *et al*., 2001). The semi-synthetic derivatives of artemisinin have improved pharmacokinetic properties and are also of current clinical use, artesunate being the most frequently used in combination therapy and in cases of resistant and uncomplicated *P. falciparum*.

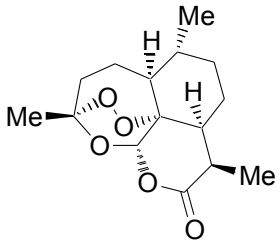

(9)

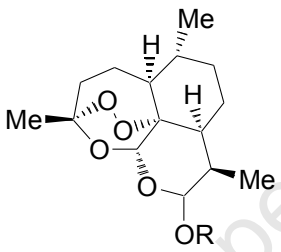

(10) R = H
(11) R = Me
(12) R = Et
(13) R = $CO(CH_2)_2COONa$
(14) R = $CH_2(p\text{-}C_6H_4)CO_2H$

Figure 1.5 Artemisinin and its semisynthetic derivatives

Artemisinins act against the asexual blood stage of the parasites life cycle. Since an artemisinin derivative lacking the endoperoxide bridge (deoxyartemisinin) is devoid of antimalarial activity, the possible reactivity of this peroxide function within the parasite is the key factor of the pharmacological activity of these molecules (Klayman, 1985). This group of antimalarials is the most rapidly acting and is effective against multi-drug resistant strains of the parasite. Although the precise mode of action of artemisinin and its derivatives is not completely understood, it is proposed that the endoperoxide bridge is cleaved to generate free radicals. The free radicals are strong alkylating agents and form covalent bonds with various parasite proteins.

Artemisinin based combination therapies (ACT's) combine one of the derivatives of artemisinin with partner drugs (*viz*. mefloquine, lumefantrine, amodiaquine). ACT's have now been adopted as the first line of treatment. The combination of drugs with

different modes of action considerably reduces the risk of selecting resistant mutants in the parasite population. ACT's produce faster clinical recovery, prevent deterioration from uncomplicated to severe malaria and reduce the risk of transmission.

1.6 Antimalarial Drug Resistance and the Need for New Antimalarials

For most of the twentieth century, malaria was treated with the readily available, inexpensive and effective drugs chloroquine and pyrimethamine-sulphadoxine. But from the 1960's onwards these drugs succumbed to the rapid emergence and spread of drug resistant strains of the parasite (Fidock, 2010). The reasons for the development and spread of drug resistance involve the interaction of drug-use patterns, characteristics of the drug itself, human host factors, parasite characteristics, and vector and environmental factors (Ridley, 2002). However, only gene mutations confer resistance to the parasites in nature.

Early theories on chloroquine resistance were that resistant parasites accumulated less chloroquine than sensitive parasites. Thus lethal concentrations of the drug are prevented from reaching the parasitic food vacuole. The decrease in chloroquine accumulation can be attributed to a higher rate of chloroquine efflux, a lower rate of chloroquine uptake, or varying combinations of both these processes (Saliba *et al*., 1998). More recent studies have highlighted the role of mutations in the *P. falciparum* chloroquine-resistance transporter (PfCRT) protein in the molecular basis of parasite resistance to the quinoline antimalarials (Bray *et al*., 2005; Sidhu *et al*., 2002; Zishiri *et al*., 2011). PfCRT is an integral membrane protein of the intra-erythrocytic parasite's digestive vacuole, the organelle in which chlorquine exerts its antimalarial effect by interfering with the formation of hemozoin. It evidently functions as a transporter directly mediating the efflux of chloroquine from the digestive vacuole. Antifolate resistance is generally due to a combination of mutations in the target enzymes and the use of an alternative pathway to recover folate.

The artemisinins are currently amongst the most effective and widely used antimalarial drugs although recurrence is associated with the monotherapy of artemisinin and its derivatives at a high rate. This is not because of resistance in the parasite, but because of the drug's phamacokinetic properties. ACT's are used to prevent recrudescence (Bloland, 2001). There is much evidence to support the use of combination ACT's, however several problems prevent its wide use in the areas where its use is most advisable; which include problems identifying the most suitable drug for different epidemiological situations, the expense of combined therapy (it is over 10 times more expensive than traditional mono-therapy), how soon the programmes should be introduced and problems linked with policy implementation and issues of compliance.

Despite the marked success of intense elimination campaigns based on ACT's and insecticide-treated bednets, the prospect of resistance remains. There is reported evidence of reduced clinical response to ACT's (Dondorp *et al*., 2009; Gamo *et al*., 2010). *P. falciparum* from patients in Pailin, western Cambodia, had significantly reduced *in vivo* susceptibility to artesunate compared to parasites from patients in Wang Pha, northwestern Thailand. The artesunate resistance was characterized by relatively slow parasite clearance, with minimal heterogeneity among patients. The reduced parasitological responses could not be explained by pharmacokinetic or other host factors.

No new class of antimalarials has been introduced clinically since 1996, owing to the inherent difficulties of antimalarial drug discovery, as well as relative lack of public and commercial resource commitment towards antimalarial research (Gamo *et al*., 2010). Due to the increased costs of developing and registering new products and the prospect of low commercial returns, pharmaceutical companies, particularly the multinationals, have little interest in developing a new cure despite the need (Ramachandran, 2002).

The sequencing of the *Plasmodium* genome and increased understanding of the parasite's biology (Guiguemde *et al*., 2010) has not yet led to new antimalarials and

target-based lead discovery has proved costly and inefficient, generally due to lack of whole-cell activity. With no vaccine on the immediate horizon, mosquito control, chemotherapy and chemoprophylaxis remain the major methods of keeping malaria in check. Malaria control is at a pivotal point. Continued effectiveness and use of ACT's and vector control efforts, could lead to a complete eradication of the disease. Alternatively, resistance could sabotage the usefulness of artemisinins, and cause resurgence in malaria.

Thus there is a real need to continue the search for new classes of antimalarial agents that are effective against multi-drug resistant *P. falciparum,* safe, affordable and simple to use. One approach to this is the investigation of medicinal plants, which have historically provided useful antimalarials.

1.7 Medicinal Plants

Although modern medicine is well established in most parts of the world, the World Health Organisation (WHO) estimates that 80% of the world's population relies solely on traditional medicine for their primary health care needs (World Health Organisation, 1995). Plants of medicinal value have been used effectively for centuries in traditional medicine. Medicinal plants are considered a major source of biologically active natural products that may serve as commercially significant entities themselves or provide lead structures for the development of modified derivatives possessing enhanced activity and/or reduced toxicity.

Traditional medicines include crude plant extracts, or combinations of several medicinal plants, which contain numerous components that are thought to contribute to the overall therapeutic effect. Because the chemical compounds in the different plant components are often quite different, usually only a specified plant part is used medicinally (*viz*. leaves, roots, bark or fruit). The method of preparation is crucial. Activities including the addition of appropriate volumes of solvents such as water or alcohol to a specified amount of fresh or dry plant material, boiling for a specified

length of time or partial burning to achieve a desired colour are important and can serve to neutralize certain toxins. Dosage forms (*viz*. tinctures, extracts, ointments or enemas) as well as the method of administration (*viz*. orally, topically or nasally) are also critical and are conveyed by the healer (Van Wyk *et al*., 2000).

Plant-based traditional medicine systems continue to play an essential role in healthcare. Because of the importance of medicinal plants the WHO encourages their use not only under an empirical basis, but also under a scientific approach. The advantages gained from a scientific approach to traditional plant remedies in developing countries, where they have fundamental importance, are numerous.

Firstly it would allow natives to gain some independence from developed countries in the preparation of plant-derived medications, and it would promote the establishment of sustainable supply and extraction industries, which could prove to be a vital aspect for economic development. Proving the efficacy of traditional medicines, would also allow the local medium-large scale cultivation of medicinal plants with an obvious benefit for the national economy. Finally, from an environmental point of view, the proof of therapeutic value of selected medicinal plants would help to conserve species that would otherwise be depleted by unsustainable harvesting activities (Caniato and Puricelli, 2003).

An estimated 70% of South Africans regularly use traditional medicines, most of which are derived from plant species indigenous to the region. South Africa represents only 0.04% of the land surface area of the world, yet nearly 10% of all known plant species occur here. There are over 24 000 plants indigenous to South Africa. Approximately 3000 species of plants are used as medicines, and some 350 of these are the most commonly used and traded medicinal plants. Some South African medicinal plant extracts are used worldwide. An extract of *Pelargonium sidoides* is commercially traded as a remedy for bronchitis (“Umckaloabo”) by the Germans. Devil’s claw (*Harpagophytum procumbens*) products are used to treat rheumatism and arthritis, and as a general heath tonic. The bitter yellow juice exuded from just

below the surface of the leaves of Cape aloes (*Aloe ferox*) is dried by an age old method to form a dark brown resinous solid which is traded internationally as a laxative. (Van Wyk *et al*., 2000).

1.8 Drugs from Plants

There are two basic approaches to drug discovery: rational drug design and the traditional method of random screening. Rational design-engineering of new drug molecules from scratch with the aid of computers and molecular biology requires knowledge of the drug target such as a receptor or an enzyme. So far, it has had only limited payoffs, although it has promising potential. In random screening many synthetic chemicals or natural products are indiscriminately tested for biological activity. Because this method is both costly and time-consuming, there has been a great need for better efficacy in strategic research and development planning for pharmaceutical companies. The strategy of developing new drugs based on medicinal plants has an advantage over random screening, since it is guided by experience from a long history of clinical practice.

For many centuries plants have been the primary source of crude drugs used to alleviate human sickness. The isolation of the analgesic morphine **(15)** from the opium poppy (*Papaver somniferum*) in 1819 and quinine **(1)** from *Cinchona bark* in 1820, laid the foundation for the purification of pharmacologically active compounds from medicinal plants (Butler, 2004). More than 25% of all drugs in clinical use today originated from plants or are derivatives of natural products. Well known examples include artemesinin **(9)**, extracted from the bark of the *Artemisia annua*; the anticancer drug, taxol **(16)**, from the bark of *Taxus brevifolia*; and salicylic acid **(17)** which served as a template for aspirin **(18)**, originally isolated from the bark of the *Salix* species. In addition, crude herbal preparations are also popular and some examples include *Oenothera biennis* (Evening primrose) used in cosmetics, *Hypericum perforatum* (St John's Wort) used as an antidepressant, and *Panax ginseng* (Ginseng) taken as a treatment for diabetes and sexual dysfunction.

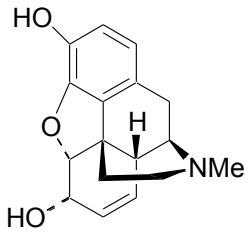

(15)

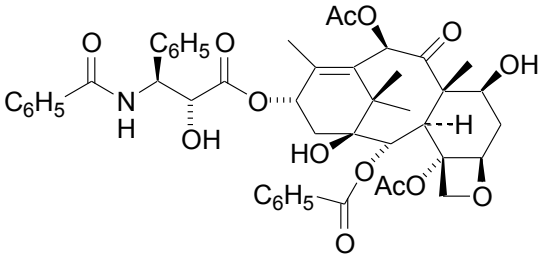

(16)

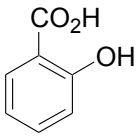

(17)

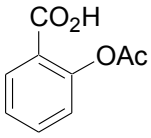

(18)

Figure 1.6 Examples of plant-derived drugs

The active ingredients in medicinal plants are chemical compounds that act directly or indirectly to prevent or treat a disease or ailment and maintain health. Plants investigated for pharmacologically active compounds are usually selected on the basis of ethnomedicinal information as there is a correlation between biological activity and the traditional use of the plant. In selecting plants that may contain biological agents, generally a targeted approach to plant collection is adopted based on the belief that plants that have acquired the status of a traditional herbal remedy have reasonable proof of safety and efficacy from their history of use and have a higher probability of yielding an active substance.

The chemical diversity and stereospecificity of complex natural products are the main attractions of working with plants as opposed to synthetic chemistry approaches. In developing a drug from a plant-derived lead compound, attempts may be made to produce chemical analogues of the active principle with enhanced antiplasmodial activity and reduced host toxicity. Guides for conducting this work are often obtained from the original plant source since plant constituents often occur as a group of

structurally related metabolites, making it possible to isolate analogues of the active compound and obtain information on structure-activity relations.

There has been a resurgence in natural product drug discovery, as is evident in the number of plant-based drugs in clinical trials, mainly for the treatment of cancer, immunological and CNS (central nervous system) related diseases (Saklani and Kutty, 2008; Newman and Cragg, 2007). Considering that only a small percentage (10 – 15%) of higher plant species have been investigated for pharmacological activity, it is most likely that plants will continue to offer novel leads for drug development.

1.9 Antimalarials from Plants

Historically the majority of the antimalarial drugs have been derived from medicinal plants or from structures modeled on plant lead compounds. Quinine **(1)**, the first effective antimalarial drug is still in clinical use today and the more recently discovered artemisinin **(9)** is the template for several semi-synthetic derivatives with enhanced animalarial activity. In light of this historic success and the fact that most indigenous people living in malaria endemic areas use traditional medicines to fight this disease, there is every possibility that ethnopharmacological approaches could lead to new antimalarial agents.

The development of continuous culturing of *P*. *falciparum* (Trager and Jensen, 1976) and subsequent *in vitro* assays (Desjardins *et al*., 1979; Makler *et al*., 1993; Schulze *et al*., 1997) made it possible to screen plant extracts for antiplasmodial activity and use bioassay-guided fractionation to isolate active principles. The investigation of a range of plants used in traditional medicine for the treatment of malaria in various countries has led to the discovery of a large number of antimalarial compounds with significant structural variety (Schwikkard and Heerden, 2002). Table 1.1 lists some of these compounds, which belong to different secondary metabolite classes, and the

traditional medicines from which they were isolated (Caniato and Puricelli, 2003; Kaur *et al*., 2009).

South Africa's rich biodiversity and long history of traditional medicinal plant use has also prompted several studies to evaluate local indigenous plants for antimalarial properties (Clarkson *et al*., 2004; Nundkumar and Ojewale, 2002; Prozesky *et al*., 2001). A recent review (Pillay *et al*., 2008) concluded that the identification of compounds from South African plants implicated in the treatment of malaria suggests that these compounds may play a role in the medicinal properties of the plant, but their potential for the development of antimalarial drugs was limited by inherent toxicity and lack of selectivity. This is often the case with antimalarial compounds identified from plants, and together with low bioavailability and/or poor solubility, accounts for the limited number that reach drug candidate status.

Table 1.1 Examples of classes of compounds with antimalarial activity isolated from medicinal plants

Class of compound	Compound	Plant	Plant part	Country of plant origin
Quinones	1-hydroxybenzoiso-chromanquinone	*Psychotria camponutans*	Stem & roots	Panama
Triterpenes	Lupeol	*Vernonia brasiliana*	Leaves	Brazil
Diterpenes	Ferruginol	*Harpagophytum procumbens*	Roots	South Africa
Sesquiterpenoids	16,17-Dihydrobrachy-calyxolide	*Vernonia brachycalyx*	Leaves	Kenya
Quassinoides	Bruceolide	*Brucea javanica*	Fruits	China
Limonoids	Fissinolide	*Khaya senegalensis*	Bark	Sudan

Class of compound	Compound	Plant	Plant part	Country of plant origin
Alkaloids	Ancistroheynine A	*Ancistrocladus heyneanus*	Roots	India
Lignans	Justicidin B	*Phyllanthus piscatorum*	Aerial parts	Venezuela
Flavanoids	Exiguaflavanone A	*Artemesia indica*	Stems	Thailand
Chalcones	(+)-Nyasol	*Asparagus africanus*	Roots	Kenya
Xanthones	Cowaxanthone	*Garcinia cowa*	Bark	Thailand
Coumarins	*O*-Methylexostemin	*Exostema mexicanum*	Stem bark	Latin America

1.10 Antimalarial Drug Discovery

Biological testing for antimalarial activity in plants has progressed over the years. In the 1950s, the screening of crude plant extracts was based on avian malarias using *in vivo* tests against *P. gallinaceum* in chicks and against *P. cathemerium* and *P. lophurae* in ducklings. In the 1970s, *in vitro* procedures were developed utilizing *P. falciparum* cultures in human red blood cells, a technique that enabled the development of a microdilution assay. This technique, compared to previous ones active on human malarias, is useful to assess *in vitro* antimalarial activity of crude extracts prior to the isolation of active principles (Caniato and Puricelli, 2003).

One such *in vitro* assay is the parasite lactate dehydrogenase (pLDH) assay. pLDH is a terminal enzyme in the glycolytic pathway of *Plasmodium spp.* and plays an important role in the parasites anaerobic carbohydrate metabolism. As malaria parasites principally rely on anaerobic glycolysis, they require the regeneration of nicotinamide adenine dinucleotide (NAD) for the continuous flux of glucose through this pathway (Noedl *et al*., 2003). On the basis of the discovery that pLDH is distinguishable from host LDH using the 3-acetylpyridine dinucleotide analogue of NAD (ADAP), Makler *et al*.(1993) developed a drug-sensitivity assay that determines

inhibition profiles by measuring the enzymatic activity of pLDH. Other *in vitro* antiplasmodial assays include those based on flow cytometric activity (Prozesky *et al*., 2001) and the titrated hypoxanthine incorporation method (Kaur *et al*., 2009).

An *in vivo* screening assay is possible in mice using a natural infection with *P. berghei*. These methods allow the development of strains resistant to chloroquine or to other antimalarials by a passage in the presence of increasing concentrations of the drug. *In vitro* tests are considered more practical, quicker and less expensive than *in vivo* cultures and not all antimalarial drugs are active in the *P. berghei* mouse model. In addition, the *in vivo* model requires significantly higher amounts of drugs (at least 1 g of extract) when compared to the *in vitro* assays which require a few mg of extract. The advantage of the *in vivo* model is that at the same time it gives a measure of toxicity.

Detailed evaluation of antimalarial drugs is done in the Aotus monkey (*Aotus trivirgatus*) using *P. falciparum* infection or in the Rhesus monkey (*Macaca mulata*) with *P. cynomolgi* B infection (Caniato and Puricelli, 2003). Of the numerous extracts and compounds studied in primary screens *in vitro*, very few reach this stage of investigation.

In researching plants which are frequently mentioned as antimalarials in literature it is often found that these do not necessarily show high activity in *in vitro* tests. This can partly be explained by the fact that many plants are used in the treatment of malaria, not for their antiparasitic effects but because of other therapeutic activities. These include reducing fever, calming convulsions and headache, and possibly even immuno-stimulatory effects. Another problem is that some plants are given in a mixture and are possibly only active in this combination due to synergistic effects. Also, an *in vitro* assay cannot precisely reproduce the *in vivo* situation. Certain plant extract components might only become active after specific metabolic processes *in vivo* (Gessler *et al*., 1994).

Other problems commonly encountered when investigating medicinal plants as a source of antimalarial drugs is that crude extracts or compounds show *in vitro* activity but are extremely toxic or those which are active *in vitro* fail to display *in vivo* activity. If a compound destroys parasites, it is logical to screen for toxicity *in vitro* using human cells in culture. When a compound is found to destroy human cells at similar concentrations, its potential as a useful drug is limited as the safety margins will be too slender. The difficulty arises from the fact that protozoa share many biochemical pathways with the human host thereby limiting the antimalarial drug's selectivity to kill the parasite without harming mammalian cells. The pharmacokinetic and pharmacodynamic properties of the extract or compound determine whether it will display *in vivo* activity. This includes absorption, distribution to the action site and whether the compound is metabolized too rapidly or to a less active form (Kirby, 1996).

The current productivity crisis in drug discovery and development may be overcome by adopting a multidisciplinary approach and combining the novel molecular diversity of natural products with total and combinatorial synthetic methodologies, and including the manipulation of biosynthetic pathways (combinatorial biosynthesis). Despite their inherent limitations (*viz*. toxicity, bioavailability, solubility), antimalarial compounds discovered from plant sources provide useful bioactive synthons, which may be synthetically modified to improve their drug-like properties.

CHAPTER 2

Antiplasmodial Activity of *Trema orientalis*

2.1 Background and Aims of this study

South Africa boasts remarkable biodiversity and a rich cultural heritage of medicinal plant use. A number of extracts from South African plants have been evaluated for *in vitro* antimalarial activity but little is known about their active constituents (Pillay *et al*., 2008). In light of this and the pressing need for new antimalarial drugs, the South African Department of Science and Technology awarded an innovation fund to a national multidisciplinary consortium to further evaluate South African medicinal plants for the treatment of malaria.

A survey of relevant literature (30 books) on medicinal plant use in East and Southern Africa revealed approximately 700 taxa associated with malaria and/or fever. All 623 taxa, occurring indigenously or naturalised within the Flora of Southern Africa (FSA) region, were ranked using weighted criteria (primarily ethnobotanical and chemotaxanomic). From the ranked list, over 134 species representing 54 families, were collected throughout South Africa and extracts thereof were tested for *in vitro* activity against a chloroquine-sensitive (D10) strain of *P. falciparum* using the pLDH assay. Sixty-six species (49%) were reported to show promising antiplasmodial activity ($IC_{50} \leq 10$ μg/ml), of which 17% (23 species) were considered highly active ($IC_{50} \leq 5$ μg/ml) (Clarkson *et al*., 2004).

One of the "highly active" plant extracts originating from this screening programme, was from *Trema orientalis*, and further investigation of this hit by the Council for Scientific and Industrial Research (CSIR) formed the basis of this study. The research undertaken was aimed at:

1. Investigating the *in vitro* and *in vivo* antiplasmodial properties of the plant extract/s
2. Comparison of a classical and accelerated approach to bioassay-guided fractionation to identify the active ingredient/s

3. Isolation and characterization of the active compounds
4. Total synthesis of the active natural product/s
5. Analogue generation based on identified pharmacophore/s

2.2 *Trema orientalis*

2.2.1 Botanical Description and Distribution

Trema belongs to the botanical family Ulmaceae and is a genus of about 30 species of evergreen trees, occurring in subtropical and tropical regions of southern Asia, northern Australasia, Africa, South and Central America, and parts of North America (Wikipedia, 2010). They are fast growing pioneer trees or shrubs, reaching 10 – 20 m in height. In South Africa only one species, *i.e. T. orientalis*, occurs naturally.

T. orientalis (Linn.) Blume is more commonly known as the pigeon wood tree. The name 'Trema' is based on the Greek word for a hole and alludes to the trees pitted seed and 'orientalis' is Latin for eastern or 'of the orient'. The common name pigeon wood is derived from the fact that pigeons are frequently seen nesting in these trees (World Agroforestry Centre, 2010).

T. orientalis is fast growing shade tree with soft foliage that may be evergreen or deciduous depending on climatic conditions. The species is very variable in growth habit, ranging from a shrub to a slender, spreading tree 10 - 18 m in height. Its height is proportional to the amount of water it receives. It resembles the White Stinkwood (*Celtis africana*) superficially, but can be distinguished by certain leaf and fruit characteristics (University of Pretoria Botanical Garden, 2006).

The bark of *T. orientails* is smooth and light grey with longitudinal lines and corky spots. The leaves are simple, alternate and stipulate. Flowers are inconspicuous, greenish, usually unisexual and appear from late winter to autumn. Fruit are small, round, fleshy and green, turning glossy black when ripe (Malan and Notten, 2005).

Figure 2.1 *Trema orientalis* growing in Pinetown, Kwazulu-Natal

The trees are found in the higher rainfall areas of eastern and northern South Africa; the Eastern Cape, KwaZulu-Natal, Swaziland, Mpumalanga, Gauteng and the Northern Province. It does not occur south of the Kei River.

2.2.2 Medicinal Usage

The young leaves are eaten as spinach by the Zulus, who also use the roots and bark medicinally (Hutchings, 1996). Various plant parts are also used in traditional medicine in West Africa, Tanzania, east Africa and Madagascar.

Fruit and leaf infusions or tonics are used to treat bronchitis, pneumonia and pleurisy and coughs. Bark is used for dysentery, as an inhalant for chest diseases and as a vermifuge. Stems and twigs are used for coughs and other respiratory ailments, fevers, toothache and venereal diseases. Pods and seeds are used for tired muscles and aching bones (Hutchings, 1996; Watt and Breyer-Brandwijk, 1962).

A decoction of the aerial parts of the plant is reportedly used to treat malaria in Madagascar (Jenkins, 1987; Rasoanaivo *et al*., 1992).

2.2.3 Chemical Constituents

Phytochemical investigations of *T. orientalis* growing in various parts of the world have led to the identification of several classes of compounds including triterpenoids, sterols, fatty acids, xanthones, coumarins, and glucosides.

The Nigerians, Ogunkoya *et al*., isolated simiarenol **(19)**, simiarenone **(20)**, trematol **(21)**, a long chain hydrocarbon and β-sitosterol from the light petroleum extract of *T. orientalis* stem-bark (Ogunkoya *et al., 1972a;* Ogunkoya *et al., 1972b;* Ogunkoya *et al*., 1973; Ogunkoya *et al*., 1977).

Tchamo *et al*. studied the trunk and root barks of *T. orientalis*, which grows as a shrub in Cameroon, and reported xanthone; secoiridoid and ursane skeletons in the Ulmaceae for the first time (Tchamo *et al*., 2001). Methylswertianin **(22)**, decussatin **(23)**, 1-*O*-glucosyldecussatin **(24)**, 1-O-primeverosyl-decussatin **(25)**, sweroside **(26)**, 2α, 3α, 23-trihydroxyurs-12-en-28-oic acid **(27)**, 2α, 3β-dihydroxyurs-12-en-28-oic acid **(28)**, lupeol **(29)**, simiarenone **(20)**, β-sitosterol, 3-*O*-β-glucopyranosyl-β-sitosterol, scopoletin, (-)-epicatechin, *p*-hydroxybenzoic acid and hexacosanoic acid were identified. They later reported on the isolation of two novel dihydrophenanthrene constituents **(30)** and **(31)**, and orientoside A **(32),** a novel phenyldihydroisocoumarin (Dijoux-Franca *et al*., 2001).

The Taiwanese reported the isolation of (+)-syringaresinol **(33)**, (-)-ampelopsin F **(34)**, *N*-(trans-*p*-coumaroyl)tyramine **(35)**, *N*-(trans-*p*-coumaryl) octopamin **(36)**, 3,5-dimethoxy-4-hydroxyphenyl-1-*O*-β-D-glucoside, (-)-epicatechin, (+)-catechin, and trans-4-hydroxy-cinnamic-acid from the stem of *T. orientalis* (Kuo *et al*., 2007).

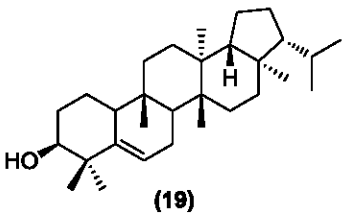

(19)

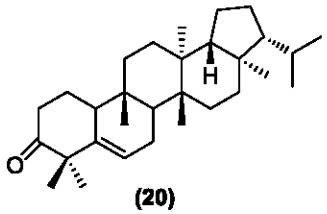

(20)

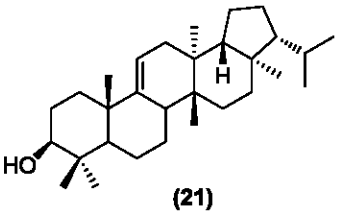

(21)

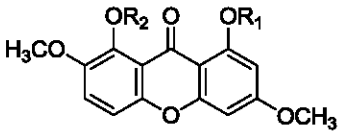

	R_1	R_2
(22)	H	H
(23)	H	Me
(24)	Glc	Me
(25)	Prim	Me

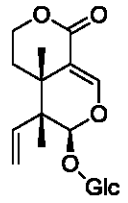

(26)

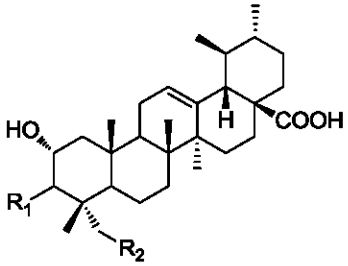

	R_1	R_2
(27)	α-OH	OH
(28)	β-OH	H

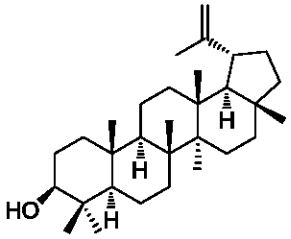

(29)

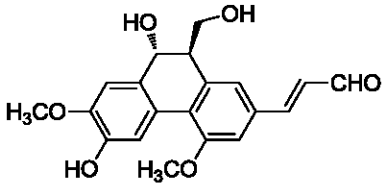

(30)

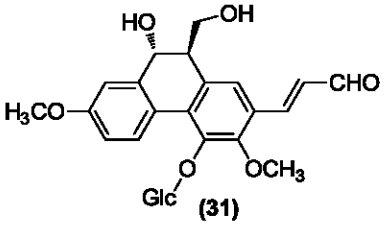

(31)

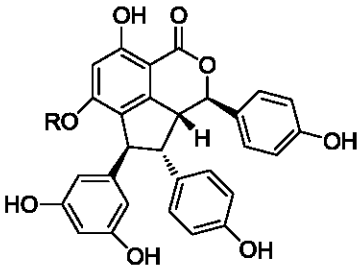

(32) R = α-arabinopyranosyl

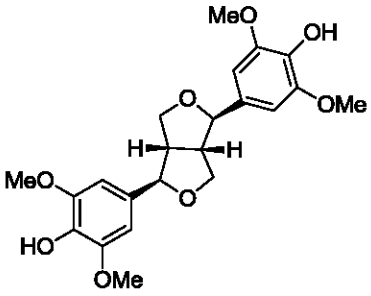

(33)

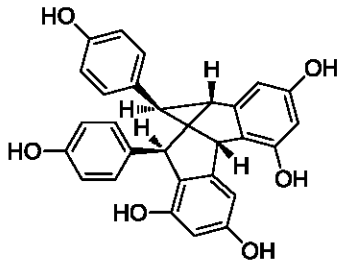

(34)

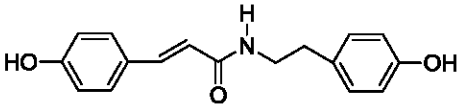

(35)

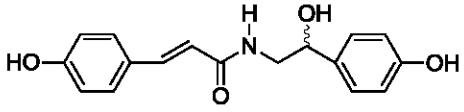

(36)

2.2.4 Biological Properties

The cytotoxic, antitumour and antimicrobial activity of extracts of the *T. orientalis* have been studied (Akinyemi *et al*., 2005; Chowdhury and Islam, 2004). An aqueous stem bark extract of the plant was also reported to significantly reduce blood glucose in STZ-induced diabetic rats by a mechanism different from that of sulphonylurea agents (Dimo *et al*., 2006). A flavanoidal mixture from *T. orientalis* was shown to possess strong CNS depressant properties, protecting 50% of experimental animals against electroshock convulsions (Chauhan *et al*., 1988).

Extracts of *T. guineense*, reported to be a synonym of *T. orientalis* (Hutchings, 1996), showed significant analgesic, anti-inflammatory and antiarthritic activity in rodents. These pharmacological effects were evaluated using the acetic acid induced writhing test and hot plate method, the carrageenin-induced Oedema assay and Newbould's adjuvant arthritis test, respectively (Barbera *et al*., 1992). An ethanolic extract of *T. guineense* leaves was evaluated for its neuropharmacological properties in rodents and was found to induce hypothermia, significantly shorten the latency to sleep and prolong the duration of chemically induced sleeping time and significantly delay the onset of chemically induced clonic seizures; suggesting that the plant may contain compounds with a tranquilizing and/or sedative action (N'Gouemo *et al*., 1994).

There are no reports on the investigation of the antimalarial properties of *T. orientalis*. However, extracts of the stem bark of a related species, *Trema micrantha*, was found to be weakly active *in vitro* (62% inhibition at 100 µg/ml) against a chloroquine resistant strain (Indo), but showed good activity *in vivo* (81% inhibition at 100 mg/kg) using a classical 4-day suppressive test against *P. vinckei petteri* 279BY (Muñoz *et al*., 2000).

2.3 *In vitro* Antiplasmodial Activity of *T. orientalis* Extracts

T. orientalis was selected for a national antimalarial screening programme (Clarkson *et al*., 2004) based on its ethnobotanical links to malaria (Jenkins, 1987; Rasoanaivo *et al*., 1992). The sequentially prepared 1:1 dichloromethane/methanol (DCM/MeOH)

and aqueous extracts of *T. orientalis* twigs, part of CSIR's historical extract repository, were tested *in vitro* against a chloroquine-sensitive (D10) strain of *P. falciparum* in duplicate in the pLDH assay (Table 2.1).

Table 2.1 *In vitro* antiplasmodial activity of *T. orientalis* extracts

Extract	D10 (Experiment 1) IC_{50} (μg/ml)	D10 (Experiment 2) IC_{50} (μg/ml)	K1 IC_{50} (μg/ml)
P05644B (1:1 DCM/MeOH)	3.0	2.2	1.7
P05644C (Aqueous)	>10	>10	-

The active component in the twigs of *T. orientalis*, responsible for the observed antiplasmodial activity, was concentrated in the organic extract, P05644B. It was found to be significantly active against the D10 strain of the parasite, having a 50% inhibitory concentration (IC_{50}) value of less than 5μg/ml. The aqueous extract (P05644C) was relatively inactive; only an IC_{50} less than 10 μg/ml was considered active at the extract level (Clarkson *et al*., 2004).

The organic extract was subsequently tested against the K1 strain of *P. falciparum* and was found to have similar activity (IC_{50} 1.7 μg/ml) against this chloroquine-resistant strain. It was therefore prioritized for bioassay-guided fractionation to isolate and identify the active compounds.

2.4 Bioassay-guided Fractionation of the *T. orientalis* Organic Extract

Bioassay-guided fractionation, based on *in vitro* antiplasmodial activity against the D10 *P. falciparum* strain, was conducted on the 1:1 DCM/MeOH extract of the twigs of *T. orientalis*.

Figure 2.2 outlines the stepwise fractionation of the organic extract, P05644B, guided by observed antiplasmodial activity against the D10 *P. falciparum* strain. As the extract showed activity against both the chloroquine-sensitive (D10) and resistant

(K1) strains, the D10 strain was selected as the primary indicator for activity as it is generally easier to culture than the K1 strain. The crude extract was subjected to a liquid/liquid partitioning process, separating the components into three fractions of varying polarity to yield a hexane- (**1A**), dichloromethane- (**1B**) and aqueous- (**1C**) soluble fraction. The choice of partitioning between these three solvents is based on a standard method to remove fatty acids (concentrated in the hexane fraction) and tannins (concentrated in the aqueous fraction) from the more biologically attractive secondary metabolites (concentrated in the dichloromethane fraction).

Enhanced antiplasmodial activity was observed for the dichloromethane-soluble fraction **1B** (IC_{50} 1.6 μg/ml) while the hexane-soluble fraction **1A** showed moderate activity (IC_{50} 6.4 μg/ml). Both these fractions were further purified by silica gel column chromatography to yield 16 fractions each. Further fractionation of 1A did not improve the antiplasmodial activity as none of the sub-fractions showed any significant activity. The further fractionation of 1B yielded sub-fraction 3G, with an improved IC50 of 0.8 μg/ml.

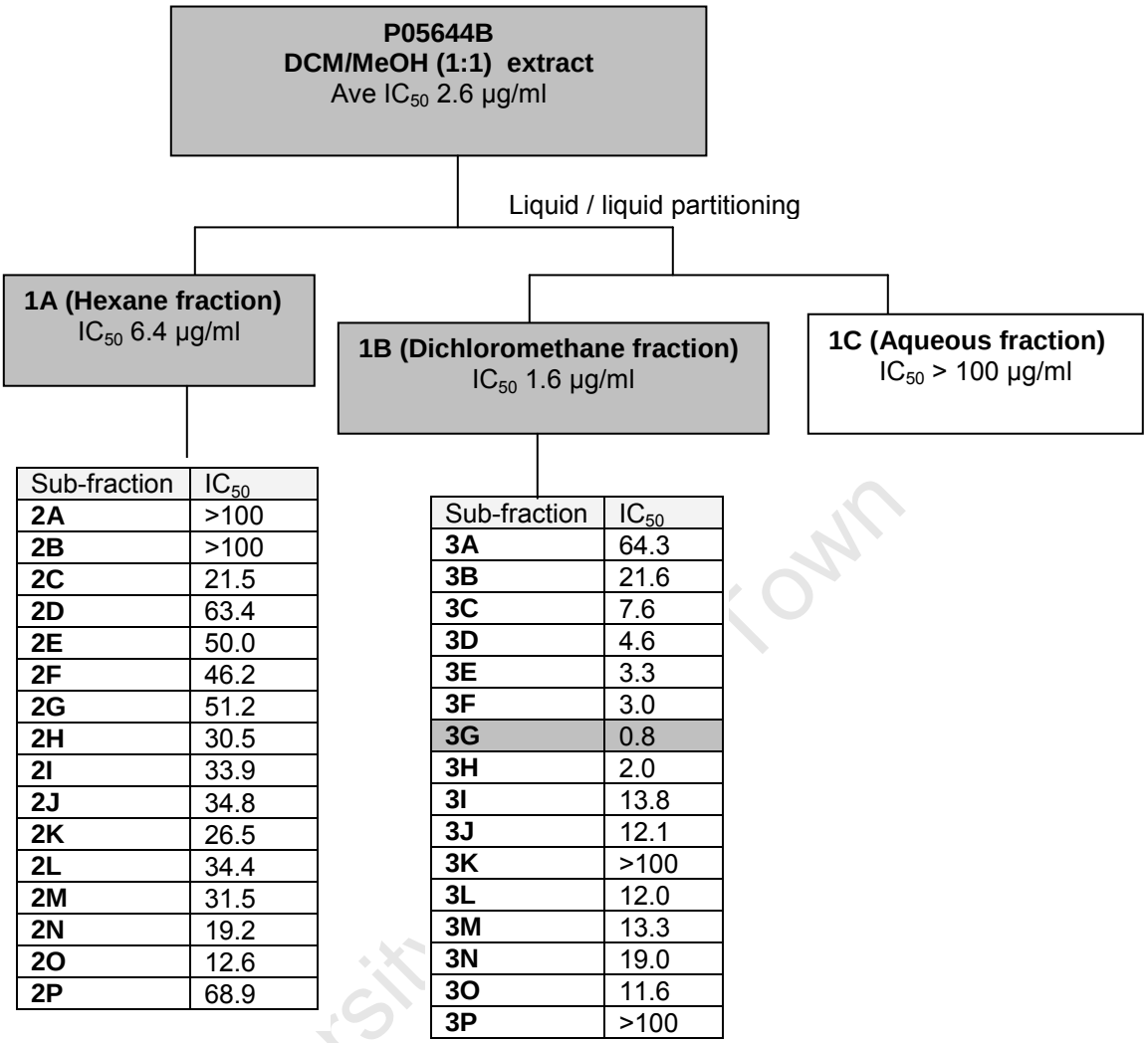

Sub-fraction	IC_{50}
2A	>100
2B	>100
2C	21.5
2D	63.4
2E	50.0
2F	46.2
2G	51.2
2H	30.5
2I	33.9
2J	34.8
2K	26.5
2L	34.4
2M	31.5
2N	19.2
2O	12.6
2P	68.9

Sub-fraction	IC_{50}
3A	64.3
3B	21.6
3C	7.6
3D	4.6
3E	3.3
3F	3.0
3G	0.8
3H	2.0
3I	13.8
3J	12.1
3K	>100
3L	12.0
3M	13.3
3N	19.0
3O	11.6
3P	>100

Figure 2.2 Bioassay-guided fractionation of P05644B. IC_{50} values are in µg/ml

Fraction 3G was also bioassayed against a Chinese Hamster Ovarian (CHO) cell line as a measure of cytotoxicity (Table 2.2). It was found to have a promising selectivity index (SI > 100), which is a ratio of cytotoxicity versus bioactivity. TLC and HPLC analysis of 3G revealed that it was a mixture of at least 5 compounds. However; due to the low yield of fraction 3G (3.2 mg), further fractionation was not practical. A recollection of plant material was required to further pursue the bioassay-guided fractionation.

Table 2.2 *In vitro* antiplasmodial activity and cytotoxicity of fraction 3G

Fraction	D10 IC_{50} (μg/ml)	CHO IC_{50} (μg/ml)	SI[a]
3G	0.8	81.5	101.9

[a] Selectivity index (SI) = cytotoxicity CHO IC_{50} / antiplasmodial D10 IC_{50}

2.5 Recollections of *T. orientalis* Twigs

Following the first observation of antiplasmodial activity and bioassay-guided fractionation attempt, several recollections of *T. orientalis* were undertaken. Plant material from various regions of the KwaZulu-Natal North coast was collected at different times of the year. Extracts of other plant parts (*viz*. the stem bark and leaves) were also prepared and bioassayed. However, the activity was found to be restricted to the young growing twigs of the trees and this was shown to be reproducible between the 1:1 DCM/MeOH twig extracts from various collections (Table 2.3). An *in vivo* evaluation of the organic twig extract from the fourth recollection (P05644-4B) was subsequently conducted.

Table 2.3 *In vitro* antiplasmodial data of recollected *T. orientalis* twig extracts

Extract	Date of collection	Collection area	D10 IC_{50} (μg/ml)	K1 IC_{50} (μg/ml)
P05644B (Original organic extract)	October 2001	Darnall	2.0	2.8
P05644-1B (1st recollection)	April 2003	Mtunzini	9	-
P05644-2B (2nd recollection)	July 2003	Darnall	2.0	-
P05644-3B (3rd recollection)	January 2004	Darnall / Zinkwazi	1.4	3
P05644-4B (4th recollection)	December 2005	Mtunzini	2.8	-
P05644-5B (5th recollection)	March 2006	Darnall	2.8	-

2.6 *In vivo* evaluation of *T. orientalis* semi-purified extract

The semi-purified dichloromethane fraction, produced through liquid/liquid partitioning of the crude extract, showed improved potency *in vitro* (*cf* Figure 2.2). Analysis of this semi- purified fraction from the 4th recollection (P05644-4B) by HPLC (UV/MS) revealed that it was still a complex mixture of 10-15 major compounds and more than 70 minor compounds (Appendix I). P05644-4B was evaluated for *in vivo* antiplasmodial activity against *P. berghei* using a 4-day suppressive test (Raw data in Appendix II). The extract was administered by subcutaneous injection at a dose of 500 mg/kg.

The survival rate of the mice is summarized in Figure 2.3. Of the four mice in the control (untreated) group, two died on day 6 and all were dead on day 7. The experimental group (treated with extract P05644-4B) showed a high survival rate, with 60% survival up to day 20. The mice in this group did not die from malaria but were sacrificed on day 20 following the ethics protocol. The survival results of the experimental group were comparable to that of the chloroquine control group.

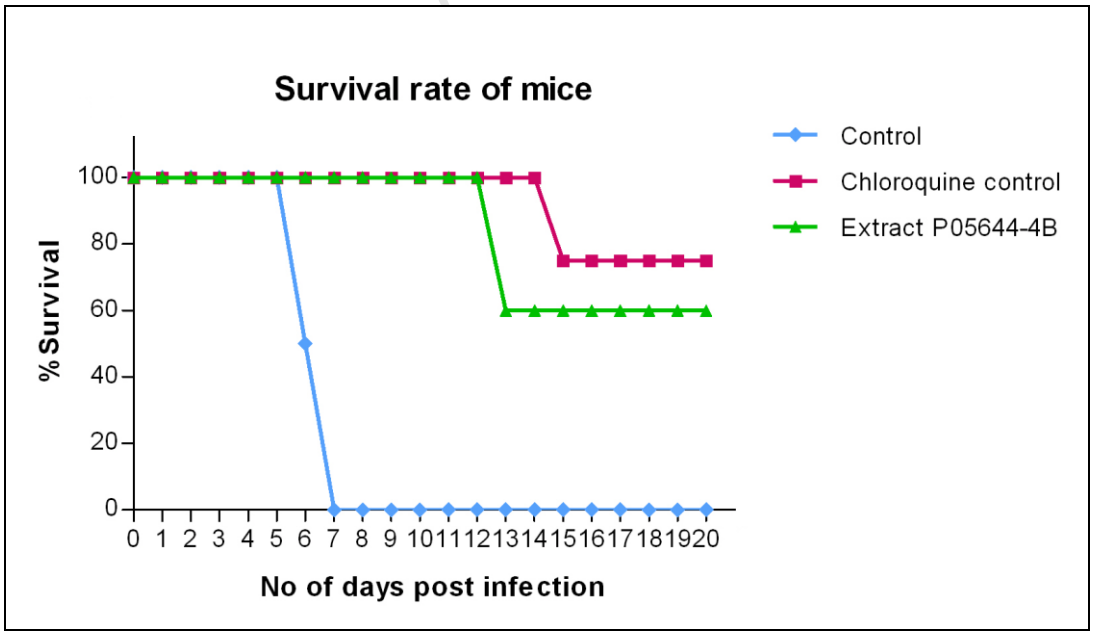

Figure 2.3 The survival rate of mice in each group after infection with *P. bergei ANKA*

The parasitemia percentages, summarized in Figure 2.4, were more indicative of the parasite suppression effect in the infected mice. Over the first four days the extract showed ~40% parasite suppression compared to the control group. The untreated group (control) had parasitemia of 28.4% on day 6 which led to the death of the entire group on day 7; whereas 60% of the mice in the experimental group survived with parasitemia levels above 47% on day 13 and continued to survive with significantly high parasitemia levels until they were sacrificed on day 20.

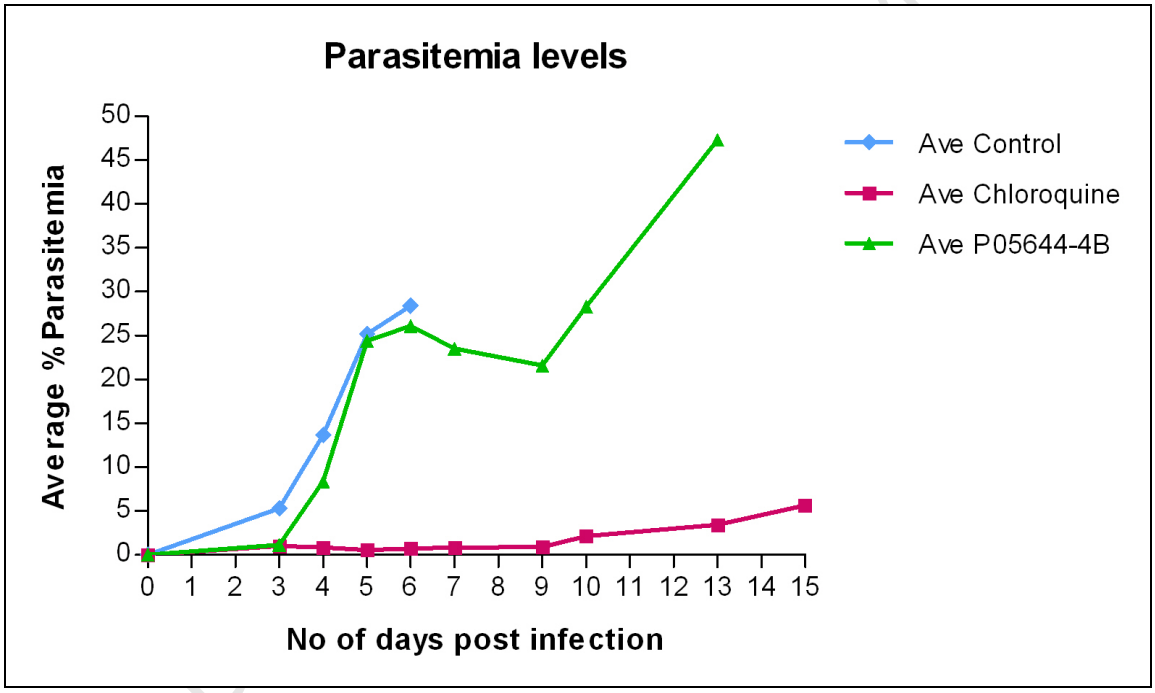

Figure 2.4 The average percentage parasitemia in each group at any given day after infection

The gradual weight loss observed amongst all the animals in the experimental group (Figure 2.5) confirmed that the mice were sick.

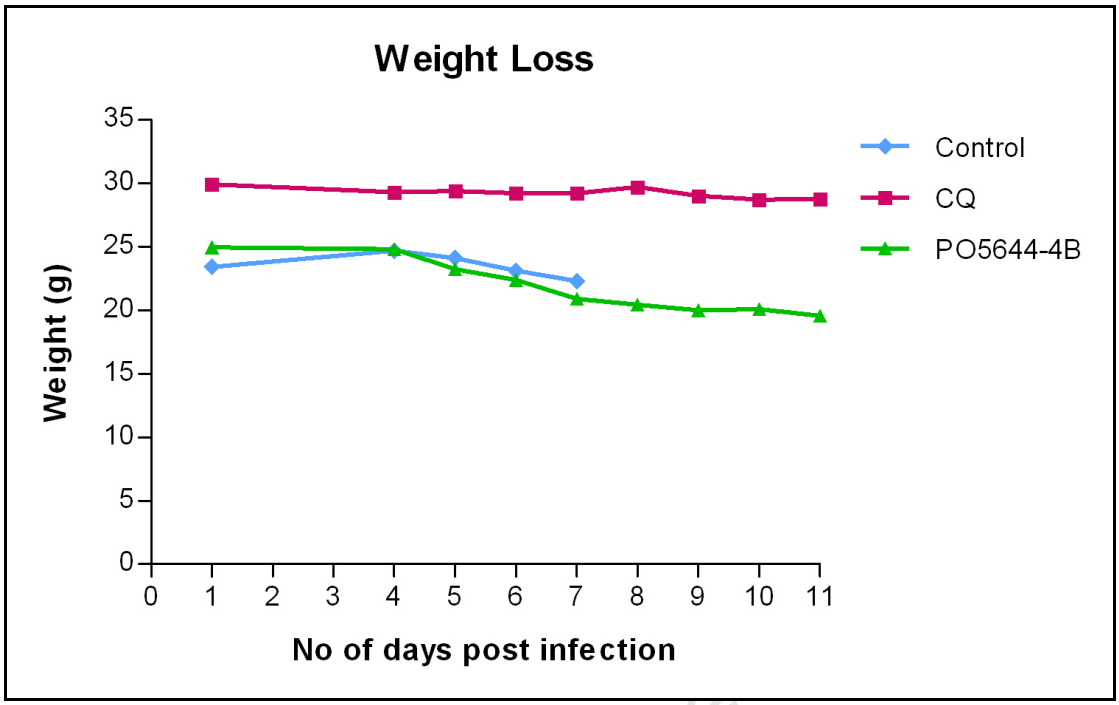

Figure 2.5 The weight loss of infected mice over time

Overall, the extract did not show good antimalarial activity due to the high parasitemia levels observed compared to chloroquine treatment. The efficacy of chloroquine is characterized by an almost immediate effect and a rapid reduction of parasitaemia. However, the semi-purified extract clearly prolonged the survival period of treated mice. The increased tolerance of high percentages of parasitemia in the blood indicates that the semi-purified extract could have either immune modulatory properties or some other kind of antimalarial effect (*viz.* parasite growth inhibition).

2.7 Bioassay-guided fractionation of P05644-5B

The first four recollections of *T. orientalis* twigs (Table 2.3) were relatively small scale (5 – 20 kg) and due to their low yields, bioassay-guided fractionation of extracts from these historical collections proved unsuccessful in identifying the active compounds.

A bulk recollection was subsequently undertaken in March 2006, followed by large scale extraction (to yield extract P05644-5B) and bioassay-guided fractionation (summarized in Figure 2.6). The purification, guided by results of previous

fractionation attempts, was based primarily on size-exclusion and reverse-phase chromatography to avoid considerable mass loss observed through silica gel chromatography.

The dichloromethane fraction **4B**, prepared by liquid/liquid partitioning (i) of the DCM/MeOH (1:1) extract, served to concentrate the actives in a less complex matrix. Purification of the dichloromethane fraction **4B** was initiated using vacuum liquid chromatography (VLC) (ii). Of the ten pooled fractions generated (**5A** - **5J**) only two (**5D** and **5E**) were found to retain biological activity and were combined and further purified by size-exclusion gel chromatography (iii). Four of the five fractions (**6A** – **6E**) subsequently generated showed improved biological activity but based on the results and yields only fraction **6D** was selected for further purification. Fraction **6D** was separated by reverse-phase solid phase extraction (SPE) (iv) and yielded 6 pooled fractions (**7A** – **7F**). Only fraction **7D** showed significant retention of biological activity and was further purified by reverse-phase semi-preparative HPLC (v).

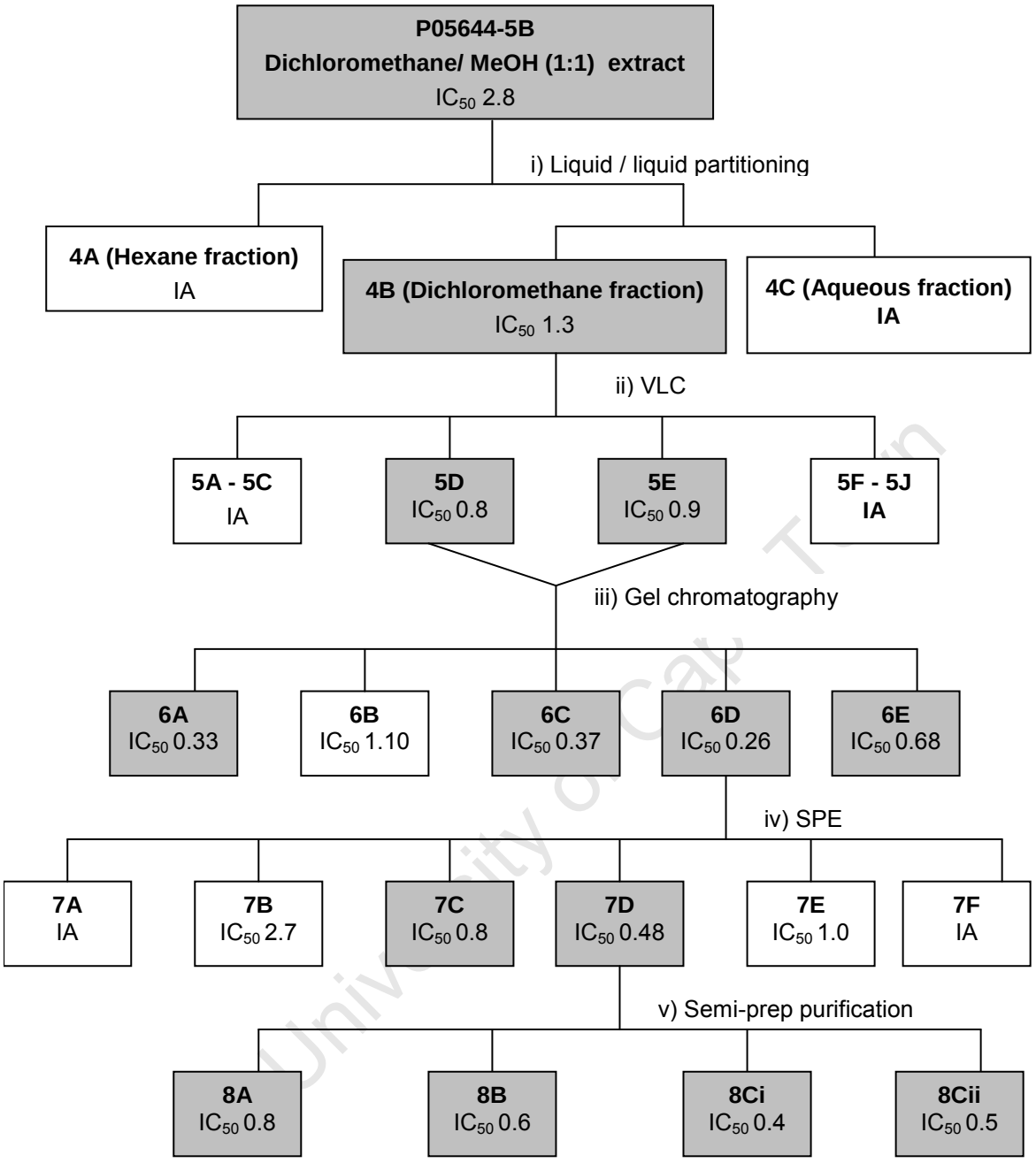

Figure 2.6 Bioassay-guided fractionation of PO5644-5B. IC_{50} values are in μg/ml. IA = Inactive at the maximum concentration tested (100 μg/ml)

Four fractions (**8A**, **8B**, **8Ci** and **8Cii**) were generated and all of these showed significant biological activity (< 1 μg/ml).

Preliminary TLC, ^{1}H NMR and MS analysis revealed that **8A** was a mixture of diastereomers; **8B** was a mixture of 3 – 4 compounds, while **8Ci** and **8Cii** were the partially separated diastereomers of a single compound. The HPLC separation of 7D to give the diastereomers **8Ci** and **8Cii** was not optimal as the NMR's of each showed traces of the other diastereomer. However; the NMR data of each diastereomer could be amply discerned for characterization.

2.8 Identification and Characterization of Compounds (8A), (8Ci) and (8Cii)

The mixture of the pair of diastereomeric compounds **8A**, and the partially separated diastereomers **8Ci** and **8Cii**, were identified and characterized by mass spectrometry (HR QTOF ESI-MS) and NMR experiments. The structural assignments of the compounds are based on detailed studies of the high-field ^{1}H and ^{13}C NMR spectral data (chemical shifts and coupling constants) and standard two-dimensional (2D) NMR techniques (Croasmun and Carlson, 1987; Sanders and Hunter, 1987).

The proton-proton connectivity patterns were established by 2D (^{1}H,^{1}H) correlation spectroscopy (COSY) experiments. The multiplicities of the different resonances in the ^{13}C spectra were deduced from the proton-decoupled CH, CH_2 and CH_3 subspectra obtained using the DEPT (distortionless enhancement by polarisation transfer) pulse sequence. The ^{13}C resonances were partly assigned by correlation of the proton-bearing carbon atoms with specific proton resonances in 2D (^{13}C,^{1}H) heteronuclear single quantum correlation (HSQC) experiments. The assignment of the quaternary carbon atoms and the deduction of the long-range (more than one bond) connectivity pattern was facilitated by 2D (^{13}C,^{1}H) heteronuclear multiple bond coherence (HMBC) experiments. Correlations observed in nuclear Overhauser enhanced spectroscopy (NOESY) experiments provided information on the relative stereochemistry of the compounds.

2.8.1 Structural Elucidation of Compound 8Cii

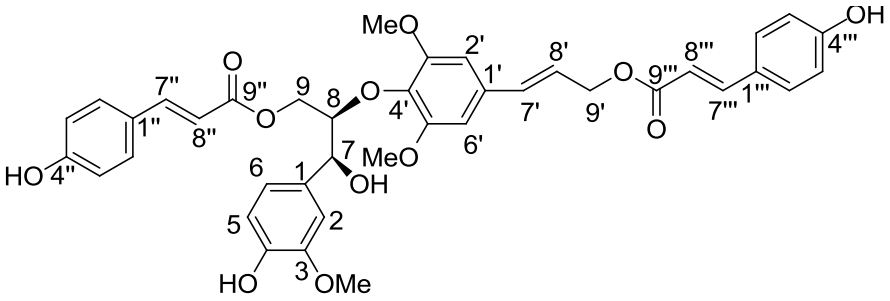

8Cii

Compound **8Cii** was isolated as a colorless gum. The ESI-MS showed a molecular ion with an m/z 697.2288 $[M-H]^-$ corresponding to an accurate mass of 698.2367 and allowing the molecular formula of **8Cii** to be deduced as $C_{39}H_{38}O_{12}$.

Resonances were concentrated in the downfield oxygenated (δ_H 3.7 – 5.0 ppm) and the olefinic regions (δ_H 6.2 – 7.7 ppm) of the ^1H NMR spectrum. Characteristic chemical shifts , splitting patterns and coupling constants identified two para substituted aromatic rings at δ_H 7.48 (2H, d, J = 8.8 Hz, H-2" and H-6"), δ_H 7.55 (2H, d, J = 8.8 Hz, H-2"' and H-6"') and δ_H 6.73 – 6.90 (H-3", H-5", H-3"' and H-5"'). Each ring was found to correlate to a *trans* double bond at δ_H 6.25 (H-8") and δ_H 6.38 (1H, H-8"'). The olefinic protons H-7" (δ_H 7.37) and H-7"' (δ_H 7.64) correlated to *α,β*-unsaturated carbonyls at δ_C 167.1 (C-9") and δ_C 167.3 (C-9"'); respectively. Also, two aromatic oxygenated carbons δ_C 160.9 (C-4" and C-4"') and δ_C 167.3 (C-9"') correlating to H-2" (and H-6") and H-2"' (and H-6"'); repectively, suggested that **8Cii** contained two 4-hydroxycinnamoyl groups.

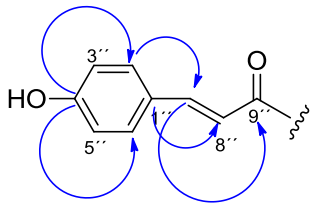

Figure 2.7 Major HMBC correlations categorizing 4-hydroxycinnamoyl fragment

Three methoxy groups (δ_C 56.1, 3-O<u>C</u>H$_3$ and δ_C 56.5, 3'-O<u>C</u>H$_3$ and 5'-O<u>C</u>H$_3$), two oxygenated methylenes (δ_C 65.1, C-9 and δ_C 65.0, C-9') and two oxygenated methines (δ_C 74.5, C-7 and δ_C 86.7, C-8) were found in the more upfield region of the ^{13}C NMR and DEPT spectra of **8Cii**. An additional two aromatic rings were also identified. Chemical shifts, splitting patterns and coupling constants of ring A were consistent with a 1,3,4-trisubstituted aromatic pattern. The methoxy groups were assigned on the basis of the HMBC correlations. The methoxyl at δ_H 3.79 (3H, s, 3-OC<u>H</u>$_3$) was found to correlate to C-3 (δ_C 148.0) while ring B was found to possess two methoxy groups (δ_H 3.86, 6H) attached to C-3' and C-5' (δ_C 153.9) in a symmetrical manner.

Further analysis of the ^{1}H, HSQC and ^{1}H-^{1}H COSY NMR spectra identified a third trans double bond at δ_H 6.68 (1H, br d, J = 15.9 Hz, H-7') and δ_H 6.39 (1H, dt, J = 15.9 Hz, 6.2 Hz, H-8') correlating to H-9' (δ_H 4.81). HMBC and COSY correlations were also observed between H-7 (δ_H 4.99), H-8 (δ_H 4.31) and the methylene protons H-9a (δ_H 4.44) and H-9b (δ_H 4.02). Based on this information and further HMBC correlations between H-7 and the aromatic carbon C-2 (δ_C 104.7) and between H-7' and the C-2' and C-6' (δ_C 111.4) aromatic carbons, it was evident that compound **8Cii** contained two C$_6$-C$_3$ units, linked by an ether bond between the oxygenated carbon, C-8 and the phenolic carbon, C-4' (δ_C 133.3), identifying it as a 8-*O*-4' neolignan derivative (Figure 2.8) (Agrawal and Thakur, 1985; Gellerstedt *et al*., 1995).

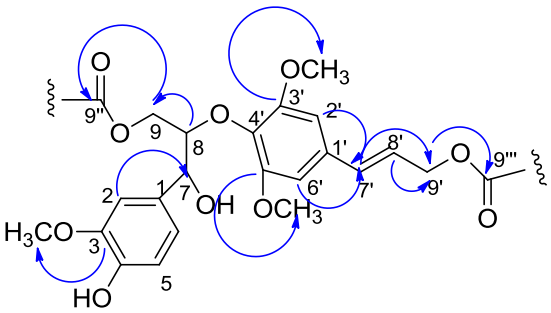

Figure 2.8 Major HMBC correlations identifying 8-*O*-4' neolignan core

Key HMBC correlations from H-9' to C-9''' (δ_C 167.3) and H-9 to C-9'' (δ_C 167.1) revealed that the two 4-hydroxycinnamoyl groups were attached to C-9 and C-9' as

esters. The coupling constant between H-7 and H-8 was 7.1 Hz, which suggested that the relative configuration between these two protons is *threo* (Zhong and Xian, 2003). Thus compound **8Cii** was structurally elucidated as *threo*-1-(4-hydroxy-3-methoxyphenyl)-2-[2,6-dimethoxy-4-{(1*E*)-3-(4-hydroxycinnamoyl)-1-propenyl}phenoxy]-3-(4-hydroxycinnamoyl)propan-1-ol.

2.8.2 Structural Elucidation of Compound 8Ci

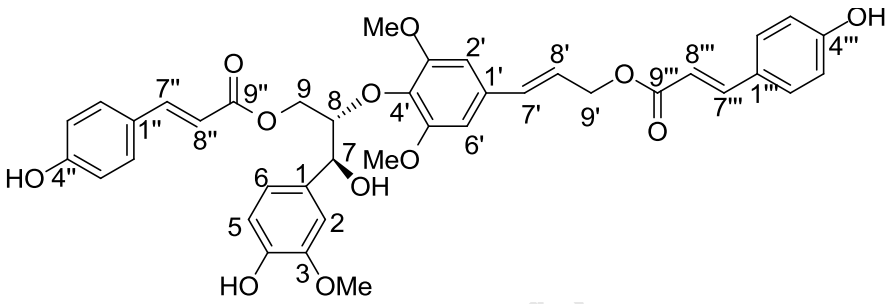

8Ci

Compound **8Ci** was also a colorless gum with essentially the same accurate mass (698.2384) and corresponding formula ($C_{39}H_{38}O_{12}$) as **8Cii**. The ^{1}H NMR spectrum of compound **8Ci** closely resembled that of **8Cii**. The most obvious difference was the chemical shift of H-8 (δ_H 4.58) and splitting pattern of H-7 (δ_H 4.97, 1H, br d, J = 3.3 Hz). The smaller coupling constant suggested that the relative configuration between H-7 and H-8 was erythro (Zhong and Xian, 2003). A thorough investigation of the ^{1}H, ^{13}C, HSQC, HMBC, COSY and NOESY experiments performed on this compound confirmed that **8Ci** was the *erythro* diastereomer of **8Cii** *i.e*. *erythro*-1-(4-hydroxy-3-methoxyphenyl)-2-[2,6-dimethoxy-4-{(1*E*)-3-(4-hydroxycinnamoyl)-1-propenyl}phenoxy]-3-(4-hydroxycinnamoyl)propan-1-ol.

2.8.3 Structural Elucidation of Compound 8A

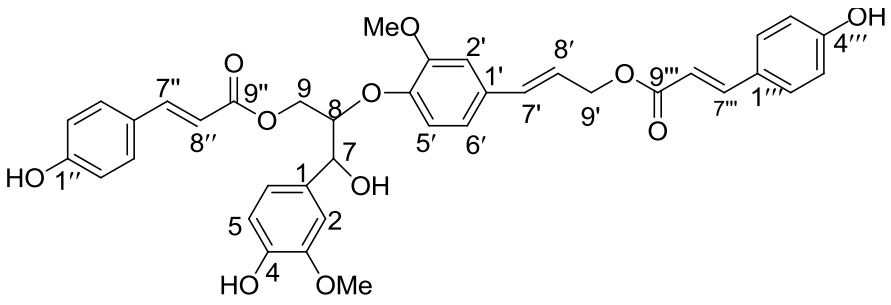

8A

Compound **8A**, also a colorless gum, showed a molecular ion peak with an m/z 667.2197 $[M-H]^-$ corresponding to an accurate mass of 668.2276 allowing the molecular formula to be deduced as $C_{38}H_{36}O_{11}$, one methoxy group less than that of **8C**. This was supported by the 1H and 13C NMR data of **8A** which revealed that this compound was also a 8-*O*-4' neolignan analogue, differing from **8C** only in the substituent pattern of ring B. NMR data of ring B in **8A** was consistent with a 1,3,4-trisubstituted aromatic ring, confirming that only one methoxy group was attached to C-3'.

The undisputed doubling of resonances in the ^{1}H and ^{13}C NMR spectra of **8A**, especially the well resolved characteristic signals of C-7 (δ_C 73.3 and 73.8) and C-8 (δ_C 83.4 and 84.1), confirmed that **8A** was a mixture of *threo* and *erythro* isomers (in approximate 1:1 ratio).

Therefore, compound **8A** was identified as a mixture of *threo*- and *erythro* -1-(4-hydroxy-3-methoxyphenyl)-2-[2-methoxy-4-{(1*E*)-3-(4-hydroxycinnamoyl)-1-propenyl}phenoxy]-3-(4-hydroxycinnamoyl)propan-1-ol.

The natural product could not be further resolved and NMR assignments of the two diastereomers was deferred till the compound could be diastereoselectively synthesized (Chapter 3).

2.9 Characterization of Compounds 8A and 8C

A literature search revealed that compounds **8C** and **8A** were previously isolated from the twigs of the Indonesian tree, *Artocarpus dadah* and were subsequently named dadahol **A** and **B**; respectively (Su *et al*., 2002). In this previous report, the authors had transposed the NMR signals of the 9- and 9′-coumaroyl groups. These were unambiguously assigned here due to access to 2D NMR data, as well as NMR data of the respective monoesters synthesized in Chapter 3.

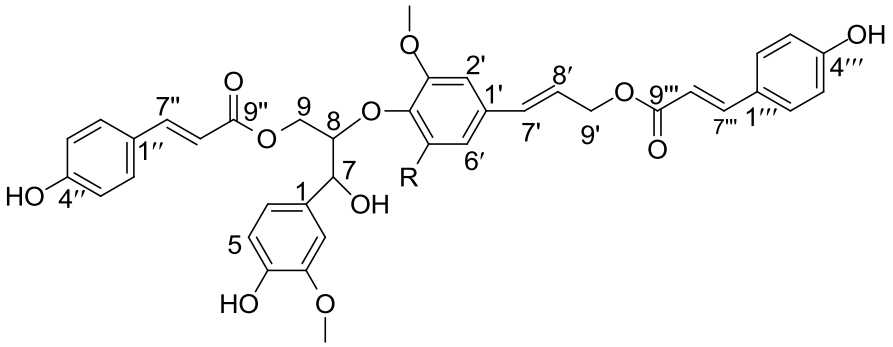

8C R = OMe; Dadahol A
8A R = H; Dadahol B

Although this is the first report of their isolation from *T. orientalis* twigs it is not an unexpected result as lignans and neolignans are the structural units of lignoid polymers (lignin) which occur in woody plants. They are characterized by the common constitutional feature of two C_6-C_3 (*n*-propylbenzene) residues (Figure 2.9) (Haworth, 1942). For nomenclature purposes, the C_6-C_3 is numbered from 1 to 6 in the ring, starting from the propyl group, and the propyl group numbered from 7 (or α) to 9 (or γ), starting from the benzene ring. The numbers are primed in the second C_6-C_3 unit.

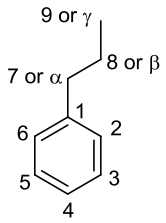

Figure 2.8 Two common ways of labeling the carbon atoms in *n*-propylbenzene residue of lignans

When the two units are linked by a bond between the central (8 and 8´) carbon atoms, the compound is referred to as a lignin. The lignans can be divided into six subgroups, based on general structures (Figure 2.9).

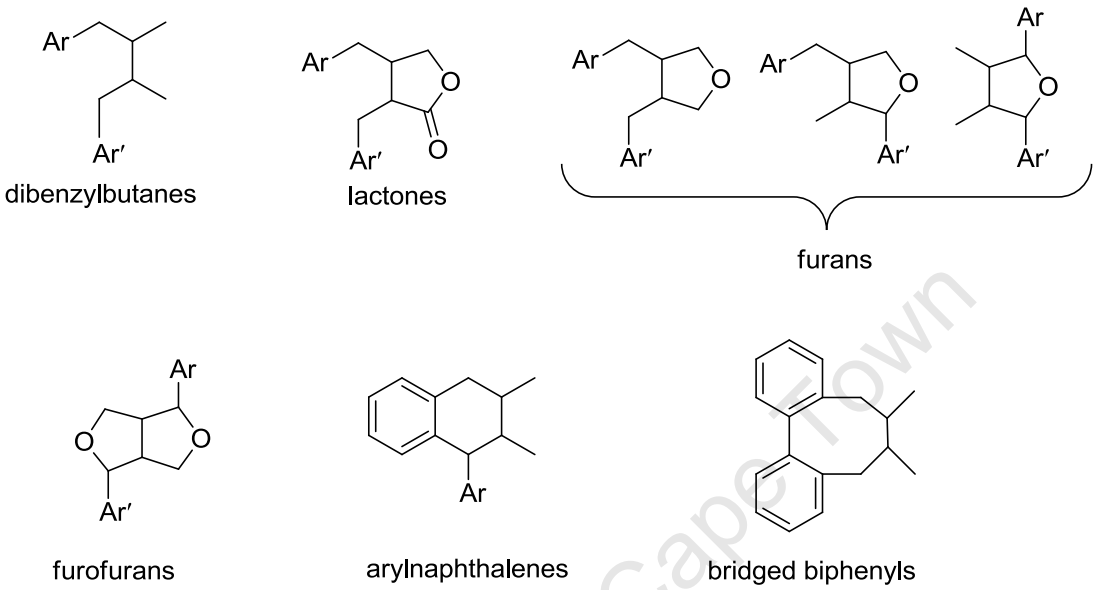

Figure 2.9 Lignin types

The term neolignans is used in the absence of the C-8 and C-8´ (*β*-*β*) bond, where the C_6-C_3 units are linked by another carbon-carbon bond. And when there are no direct carbon-carbon bonds between the C_6-C_3 units and they are instead linked by an ether oxygen atom, as in dadahols A and B, the term oxyneolignan is used (Moss, 2000). There are more that fifteen subgroups of neolignans; these are most readily designated by specifying the points of union between the C_6-C_3 units (Whiting, 1985). The two phenylpropanoid units of dadahols A and B are linked via C-8 of the first unit and the oxygen of the hydroxyl substituent at C-4´ in the second unit, therefore further characterizing them as 8-*O*-4´ (or *β*-*O*-4) oxyneolignans (Agrawal and Thakur, 1985; Gellerstedt *et al*., 1995).

Lignans and neolignans show enormous structural diversity, varying substantially in oxidation level, substitution pattern and the chemical structure of their basic carbon framework. The aryl moieties of these phenylpropane dimers are primarily substituted

with hydroxyl (phenolic) or their corresponding methyl ethers and methylene dioxy functionalities (Jensen *et al*., 1993). 3-Methoxy-4-hydroxyphenyl (guaiacyl), 3,4-dimethoxyphenyl (veratryl), 3,5-dimethoxy-4-hydroxyphenyl (syringyl) 3,4,5-trimethoxyphenyl and 3,4-methylenedioxyphenyl (piperonyl) (Figure 2.10) are the most commonly occurring aromatic rings found in lignans (Umezawa, 2003). The neolignan core of dadahol B is composed of two guaiacyl rings while in dadahol A the B ring is syringyl.

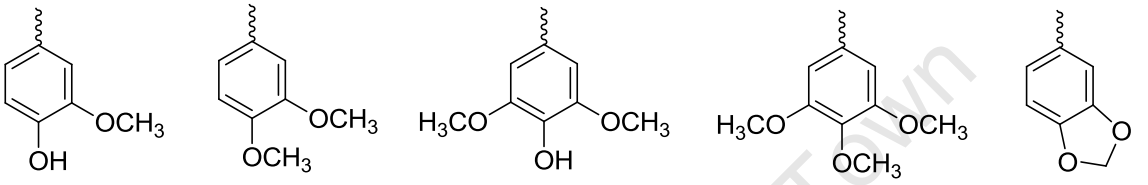

Figure 2.10 Principal aromatic structures of lignans

Two cinnamic acid residues are attached to the terminal hydroxyls of the oxyneolignan core of dadahols A and B as 4-hydroxycinnamoyl (*p*-coumaroyl) groups. *p*-Coumaric acid is a precursor in the lignan biosynthetic pathway.

The presence of two chiral carbons (C-7 and C-8) in dadahols A and B implies that two possible diastereomers, *erythro* and *threo*, can be present. With the possibility of free rotation around the C-7 and C-8 bond, it is difficult to determine the stereochemistry of such units and there appears to be no straightforward guideline. According to Zhong and Xian (2003) the relative stereochemistry between C-7 and C-8 should be in the *erythro* form if the coupling constant between them measured by ^{1}H NMR is small (J = 2.7 – 5.0 Hz). If the coupling constant measured is larger (J = 6.0 – 8.6 Hz), the configuration is in the *threo* form. Although there appears to be some confusion and contradicting reports in literature regarding the determination of *threo* and *erythro* stereochemistry, published data for *erythro* dadahol A (Su *et al.*, 2002) and similar 8-*O*-4´oxyneolignans (Seca *et al*., 2001; Paula *et al*., 1995) substantiated the observations of Zhong and Xian (2003), therefore this guideline was used to determine the relative stereochemistry of the dadahol A diastereomers (**8Ci**

and **8Cii**). Ideally, X-ray crystallography would have been the best approach to confirming the relative stereochemistry of the natural products but unfortunately crystallization attempts were unsuccessful.

As plant metabolites often exist as part of a family of related compounds it is likely that other less active neolignan analogues were also present in the *T. orientalis* extract. Several other fractions (*viz*. **6A**, **6D**, **6E** and **7C** in Figure 2.6) showed considerable activity but the further fractionation of these were not pursued as the bioassay-guided fractionation process employed focused on the identification of the major active compounds. These fractions could contain analogues of dadahols A and B, which contribute to the activity of the crude extract. Fraction **8B** (Figure 2.6) provided evidence of this. It was found to be an inseparable mixture of at least 3 minor compounds with similar R*f*'s, NMR and MS profiles to **8A** and **8C**. Dadahols A and B were subsequently recognized as major components of the semi-purified extract, P05644-4B (Appendix I), which increased tolerance of *P. berghei* infected mice to high percentages of parasitemia (Section 2.6).

2.10 Classical versus Accelerated Bioassay-guided Fractionation Approach

The bioassay-guided fractionation approach that was used to identify the active compounds, **8A** and **8C**, is regarded as classical bioassay-guided fractionation. Basically, this entailed the bioassaying of the crude plant extract in a primary screen, followed by a purification process whereby the active extract underwent iterative steps of activity-guided fractionation to identify the active compounds. For *T. orientalis*, this entire process spanned over 2-3 years, requiring numerous recollections, bulk extractions and fractionation steps (Figure 2.1 and Figure 2.6).

The classical approach of bioassay-guided fractionation to target the active constituents is not only time consuming, but often leads to the re-discovery of known compounds, and loss of activity in the course of the purification is not uncommon as the process may neglect interesting compounds with minor biological activity. These secondary active compounds discarded during the traditional approach may

contribute to the overall activity of the extracts and present interesting chemical scaffolds that could make them preferential candidates for their chemical optimisation (hit-to-lead and lead-optimisation) into therapeutic candidates.

Transformations in the drug discovery process over the last decade have stimulated new requirements for natural product research and more targeted approaches are being adopted in order to identify promising candidate molecules upfront and accelerate the development process (Fura *et al*., 2004; Potterat and Hamburger, 2006). An accelerated natural product drug discovery process, based on the "HPLC biogram" approach (Shu *et al*., 2002), was recently implemented at CSIR Biosciences. The approach is based on rapid bioassay-guided plant metabolite detection and characterization - a schematic illustration of the "HPLC biogram" method is shown in Figure 2.11.

Plant extracts are separated by semi-preparative HPLC and fractions are collected into 96-well plates. The fractions are subjected to one or more relevant bioassays (on-line or off-line). Fraction collection is time based, resulting in a direct relationship between the well's position in the plate and a corresponding region on the HPLC chromatogram. This allows assignment of activity to a particular component or range of components of the mixture. The active peaks are correlated back to HPLC/UV/MS profiles and followed up with UV/MS spectral analysis for structure characterization.

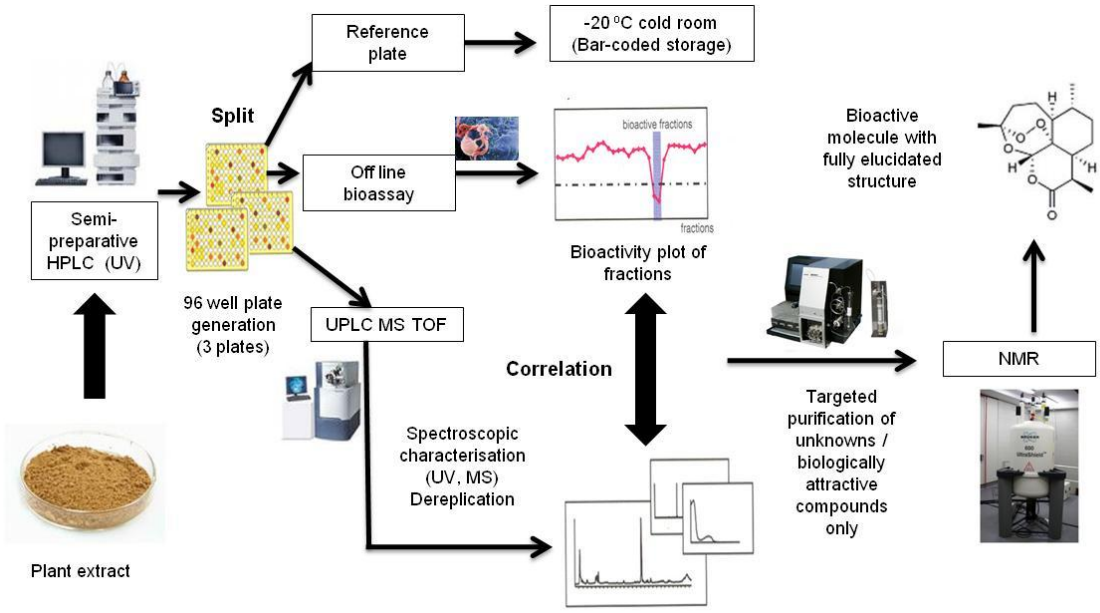

Figure 2.11 "HPLC biogram" approach

When applied to the discovery of bioactive natural products, the "biogram" methodology allows for early recognition of active compounds in complex plant extracts in a rapid and efficient manner while minimizing time and effort spent on inactive, known or otherwise uninteresting compounds. It therefore facilitates decision-making in initiating re-isolation or scale-up of active compounds for full structural and biological evaluation. If the bioassay employed is robust and as sensitive as the analytical method, both with a good "signal/noise" ratio, the "biogram" method can provide rapid and efficient detection and characterization of very minor bioactive compounds, previously undetected by other physical methods.

T. orientalis was included as part of the validation process, in order to compare the time frame and actives identified via the "HPLC biogram" approach to that of the historical approach. The dichloromethane fraction (**4B**; Figure 2.6) obtained through liquid-liquid partitioning of the *T. orientalis* crude extract (P05644-5B) was fractionated into a 96-well microtitre plate using semi-preparative HPLC. The selection of the dichloromethane fraction (**4B**) for the 96-well plate fractionation was based on the enriched antiplasmodial activity (*cf.* Section 2.7) and lack of fatty acids and tannins (*cf.* Section 2.4) in this semi-purified extract relative to the crude extract.

The semi-purified extract, **4B**, and 96-well plate were subjected to *in vitro* bioassays at the Swiss Tropical and Public Health Institute (Swiss TPH) against the various micro-organisms responsible for the so-called 'neglected' diseases *i.e. Trypanosoma brucei rhodesiense*, *Trypanosoma cruzi, P. falciparum* and *Leishmania donovani*. Cytotoxicity was also evaluated using rat skeletal myoblast (L-6) cells. In a pre-screen, the extract showed selective activity against a chloroquine-resistant (K1) *P. falciparum* strain (Table 2.4).

Table 2.4 Activity and cytotoxicity of *T. orientalis* extract (IC_{50}'s in µg/ml)

Organism/ Cell line	*T.b. rhodesiense*	*T. cruzi*	*L. donovani*	*P. falciparum* K1	Cytotoxicity L6
Melarsoprol	0.004				
Benznidazole		0.314			
Miltefosine			0.175		
Chloroquine				0.07	
Podophyllotoxin					0.004
T. orientalis semi-purified extract (**4B**)	10.24	18.72	8.32	1.54	29.41

The 96-well plate fractions were subsequently bioassayed against *P. falciparum* K1 at two concentrations, 4.8 and 0.8 µg/ml (See Appendix III) using the ^{3}H-hypoxanthine incorporation assay. Wells which showed more than 50% inhibition of the parasite at the lower concentration were considered active. The activity profile at 0.8 µg/ml is depicted in Figure 2.12 and shows that there were three active regions, wells A1 – A4, wells C6 – E4 and well G7.

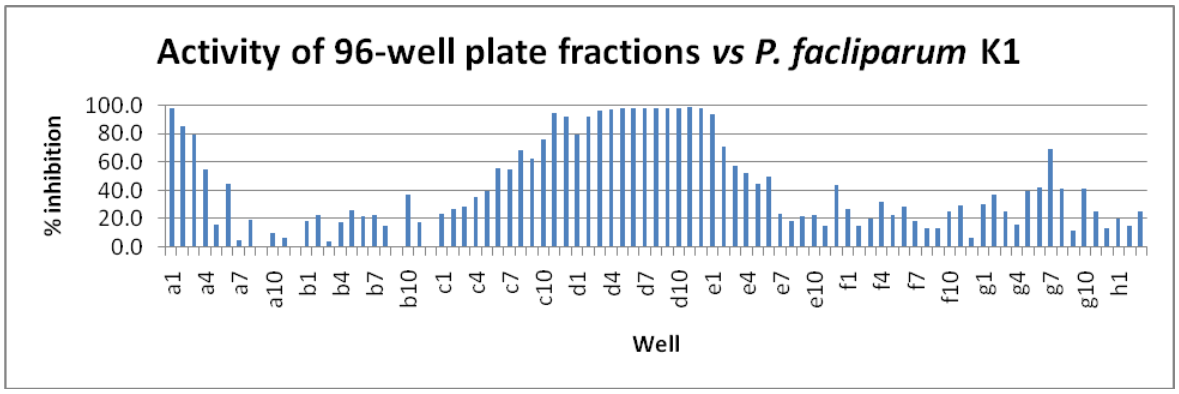

Figure 2.12 Activity profile of 96-well plate fractions at 0.8 µg/ml

IC_{50} values were determined for these wells (Figure 2.13). They were also evaluated for toxicity to L6 cells (Appendix III).

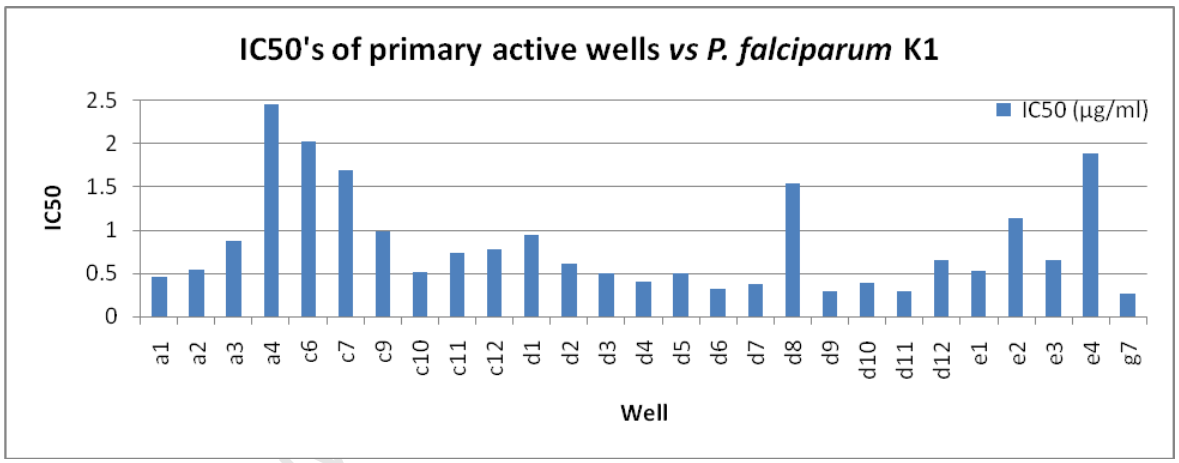

Figure 2.13 Plot of IC_{50} values in µg/ml

Based on the serial dilution assay eight wells showed IC_{50} values less than 0.5 µg/ml with selectivity indices (SI, ratio of cytotoxicity to antiplasmodial activity) greater than 10 (Table 2.5).

Table 2.5 Summary of activity and cytotoxicity of most active fractions

Fraction/ Well	*P. falciparum* K1 IC_{50} (ug/ml)	Cytotoxicity L6 IC_{50} (ug/ml)	SI
A1	0.459	5.19	11.3
D4	0.403	4.83	12.0
D6	0.324	3.32	10.2
D7	0.374	9.1	24.3
D9	0.296	10.7	36.1
D10	0.381	8.9	23.4
D11	0.286	9.1	31.8
G7	0.256	8.5	33.2

The corresponding wells of a duplicate plate were analysed by UPLC-TOF-MS and bioactivity was correlated with the spectral data of the well components. In order to determine if the active wells contained the same or a common region/compound their Base Peak Intensity (BPI) (negative mode) chromatograms were compared (Appendix IV). The chromatograms showed that wells D4-D7 and D9-D11 were identical. Well G7, which had the lowest IC_{50}, was found to be an unresolved mixture of weakly UV-active apolar compounds that eluted during the column wash, and was subsequently not further analysed. One representative well from each of the other regions was analyzed in more detail and major peaks occurring in both the BPI (ES-) and UV chromatograms were identified (Figure 2.14).

Accurate mass and UV maxima data for each of these peaks were then used to search the Dictionary of Natural Products (DNP) database (Chapman & Hall, 2010) for possible structures (Appendix V).

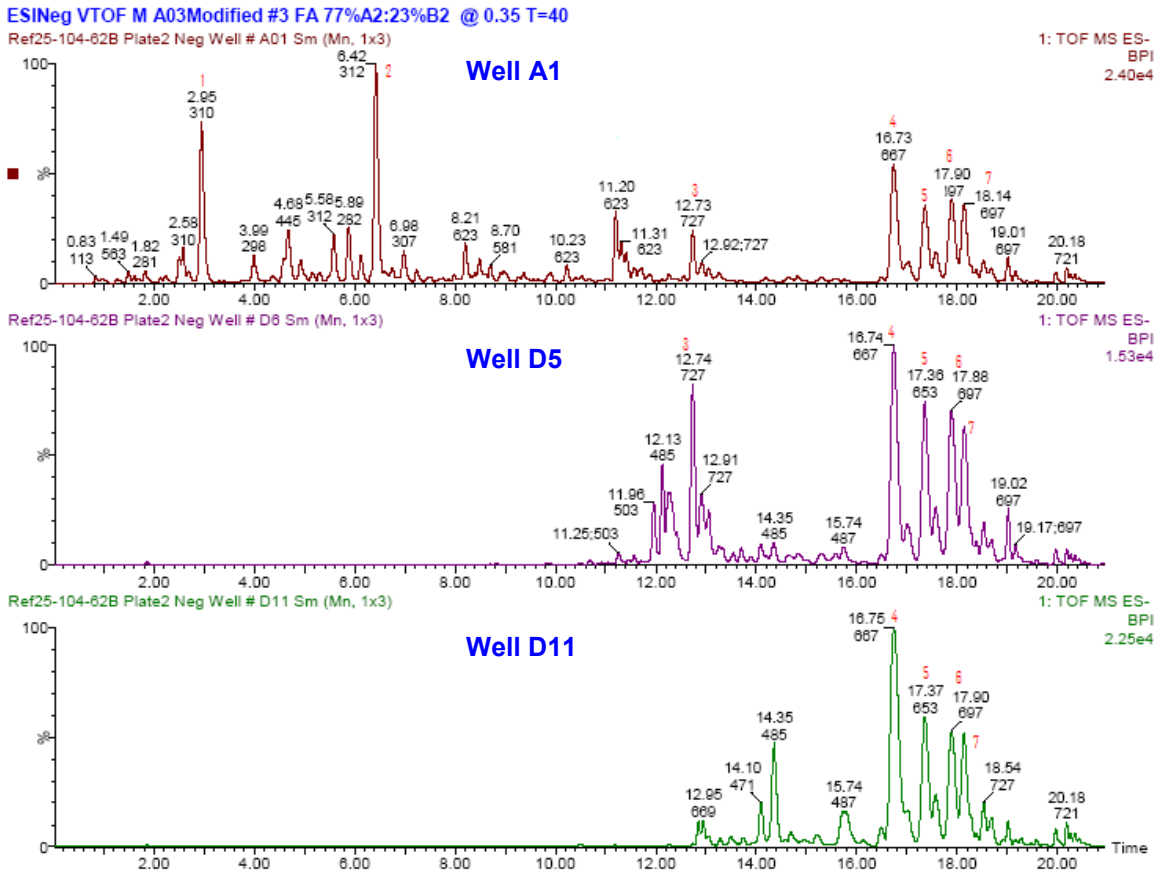

Figure 2.14 ES- BPI chromatograms of representative active wells

Peak 1, with a retention time (rt) of 2.93 min, showed a molecular ion with an m/z 328.1166 $[M-H]^-$ corresponding to an accurate mass of 329.12454 and UV maxima peaks at 220 and 318 nm. A search on DNP based on the accurate MS and UV data of this compound identified the possible structure of this compound as *N*-trans-feruloyl-*S*-octopamine, a close analogue of *N*-(trans-*p*-coumaryl)-octopamin **(36)** which has been previously isolated from *T. orientalis* (Kuo *et al*., 2007).

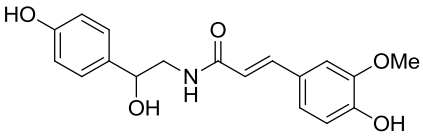

N-trans-Feruloyl-*S*-octopamine

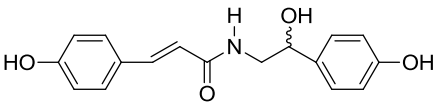

(36) N-trans-*p*-coumaryl)-octopomin

A DNP search based on the accurate mass (313.1284) and UV maxima (219 and 318 nm) of peak 2 (rt 6.42 min) resulted in two possible alkaloid structures; Cassiarine B

or *N*-trans-Caffeoyl-*O*-methyltyramine; the latter compound being the more obvious choice due to its structural relation to alkaloids previously isolated from *T. orientalis* (Kuo *et al*., 2007).

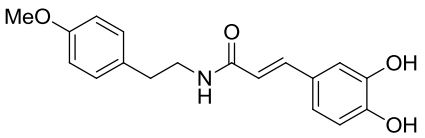

N-trans-Caffeoyl-*O*-methyltyramine

Peak 4 (rt 16.74), showing a molecular ion with an m/z 667.2184 $[M-H]^-$ corresponding to an accurate mass of 668.22634 and UV maxima peaks at 222 and 310 nm, resulted in just one hit in the DNP search *i.e*. dadahol B. Peaks 6 and 7 had almost identical accurate mass (697.23944 and 697.23844; respectively) and UV maxima (222, 310 and 223, 310 nm; respectively) and searches using this data revealed that these two peaks most likely corresponded to the two diastereomers of dadahol A. The tentative identification of peaks 4, 6 and 7 was confirmed by comparison of their retention times with those of dadahol A and B standards using the same UPLC analytical method.

No possible hit structures were obtained based on the accurate mass and UV maxima of peak 3 (rt 12.73 min) and peak 5 (rt 17.38 min). However, based on their similar rt's, MS and UV maxima profiles to peaks 4, 6 and 7 it is likely that these compounds are closely related to dadahols A and B. Peak 3 with an accurate mass of 728.25004 correlates to a possible analogue of dadahol A, which has an additional methoxy substituent (Exact mass calculated for $C_{40}H_{40}O_{13}$: 728.25). Similarly, the accurate mass of peak 5 (654.24754) suggests that it could be an analogue of dadahol B, where one of the methoxy substituents is replaced with a hydroxyl (Exact mass calculated for $C_{37}H_{34}O_{11}$: 654.21). There are several other minor peaks with similar MS and UV profiles in the regions of peaks 3 – 7 that are also likely to be analogues of dadahols A and B with different substituent patterns.

Peaks 4 -7 were relatively major compounds common to all the active wells and the spread of this over the 96 well plate suggests that the separation was not ideal due to

column overload and that there might have been some carry-over of the actives between successive runs due to insufficient washing of the column between runs. However, the 96-well microtiter fractionation approach not only confirmed dadahol A and B as the major bioactives, but also served to identify other possible compounds which might be contributing to the overall activity of the extract. This physio-chemical process was achieved with a few hundred mg of extract over a couple of months as opposed to the classical bioassay-guided fractionation approach which required bulk recollections and took at least two years to identify the actives.

The accelerated approach therefore represents a highly suitable tool for the identification of biologically attractive molecules and the profiling of extracts with pharmacological potential. The limitations of this approach lies in the facts that it is more suited to the dereplication of known compounds with published accurate mass and UV maxima data and is dependent on access to regularly updated electronic databases. In that respect, the “HPLC biogram” approach cannot fully replace the traditional bioassay-guided fractionation approach.

CHAPTER 3

Diastereoselective Synthesis of Dadahol B

3.1 Monolignol Biosynthesis

Monolignols are monomeric phenolic compounds with a phenylpropane carbon skeleton, derived from the aromatic amino acid phenylalanine. The aromatic amino acids (L-phenylalanine, L-tyrosine and L-tryptophan) are synthesized from the carbohydrate precursors *D*-erythrose-4-phosphate (derived from the pentose phosphate pathway) and phosphoenolpyruvate (from glycolysis) via shikimic acid (Ganem, 1978; Haslam, 1974).

Several other major classes of plant metabolites are derived from phenylalanine, including flavanoids, coumarins, stilbenes and benzoic acid derivatives (Dixon and Paiva, 1995). The initial steps in the biosynthesis of all these compounds are shared through the phenylpropanoid pathway.

Lignin biosynthesis begins in the cytosol with the synthesis of monolignols from the amino acid phenylalanine as outlined in Scheme 3.1 (Boudet and Grima-Pettenati, 1996; Campbell and Sederoff, 1996; Whetten and Sederoff, 1995). As the first step, phenylalanine (**a**) is deaminated to yield cinnamic acid (**b**) by the action of phenylalanine ammonia-lyase (PAL) (**1**). Cinnamic acid is hydroxylated to *p*-coumaric acid (**c**) by cinnamate-4-hydroxylase (C4H) (**2**), a cytochrome P-450-linked monooxygenase. *p*-Coumaric acid is in turn activated to *p*-coumaroyl-coenzyme A (CoA) (**d**) by *p*-coumarate-CoA ligase (4CL) (**6**). The activated thioester is the precursor for the synthesis of flavanoids, stilbenes and other phenylpropanoids as well as the monlignol *p*-coumaryl alcohol (**f**).

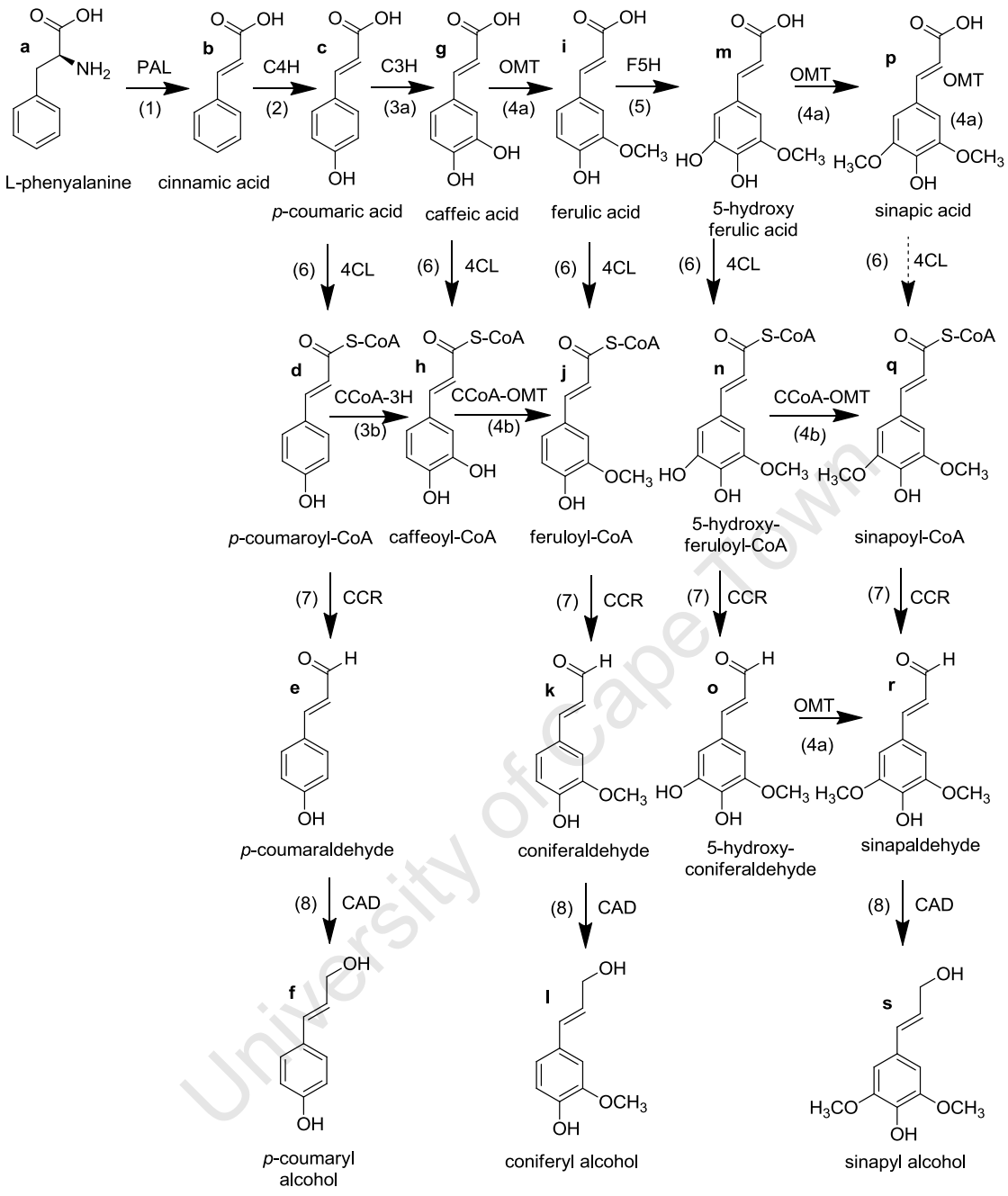

Scheme 3.1 Overview of the monolignol biosynthetic pathway

p-Coumaric acid and *p*-coumaroyl-CoA can both be hydroxylated at the 3 position to yield caffeic acid (**g**) and caffeoyl-CoA (**h**), respectively, but the responsible enzymes (**3a** and **3b**) are not well studied. The newly added hydroxyl group can be methylated by *O*-methyltransferase (OMT) (**4a** or **4b**) to

give ferulic acid (**i**) or feruloyl-CoA (**j**) Caffeic acid and ferulic acid can be activated to their corresponding CoA thioesters by 4CL (**6**).

Ferulic acid can be hydroxylated by ferulate 5-hydroxylase (F5H) (**5**), another P-450-linked monooxygenase, to yield 5-hydroxyferulic acid (**m**), which is also a substrate for 4CL. The 5-hydroxyferulic acid can be methylated by OMT (**4a**) to produce sinapic acid (**p**). The corresponding methylation of 5-hydroxyferuloyl-CoA to sinapoyl-CoA has also been described and is most likely catalysed by caffeoyl-CoA 3-O-methyltransferase (CCoA-OMT) (**4b**). Activation of sinapic acid to sinapoyl-CoA is possible but occurs ineffectively in most plants tested.

Reduction of the CoA thioesters to the corresponding aldehydes is catalysed by cinnamoyl-CoA reductase (CCR) (**7**). Caffeoyl aldehyde is not shown as it has no known physiological role. Further reduction of the aldehydes by cinnamyl alcohol dehydrogenase (CAD) (**8**) yields the three monolignol monomers: *p*-coumaryl alcohol (**f**), coniferyl alcohol (**l**) and sinapyl alcohol (**s**).

The order in which hydroxylation, methylation, thioactivation and reduction reactions occur during monolignol synthesis may vary at one or more levels, although the extent and physiological significance of this variation are unclear.

The monolignols *p*-coumaryl alcohol, coniferyl alcohol and sinapyl alcohol are relatively toxic and unstable. Glycosylation on the phenolic hydroxyl group yields the monolignol glucosides 4-hydroxycinnamyl alcohol glucoside, coniferin and syringin, respectively. The attached glucose renders them water soluble and less toxic. Once transported through the cell membrane to the apoplast, *β*-glucosidase releases the three alcohols from their glucosides and makes them available for further processing by phenol dehydrogenases (oxidative enzymes) (Freudenberg, 1965).

3.2 Oxidative Coupling of Monolignols: Dehydrodimerisation

The dimeric lignans (homodimers), dilignols (heterodimers) and the structural units in polymeric lignin are formed by the so-called oxidative coupling reaction of monolignols. There are three modes of coupling mechanisms in pteridophytes and woody gymnosperms/angiosperms, each having evolutionary significance (Lewis and Davin, 1994). The first involves monolignol oxidations catalysed by H_2O_2-dependent peroxidases to yield lignan dimers. Woody plants also contain laccases, O_2-dependent oxidases containing four copper atoms, which catalyse the coupling of coniferyl/sinapyl alcohols to give racemic (neo)lignans. In contrast, optically active lignans are formed by stereoselective coupling catalysed by more specific weakly characterized O_2-requiring oxidases.

Dehydrodimerisation is based on the oxidative coupling of monolignols where two phenoxy radicals are first generated in a one-electron oxidation reaction by an oxidant system such as peroxidases/H_2O_2, where peroxidase is a catalyzing enzyme and H_2O_2 is an oxidant (Setälä, 2008). The oxidant penetrates into the active site of the enzyme forming an activated enzyme which is capable of oxidising a substrate. The monolignol penetrates into the active site of the enzyme to form a monolignol-enzyme complex. The ratio and availability of monolignols in the reaction side of the cell wall together with oxidizing enzymes are important factors. The relative reactivities (redox potentials) of the monolignols are important in cross-coupling reactions (heterodimerisation) (Syrjänen and Brunow, 1998).

The postulated dehydrogenation and one-electron oxidation of the monolignol monomer generates phenoxyradicals. Delocalization of the unpaired electron spin density over the aromatic and double bond ring system of the phenoxy radical, gives several resonance forms and positions that can react with each other (Scheme 3.2).

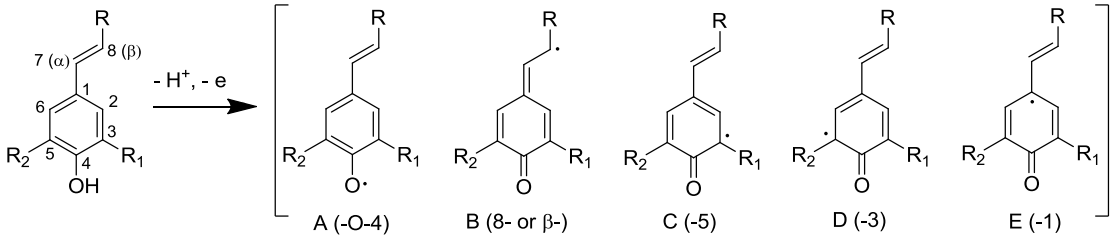

Scheme 3.2 Resonance forms (A-E) of a phenoxy radical

3.2.1 Regioselectivity in Phenoxy Radical Coupling

Two phenoxy radicals subsequently couple to form quinone methide intermediates. How the radicals are initially coupled, which reaction route is selected and the ratio of possible dimeric products are primarily dependent on the stereoelectronic effects related to the structure of the phenoxy radical, but the catalyst/oxidant system and reaction conditions can also have significant effects.

The different kinds of C-C or C-O bonds formed when one phenoxyradical couples to another are represented in Scheme 3.3. The *β*-*β*, *β*-5 and *β*-*O*-4 couplings are the most common in lignan and lignin structures. The 4-*O*-5' (A + C) and 5-5' (C + C) couplings are only possible if there are no substituents in the C-5 (and/or C3) position of the aromatic ring and are most likely to occur if there is no *β*-radical coupling possibility. *β*-1 (8-1') (B + E) coupling is possible if there is no *β*-radical coupling possibility in another phenoxy radical forming compound and more likely if the C-3 and/or C-5 positions in the aromatic ring are blocked. Other coupling products have not been observed most likely due to instability or steric hindrance.

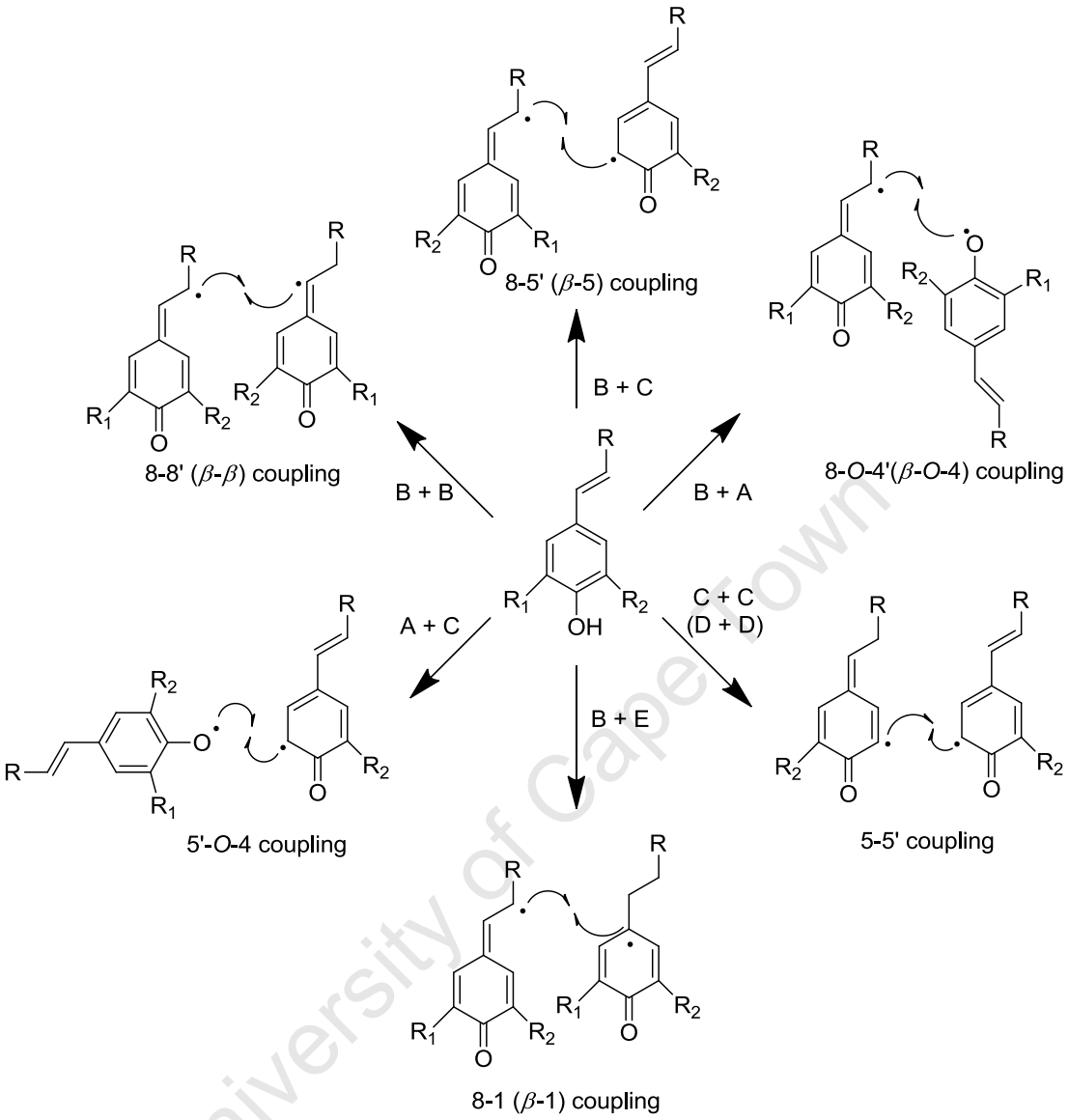

Scheme 3.3 Possible coupling of resonance stabilized phenoxy radicals generated from 4-hydroxy monolignols

Factors which control the formation of various dimeric products have been studied using molecular dynamic calculations (Elder and Ede, 1995), semi-empirical molecular orbital calculations (Shigematsu *et al*., 2006, Elder and Worley, 1984), density functional theory (Durbeej and Eriksson, 2003b, Durbeej and Eriksson, 2003a) and computational and simulation methods (Houtman, 1999, Russell *et al*., 1996).

Kinetic arguments were used to explain the product distribution in the case of coniferyl alcohol. Tereshima and Atalla (1995) studied pH effects and measured the product distribution of coniferyl alcohol dimers and oligomers in various water/diglyme mixtures. Based on this and molecular dynamic (MD) calculations Houtman (1999) proposed a mechanism by which the solvent environment determines the product distribution of dimers. In water the coniferyl alcohol radicals are not free to adopt all possible orientations, resulting in a modified product distribution ratio since the outcome is most likely determined by the relative orientations of the molecules at the moment the orbitals of two centers of unpaired spin density overlap. In contrast, the relative orientations of the molecules seem to be freer in glycerol, and thus the product distribution is more comparable to that predicted from a statistical analysis of the probability of forming each product, assuming an equal likelihood of each relative orientation.

Phenoxy radicals are assumed to initially form π-complexes that have to be superimposed in a way that enables the maximum overlapping of single-occupied molecular orbitals (SOMO) while the stereoelectronic repulsions of substituents on the aromatic ring and C_3-side chain have to be minimized (Setälä, 2008). The different configurations of the intermediate π-complexes may also play a significant role in the regioselectivity of phenol oxidative coupling reactions. The π-complexes (sandwich model) lead to the σ-complexes (quinone methide intermediates) resulting in transition states (Chioccara *et al*., 1993). The quinone methides may be in equilibrium with the π-complexes or each other (Scheme 3.4).

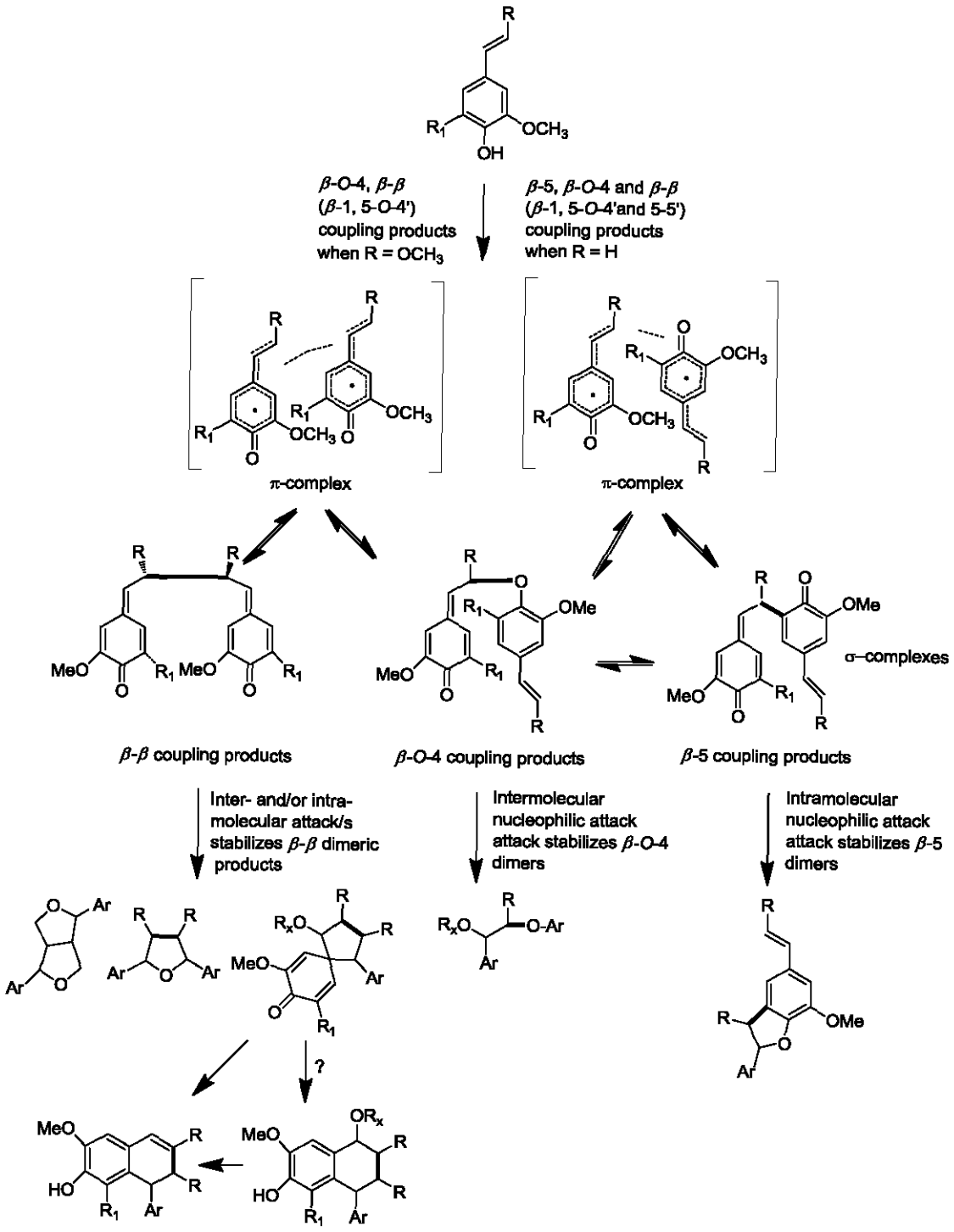

Scheme 3.4 Possible phenoxy radical coupling routes and mechanisms to different structures

The stabilisation of the α-carbon in quinone methide intermediates by the addition of nucleophiles (R_x-OH) is essentially also a reversible reaction, and competes with the intramolecular nucleophilic attack. It depends on the nature and availability of nucleophiles in the reaction matrix, on the structure of the quinone methide, on the solvent system (solvolysis, H-bonding, and bulk effects) as well as the type of catalysis (*viz*. acid or base catalysed, pH dependence, solvent catalysis) (Setälä, 2008).

The quinone methides are electrophilic in nature and good Michael acceptors allowing nucleophiles to be readily added under mild conditions to the quinone methide exocyclic methylene group to form benzylic adducts. The formation and subsequent reactions of quinone methides are highly dependent on the presence of electron-withdrawing and –donating groups in the aromatic ring: electron-donating groups promote initial quinone methide generation and electron-rich groups lead to slower but more selective reaction with nucleophiles (Weinert *et al*., 2006). Nucleophilic addition to a quinone methide can be an intramolecular attack of a substituent on the dimeric intermediate (such as in the formation of *β*- dimers), or an attack by other nucleophiles existing in the reaction matrix (*viz*. stabilization of *β*-*O*-4 dimers).

3.2.2 Stereoselectivity in Phenoxy Radical Coupling

The coupling of two phenoxy radicals leads to new stereogenic centers. If stereocontrol is exerted due to a catalyst and/or environment and/or chiral auxiliaries in the monolignol, the reaction can lead to pure enantiomers. Natural lignans often exist in enantiopure forms. The regio- and stereospecificity of bimolecular phenoxy radical coupling in lignan and lignin biosynthesis are clearly controlled in some manner *in vivo*. In contrast, *in vitro* coupling reactions using oxidases, such as laccases, have lacked strict regio- and stereospecific control. That is, if chiral centers are generated during *in vitro* coupling, the products are racemic, and different regiochemistries can result if more than one potential coupling site is present. Thus

the ability to generate a particular coupling product *in vitro*, is not under explicit control (Davin *et al*., 1997).

For instance, one-electron oxidation of the monolignol, *E*-coniferyl alcohol **(37)**, results in "random" bimolecular coupling to initially afford three possible quinone methide intermediates, which ultimately undergo inter- or intra-molecular nucleophilic attack to yield the dimeric products, (±)-dehydrodiconiferyl alcohols **(38)**, (±)-pinoresinols **(39)** and (±)-guaiacyglycerol *β-O*-4-coniferyl alcohol ethers **(40)** (Scheme 3.5).

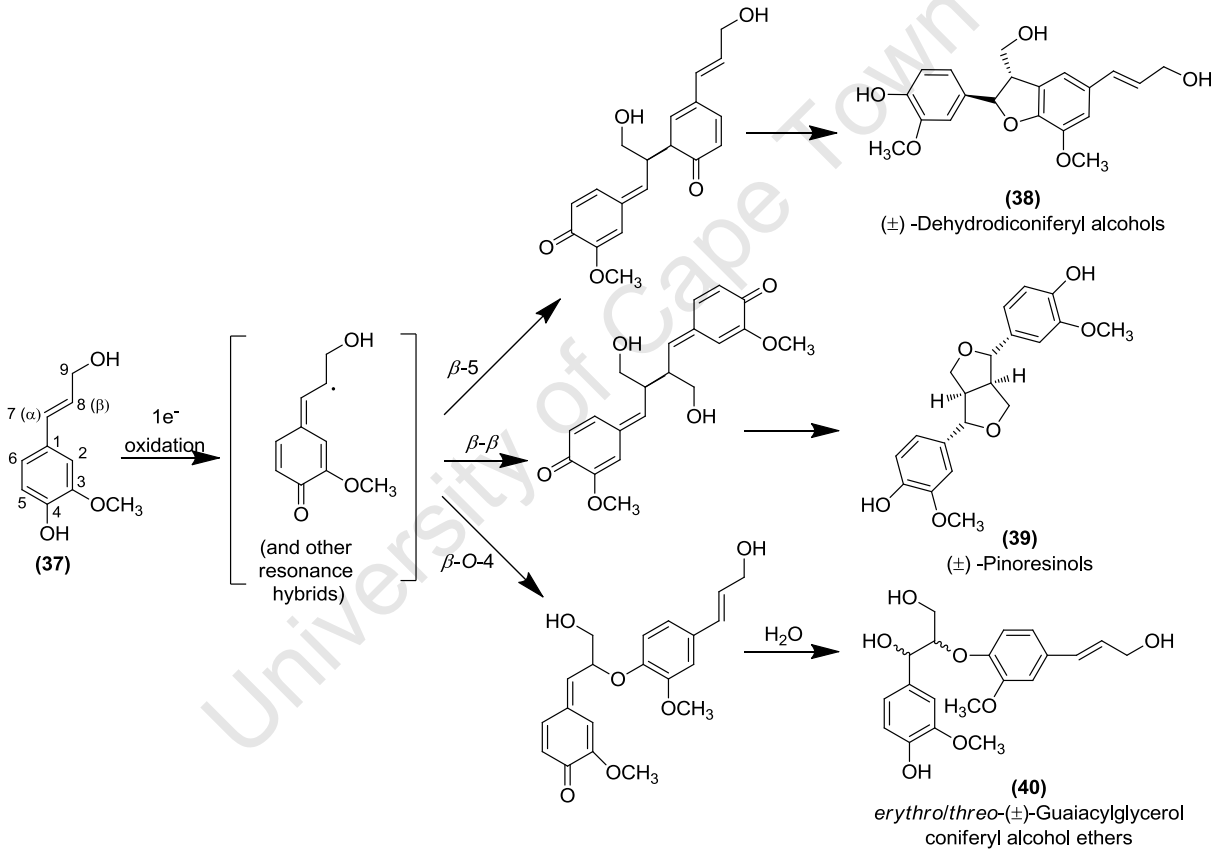

Scheme 3.5 Bimolecular phenoxy radical coupling intermediates and products from *E*-coniferyl alcohol

β-O-4 coupling can give rise to *erythro* and *threo* isomers while *β*-5 type coupling nearly always results in pure *trans* isomers (Scheme 3.6). The *erythro*/*threo* ratio of *β-O*-4-structures is an important structural characteristic of lignin (Akiyama *et al*., 2003).

The stereochemistry in forming these isomers is believed to be kinetically controlled (Ralph *et al*., 2004). *In vitro* experimental results are lacking, unreliable, non-systematic and have varied quite significantly making it difficult to draw fundamental conclusions on the correlations between the *erythro*/*threo* ratio and the reacting species (quinone methides and nucleophiles), the effect of the monolignol structure, and the reaction conditions.

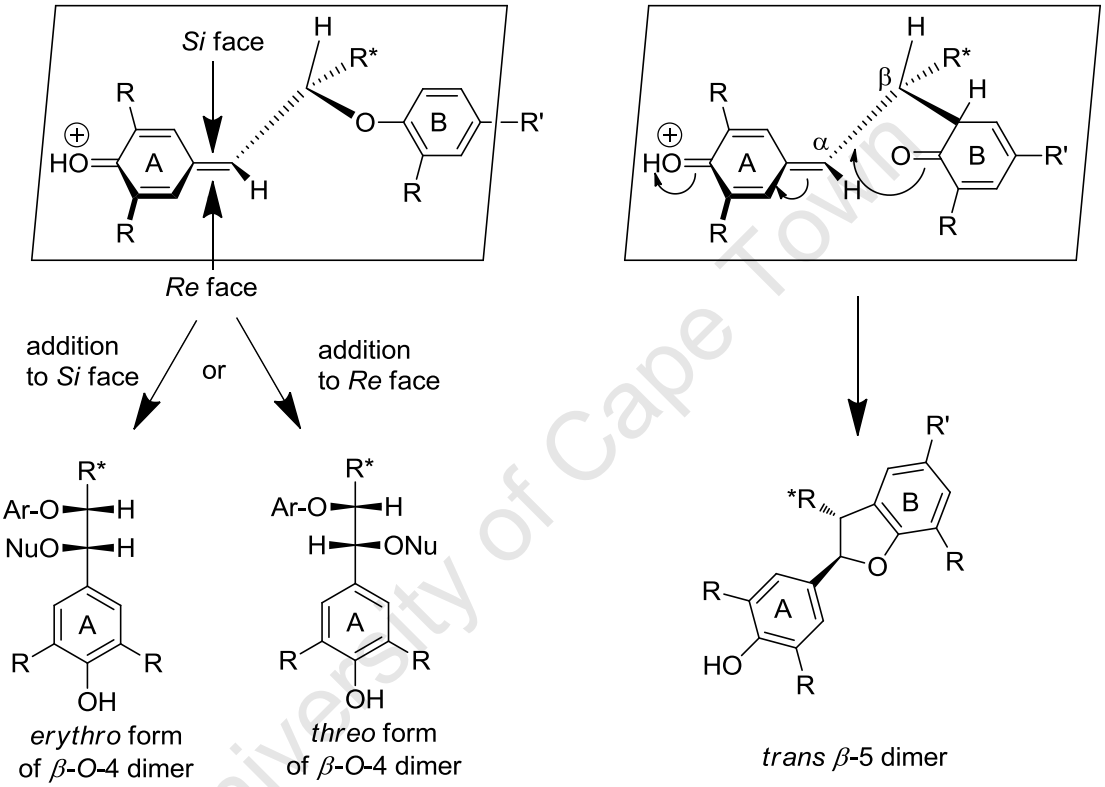

Scheme 3.6 Schematic diagram showing the acid catalysed addition of a nucleophile to a quinone methide intermediate and formation of *erythro* and *threo* isomers of *β-O*-4 dimers and C_{α}-C_{β} trans *β*-5 dimer

Soluble and insoluble enzymes prepared from *Eucommia ulmoides*, incubated with 30 mM coniferyl alcohol for 60 min, were shown to enantioselectively form (-)-*erythro*, (+)-*erythro* and (+)-*threo*, (-)-*threo*-GGCE's respectively (Alam *et al*., 2008).

A 78-kilodalton protein, isolated from *Forsythia* species, has been shown to affect stereoselective bimolecular phenoxy radical coupling *in vitro* in the presence of an oxidase or one electron oxidant. Lacking a catalytically active (oxidative) center itself, its mechanism of action is presumed to involve capture of coniferyl alcohol-derived free radical intermediates, with consequent stereoselective coupling to yield (+)-pinoresinol (Scheme 3.7). The directing protein (DP) therefore acts as a chiral inducer.

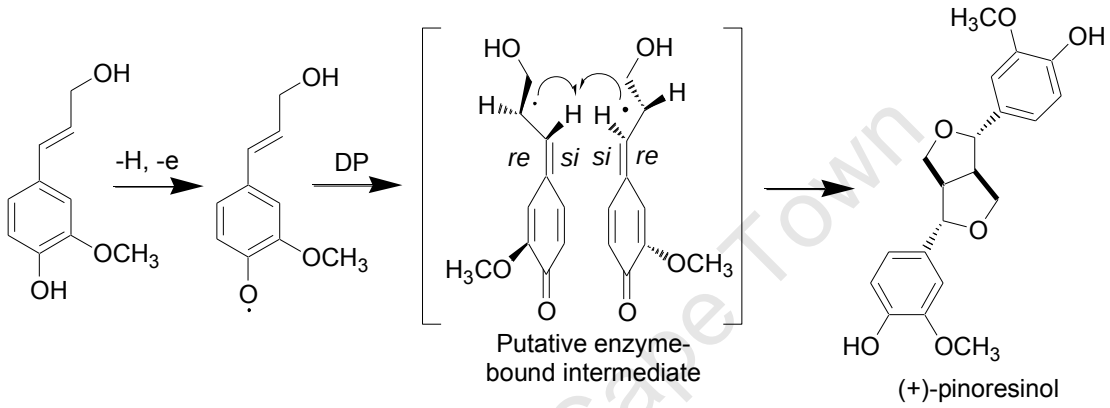

Scheme 3.7 The formation of (+)-pinoresinol by directing protein (DP) mediated coupling of coniferyl alcohol

3.3 Retrosynthesis: Dadahol B

Retrosynthetic analysis of dadahol B (Scheme 3.8) revealed that disconnections at the ester groups leads to *p*-coumaric acid **(41)** and a guaiacyglycerol *β*-*O*-4-coniferyl alcohol ether (GGCE) **(40)** moieties. GGCE contains two guaiacyl rings with two methoxy groups and is recognised as the biomimetic bimolecular oxidative coupling product of coniferyl alcohol **(37)** - the radical species of coniferyl alcohol bears one guaiacyl ring with one methoxy group. The monolignol (4-hydroxycinnamyl alcohol) **(37)** is the reduction product of the corresponding *p*- hydroxycinnamyl ester **(42)**, which is ultimately prepared from the readily available benzaldehyde, vanillin **(43)**, via a classical Wittig reaction.

Other retrosynthetic routes were considered but were deemed less practical as these required synthetic routes with several more steps and specialized reagents.

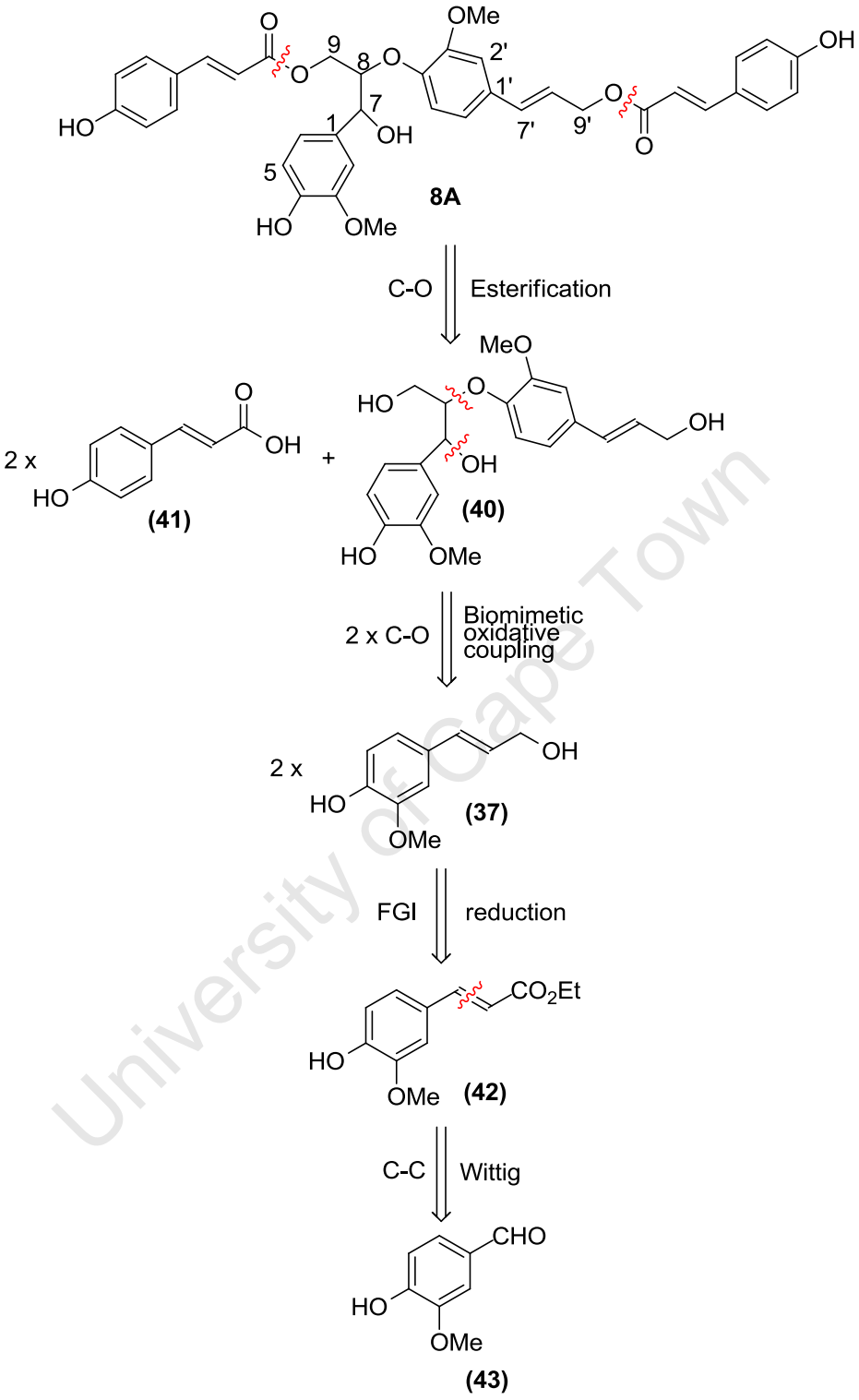

Scheme 3.8 Retrosynthesis of dadahol B

3.4 Total Diastereoselective Synthesis of Dadahol B

Scheme 3.9 summarises the synthetic route adopted to synthesise the two diastereomers of dadahol B using readily available starting materials.

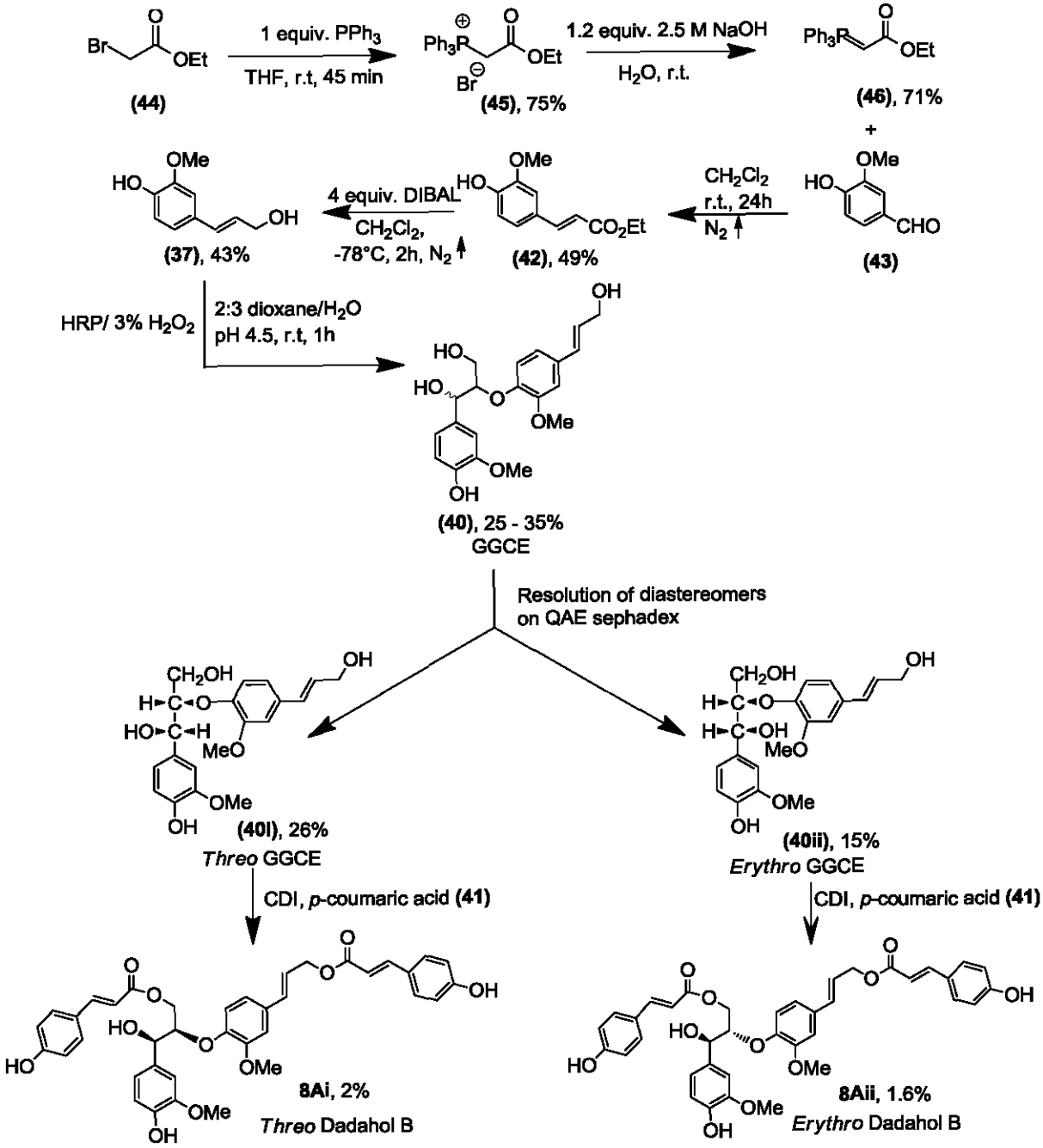

Scheme 3.9 Diastereoselective synthesis of dadahol B

3.4.1 Synthesis of the Monolignol: Coniferyl Alcohol

Ethyl bromoacetate **(44)** was reacted with triphenylphosphine to produce the triphenylethoxycarbonylmethylphosphonium bromide salt **(45)**. The phosponium ylide, or Wittig reagent **(46)**, was prepared by reaction of the phosphonium salt with a base (sodium hydroxide). The Wittig reaction between vanillin **(43)** and the Wittig reagent **(46)** proceeds at room temperature but is slow and low yielding due to the anion-stabilizing/electron withdrawing nature of the $-CO_2Et$ substituent.

Stabilized ylides such as **(46)** tend to be less reactive than other ylides and predominately give *E*-alkenes. This selectivity has been attributed to the fact that stabilized ylides react with aldehydes under thermodynamic control (Vedejs and Peterson, 1994). Therefore, the less crowded *trans*-oxaphosphetane intermediate is favoured (Scheme 3.10). The major product 4-hydroxy-*trans*-cinnamyl ester (ethyl ferulate) **(42)** (~ 50 % yield) was separated from minor (> 5 % yield) corresponding *cis* ester by silica gel column chromatography.

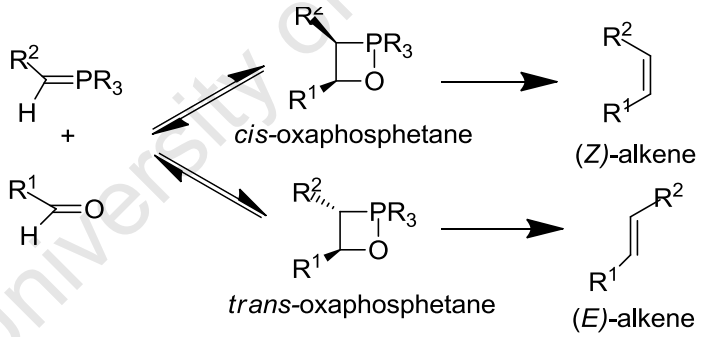

Scheme 3.10 Wittig reaction mechanism

Diisobutylaluminum hydride (DIBAL) was used to reduce ethyl ferulate **(42)** to the monolignol, *E*-coniferyl alcohol **(37)**. DIBAL is a versatile reducing agent useful in achieving stereo- and chemoselective reductions, particularly in the case of unsaturated carbonyl compounds. Alternative reducing agents, such as lithium aluminum hydride, yield varying amounts of saturated alcohol due to competing 1,4- *vs* 1,2-attack by the hydride (Quideau and Ralph, 1992).

3.4.2 Oxidative Coupling of *E*-coniferyl Alcohol

Biomimetic oxidative coupling of *E*-coniferyl **(37)** alcohol provided a straightforward and reproducible method for the preparation of the core neolignan structure (GGCE) **(40)**. Oxidant systems and reaction conditions which favoured the formation of the *β*-*O*-4 (8-*O*-4') dimer were investigated. Enzymatic systems such as peroxidase/H_2O_2 and laccase/O_2 were more successful than inorganic oxidants such as Ag_2O.

The best yields of *β*-*O*-4 dimer **(40)** (25 – 35%) were obtained using horseradish peroxidase (HRP) as a catalyst with hydrogen peroxide (H_2O_2) as an oxidant, in a 2:3 (v/v) dioxane/water mixture at pH 4 - 4.5 (Houtman, 1999; Terashima and Atalla, 1995).

HRP is a heme-containing enzyme from horseradish (*Armoracia rusticana* P. Gaertn., B.Mey. & Scherb.; Cruciferae) roots. The stability and activity of HRP is dependent on the concentration of H_2O_2, which can inhibit the enzyme at too high a concentration. The molar ratio of coniferyl alcohol / oxidant was generally 1:0.5 because one H_2O_2 can generate two phenoxy radicals.

Terashima and Atalla (1995) measured the product distributions from the dimerization of coniferyl alcohol in various water/diglyme mixtures and observed that a small addition of diglyme (20%) dramatically increased the production of *β*-O-4 dimers at the expense of the *β*-5 and *β*-*β* dimers (Scheme 3.5). Similar effects were observed for water/dioxane and water/glycerol mixtures.

The amount of organic solvent is generally kept as low as possible to prevent denaturing of the enzyme. HRP has been found to be fairly active even at high concentrations of organic solvents (Ryu and Dordick, 1989). According to kinetic studies, the apparent K_m values (enzyme-substrate interactions) in dioxane/water mixtures increases as the substrate hydrophobicity increased, whereas in aqueous buffer, the apparent K_m values remained relatively constant. Values of V_{max} (catalytic

turnover), i.e. V_{max}/K_m, were reduced because of a stronger binding of substrates to HRP (Ryu and Dordick, 1992; Ryu and Dordick, 1989).

pH also affects the dimerization of coniferyl alcohol. Among the contributing structures to the resonance hybrid of the coniferyl alcohol radical, the phenoxy radical (resonance form A in Scheme 3.2) is greater under acidic than neutral conditions, and will therefore give more *β*-O-4 dimer (Terashima and Atalla, 1995). The formation of *β*-O-4 dimer differs from the other two coniferyl alcohol dimers (*β*-*β* and *β*-5; Scheme 3.5) in that it requires the addition of water to the intermediate quinone methide; this is an acid catalysed reaction which is very slow at neutral pH.

A dioxane/water mixture at pH 4 – 4.5 was established as the most suitable matrix for scale-up of the oxidative coupling reaction since it allowed for optimal yields and easier recovery of *β*-O-4 dimer **(40)**. No significant change in pH occurs during the reaction. Due to reduced peroxidase activity, the reaction slowed after one hour and addition of more peroxidase and H_2O_2 usually completed the dimerisation process.

In all experiments, trace quantities (< 5%) of *β*-*β* dimers (pinoresinol) **(39)** and variable amounts of oligomeric products, that were not further characterized, were obtained. However, the major products were GGCE **(40)** (25-35% yield) and DHCA **(38)** (10-15%) (Scheme 3.11), even after an excess of H_2O_2 was added; while the relative ratio of the two was fairly constant regardless of the reaction time. This indicates that the reactivity of the monomers is greater than that of the dimers, and coupling between monomer and dimers and two dimers does not occur readily as long as they are in dilute solution. This may be due to steric hindrance factors or substrate specificity of peroxidase between monomer and dimer.

Oxidative coupling results in carbon-carbon and carbon-oxygen bond formation. Subsequently, new chiral centers are formed. Peroxidases have not been observed to catalyse the oxidative coupling of phenols in an enantioselective way without the help of so-called dirigent proteins (Davin *et al*., 1997). No diastereoselection between

threo **(40i)** and *erythro* **(40ii)** forms of GGCE was observed in the HRP-catalysed oxidative coupling of *E*-coniferyl alcohol. The ^{1}H NMR of the synthesized GGCE **(40)** revealed that the diastereomeric ratio was ~1:1.

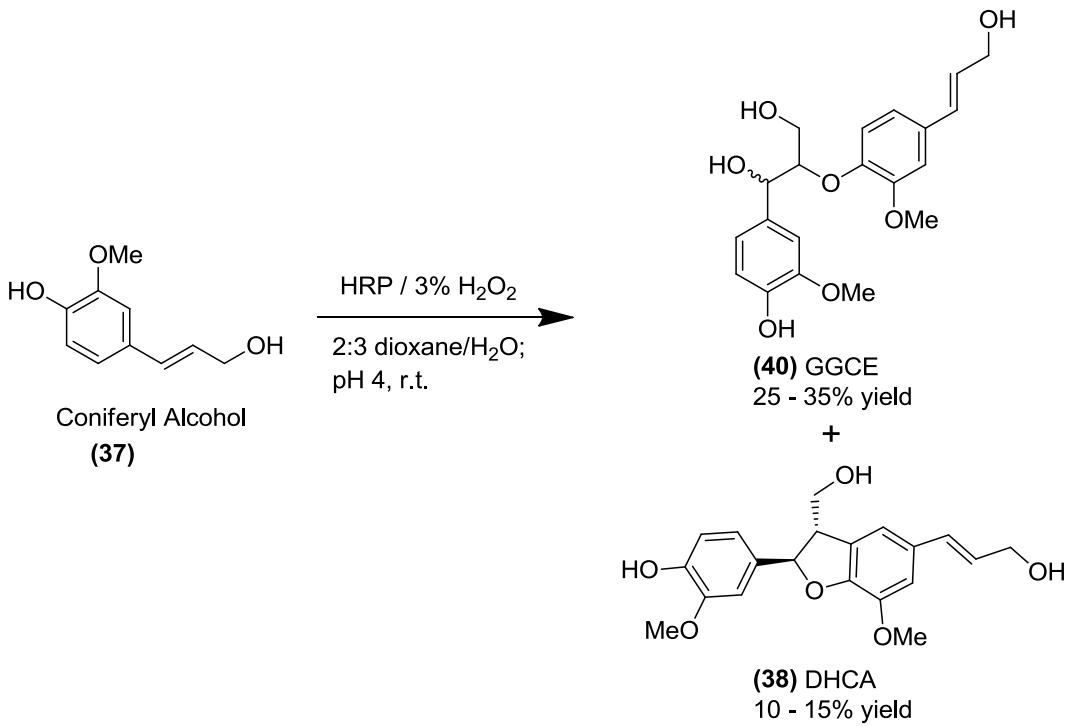

Scheme 3.11 Major products of oxidative coupling of *E*-coniferyl alcohol

3.4.3 GGCE Esterification

To complete the synthesis of dadahol B, GGCE **(40)** needed to be coupled with two *p*-coumaric acid **(41)** molecules at the C-9 and C-9' positions (Scheme 3.12).

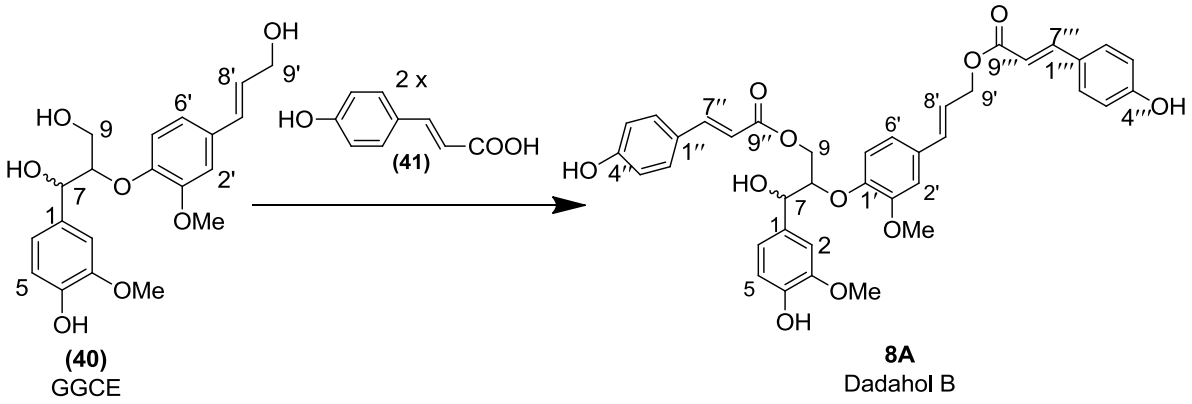

Scheme 3.12 Coupling of GGCE with 2 x p-coumaric acid to yield dadahol B

Phenolic alcohols and phenolic acids are not easily amenable to esterification reactions. Varying degrees of chemoselectivity have been achieved with strong protic acids (Fischer esterification), Lewis acid-catalysed acylations, enzymes, condensing agents (*viz*. *N*, *N*'-dicyclohexylcarbodiimide, DCC) and catalytic quantities of promoters (*viz.* 4-dimethyaminopyridine, DMAP). However, harsh reaction conditions, the requirement of a large excess of one of the reagents, long reaction times and modest yields limit the scope and versatility of these esterification techniques to more hydroxylated and sensitive substrates (Appendino *et al*., 2002; Nahmany and Melman, 2004).

Several methods for the acylation of vanilinol **(47)** (Scheme 3.13) were investigated (Appendino *et al*., 2002). Reactions of symmetric and mixed anhydrides and acyl chlorides in the presence of pyridine or triethylamine/DMAP were found to give comparable rates for the acylation of the phenolic and alcohol hydroxyls. Even reactions of a carboxylic acid/carbodiimide/DMAP system showed similar rates for the formation of alkyl and aryl esters.

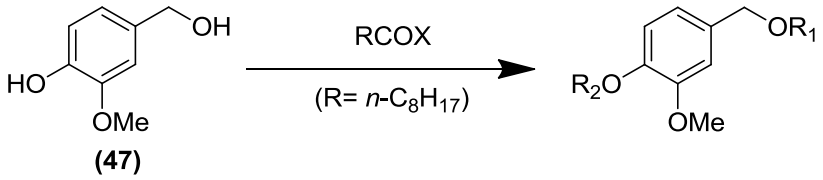

Scheme 3.13 Acylation of vanilinol

The esterification of phenolic alcohols and phenolic acids via acyl nucleophilic substitution under nucleophilic catalysis requires protection of the phenolic hydroxyls, since acids activated *in situ* or *ex situ* show poor discrimination between hydroxyls bound to aliphatic and aromatic carbons. Since deprotection of polyphenolic esters is often not a trivial operation, the more rational alternative would be to switch from carbonyl to hydroxyl activation - phenolic carbons are not substrates for S_N2-type reactions. For instance, the cesium salts of phenolic acids have been reported to chemoselectively react with alkyl halides, but with modest yield and with an excess of halides (Stüwe *et al*., 1989). But this approach cannot be directly extended to multifunctional substrates such as phenolic alcohols.

More specialised techniques like the Mitsunobu esterification, using the diisopropyl azodicarboxylate (DIAD) and triphenylphosphine (TPP) complex as a condensing agent, has been successfully applied to the chemoselective esterification of polyphenolic acids with polyphenolic alcohols. This is demonstrated by the condensation of hydroxytyrosol **(48)**, a major antioxidant of olive oil, with gallic acid **(49)** (Appendino *et al*., 2002) (Scheme 3.15). Ester **(50)** was previously prepared in five steps with a 5% overall yield (Tillekeratne *et al*., 2001). The S_N2-mechanism of the Mitsunobu reaction rules out aromatic carbons as electrophilic substrates, while generation of the nucleophilic species by deprotonation with a stabilized azaenolate, a relatively weak base (Hughes *et al*., 1988), ensures that carboxylates rather than phenolates are formed, provided that stoichiometric amounts of reagents are used.

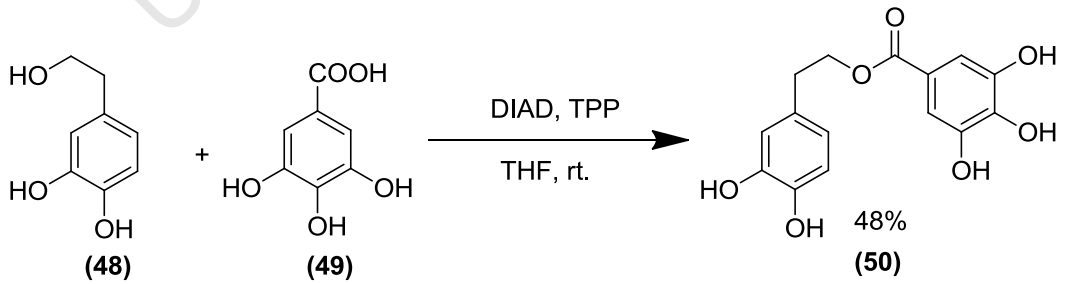

Scheme 3.15 Mitsunobu esterification of hydroxytyrosol

In theory, the difference in electronic properties and acidity between alcohols and phenols could be manipulated to control the chemoselectivity of esterification. The oxygen atoms in phenols generally have lower basicity and nucleophilicity - K_b of phenol is about 10^6 times lower than that of methanol.

However, the challenge in selectively esterifying a substrate like GGCE **(40)**, lies in the fact that it contains four potential reaction sites with varying properties *i.e*. an allylic hydroxyl (at C-9'), a primary hydroxyl (at C-9), a secondary hydroxyl (at C-7) and a phenolic hydroxyl (at C-4).

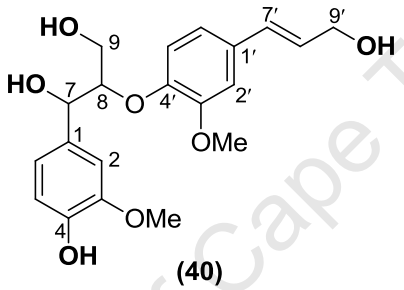

(40)

3.4.3.1 Acid Chloride Esterification

To assess the reactivity of the different GGCE hydroxyls, a simple acid chloride esterification (Scheme 3.16) was conducted. 2.5 Equivalents of cinnamic acid **(51)** were treated with oxalyl chloride to yield the corresponding acid chloride **(52)**. In the presence of triethylamine, the acid chloride reacts with unresolved GGCE **(40)** to give two primary products, the *erythro* 4,9-diester **(53)** and the 4-monoester **(54)** as a diastereomeric mixture.

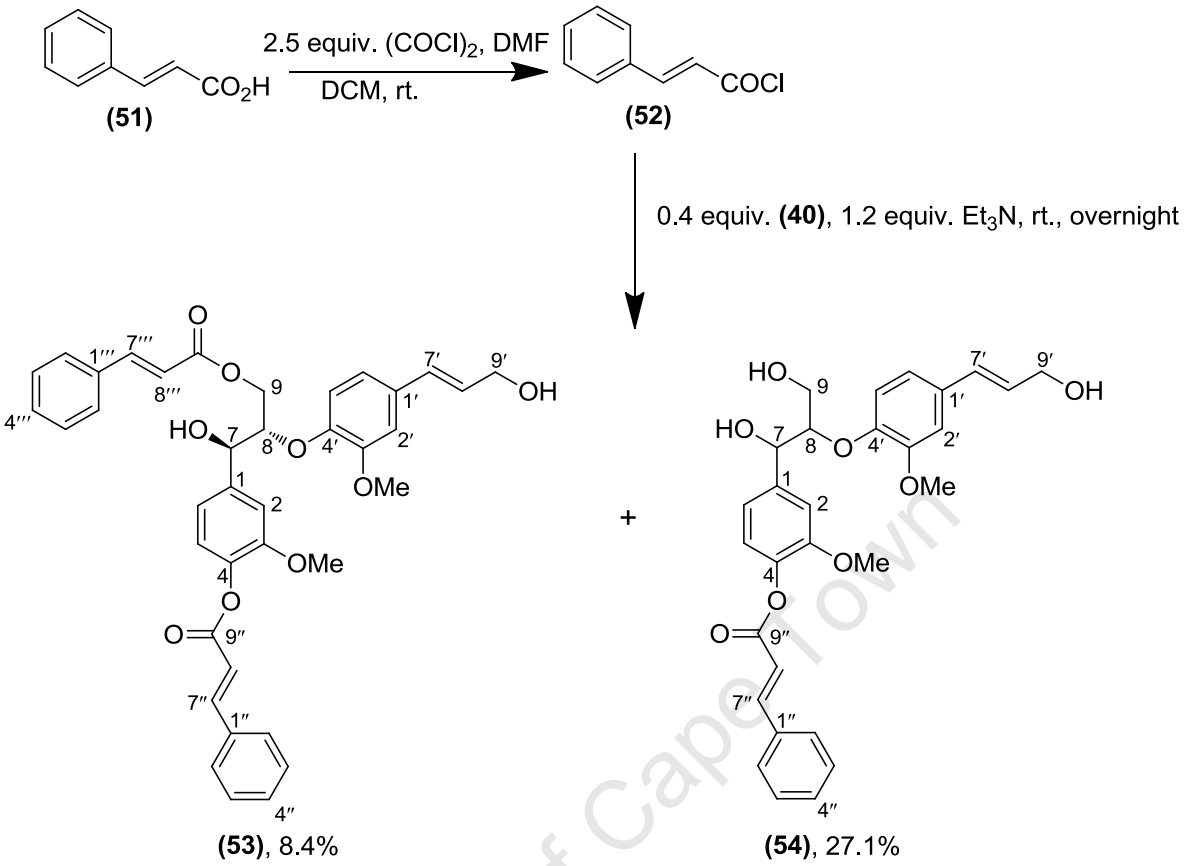

Scheme 3.16 Acid chloride esterification of GGCE

The phenolic hydroxyl was the most reactive, followed by the primary hydroxyl at C-9. As expected, the tertiary hydroxyl at C-7 was completely unreactive, but surprisingly, so was the allylic hydroxyl (at C-9').

This selectivity can be attributed to the alkaline reaction conditions. In the presence of even weak bases, deprotonation of the phenolic moiety tends to be the main factor controlling the chemoselectivity of acylation (Nahmany and Melman, 2004). In the presence of triethylamine, the phenolic hydroxyl of GGCE deprotonates producing phenolate anions that is acylated in preference to the less acidic hydroxyl groups.

3.4.3.2 Protection and Alternative Esterification Methods

To circumvent the selectivity issue observed in the acid chloride esterification, phenolic protection as well as alternative esterification techniques, were investigated. In several instances, the *β*-5 dimer, DHCA **(38)**, was used as an alternative substrate (*cf*. Chapter 5) since the relative hydroxyls of DHCA **(38)** were found to have similar properties and reactivities to those of GGCE **(40)** (Figure 3.1).

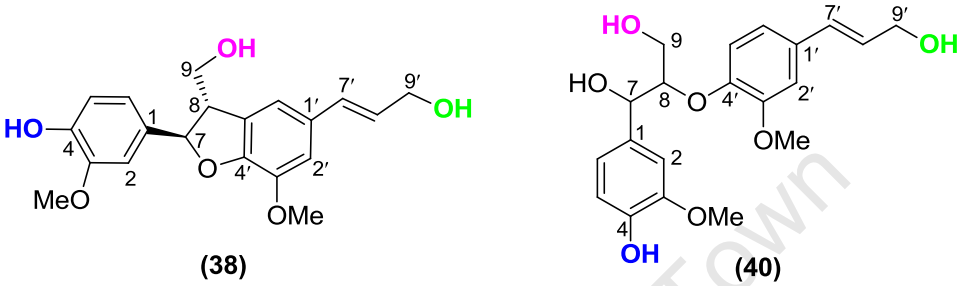

Figure 3.1 Comparison of DHCA and GGCE hydroxyls

Table 3.1. summarises the reactivities of the different DHCA/GGCE hydroxyls to various protection and esterification methods attempted (based on literature precedence and available reagents). The rationale and results of these are discussed further in Chapter 5.

Table 3.1 Summary of results of protection and esterification reactions on DHCA and/or GGCE

Reaction/Conditions	Reaction at position/s:							
	4	**9**	**9'**	**4,9**	**4,9'**	**9,9'**	**7,9**	**4,9,9'**
TBS-Cl (1.1 equiv.), Imidazole, DMAP, THF, rt.	-	-	X	-	-	X	-	-
TBS-Cl (1.1 equiv.), Imidazole, DMAP, THF, 0°C	-	-	X	-	-	-	-	-
TBS-Cl (1.1 equiv.), Et_3N, DMAP, THF, 0°C	-	-	X	-	-	-	-	-

Reaction/Conditions	Reaction at position/s:							
	4	9	9'	4,9	4,9'	9,9'	7,9	4,9,9'
TBS-Cl (1.1 equiv.), 2,6-lutidine, CH_3CN, 0°C	-	-	X	-	-	-	-	-
DHP (1.5 equiv.), PPTS, DCM, rt.	-	-	X	-	-	-	-	-
TrCl (1.05 equiv.), Et_3N, DMAP, DCM, 0°C	X	-	-	-	-	-	-	-
Acetone/DMP (1:1), PPTS, rt.	-	-	-	-	-	-	X	-
Acid chloride (2.5 equiv.), Et_3N, THF, rt.	X	-	-	X	-	-	-	-
Acid chloride (1.1 equiv.), Et_3N, THF, 0°C	X	-	-	-	-	-	-	-
Acid (2 equiv.), DCC, DMAP, DCM/THF (1:1), 0°C → rt	X	-	-	X	-	-	-	-
Acid (2 equiv.), DCC, DMAP, DCM/THF (1:1), rt → 60°C	X	-	-	X	-	-	-	-
Acid (1 equiv.), $(CF_3CO)_2O$, THF, 60°C	-	-	-	-	-	-	-	-
Acid (2.5 equiv.), DIAD, PPh_3, THF, 0°C	-	-	-	-	-	-	-	-
Acid (2 equiv.), CDI, DMAP, 70°C	-	X	X	-	X	X	-	X

Both DHCA **(38)** and GGCE **(40)** proved fairly fragile, showing a tendency to decompose or polymerise even under mildly acidic or basic conditions. Reaction yields were modest, even simple silylation was not resoundingly successful, with more than half the substrate not yielding any recoverable product and favouring the 9'-position. The specialized Mitsunobu esterification which is reported to distinguish between alcohol and phenol hydroxyls in esterification reactions (Appendino *et al*., 2002) also proved unsuccessful with no reaction occurring between the substrates. In other cases, desirable products were difficult to separate from each other as well as unreacted starting materials and degradation/polymerization products; acetonidation

of the 7,9-positions of GGCE **(40)** yielded a complex mixture of several inseparable unstable products.

In terms of selectivity, of the various approaches attempted, only CDI (*N*,*N*'–carbonyldiimidazole) coupling proved successful in obtaining the desired 9,9'-diester. CDI coupling of GGCE **(40)** with 2 equivalents of cinnamic acid **(51)** resulted in a mixture of products, the major products being the triester **(55)**, and the diesters **(56)** and **(57)** (Scheme 3.17). Although the reaction was slow and low yielding, it was possible to separate and individually characterise the *threo* **(56)** and *erythro* **(57)** forms of the 9,9'-diester.

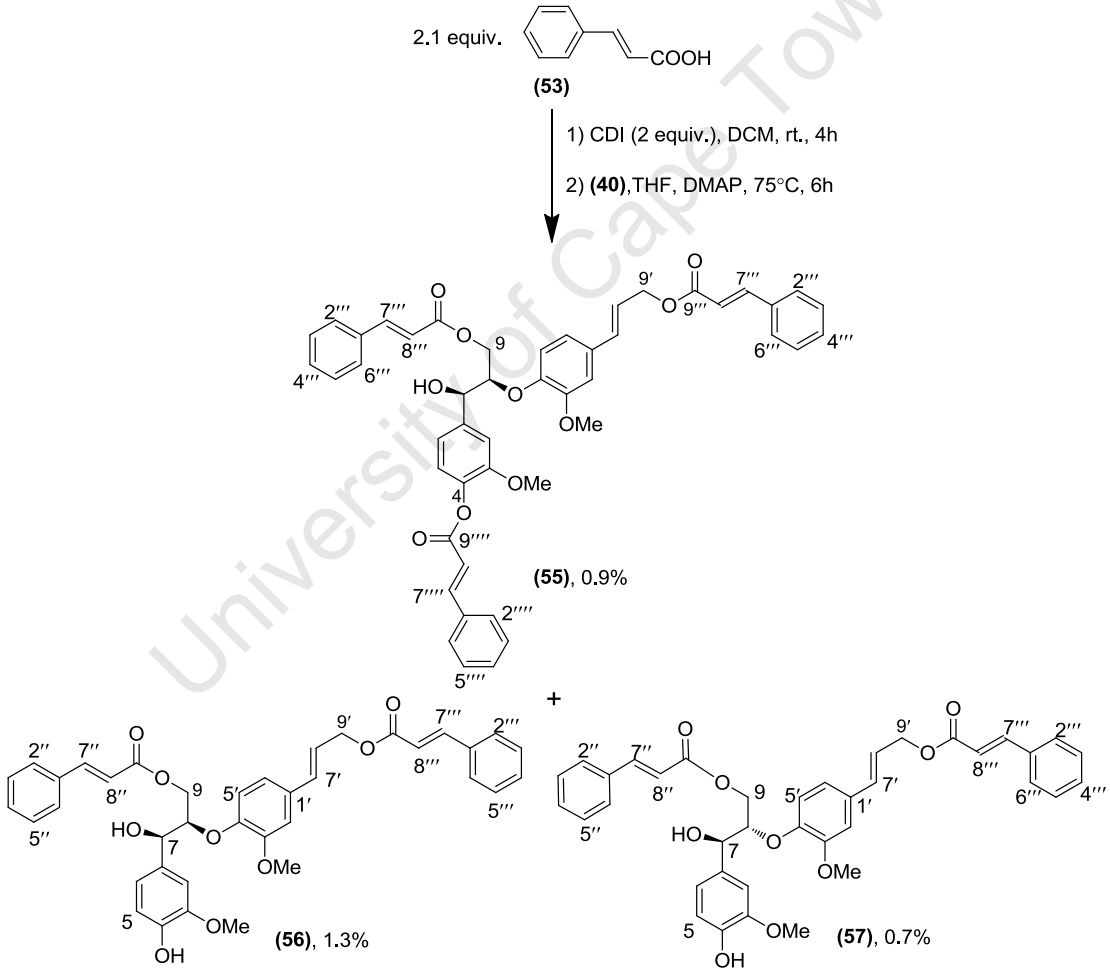

Scheme 3.17 CDI coupling of GGCE with cinnamic acid

However, in attempting the same reaction between GGCE and silylated *p*-coumaric acid **(41)**, an inseparable diastereomeric mixture of the *threo* and *erythro* forms of dadahol B **8A2** was recovered (Scheme 3.18) in modest yield (8.2%). The diastereomeric forms of GGCE **(40)** would therefore need to be resolved before esterification.

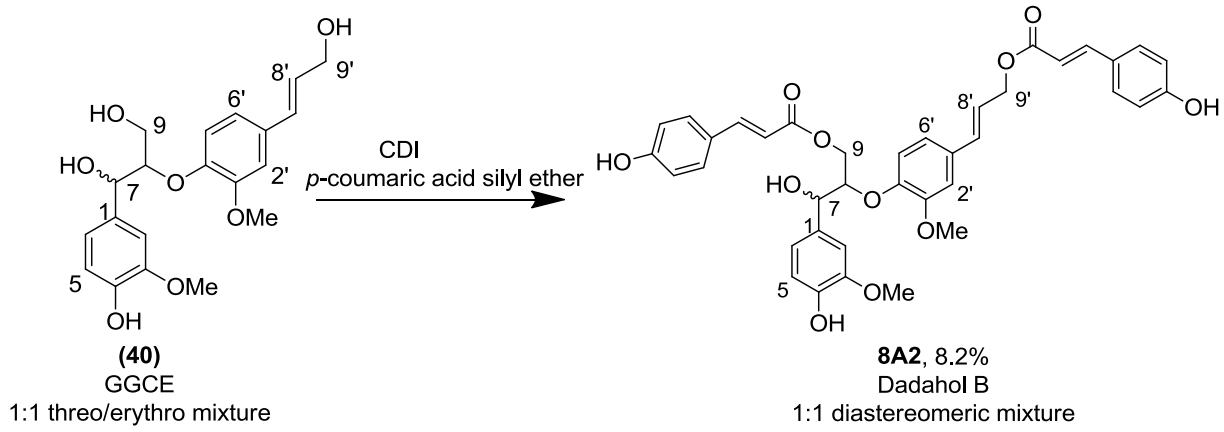

Scheme 3.18 CDI coupling of GGCE with *p*-coumaric acid

3.4.4 GGCE Diastereomer Separation

The *threo* **(40i)** and *erythro* **(40ii)** forms of GGCE were inseparable by conventional column chromatography and semi-preparative HPLC methods. The separation of diastereomers of lignin-related diol compounds based on ion exchange chromatography on an anion exchanger using a borate solution as the eluent was first introduced by Berndtsson and Lundquist (1977). This method and modifications thereof has since been applied in various studies (Ibrahim and Lundquist, 1994; Karlsson *et al*., 1990; Kristersson *et al*., 1980; von Unge *et al*., 1988).

The preparative separation of the diastereomers of GGCE **(40)** was achieved on an ion exchanger with polysaccharide matrix (QAE Sephadex A-25), using 0.06 M potassium tetraborate ($K_2B_4O_7$) in EtOH/water (1:4) as the eluent. QAE (Quaternary aminoethyl) Sephadex is a strong anion exchanger. The ion exchange group is

diethyl-(2-hydroxy-propy)aminoethyl which remains charged and maintains consistently high capacity over a wide pH range.

The *threo* isomer **(40i)** eluted from the column in advance of the *erythro* isomer **(40ii)**. The elution volumes of both diastereomers were large (400 – 500 ml) and the symmetrical elution peaks and difference in elution volume (~ 60 ml) allowed for the complete separation of the GGCE diastereomers.

The *erythro* form gives the stronger borate complex and elutes after the *threo* form. This is expected from a conformational analysis of the borate complexes; in the borate complex of the *threo* form (Figure 3.2), the bulky aryl substituents are *cis* orientated and energetically unfavourable interactions between these groups cannot be avoided (Ibrahim and Lundquist, 1994).

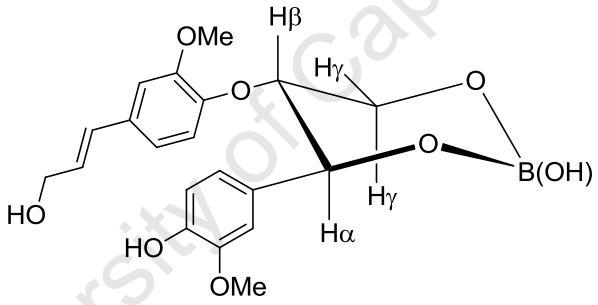

Figure 3.2 Boric acid complex of *threo* GGCE

Work-up of the fractions containing the *threo* or *erythro* forms of GGCE gave mixtures of the compounds, their boric acid complexes and some degradation products. The boric acid was removed by repeated addition and evaporation of methanol. The pure diastereomers were then separated from their degradation products by silica gel column chromatography.

Most of the degradation products were found to be oligomeric in nature and were not further characterized. The ^{1}H NMR of one of the by-products that was recovered showed a triplet at δ_H 1.58 coupled to a quartet at δ_H 3.50 (J = 7.0 Hz), which correlated to C-9' in the HMBC. The ESI-MS data of this compound [m/z 404.179;

$C_{22}H_{28}O_7$] supported the addition of an ethyl group to GGCE **(40)**. Thus, it was confirmed that the allylic alcohol of GGCE **(40)** was ethylated during the ion-exchange chromatography, even though the nucleophilic double bond is more likely to react with acid.

A possible mechanism for this is that the allylic alcohol was preferentially protonated during the acidic conditions of ion exchange chromatography and the generated protonated intermediate undergoes dehydration to yield two possible resonance-stabilized carbocation intermediates **(58)** and **(59)**. Presumably, nucleophilic attack *via* the more stable (disubstituted double bond-containing) carbocation **(59)** by ethanol yielded the observed product, the 9'-ethoxy boric acid complex of GGCE **(61)** (Scheme 3.19). Once the boric acid was removed, the ethylated analogue of GGCE **(62)** was recovered by silica gel column chromatography.

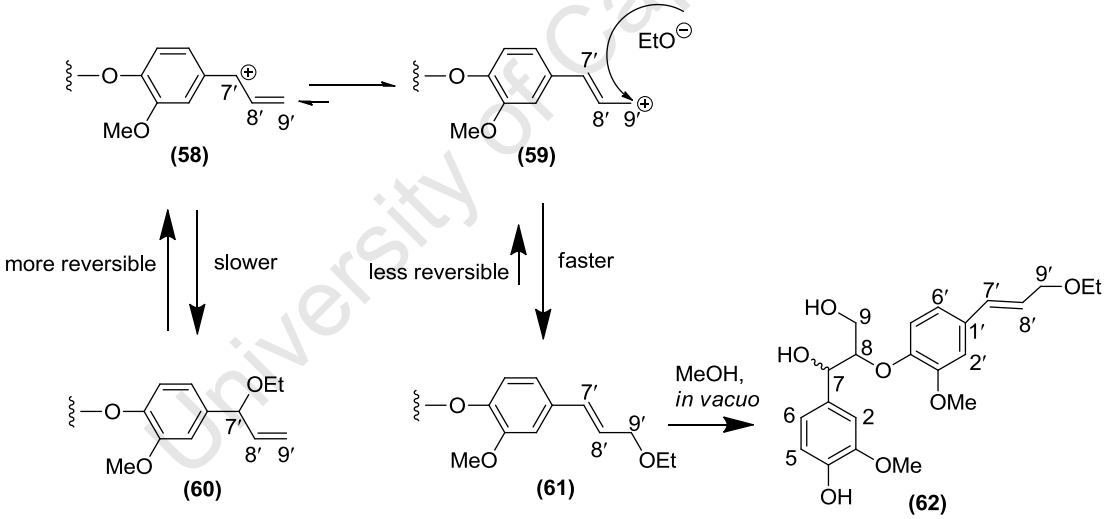

Scheme 3.19 Proposed mechanism of GGCE ethylation

3.4.5. Diastereoselective CDI coupling

Each resolved GGCE diastereomer, **(40i)** and **(40ii)**, was subsequently coupled with *p*-coumaric acid **(41)** using CDI **(63)** as the activating agent. CDI is a highly active carbonylating agent which contains two acylimidazole groups that can activate carboxylic acid groups by forming *N*-acylimidazoles **(64)** (Scheme 3.20). The reaction

is usually driven forward by the liberation of carbon dioxide and imidazole (**65).** The active carboxylate reacts with hydroxyl groups to form ester linkages.

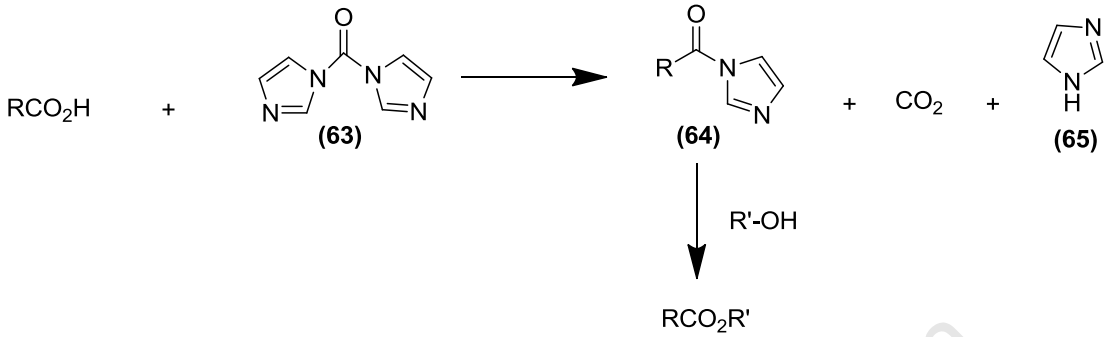

Scheme 3.20 Esterification via CDI activation of carboxylic acids

Methods of improving yields in CDI activated esterification reactions were investigated. Since purity of CDI may be variable due to its water sensitivity, an excess was used to ensure complete conversion of the carboxylic acid to the acylimidazole. It has been suggested that the alcohol might react faster with the residual CDI than the acylimidazole, contributing to overall low yields of the ester. The activation step was conducted in anhydrous DMF, known to drive the reaction forward (Bode *et al*., 1994).

The *p*-coumaric acid **(41)** was silylated **(66)** to limit homogenous coupling of the phenolic acid. Since alcoholysis of the intermediate acylimidazole is slow (Wipf, 2005), the reaction mixture had to be heated for several hours at 70ºC. Catalytic amounts of base (*viz.* Na_2CO_3, NaH) were added to convert the alcohol to the alkoxide, which is reported to drive the esterification reaction forward (Wipf, 2005). The base catalyst was added after formation of the *N*-acylimidazoles **(64)** from the acid as indicated by the cessation of evolution of carbon dioxide. The subsequent alkaline reaction conditions resulted in the loss of the silyl protective groups, thus eliminating the need for an additional deprotection step. Consequently, overall yields were low but sufficient for the isolation and characterisation of each dadahol B diastereomer, **8Ai** and **8Aii,** as well as the some of the 9- and 9'-monoesters, **(67)** – **(69)** and one of the other possible diesters, **(70)** (Schemes 3.21 and 3.22). Traces of

the 4,9,9'-triesters were also recovered but low quantities and complexity of NMR's did not allow for full characterisation.

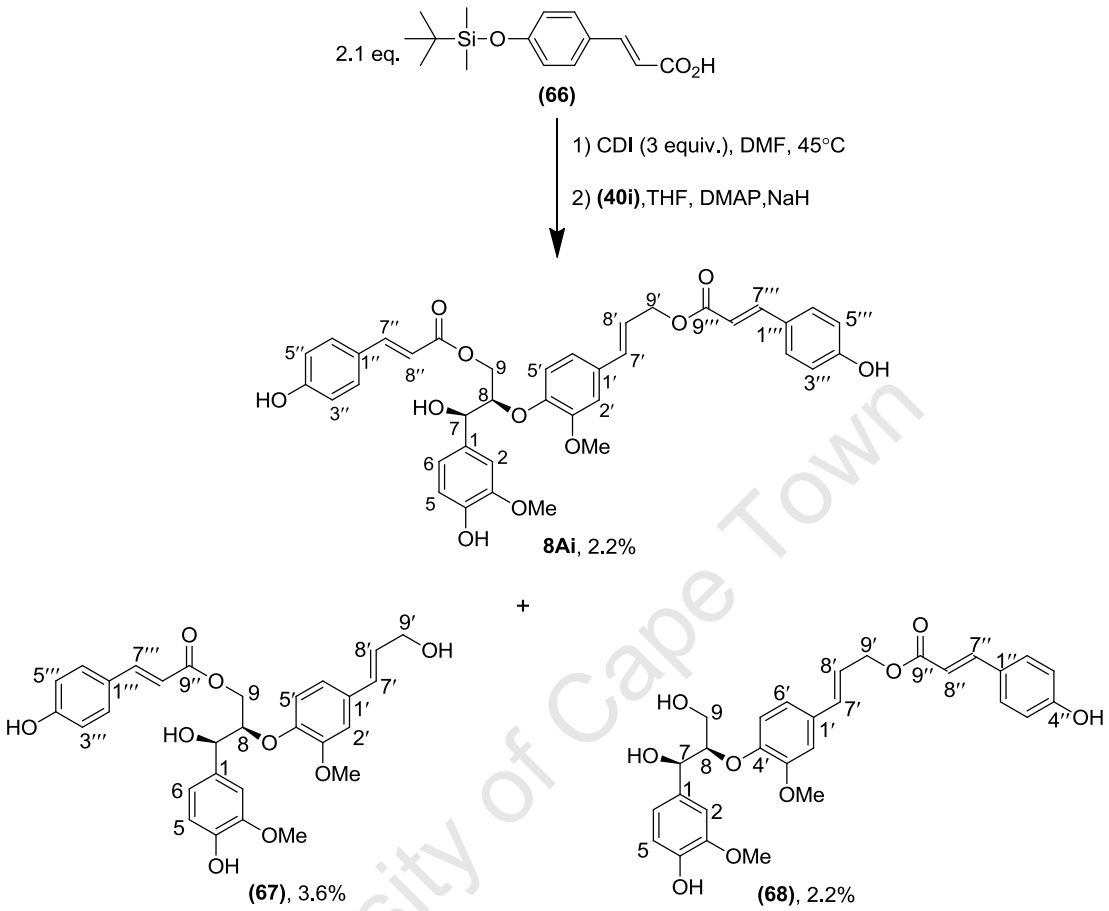

Scheme 3.21 CDI esterification of *threo* GGCE

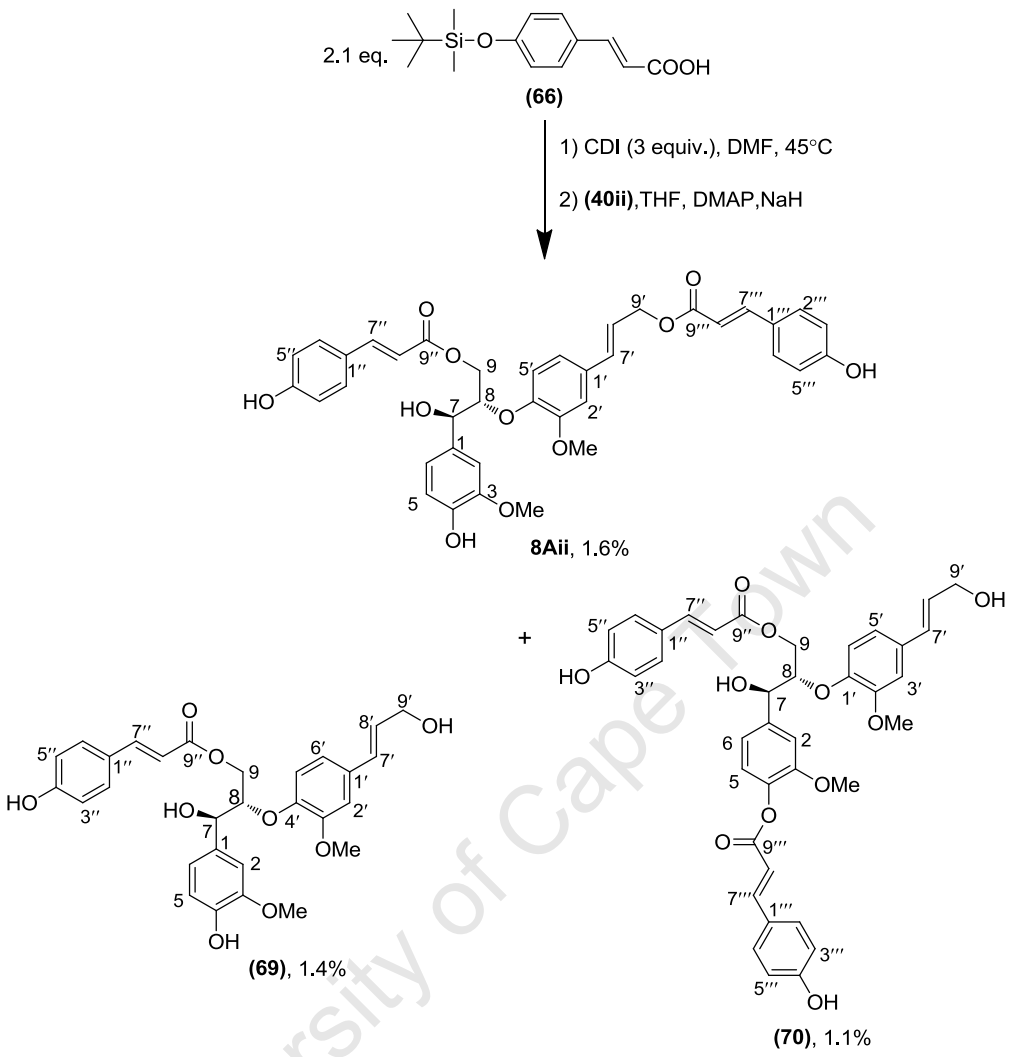

Scheme 3.22 CDI esterification of *erythro* GGCE

The ^{1}H NMR of the natural product **8A** (~1:1 diastereomeric mixture) was subsequently resolved by comparison with the spectroscopic data of the synthesised *threo* **8Ai** and *erythro* **8Aii** forms of dadahol B (Appendix VI). NMR data of the monoesters were also useful in resolving ambiguous resonances of dadahols A (*cf* Chapter 2) and B.

CHAPTER 4

Biological Properties of Dadahols A and B

4.1 Biological Properties of Lignans and Neolignans

Many lignans and neolignans from plants display important physiological functions in plants and human health. Because they have been shown to display potent antimicrobial, antifungal, antiviral, antioxidant, insecticidal and antifeeding properties, lignans probably play an important role in plant defense against various biological pathogens and pests. They may also participate in plant growth and development. In addition to their purpose in nature, lignans and neolignans also possess significant pharmacological activities which include antitumor, anti-inflammatory, immunosuppressive, cardiovascular, antiviral and antioxidant actions (Saleem *et al*., 2005).

Many naturally-derived lignans and neolignans have served as lead compounds for organic synthesis of derivatives to optimize activity and to study structure-activity relationships (Apers *et al*., 2003). Although their molecular backbone consists only of two phenylpropane units, lignans and neolignans show enormous structural diversity, offering a huge library of natural compounds, unsurpassable by modern combinatorial chemistry techniques. The exploration of the chemical diversity of naturally occurring lignans and neolignans has already resulted in the characterization of many interesting lead compounds in various therapeutic areas, some of which are highlighted here.

4.1.1 Antitumoural Activity

Podophyllotoxin **(71)**, a cytotoxic arytetralin lactone originally isolated from *Podophyllum peltatum* L., is the first and best known example (Canel *et al*., 2000). Its antimitotic activity is due to reversible binding to tubulin, which inhibits microtubule assembly and interrupts the cell cycle. A wide range of analogues and derivatives continue to be investigated in an effort to improve upon the antitumour activities and

properties of the clinical drug etoposide **(72)** (Ward, 1999). The antitumoural activity of etoposide **(72)** and teniposide **(73)**, despite being podophyllotoxin analogues, is due to inhibition of DNA topoisomerase II. Combination of both pharmacophores has led to compounds with a dual mechanism of action, such as azotoxin **(74)**.

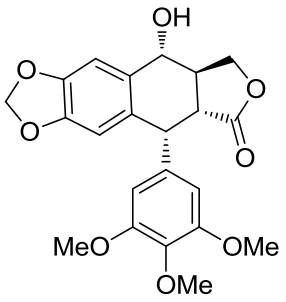

(71)

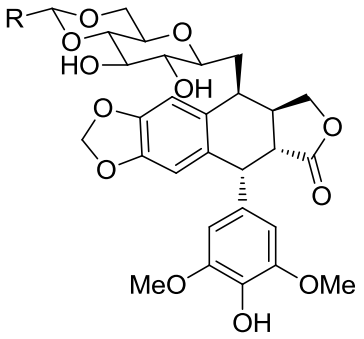

(72) R = Me
(73) R = 2-thienyl

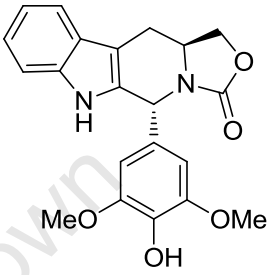

(74)

In addition to podophyllotoxin, other types of lignans and neolignans have also been identified as inhibitors of tubulin polymerization. Dihydrobenzofuran neolignans, based on the natural lead 3'-4-di-*O*-methylcedrusin **(75)** have also been investigated as potential antitumoural agents. The dimerisation product of caffeic acid methyl ester, dihydrobenzofuran **(76)**, showed the best activity against leukemia and breast cancer cell lines. Dihydrobenzofuran **(76)** appeared to inhibit mitosis at μM concentrations *in vitro*, but it lacked activity in a hollow fiber *in vivo* assay, most likely due to enzymatic hydrolysis of the methyl esters or instability and ring opening of the dihydrobenzofuran ring (Apers *et al*., 2003).

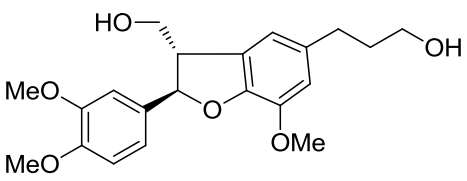

(75)

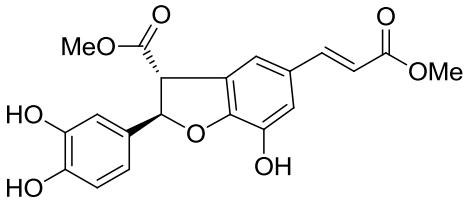

(76)

Antitumor activities of other classes of lignans have been studied and reviewed over the years (Apers *et al*., 2003; Hahm *et al*., 2005; Kong *et al*., 2005; Konuklugil, 1994). These studies suggest that lignans might be valuable as antitumor compounds in chemical carcinogenesis – they can be sedative non-toxic agents for the inhibition of apoptotic agents. Lignans that inhibit Phospholipase Cγl (PLCγl), that plays a key role in the proliferation and progression of human cancer, are also suggested as worthy candidates for chemopreventative and chemotherapeutic agents (Saleem *et al*., 2005).

There is also growing evidence that the consumption of foods rich in lignans (*viz*. wheat, oats, beans, lentils, garlic, broccoli and carrots) can decrease the risk of developing certain forms of cancer. For instance, the lignans may contribute towards the prevention of breast cancer as a result of their antiestrogenic properties whereby they interact with the estrogen receptor and modulate the action of estrogen. Alternatively they may act as antioxidants and prevent the production of carcinogens from estrogen, or they may inhibit aromatase enzyme activity and thereby contribute to the prevention of hormone dependent cancers (Ward, 1999).

4.1.2 Antiviral Activity

Several modes of antiviral activity are associated with lignans: tubulin binding (inhibition of tubulin polymerization interferes with the formation of the cellular cytoskeleton and with some critical viral processes), reverse transcriptase inhibition, intergrase inhibition, and topoisomerase inhibition. While podophyllotoxin and its derivatives were the most prominent representatives of the tubulin binding lignans, inhibition of reverse transcriptase was observed for various classes of lignans, such as dibenzylbutyrolactones, dibenzylbutanes, dibenzocyclooctadienes and arylteralins (Charlton, 1998). Dibenzylbutyrolactones derived from arctigenin **(77)** were active inhibitors of viral integrase.

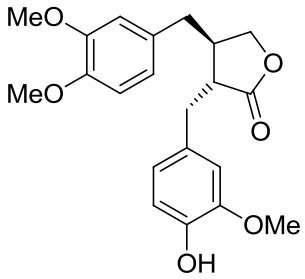

(77)

The Na and K salts of **(78)** and **(79)**, which are known tetramers of caffeic acid, have been isolated from *Arnebia euchroma* and shown to possess potent anti-HIV activity (Kashiwada *et al*., 1995).

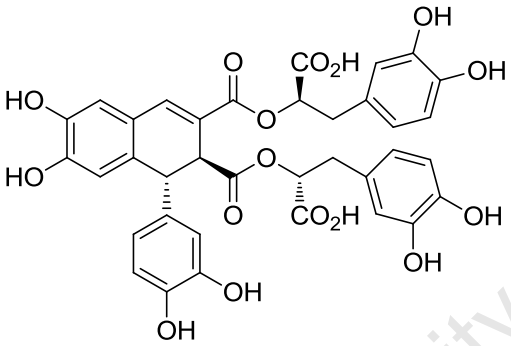

(78)

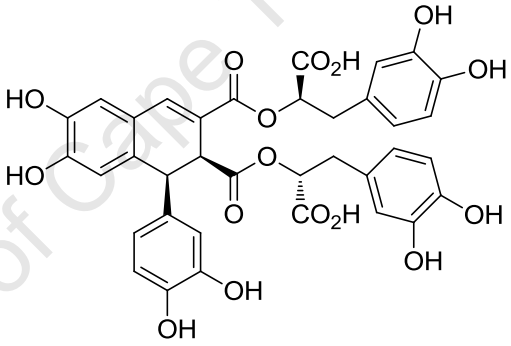

(79)

A number of lignans isolated from *Larrea tridentata* including nordihydroguaiaretic acid **(80)**, were found to suppress HIV-I replication in infected cells. A series of methylated derivates were prepared and the tetramethyl nordihydroguariaretic acid **(81)** was more active than the original lead (Hwu *et al*., 1998). This derivative, as well as the tetraacetyl nordihydroguariaretic acid **(82)**, was found to be useful in the treatment of papillomavirus infections and their associated induced human cancers (Craigo *et al*., 2000).

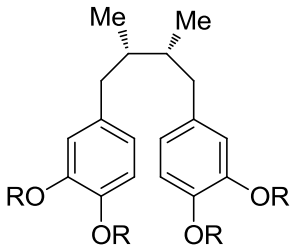

(80) R = H
(81) R = Me
(82) R = Ac

4.1.3 Antiparasitic Activity

As antiparasitics, lignans and neolignans have mostly been tested against *Trypanosoma cruzi*, the causative agent of Chagas' disease (Bastos *et al*., 1999; Cabral *et al*., 1999; Cabral *et al*., 2010; Cherigo *et al*., 2005; da Silva Filho *et al*., 2004; Lopes *et al*., 1998; Luize *et al*., 2006; Martins *et al*., 2003; Nocito *et al*., 2007).

Lopes *et al* (1998) demonstrated the potential of the tetrahydrofuran lignans, grandsin **(83)** and veraguensin **(84)**, from *Virola surinamensis* twigs to prevent the transmission of *T. cruzi* by blood transfusion. The compound (-)-methylpluviatolide **(85)**, isolated from the hexane extract of the leaves of *Zanthoxyllum naranjillo*, was highly effective against *T. cruzi in vitro* and against the bloodstream forms of the two strains *in vivo*. Healthy animals injected with (-)-methylpluviatolide did not develop infection pointing to potential use in chemoprevention (Bastos *et al*., 1999). In an *in vitro* evaluation of a series of 8-*O*-4'-neolignans based on those isolated from the Myristicaceae family, Nicoto *et al* (2007) identified compound **(86)** (3,4-methylenedioxi-7-oxo-1'-allyl-3',5'-dimethoxy-8-*O*-4'-neolignan) as having promising trypanocidal activity.

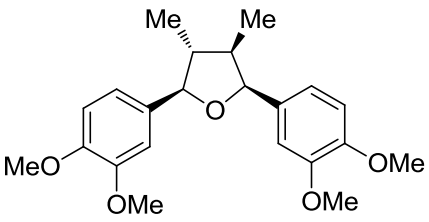

(83)

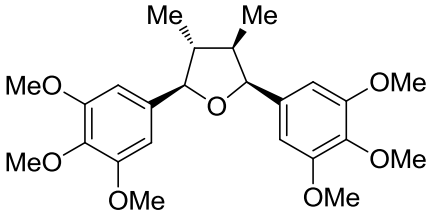

(84)

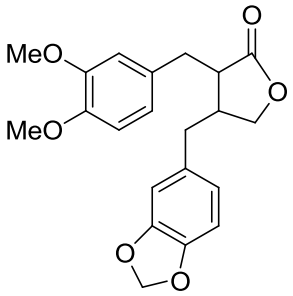

(85)

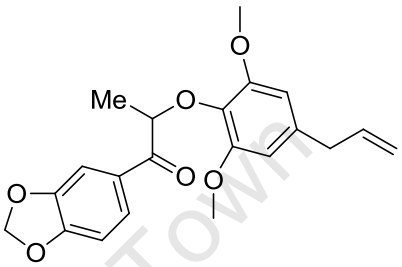

(86)

8-*O*-4'-Neolignans were also shown to have effects against *Leishmania donovani*, one of the causative agents of leishmaniasis. Based on the active principles isolated from *Virola surinamensis*, surinamensin **(87)** and virolin **(88)**, a series of compounds with ether linkages and their corresponding C-8 sulfur and nitrogen analogues were synthesized and evaluated *in vitro*. The highest selective activity against amastigotes was found in those compounds with sulfur bridges, suggesting that the C-8 sulfur bond may be a key pharmacophore in their antileishmanial activity. Of these, only compound **(89)**, (3,4-dimethoxy)-8-(4'-methyl-thiophenoxy)-propiophenone), was significantly active *in vivo*, resulting in 42% inhibition of *L. donovani* amastigotes in the liver of infected mice at a dose of 100 mg/kg orally once a day over 5 consecutive days (Barata *et al*., 2000).

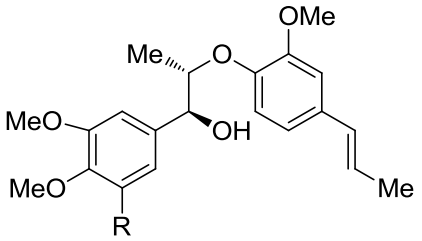

(87) R = OMe
(88) R = H

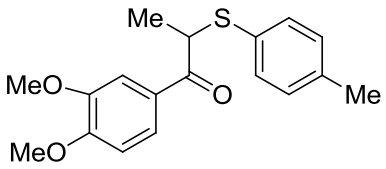

(89)

A norlignan isolated from *Asparagus africanus*, (+)-Nyasol **(90)**, was shown to potently inhibit the growth of *Leishmania major* promastigotes (IC_{50} 12 µM) and moderately inhibit *Plasmodium falciparum* schizonts (IC_{50} 49 µM) (Oketch-Rabah *et al*., 1997). Moderate antiplasmodial activities have also been reported for the 8,5'-linked lignan dehydrodiconiferyl dibenzoate **(91)** (IC_{50} 12 µM; D6) isolated from the roots of *Euterpene precatoria* (Jensen *et al*., 2002), and an arylnaphthalide lignan, justicidin B **(92)** (IC_{50} > 5.0 µg/ml; 3D7), obtained from *Phyllanthus piscatorum* (Gertsch *et al*., 2003).

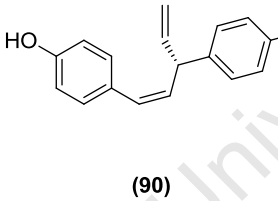

(90)

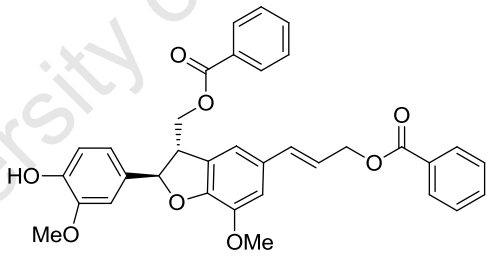

(91)

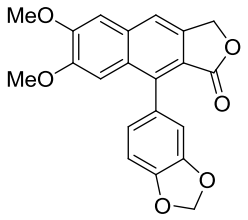

(92)

8-*O*-4'-Neolignans which have shown antiplasmodial activity include polysyphorin **(93)** (IC_{50} 0.4 µg/ml; D6) isolated from *Rhaphidophora decursiva* (Zhang *et al*., 2001) and rourinoside **(94)** (IC50 3.7 µM; D6) from *Rourea minor* (He *et al*., 2006). Antimalarial properties have also been reported for sesquilignans (Kraft *et al*., 2002), aryltetralone lignans (de Andrade-Neto *et al*., 2007) and tetrahydrofuran lignans *(*da Silva Filho *et al*., 2004).

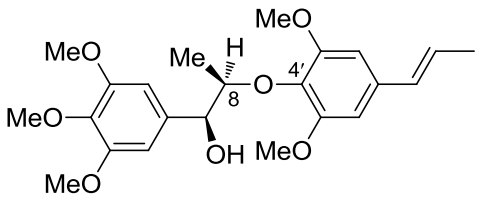

(93)

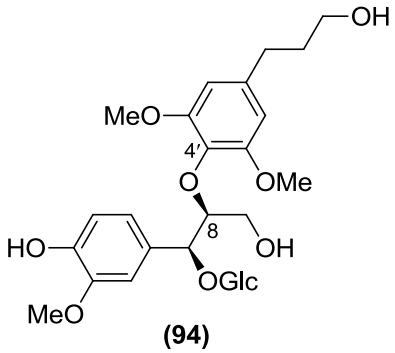

(94)

4.2 *In vitro* Antiplasmodial Activity of Dadahol A and B

Although dadahols A and B were originally isolated from an *A. dadah* twig extract by activity-guided fractionation using a cyclooxygenase-1 (COX-1) inhibition assay, they were found to be inactive (IC_{50} > 100 µg/ml) against both COX-1 and COX-2 (Su *et al*., 2002). Therefore, this is the first report of the compounds having any biological activity. Dadahol B, **8A**, and the two diastereomers of dadahol A (**8Ci** and **8Cii**) were isolated from *T. orientalis* via bioassay-guided fractionation using antiplasmodial activity against a chloroquine-sensitive (D10) strain of *P. falciparum* as the biological indicator (Figure 2.6). These compounds were subsequently bioassayed against the K1 strain to determine relative activity in a drug resistant strain, and against a Chinese Hamster Ovarian (CHO) cell line, as a measure of cytotoxicity and selectivity (Table 4.1).

Natural products **8A**, **8Ci** and **8Cii** were significantly active against the chloroquine-sensitive strain of the parasite with IC_{50}'s of 0.8 µg/ml (1.2 µM), 0.4 µg/ml (0.5 µM) and 0.5 µg/ml (0.7 µM); respectively. The resistance index (RI) gives an indication of the relative activity of the compounds in a drug resistant and sensitive strain of *P. falciparum*. The lower the RI value, the greater the likelihood that the compound will be effective against the resistant strain. The RI values of all three compounds were significantly lower than that of the chloroquine control.

Table 4.1 *In vitro* antiplasmodial activity of natural compounds against the D10 and K1 strains of *P. falciparum* and cytotoxicity against CHO cells

Compound	D10: IC_{50} (µg/ml)	K1: IC_{50} (µg/ml)	CHO: IC_{50} (µg/ml)	RI	SI (D10)
8A					
Dadahol B	0.8	1.1	71.8	1.4	90
8Ci					
Dadahol A (*erythro*)	0.4	0.6	88.3	1.5	221
8Cii					
Dadahol A (*threo*)	0.5	0.8	74.3	1.6	149
Emetine			0.05		
Chloroquine	0.015	0.13	18.5	9	1233

Selective index (SI) = IC_{50} CHO / IC_{50} D10

Resistance index (RI) = IC_{50} K1 / IC_{50} D10

The selectivity index (SI) is a ratio of cytotoxicity to antiplasmodial activity and gives a general indication of the specific activity. The greater the SI value, the greater the potential therapeutic window. The *erythro* and *threo* forms of dadahol A (**8Ci** and **8Cii**; respectively) showed limited cytotoxicity at the active concentrations (SI > 100). Dadahol B (**8A**), which was a mixture of the two diastereomeric forms, was shown to be relatively less active and selective than the dadahol A diastereomers despite differing from them by just one less methoxy group in the B ring. This observation and the fact that polysyphorin **(93)** and rourinoside **(94)**, which both have reported antiplasmodial properties (He *et al*., 2006; Zhang *et al*., 2001), also possess methoxy groups in the C-3' and C-5' positions of the B ring suggesting that this di-methoxy substitution is a key pharmacophore for antiplasmodial activity of 8-*O*-4 neoligans.

In considering basic criteria for antiparasitic drug discovery (Pink *et al*., 2005), a compound can be considered a hit if it is:

- Active *in vitro* against whole protozoa with an IC_{50} of ≤1 µg/ml
- Selective (at least tenfold more active against the parasite than against a mammalian cell line)

Based on this, dadahols A and B can be considered antiplasmodial hit compounds. The identification of antiplasmodial 8-*O*-4 neolignans from *T. orientalis* suggests that these molecules may play a role in the medicinal properties of the plant. Although their activity does not compare to chloroquine (IC_{50} 0.03 μM), the basic dadahol structure does provide an attractive scaffold for chemical modification with the aim of exploring structure-activity relationships and possibly improving overall activity and selectivity.

4.3 *In vitro* Antiplasmodial Activity of Synthetic Precursors and Analogues of Dadahol B

The diastereoselective synthesis of dadahol B (Chapter 3) resulted in several synthetic precursors and related compounds that were subjected to biological assaying, to provide some insight into structure activity relationships (Figure 4.1). The natural product **8A** was rescreened with the synthesised dadahol B diastereomers and analogues to compensate for batch to batch variation. Bioactivity was measured against the chloroquine-sensitive D10 strain of *P. falciparum*

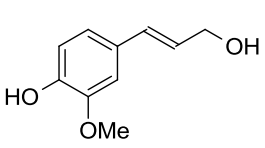

(37)
Coniferyl alcohol
IC_{50} > 100 μg/ml

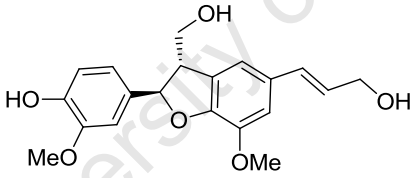

(38)
DHCA
IC_{50} = 5.97 μg/ml

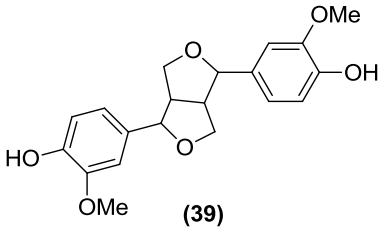

(39)
Pinoresinol
IC_{50} = 13.80 μg/ml

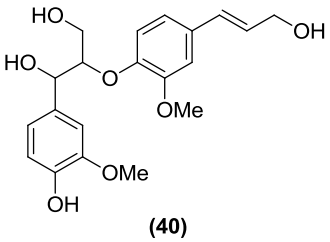

(40)
GGCE (~ 1:1 *threo/erythro)*
IC_{50} = 77.96 μg/ml

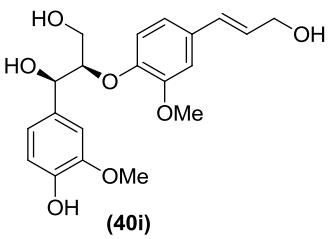

(40i)
GGCE (*threo*)
IC_{50} = 61.85 μg/ml

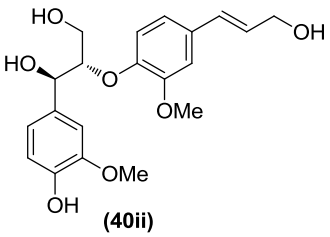

(40ii)
GGCE (*erythro*)
IC_{50} > 100 μg/ml

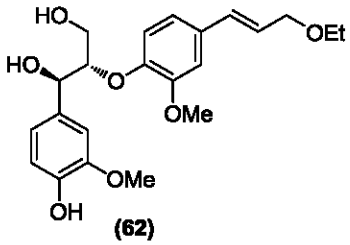

(62)
erythro 9′-ethoxy GGCE
IC_{50} = 16.39 μg/ml

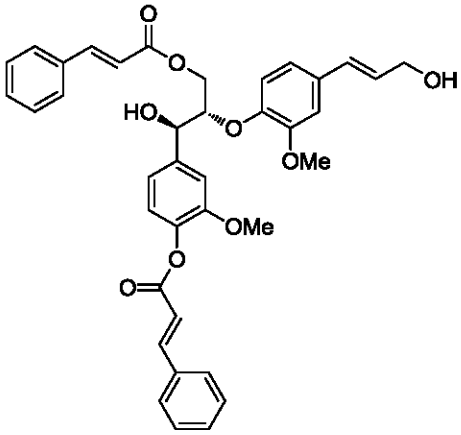

(53)
erythro 4,9-dicinnamoyl GGCE
IC_{50} = 6.09 μg/ml

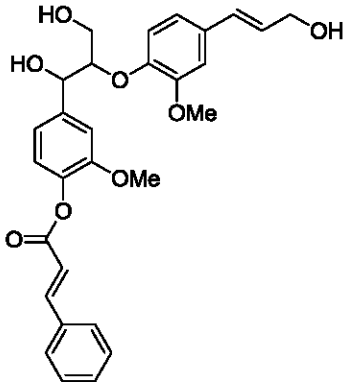

(54)
4-cinnamoyl GGCE
IC_{50} = 6.11 μg/ml

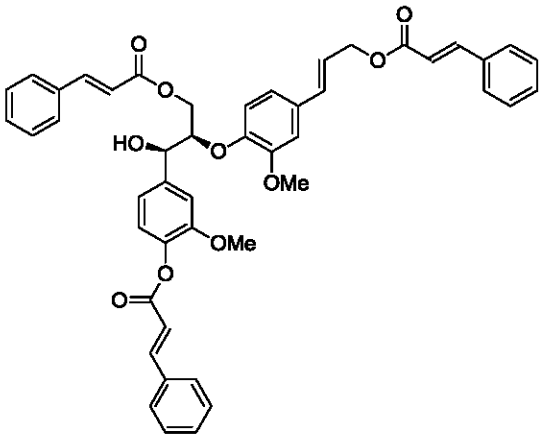

(55)
threo 4,9,9′-tricinnamoyl GGCE
IC_{50} = 2.86 μg/ml

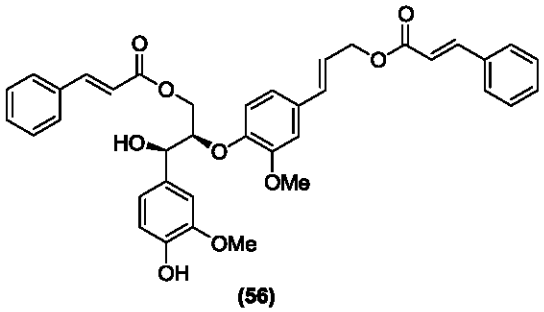

(56)
threo 9,9′-dicinnamoyl GGCE
IC_{50} = 7.31 μg/ml

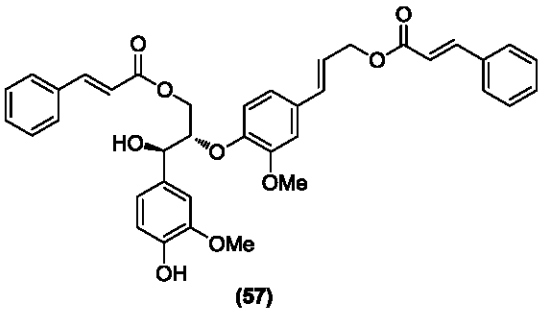

(57)
erythro 9,9′-dicinnamoyl GGCE
IC_{50} = 7.66 μg/ml

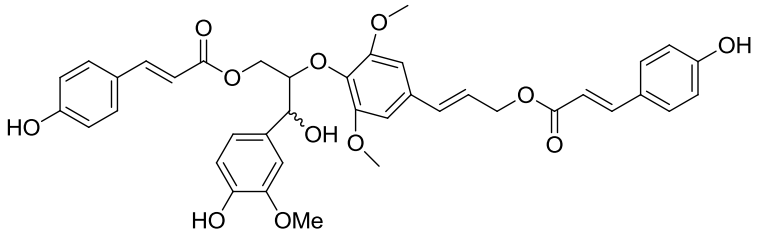

8A

Dadahol B (natural product ~ 1:1 *threo*/*erythro)*

IC_{50} = 3.39 μg/ml

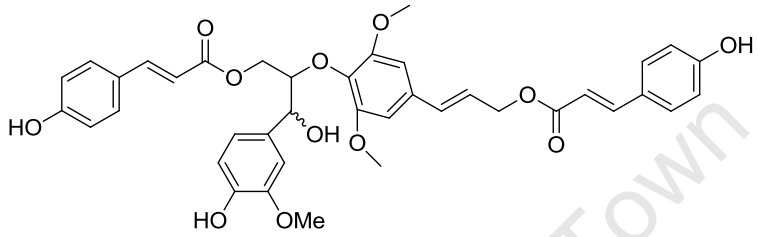

8A2

Dadahol B (synthetic product ~ 1:1 *threo*/*erythro*)

IC_{50} = 2.32 μg/ml

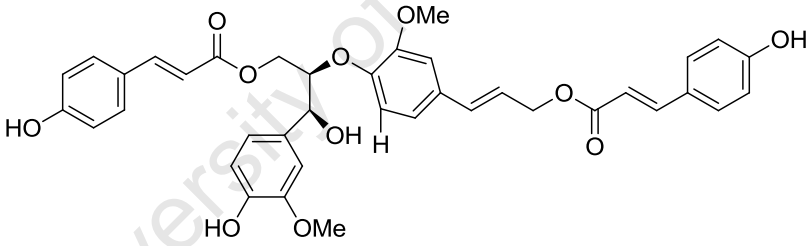

8Ai

Dadahol B (*threo*)

IC_{50} = 1.96 μg/ml

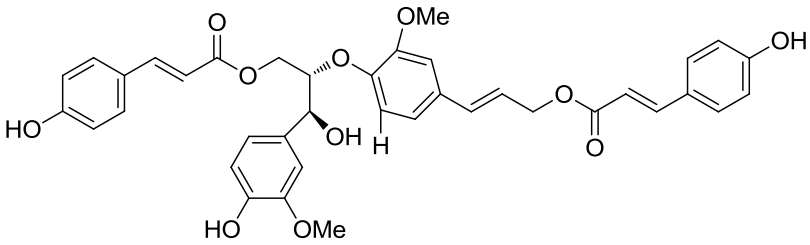

8Aii

Dadahol B (*erythro*)

IC_{50} = 3.36 μg/ml

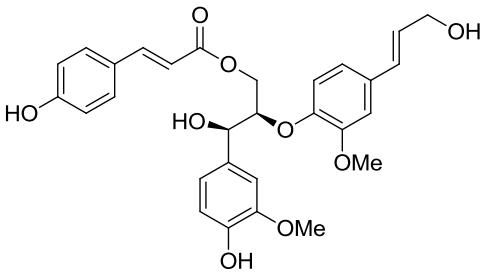

(67)
threo 9-coumaroyl GGCE
IC_{50} > 100 μg/ml

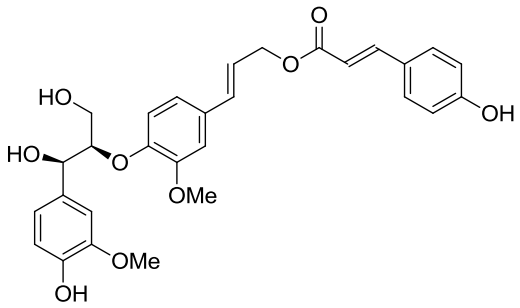

(68)
threo 9′-coumaroyl GGCE
IC_{50} = 3.28 μg/ml

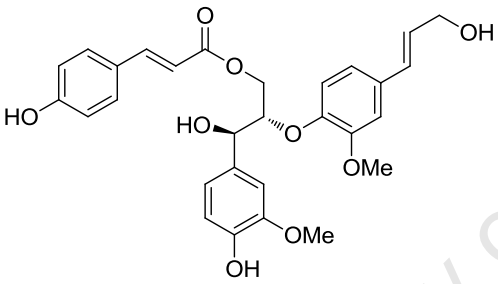

(69)
erythro 9-coumaroyl GGCE
IC_{50} = 27.46 μg/ml

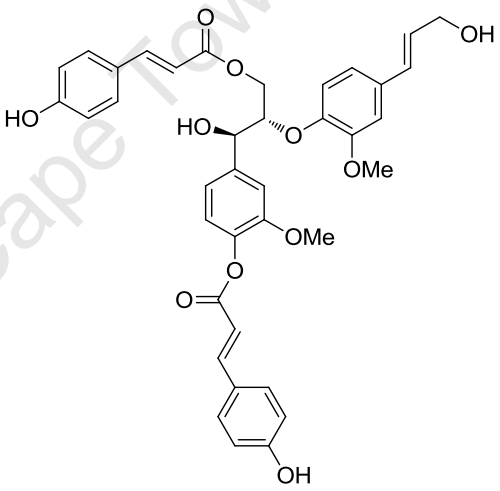

(70)
erythro 4,9-dicoumaroyl GGCE
IC_{50} = 2.96 μg/ml

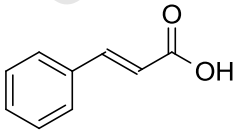

(51)
Cinnamic acid
IC_{50} > 100 μg/ml

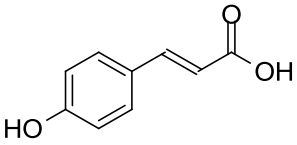

(41)
p-coumaric acid
IC_{50} > 100 μg/ml

Figure 4.1 *In vitro* antiplasmodial activity of synthetic precursors and analogues of dadahol B against the D10 strain of *P. falciparum.* Average IC_{50} of chloroquine = 0.016 μg/ml.

The monolignol, coniferyl alcohol **(37)**, did not show any activity (IC_{50} >100 µg/ml); and of the three oxidative coupling products (DHCA, pinoresinol and GGCE), the *β*-5 coupling product **(38)** showed the best antiplasmodial activity (IC_{50} 5.97 µg/ml). GGCE **(40)**, which forms the core of the natural product, did not show any significant activity in either of its diastereomeric forms. This suggests that the *p*-coumaryl groups are essential components for the antiplasmodial properties of dadahol B. However *p*-coumaric acid **(41)** itself was shown to be inactive (IC_{50} >100 µg/ml).

Cinnamic acid derivatives (CAD's) have been reported to arrest growth of all stages of intraerythrocytic *P*. *falciparum* in culture, in direct correlation with their hydrophobic character. But their application as antimalarial agents has been limited by their inherent toxicity – it has been observed that CAD's may inhibit some process in the host cell whose function is vital for parasite growth (Kanaani and Ginsburg, 1992). CAD's may inhibit ATP production in the parasite and its utilization by the host cell.

Rescreening of the natural product, dadahol B **8A**, resulted in a much higher IC_{50} (3.39 µg/ml) compared to its original bioassay result (IC_{50} 0.8 µg/ml). The pLDH assay generally gives reproducible results (Makler *et al*., 1993; Persson *et al*., 2006) and besides inter-assay variation based on different technicians conducting the assay and standard human error; this marked difference in activity can only be attributable to chemical instability or insolubility of the natural product in the culture medium. Due to the hydrophobic properties of dadahol B, it is likely to precipitate out of solution in the bioassay culture medium and the effective concentration will therefore vary with different rates of precipitation. In order to validate the original activity of the natural products, they were screened in an independent laboratory at the London School of Hygiene and Tropical Medicine and activity of both natural products was confirmed to be < 1 µg/ml against a chloroquine-sensitive (3D7) and chloroquine-resistant (K1) strain of *P. falciparum*.

The *threo* form of dadahol B, **8Ai**, was found to be relatively more active (IC_{50} 1.96 µg/ml) than the *erythro* form (**8Aii**) (IC_{50} 3.36 µg/ml). Of the various synthesized

monoesters, only the *threo* 9'-monoester **(68)** showed antiplasmodial activity (IC_{50} 3.28 µg/ml) comparable to the natural product (IC_{50} 3.39 µg/ml). Activity is lacking if just the 9-OH position is esterified, as in **(67)** and **(69)**, suggesting that this *p*-coumaryl group might not be a key pharmacophore of dadahol B. But if the phenolic or allylic position is also esterified, as in **(70)** and dadahol B **8A**, the antiplasmodial activity is more significant.

4.4 *In vivo* Antiplasmodial Activity of Dadahols A and B

In order to isolate sufficient quantities of dadahols A and B for *in vivo* biological evaluation, a targeted purification based primarily on liquid/liquid partitioning and flash silica gel chromatography was undertaken on the 1:1 DCM/MeOH extract (P05644-5B) of the twigs of *T. orientalis*. This yielded 80 mg (0.38% w/w of dry plant material) of dadahol B and 50 mg (0.25% w/w of dry plant material) of dadahol A. The compounds were isolated and evaluated as mixtures of the *threo* and *erythro* isomers due to challenges in completely resolving or stereoselectively synthesizing sufficient quantities of the individual diastereomers.

Dadahols A and B were evaluated for *in vivo* antiplasmodial activity against *P. berghei* using a 4-day suppressive test. The compounds were administered by subcutaneous injection at a dose of 100 mg/kg. The survival rate of the mice is summarized in Figure 4.2.

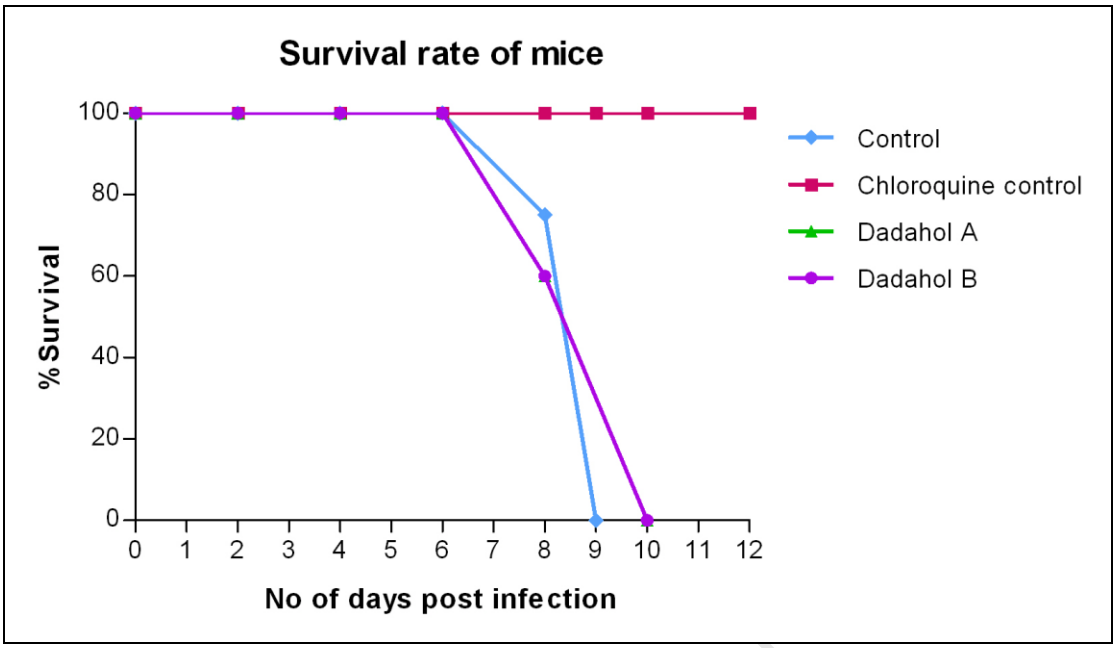

Figure 4.2 The survival rate of mice in each group after infection with *P. bergei ANKA*

In the control group, mortality was first observed on day 8. All the animals were dead on day 9. The two groups treated with dadahols A and B showed poor survival rate, with only 60% survival rate on day 8 and 100% mortality by day 10. All mice in chloroquine group survived for the duration of the experiment. There is no difference in the survival pattern between the treated groups and the control group, which shows that samples exhibited no antimalarial activity. Mice in the treated group also lost weight at more or less the same rate as the control group (Appendix VII), indicating that the treated mice were still sick.

The chloroquine group had an unusually high parasitemia of 3.7% on day 4 and even higher on day 6, reaching 5.1% (Figure 4.3). The parasitemia in the chloroquine treated group is usually maintained below 2% up to day 8-10. Nonetheless, the average percentage parasitemia in each treated group on day 6 was significantly high and more comparable to the control (untreated) group than the chloroquine treated group.

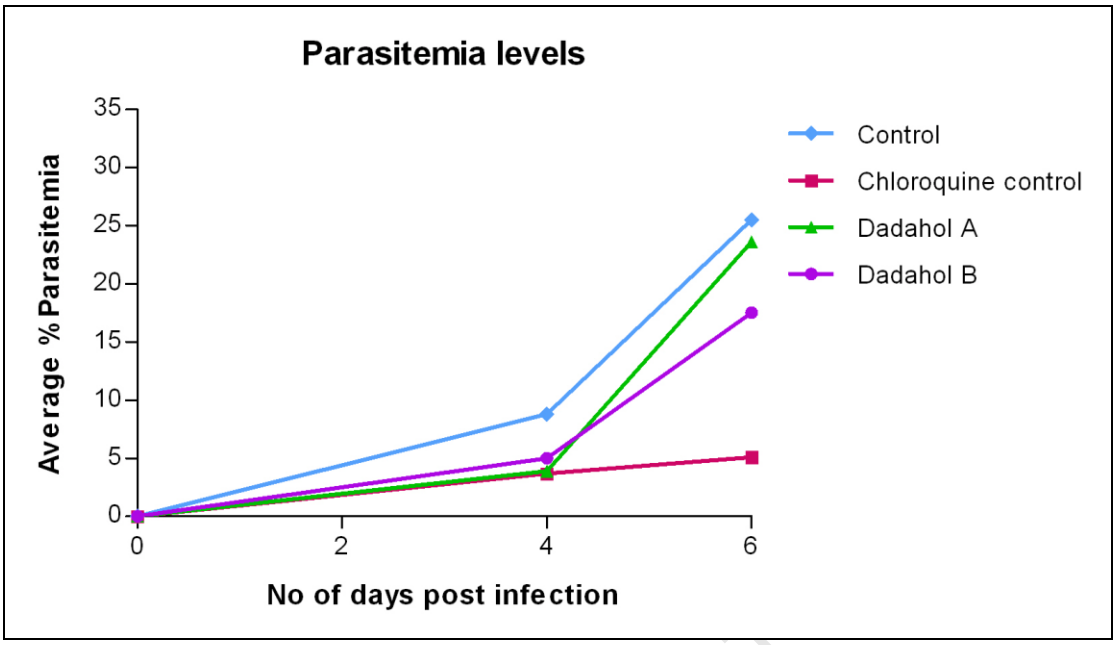

Figure 4.3 The average percentage parasitemia in each group at any given day after infection

The parasitemia reduction by each test compound is compared with that of chloroquine (Table 4.2). On day 4, the average percentage parasitemia reduction in the treated groups was comparable to the chloroquine group, but by day 6 the parasitemia reduction was significantly lower in the experimental groups compared to the choloroquine control group. This suggests that the antiplasmodial effect of the compounds does not last past the 4 days that the mice are treated. Dadahol B showed better parasite reduction than dadahol A on day 6, but overall the natural products showed poor antimalarial properties *in vivo* compared to chloroquine.

Table 4.2 The average % parasitemia and % reduction on Days 4 and 6

Group	Day 4		Day 6	
	Parasitemia (%)	Parasitemia percentage reduction (%)	Parasitemia (%)	Parasitemia percentage reduction (%)
Control	8.8		25.5	
Dadahol A	3.9	56.7	23.6	8.1
Dadahol B	5.0	42.2	17.5	31.6
Chloroquine	3.7	57.9	5.1	80.0

The *in vivo* results for dadahol A and B do not compare with that of the semi-purified *T. orientalis* extract (P05644-4B) previously evaluated (Chapter 2). The extract prolonged the survival period of treated mice and increased their tolerance to high parasitemia levels, indicative of a possible immune stimulant effect. Although dadahols A and B were relatively major components of this semi-purified extract (Appendix I), they were isolated through bioassay-guided fractionation based on *in vitro* antiplasmodial activity (which is not related to any possible immune stimulating effect), and it is possible that these were not the compounds responsible for the *in vivo* properties of the extract. As is often the case with medicinal plant extracts, the observed result could have been due to a synergistic effect of several components in the extract or more importantly the components of the extract could have been metabolized *in vivo* into metabolites with immune stimulating properties.

4.5 Pharmacokinetic Properties of Dadahols A and B

Pharmacokinetics (pK) describes the time course of a drug on entry into the body to its eventual excretion. It includes the study of the mechanisms of absorption and distribution of an administered drug/substance, the rate at which drug action begins and the duration of the effect, the chemical changes of the substance in the body (*e.g.* by CYP or UGT enzymes) and the effects of excretion of the metabolites of the drug/substance (Benet, 1984).

Pharmacokinetics is subsequently divided into several areas including the extent and rate of **a**bsorption, **d**istribution, **m**etabolism and **e**xcretion. This is commonly referred to as the **ADME** scheme. Since up or down regulation of these processes has been associated with the toxicity of many drugs, the study of ADME has been strongly connected to that of toxicology, hence the acronym, **ADMET**.

Most drugs are administered orally for the sake of convenience and compliance. Typically, a drug dissolves in the gastro-intestinal tract, is absorbed through the gut wall and then passes the liver to get into the blood. The percentage of the dose reaching blood circulation is called the bioavailablity. From there, the drug is

distributed to various tissues and organs in the body. The extent of distribution will depend on the structural and physiochemical properties of the compound. Some drugs can enter the brain and central nervous system by crossing the blood-brain barrier. Ultimately the drug will bind to its molecular target (*viz*. a receptor or ion channel) and exert its desired action.

Dadahols A and B had significant *in vitro* antiplasmodial activity but showed poor overall efficacy in a mouse model, suggesting that the compounds may have poor pharmacokinetic properties. In order to confirm this, the compounds were administered subcutaneously at a dose of 10mg/kg to healthy mice and blood samples were collected at relevant time intervals. Test compounds were subsequently extracted and levels were determined by LC-MS/MS. The test compound levels in mice were erratic and below the limit of quantification at several of the measured time points (Tables 4.3 and 4.4).

Table 4.3 Levels of Dadahol A in mice blood samples

Time (hour)	M1 (ng/ml)	M2 (ng/ml)	M3 (ng/ml)
0	0	0	0
0.5	21.1	BLQ	15.7
1.0	17.2	8.44	10.9
2.0	BLQ	14.1	25.7
5.0	46.9	25.6	BLQ
8.0	BLQ	BLQ	12.5

Table 4.4 Levels of Dadahol B in mice blood samples

Time (hour)	M1 (ng/ml)	M2 (ng/ml)	M3 (ng/ml)
0.0	0	0	0
0.5	BLQ	BLQ	13.1
1.0	31.3	11.0	9.26
2.0	24.5	20.2	26.8
5.0	BLQ	BLQ	BLQ
8.0	BLQ	BLQ	BLQ

BLQ = below limit of quantification

Levels of the natural products in mice were too low for PK analysis and modeling. The relatively low levels of the compounds in the animal samples might be an indication that these compounds are metabolized rapidly *in vivo*. This is most likely due to non-specific enzymatic cleavage of the *p*-coumaryl esters. The poor PK properties of Dadahols A and B explain their poor overall efficacy in a mouse model.

CHAPTER 5

Analogues of DHCA and GGCE

5.1 Biological Properties of DHCA and GGCE

One-electron oxidation of the monolignol, *E*-coniferyl alcohol **(37)**, results in "random" bimolecular radical coupling to afford initially dimeric products – the (±)-dehydrodiconiferyl alcohols (DHCA) **(38)**, (±)-pinoresinols **(39)**, and (±)-guaiacylglycerol 8-*O*-4'-coniferyl alcohol ethers (GGCE) **(40)** (Scheme 5.1).

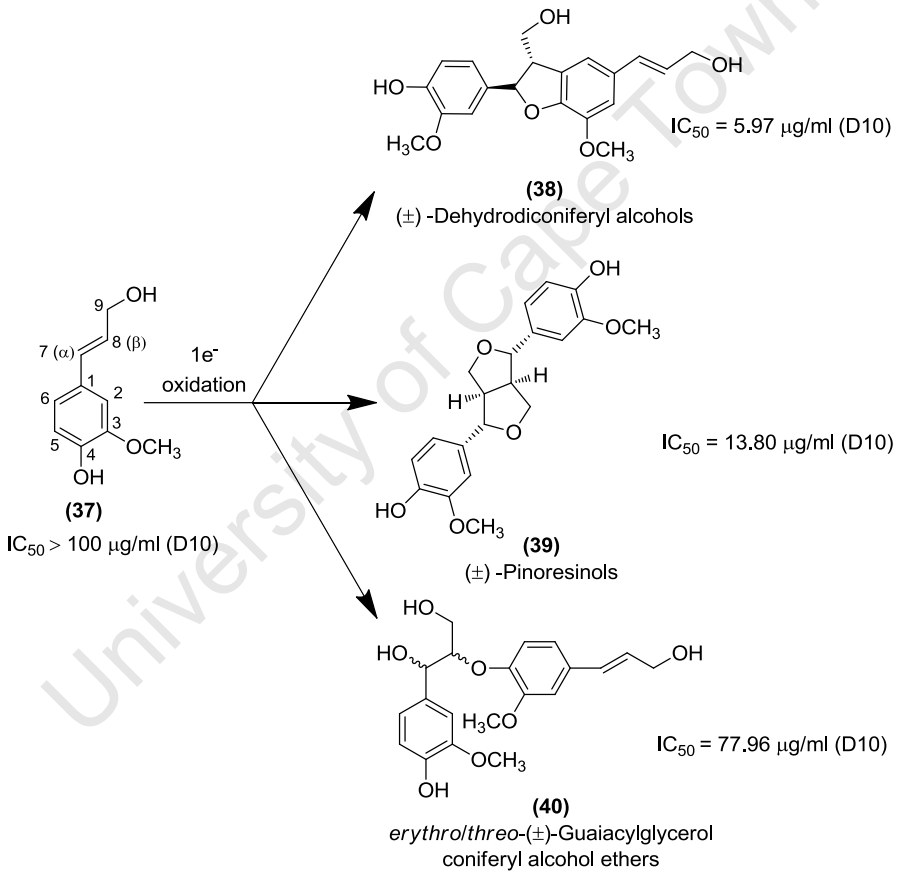

Scheme 5.1 Bimolecular phenoxy radical coupling products from *E*-coniferyl alcohol.

GGCE and its analogues have not shown any significant bioactivity while analogues of the benzofuran DHCA have been reported to have antioxidant (Takara *et al*., 2000), anti-cancer (Binns *et al*., 1987; Lee *et al*., 2007a; Lynn *et al*., 1987),

antiatherogenic (Rakotondramanana *et al*., 2007), antileishmanial (Miert *et al*., 2005) and anti-*Helicobacter pylori* (Hu and Jeong, 2006) activity. Analogues of DHCA which showed antiplasmodial activity include dehydrodiconiferyl dibenzoate **(95)** (Jensen *et al*., 2002), the gallate derivatized dihydrobenzofuran analogue **(96)** (Rakotondramanana *et al*., 2007), and dimerisation products of lipophylic esters of caffeic acid such as compound **(97)** (Miert *et al*., 2005) (Figure 5.1).

DHCA **(38)** showed better initial antiplasmodial activity than GGCE **(40)** (Scheme 5.1) and was therefore considered as an alternative scaffold for derivatisation. The similarity between the core of DHCA and highly active antiprotozoal bisamidine analogues such as **(98)**, which gave an IC_{50} of 6 nM against the chloroquine resistant K1 strain of *P. falciparum* (Bakunov *et al*., 2008), added to its attractiveness as a scaffold for analogue generation.

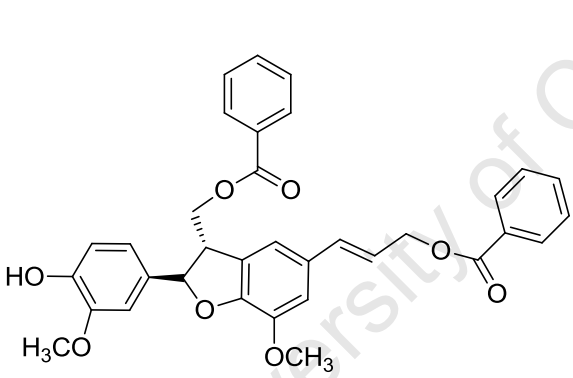

(95)

IC_{50} = 12 μM (D6)

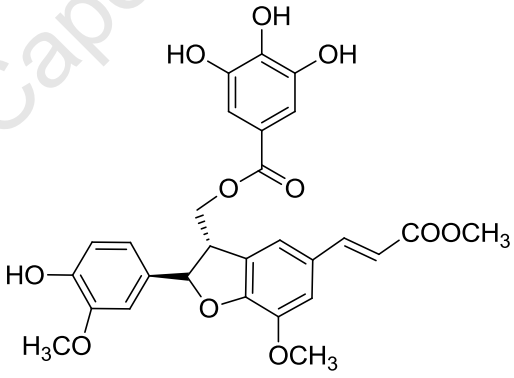

(96)

IC_{50} = 0.8 μM (FCM29)

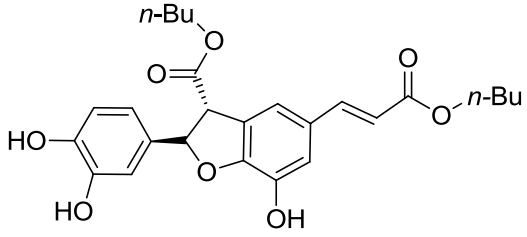

(97)

IC_{50} = 0.43 μg/ml (K1)

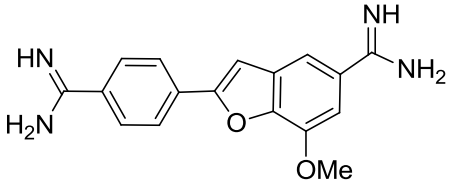

(98)

IC_{50} = 6 nM (K1)

Figure 5.1 Antiplasmodial activities of benzofuran analogues

5.2 Approaches to Derivatisation of DHCA

Based on literature precedent on antiplasmodial pharmacophores, synthetic and medicinal chemistry approaches, and making use of readily available organic reagents, a series of analogues based on DHCA **(38)** were considered with the aim of not only improving bioactivity but also to study and compare selected synthetic routes, derivatisation techniques and substitution effects.

The two approaches selected for analogue generation were:

- Optimisation of the ester moiety by preparing a range of esters from cinnamic acid derivatives (Kanaani and Ginsburg, 1992) and related bulky acids with known biological properties

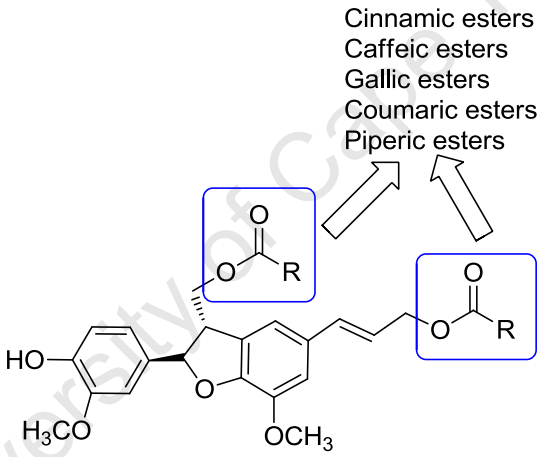

- Optimisation of the aromatic moiety using a range of readily available aromatic aldehydes with alternative substituents

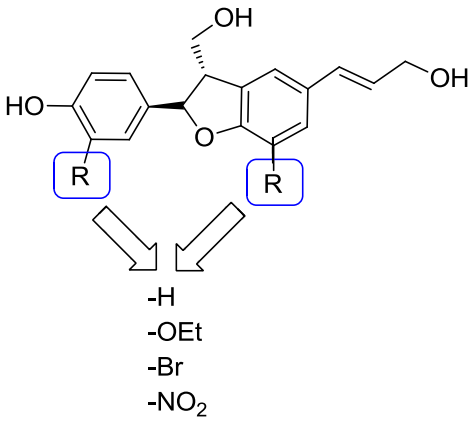

5.3 Auto-oxidation Products of DHCA and GGCE

Upon standing, the allylic alcohols of DHCA **(38)** and GGCE **(40)** were observed to gradually undergo spontaneous oxidation to their aldehyde forms, **(99)** and **(100)**; respectively (Scheme 5.2). Although compound storage under nitrogen significantly reduced this conversion, it was still necessary to remove traces of the auto-oxidation products by column chromatography prior to major processes and reactions (*viz*. GGCE diastereomer separation). Traces of auto-oxidation products were also observed as by-products during preparation and synthesis of analogues of **(38)** and **(40)**.

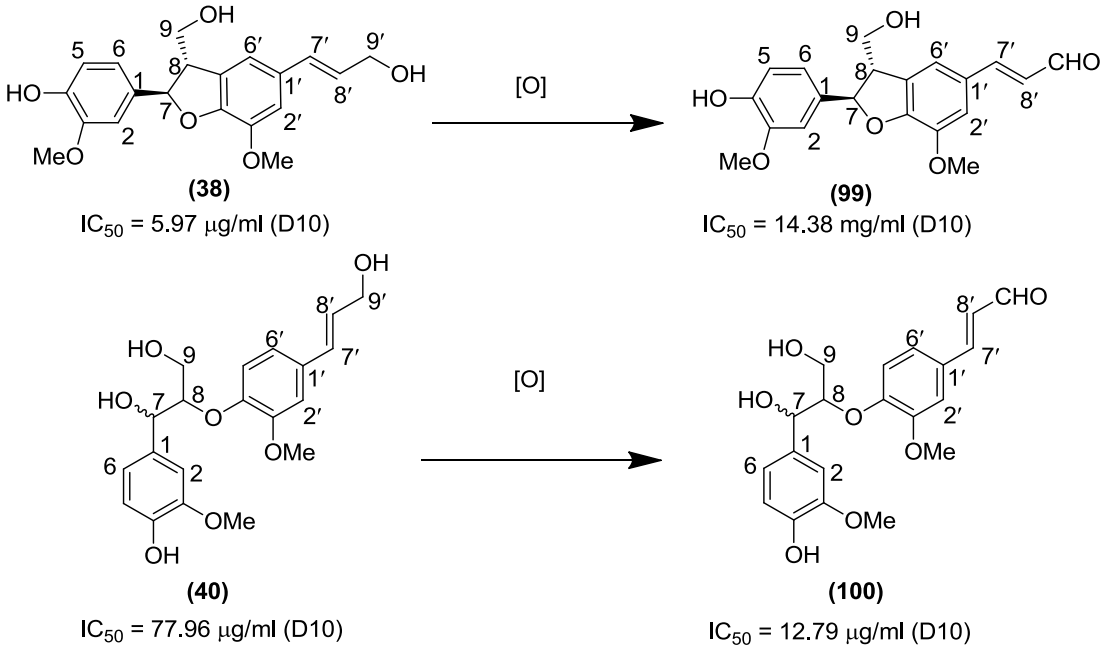

Scheme 5.2 Auto-oxidation products of DHCA and GGCE

Biological assaying of the auto-oxidation products revealed that the aldehydic form of DHCA **(99)** had reduced antiplasmodial efficacy (IC_{50} 14.38 µg/ml) while that of GGCE **(100)** showed improved activity (IC_{50} 12.97 µg/ml) relative to the parent compounds.

5.4 Alternative Preparation of DHCA

In order to produce additional quantities of the benzofuran DHCA **(38)** for derivatisation, an alternative synthesis (Scheme 5.3) was adopted using more readily available reagents ferulic acid **(101)** as the starting material and silver(I) oxide as the oxidant. In dichloromethane, DHCA **(38)** was the only major product and the yield was increased to over 20% (as opposed to the 10 -15 % yield obtained using the expensive and condition-dependent peroxidase).

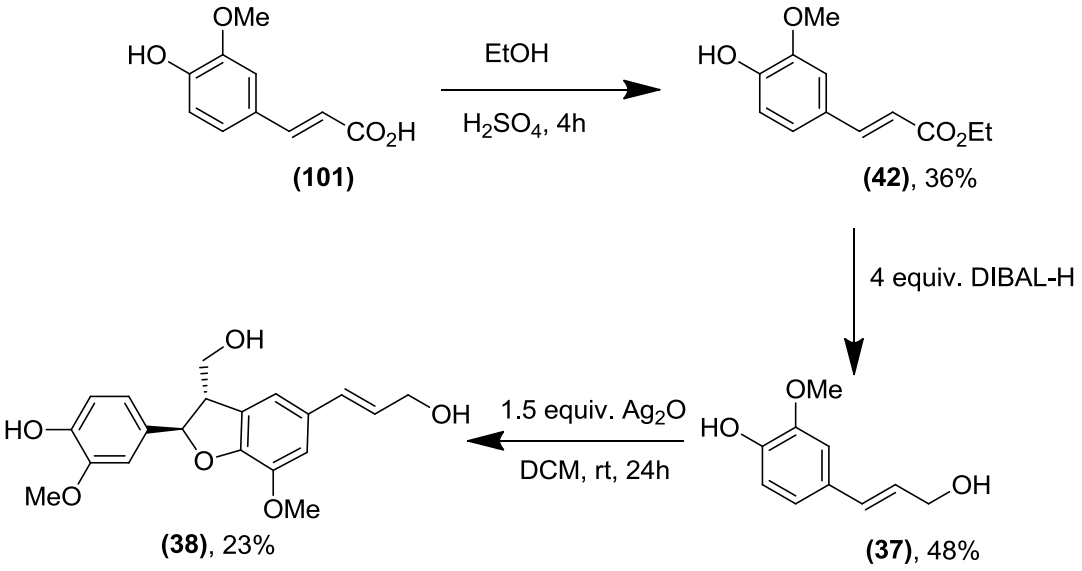

Scheme 5.3 Alternative synthesis of DHCA

In order to further improve on this yield, *N*,*N*-dimethylformamide (DMF) was investigated as an alternative solvent for the oxidative coupling reaction. However, in DMF the reaction yielded a mixture of products (Scheme 5.4), with compound **(102)** being a major product (8% yield). NMR analysis revealed that **(102)** was also a mixture of diastereomers and was closely related to GGCE, with a methoxy group in the 7-position. DMF promotes *β*-*O*-4 coupling and the *β*-*O*-4 quinone methide intermediate (Chapter 3; Scheme 3.5) most likely picked up a methoxy ion from impurities in the solvent. Trace quantities (1.4%) of the aldehyde **(103)** form of **(102)**, were also recovered. Neither of these GGCE analogues showed any antiplasmodial activity. DHCA **(38)** and its aldehyde **(99)**, were also isolated in comparable yields.

However, dichloromethane was reverted to as the solvent of choice for scale-up preparation of DHCA.

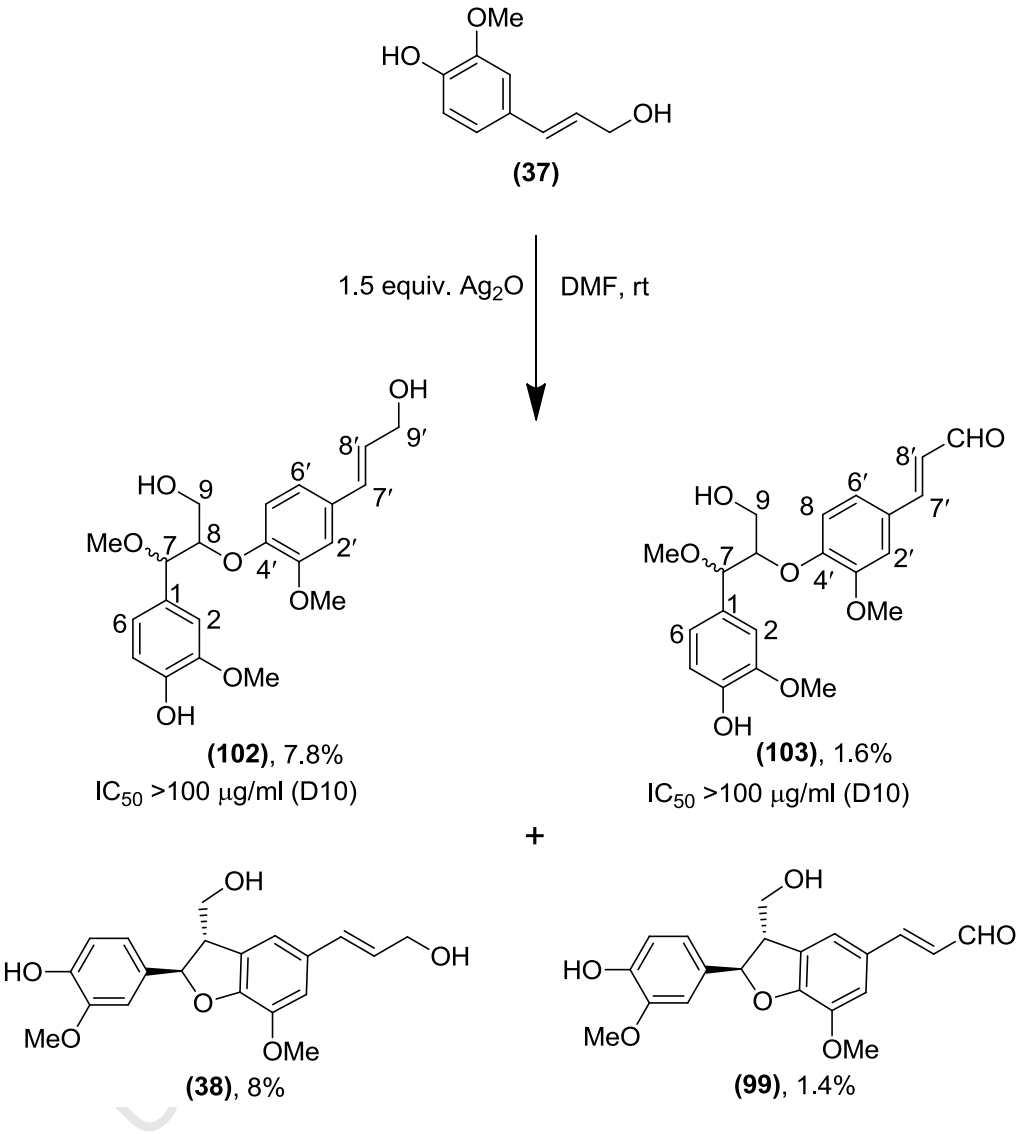

Scheme 5.4 Silver(I) oxide dimerisation of coniferyl alcohol in DMF

5.5 Acid Chloride Esterification of DHCA

Reaction of DHCA with *p*-nitrobenzoyl chloride yielded the triester, **(104)** and the diester **(105)** (Scheme 5.5.). The high reactivity of the benzoyl chloride resulted in consumption of the acyl chloride and non-selective esterification at multiple sites. The *p*-nitrobenzoyl esters were fairly inactive relative to DHCA.

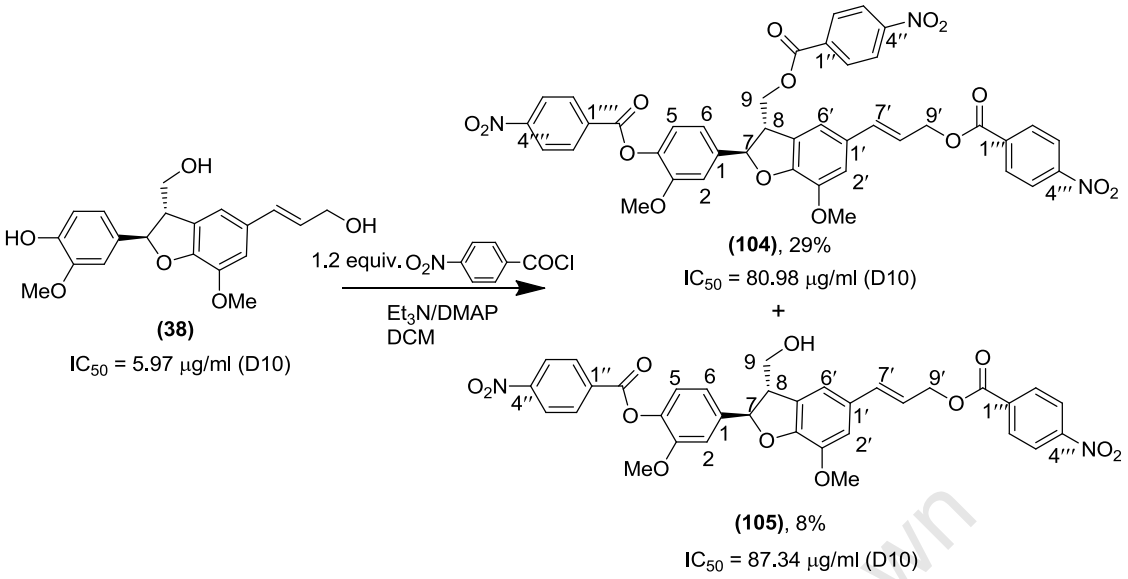

Scheme 5.5 Esterification of DHCA with *p*-nitrobenzoyl chloride

To assess if this reactivity will be the same for any acyl chloride, the acid chloride of cinnamic acid was prepared by reaction with oxalyl chloride **(106)** and a catalytic amount of DMF. The resulting Vilsmeier-Haack reagent **(107)** reacts with the acid **(51)** to give cinnamoyl chloride **(52)** (Scheme 5.6).

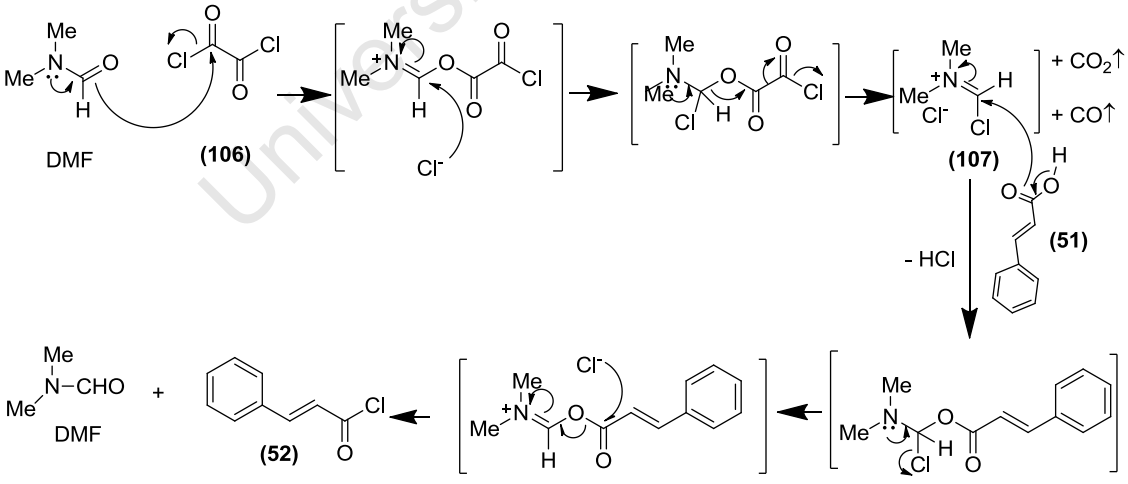

Scheme 5.6 Vilsmeier mechanism for cinnamoyl chloride formation

The reaction of one equivalent of cinnamoyl chloride **(52)** with DHCA **(38)** in the presence of triethylamine (Et_3N) led to a single fair yielding product **(108)** (Scheme 5.7.). NMR analysis revealed that there was no significant change in chemical shift of H-9 or H-9' in the proton NMR and no correlation was observed between the ester carbonyl and H-9 or H-9' in the HMBC. It was subsequently established that esterfication had occurred at the phenolic position. The deprotonation of the phenolic moiety of DHCA results in phenolate anions that are acylated in preference to the less acidic 9- and 9'-hydroxyls. This selectivity could not be altered by attempts to vary the reaction solvent, temperature or stoichiometry. Therefore the phenolic position would have to be protected in order to selectively esterify the other hydroxyls.

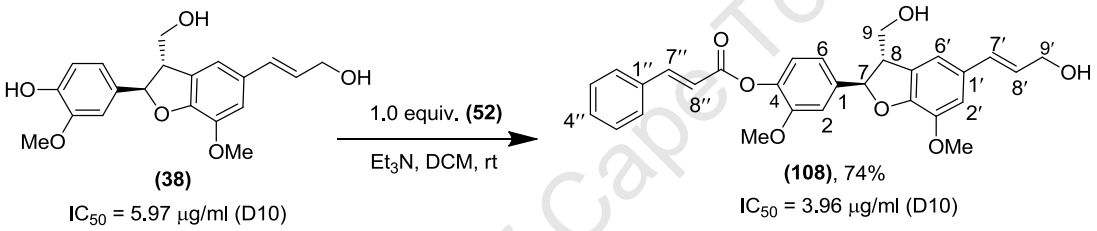

Scheme 5.7 Reaction of DHCA with cinnamoyl chloride

The 4-cinnamoyl analogue of DHCA **(108)** showed comparable antiplasmodial activity (IC_{50} 3.96 µg/ml) to the parent compound **(38)** (IC_{50} 5.97 µg/ml).

5.6 Protection of the DHCA Phenol

In order to circumvent the higher reactivity of the phenolic moiety of DHCA, it needed to be protected prior to reaction with the acid chloride. Silylation was considered as the preferred route due to the convenience of tetra-*n*-butylammonium fluoride (TBAF) deprotection and the sensitivity of the substrate to harsher deprotection methods, such as acid hydrolysis and hydrogenation.

Reaction of DHCA with 1.1 equivalents of *tert*-butyldimethylsilyl chloride (TBS-Cl) resulted in silylation of the primary hydroxyl groups in preference to the phenol to yield the silyl ethers **(109)** and **(110)** (Scheme 5.8) in low yield. Bases such as

imidazole are expected to complex with the most acidic, less hindered phenols and alcohols but in this instance, it is the allylic alcohol which is the preferred site for silylation. This selectivity to silylation was confirmed with a selection of alternate bases (2,6-lutidine and Et_3N) in the presence of a catalytic amount of 4-(dimethylamino)-pyridine (DMAP) at 0 °C. An alternative protective group, the tetrahydropyranyl (THP) group was also found to react exclusively at the allylic alcohol position.

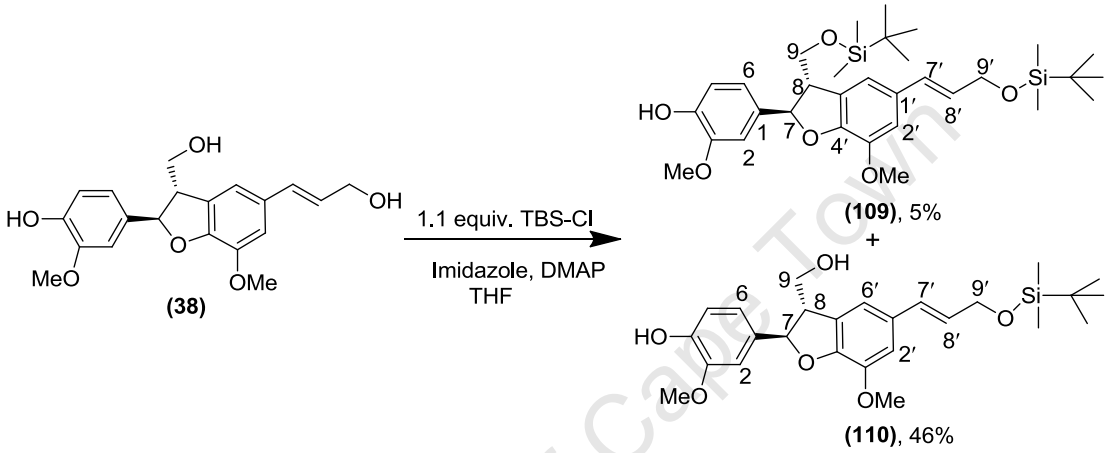

Scheme 5.8 Silyl protection of DHCA

A subsequent literature survey on the regioselective protection of hydroxylalkyl phenols confirmed that silyl and tetrahydropyranyl ethers are selectively formed at the hydroxyalkyl positions (Ballini *et al*., 1997; Sefkow and Kaatz, 1999). Perfluoroaryl derivatives, allyl bromide (van der Leij *et al*., 1981), *t*-butyoxycarbonyl (Boc) anhydride (Houlihan *et al*., 1985), acetylimidazole (Hagiwara *et al*., 1998) and trityl chloride (Sefkow and Kaatz, 1999) have all been used to selectively protect phenol groups. Most of these procedures required specialized reagents and conditions or harsh deprotection methods.

An attempt to use trityl chloride to selectively protect the phenolic position of DHCA proved successful, yielding the trityl ether **(111)** in 55% yield (Scheme 5.9). However scale-up attempts resulted in a mixture of tri- and di-trityl ethers which were difficult to separate. Deprotection also proved challenging, with even the most facile methods

recommended for acid-sensitive compounds (Pathak *et al*., 2001), resulting in complex mixtures of decomposition and rearrangement products.

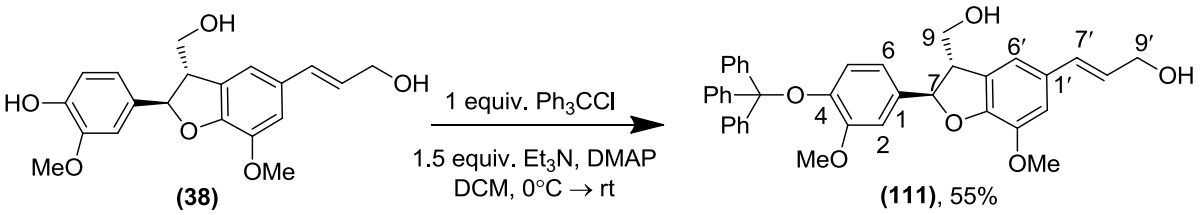

Scheme 5.9 Trityl protection of DHCA

5.7 Alternative Esterification Techniques

With phenolic protection proving unsuccessful, the next approach was to consider alternative esterification techniques.

The Mitsunobu esterification has been reported to be successfully applied to the chemoselective esterification of polyphenolic acids with polyphenolic alcohols (Appendino *et al*., 2002). However, no reaction was observed between DHCA **(38)** and gallic acid **(112)** under reported conditions (Scheme 5.10) and variations thereof (*viz*. longer reactions times, heating, and sonication).

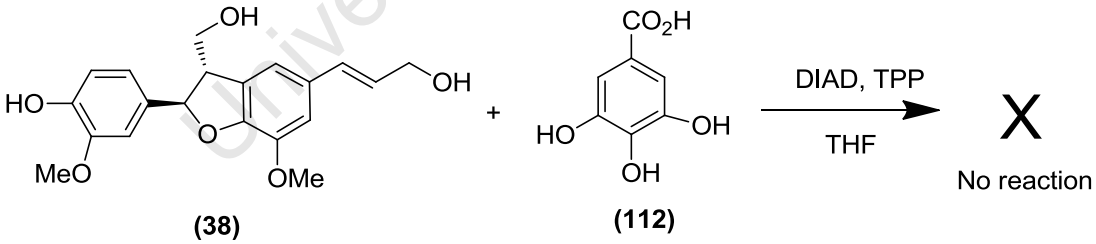

Scheme 5.10 Mitsunobu reaction between DHCA and gallic acid

In assessing other typical condensing agents used in ester synthesis, trifluroacetic anhydride also proved unsuccessful, while dicyclohexylcarbodiimide (DCC) coupling (Stechlich esterification) between DHCA **(38)** and silylated *p*-coumaric acid **(66)** in the

presence of DMAP resulted in esterification primarily at the 9-OH and 4-OH positions (Scheme 5.11) to yield the monoesters **(113)** and **(114)**.

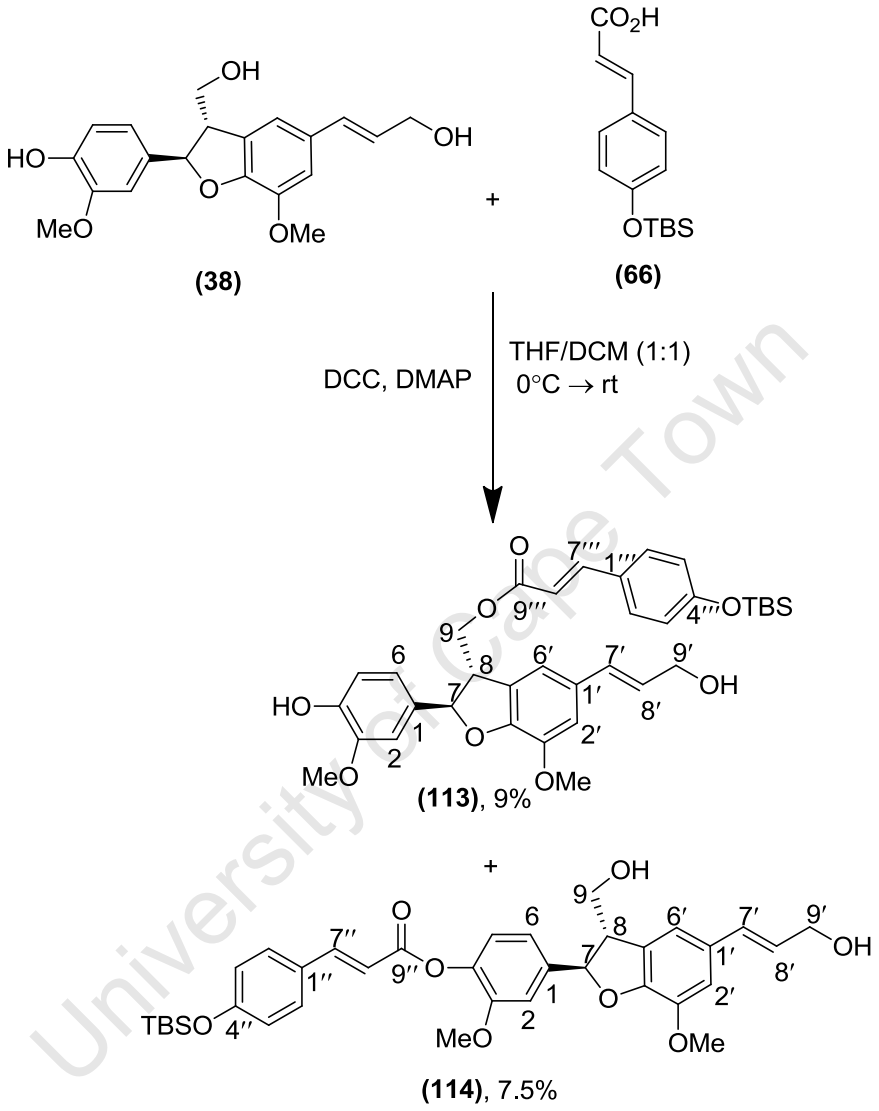

Scheme 5.11 DCC coupling between DHCA and protected *p*-coumaric acid

As with GGCE **(40)** (*cf* Chapter 3), CDI coupling proved the most selective in yielding a range of different possible esters. The reaction between DHCA **(38)** and cinnamic acid **(51)**, yielded the tricinnamoyl **(115)**, the 9,9'- **(116)** and 4,9'- **(117)** dicinnamoyl and the 9- and 9'- cinnamoyl analogues [**(118)** and **(119)**; respectively] (Scheme 5.12). Here too, the reaction was slow with poor rates of recovery. However, the

products were separable and sufficient in yield for characterisation and bioassaying. Only the 9,9'-dicinnamoyl analogue **(116)** showed comparable activity to the parent compound, DHCA **(38)** (IC_{50} 5.97 µg/ml).

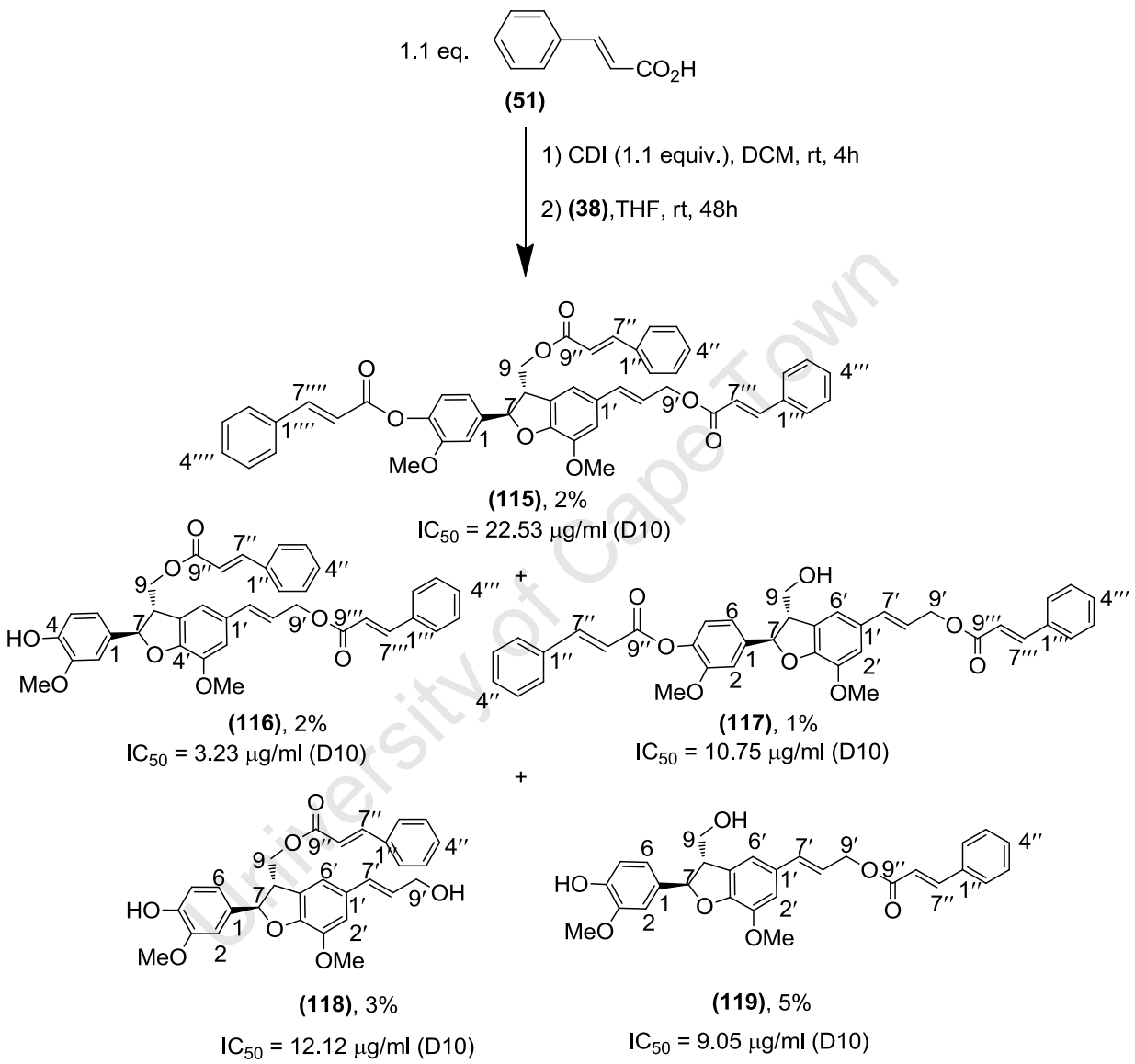

Scheme 5.12 CDI coupling between DHCA and cinnamic acid

CDI coupling between DHCA **(38)** and silylated caffeic acid **(120)** resulted in just one product in low yield (Scheme 5.13). NMR analysis revealed that this was a mixture of the 9- and 9'-caffeoyl mono-esters **(121)** and that, as previously observed, the silyl groups had been removed during the course of the reaction. The mixture was

inseparable and the antiplasmodial activity of this mixture of caffeoyl esters was found to be equivalent to that of the parent compound, DHCA **(38)**.

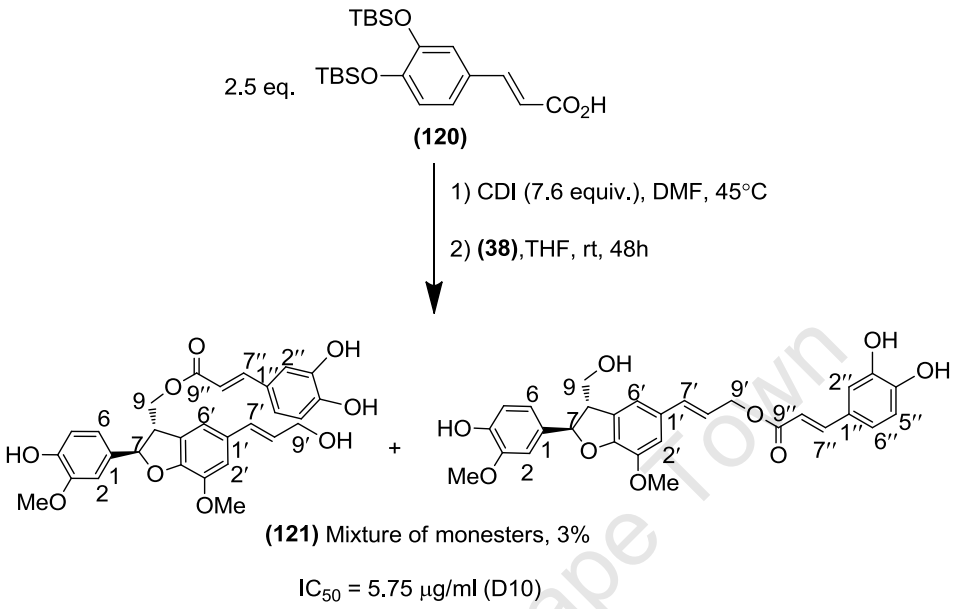

Scheme 5.13 CDI coupling between DHCA and protected caffeic acid

5.8 Alternative Routes to Esterification

Alternative routes to esterification of DHCA **(38)** were also investigated to circumvent susceptibility of protective groups and low yields achieved from CDI coupling.

5.8.1 Oxidative Coupling of Coniferyl Alcohol Esters

Based on the approach of Miert *et al*. (2005), who synthesized a series of dihydrobenzofuran lignans by oxidative dimerisation of caffeic acid esters **(122)**, the oxidative coupling of esters of coniferyl alcohol **(123)** was considered as an alternative route to preparing esters of DHCA (Scheme 5.14). However, the selective esterification of the 4-OH (as opposed to the desired 9-OH) position of coniferyl alcohol **(37)**, as well as challenges associated with oxidative coupling of bulky hydroxylated (*viz*. coumaroyl) ester substituents, made this approach impractical.

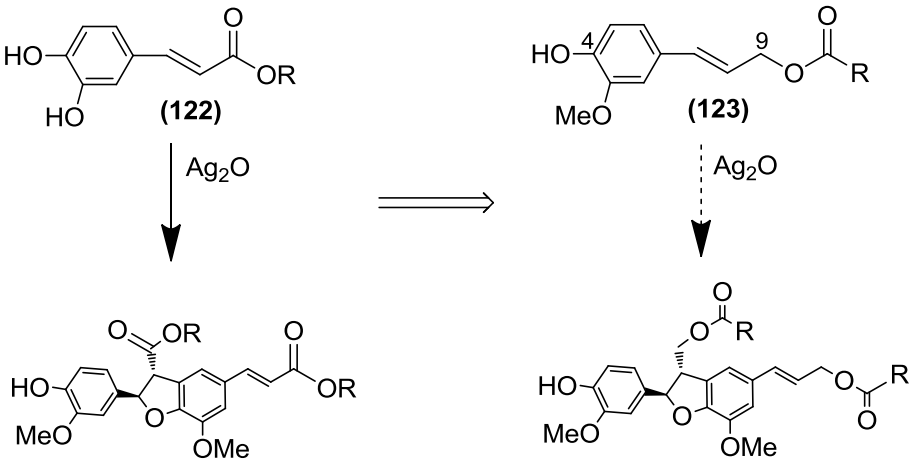

Scheme 5.14 Alternative approach to DHCA esterification based on oxidative coupling of caffeic acid esters

5.8.2 Oxidative Coupling of Ethyl Ferulate

A second approach was based on the oxidative coupling of the precursor ethyl ferulate **(42)** to yield the dimer **(124)**, which could then be protected as the silyl ether **(125)**, before reduction to the diol **(126)**, and subsequent esterification to afford the three silyl esters [**(127)** – **(129)**], which could each then be deprotected to yield the desired 9,9'-dicoumaroyl analogue **(130)**, the 9'-coumaroyl analogue **(131)** and the 9-coumaroyl analogue **(132)** (Scheme 5.15).

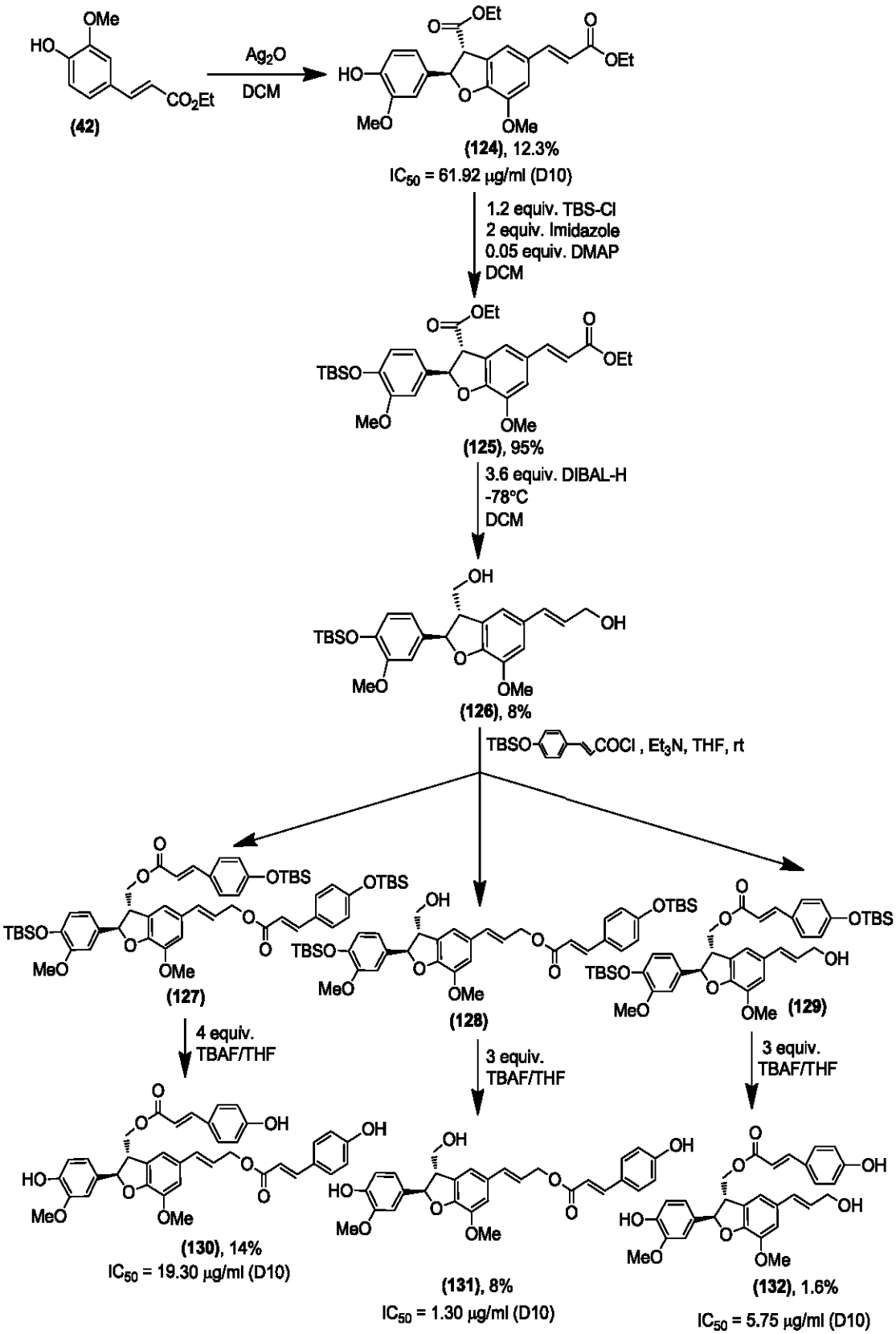

Scheme 5.15 Esterification of DHCA via ethyl ferulate coupling

The DIBAL reduction step resulted in low yields (17%) of the 4-*O*-silyl ether of DHCA **(126)**. The major products were found to be mixtures of rearrangement products such as the enol ether **(133)** (Scheme 5.16), which following deprotection to **(134)** was shown by NMR to lack the furan ring and contain an additional double bond.

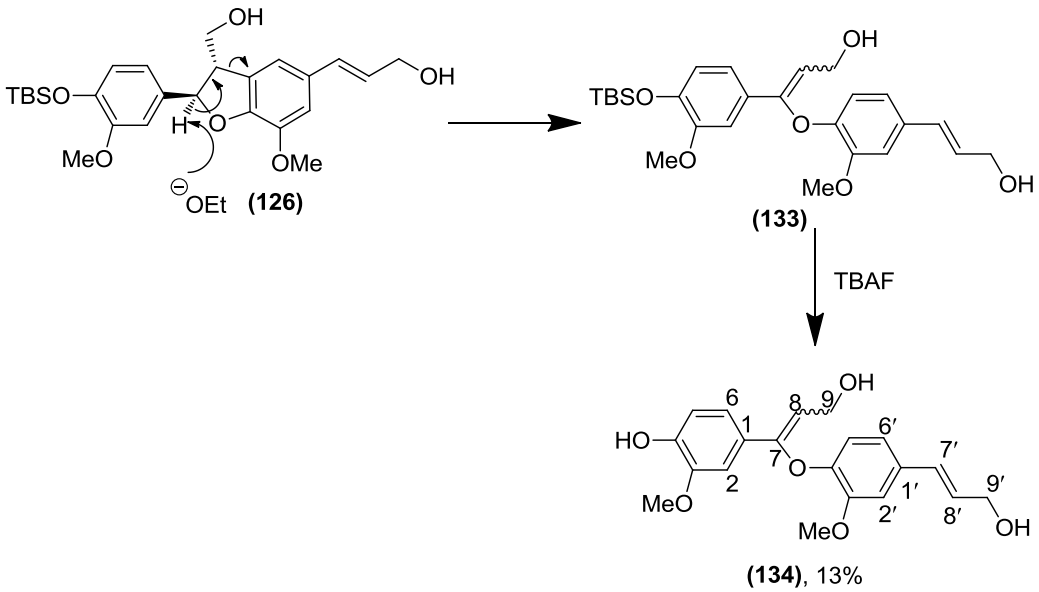

Scheme 5.16 Proposed ring opening mechanism leading to enol ether by-product

Ethyl ferulate **(42)** has been successfully reduced to coniferyl alcohol **(37)** using DIBAL-H in yields as high as 90% (Hu and Jeong, 2006). Therefore, it is most likely the conformational changes in the benzofuran afforded by the silyl group of the protected ethyl ferulate dimer **(125)** and its reduction product **(126)**, that exposes the furan moiety to ring opening side reactions. An electron withdrawing protective group (*viz.* tosylate) or a more inert reaction solvent (*viz*. toluene) might have helped improve yields; however the recovered product was sufficient to investigate the approach using at least two ester functionalities.

The piperonylic esters **(135)** and **(136)** were subsequently also prepared (Scheme 5.17) from the 4-*O*-silyl ether of DHCA **(119)**. In this case it appears that some deprotection had occurred during the esterification process to afford the 4,9,9'-tripiperonylic analogue **(136)**.

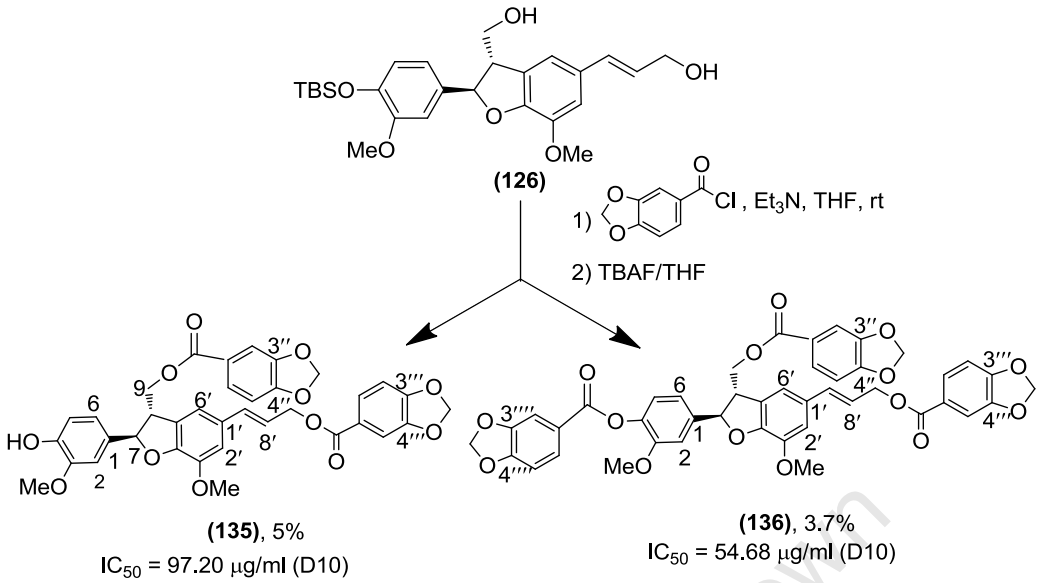

Scheme 5.17 Piperonylic ester synthesis

As the *p*-coumaric substituents of dadahol B was shown to contribute to the natural product's antiplasmodial properties, it was surprising to find that the corresponding 9,9'-dicoumaroyl analogue of DHCA **(130)** was relatively inactive (IC_{50} 19.30 µg/ml), even though DHCA **(38)** had better activity (IC_{50} 5.97 µg/ml) than the dadahol B core structure, GGCE **(40)** (IC_{50} 77.96 µg/ml). On the other hand, the 9-monoester **(132)** was equipotent (IC_{50} 5.75 µg/ml) while the 9'-monoester **(131)** showed improved activity (IC_{50} 1.30 µg/ml) relative to the parent compound, DHCA **(38)** (IC_{50} 5.97 µg/ml). Both the piperonylic esters, **(135)** and **(136)**, lacked any antiplasmodial activity at the maximum concentration tested.

5.9 DHCA and GGCE Ring Substitution

Changing the substituents on the aromatic rings of DHCA **(38)** was targeted to assess how this would affect the antiplasmodial activity of the dimer. A range of substituted monolignols were synthesised from readily available benzaldehydes (as for coniferyl alcohol: Chapter 3; Figure 3.9). These were subsequently subjected to oxidative coupling using the HRP/H_2O_2 oxidant system to yield substituted DHCA and GGCE analogues (Scheme 5.18).

Reaction yields indicated that electronic and steric effects of substituents may influence the oxidative coupling as yields of the *β*-5 dimer were relatively high despite the reaction conditions favouring *β*-*O*-4 coupling. No real conclusions can be drawn on the electronic and steric effects of the substitutents on the rate of oxidative coupling as the reaction of the ring activating ethoxy- **(137)** and electron withdrawing bromo- **(139)** substituted monolignols proceeded quickly to conclusion while, with the unsubstituted **(138)** and electron withdrawing nitro- **(140)** analogues, the reactions were slow and did not go to completion. A more detailed study using a broader range of substituents could be more useful in this respect but was beyond the scope of this study.

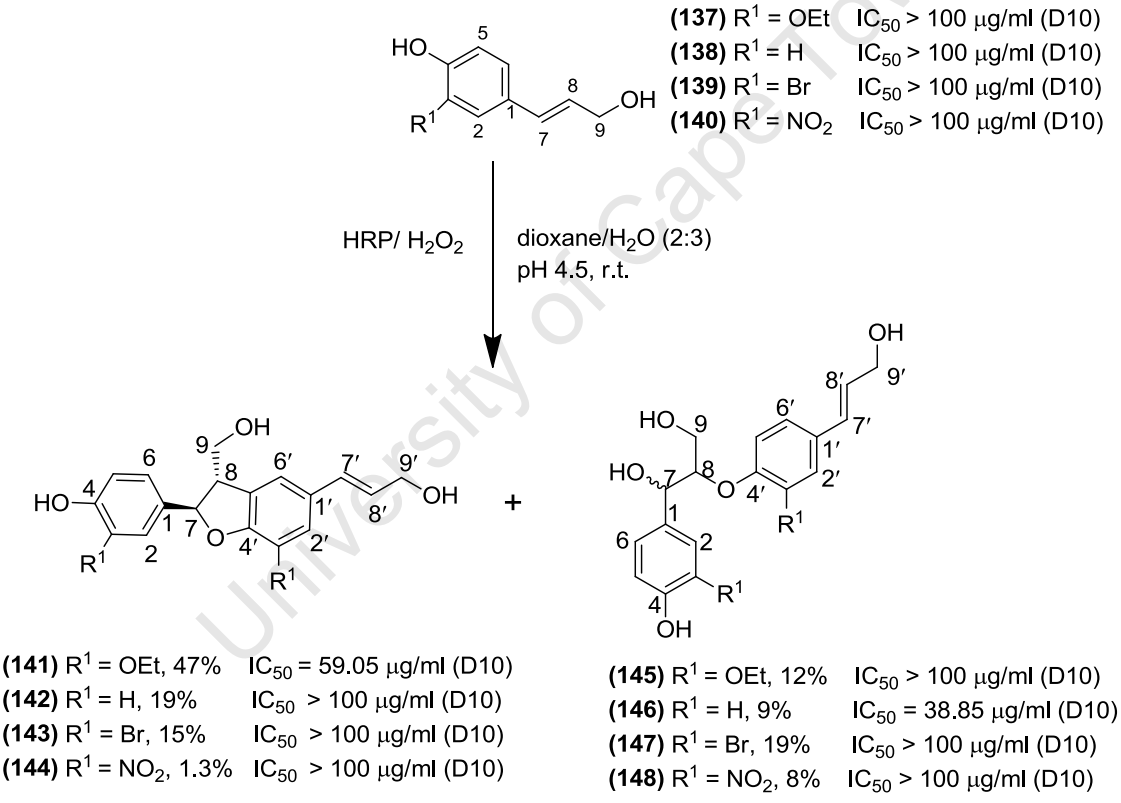

Scheme 5.18 Oxidative coupling of mono-substituted coniferyl alcohol analogues

With both *ortho* positions occupied, oxidative coupling of the dibromo-substituted monolignol **(149)** yielded only the *threo* **(150i)** and *erythro* **(150ii)** forms of the *β*-*O*-4 dimer, which were easily separable by column chromatography (Scheme 5.19a). A probable explanation for the *threo* diastereomer **(150i)** forming in preference (64%

yield) to the *erythro* diastereomer **(150ii)** (8% yield), is that due to bulkiness of the bromo substituents and exerted conformational form of the *β-O*-4 dimer quinine intermediate (*cf.* Chapter 3, Schemes 3.5 and 3.6) the nucleophilic addition of water at C-8 occurs from the less hindered face. Similarly, due to the steric effects of the bulky methoxy substituents, the dimethoxy-substituted monolignol (**151**) yielded only the *β-β* coupling product, syringaresinol **(152)** (Scheme 5.19b).

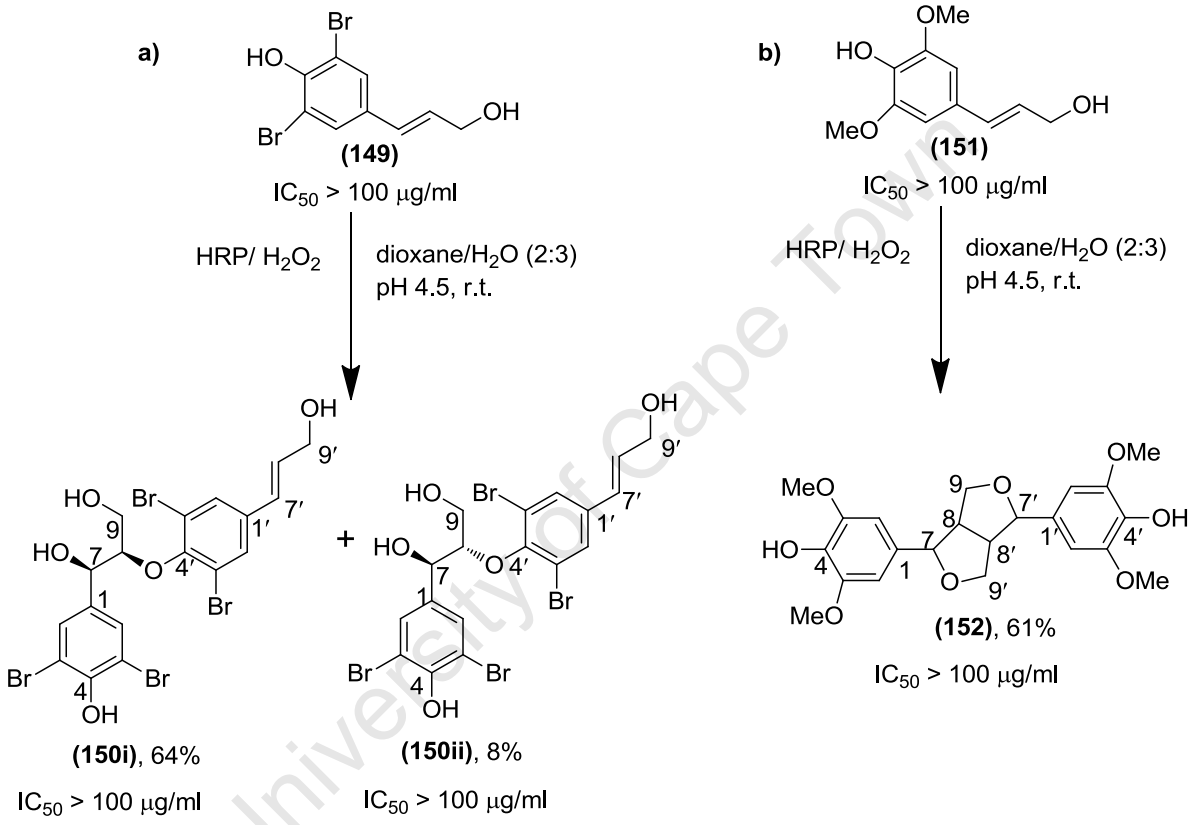

Scheme 5.19 Oxidative coupling of the disubstituted coniferyl alcohol analogues

None of the substituted coniferyl alcohol, DHCA and GGCE analogues showed any significant antiplasmodial activity.

5.10 Oxidative Cross-coupling

An important extension of oxidative coupling is the coupling between two structurally different phenols (cross-coupling). The synthesis of dadahol A (**8C**), for instance,

would require the oxidative coupling of coniferyl alcohol **(37)** and sinapyl alcohol **(151)** to form the core 8-*O*-4 neolignan core.

Oxidation of a mixture of two phenols can lead to a mixture of dimers of the individual phenols and cross-coupling products between the two phenols. When one phenol reacts faster than the other, for instance if it has a lower oxidation potential, dimerisation is favoured without formation of significant amounts of cross-coupling products (Syrjänen and Brunow, 2001).

Using a relatively basic approach the more reactive phenol, sinapyl alcohol **(151)** (oxidation potential ~ 0.38) and the oxidant (H_2O_2) were added slowly to the reaction mixture containing excess of the less reactive phenol, coniferyl alcohol **(37)** (oxidation potential ~ 0.44) (Syrjanen and Brunow, 1998). This resulted in a mixture of low yielding products, including the sinapyl alcohol *β*-*β* coupled dimer (syringaresinol) **(152)**, the *β*-5 cross-coupled product **(153)**, the coniferyl alcohol coupled dimers, DHCA **(38)** and GGCE **(40)**, and an inseparable mixture of the two cross- *β*-*O*-4-coupled products **(154) (**Scheme 5.20).

The yields of the cross-coupled products were low compared to the dimerization products, suggesting that slower modes of addition are required to promote cross-coupling. One approach to suppressing dimerisation would be to diffuse the more reactive phenol through a dialysis membrane (Syrjänen and Brunow, 2001). However this study was limited to the demonstration of this cross-oxidative coupling process and the evaluation of the bioactivity of the major products. The *β*-5 cross-coupled analogue **(153)** was the only product which showed some level of antiplasmodial efficacy (IC_{50} 8.27 µg/ml), in the same order of magnitude as that of DHCA **(38)** (IC_{50} 5.97 µg/ml).

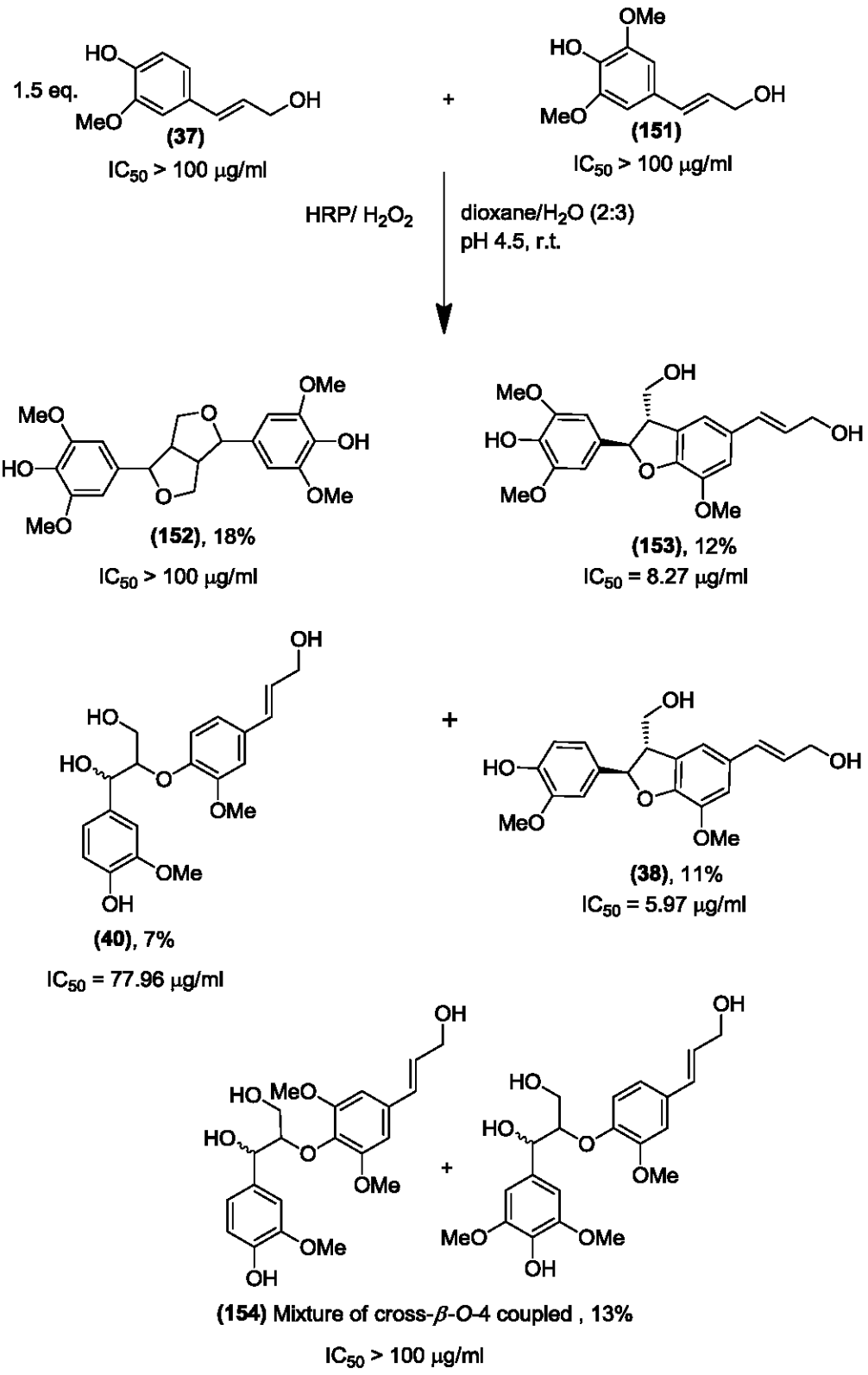

Scheme 5.20 Oxidative cross-coupling between coniferyl alcohol and sinapyl alcohol

CHAPTER 6
Conclusion

Natural products and medicinal plants still remain an important starting point for drug discovery and the identification of novel template compounds. The historical success of natural products as antimalarials and the large number of structurally diverse plant-derived compounds which have been shown to have antiplasmodial properties, provide justification for the continued effort in this area.

The identification of neolignans with antiplasmodial properties from *T. orientalis* suggests that they may play a role in the medicinal properties of the plant. Although, the neolignans themselves were shown to have poor antimalarial properties *in vivo*, the extract as a whole demonstrated some ability to prolong survival despite high levels of parasitic infection, providing further evidence of the medicinal properties of the plant. An approach worth considering is the combination of the extract with effective antimalarial drugs (*in vitro* and *in vivo*) to see if any synergistic effect is observed with the combination treatment.

The identification of dadahols A and B as the major compounds responsible for the observed antiplasmodial efficacy of the extract was confirmed by two bioassay-guided fractionation approaches using results from two independent screening laboratories (*i.e.* UCT's *p*LDH assay and Swiss TPH's ^{3}H-hypoxanthine incorporation assay) as the biological indicator. The new accelerated "HPLC biogram" methodology allowed for early recognition of the active compounds in the complex plant extract, requiring considerably less time and material compared to the classical reiterative approach. However, the accelerated approach is more suited to the dereplication of known compounds with published accurate mass and UV maxima data and is dependent on access to regularly updated electronic databases.

Although dadahols A and B are known compounds, this was the first report demonstrating any inherent biological activity. They were shown to have promising antiplasmodial activity (IC_{50} < 1 µg/ml) and selectivity (SI > 100) *in vitro*, but their lack

of antimalarial activity in an animal model and their poor pharmacokinetic properties demonstrated *in vivo*, made them unsuitable for further development as potential antimalarial drug leads. The natural products did, however, provide opportunities to study different synthetic techniques and approaches as well as investigate various structure-activity relationships. Biomimetic oxidative coupling formed the basis of these studies, proving its usefulness in the exploitation and study of biologically active lignans and neolignans.

The total diastereo-selective synthesis of dadahol B was demonstrated for the first time, allowing for the complete resolution of the proton NMR data of the *threo* and *erythro* forms. The 8-*O*-4´ neolignan core of dadahol B, *i.e.* GGCE, lacked antiplasmodial activity identifying the *p*-coumaroyl moieties (at the 9- and 9'-positions) as key pharmacophores of the natural product. The co-synthesis and bioassaying of the mono-esterified dadahol B analogues, revealed that the 9'-coumaroyl group contributed more to the bioactivity of the natural product than the ester at C-9.

DHCA, a by-product of the oxidative coupling step, showed better initial activity than GGCE, and was subsequently also used as a scaffold for analogue generation. Despite the instability of DHCA and GGCE to basic derivatisation techniques and low reaction yields, a fair number of analogues with different ester and aromatic ring substituents were synthesized. CDI coupling was shown to be the most selective esterification technique, eliminating the need to selectively protect the phenol group of the substrate. A new approach based on the oxidative coupling of the ethyl ferulate precursor, was also shown to be useful in the synthesis of 9,9'-diesters of DHCA. The aromatic ring substituent was shown to affect the rate and regioselectivity of oxidative coupling, although a more detailed study using a broader pool of substituents will be required to draw more substantial conclusions on the substituent effects.

None of the precursors, by-products or analogues synthesized in this study showed improved antiplasmodial activity relative to the natural products or chloroquine. However, opportunities exist to pursue with GGCE and DHCA as scaffolds for the

preparation of water-soluble derivatives (pro-drugs), which might result in more active and metabolically stable antimalarial lead compounds.

CHAPTER 7

Experimental

7.1 Plant Material

T. orientalis plant material was first collected in October 2001 between Darnall and the Tugela River mouth on the KwaZulu-Natal North coast (GPS co-ordinates: 31 23 307 E 29 14 66 S). The collection was undertaken by an independent plant collector contracted by the CSIR. Voucher specimen (BP00908) of the aerial plant parts was identified as *T. orientalis* (Linn.) Blume and retained at the South African National Biodiversity Institute (SANBI) Herbarium in Pretoria.

Permit applications were made to the KwaZulu-Natal Nature Conservation Board for subsequent recollections of *T. orientalis* twigs. Recollections were undertaken from the original collection site and surrounding areas by Jean Meyer, a SANBI botanist.

7.2 Extract Preparation

Plant material (152 g) was dried in an oven at 45 °C. Dried material was then ground to a coarse powder using a hammer mill. Powdered plant material was first extracted with de-ionized water and subsequently dried at 45 °C before extraction with 1:1 dichloromethane/methanol (DCM/MeOH).

For each extraction procedure the plant material was steeped in sufficient solvent for 4 - 5 h at room temperature, with occasional stirring. The solvent was subsequently drained. The aqueous extract was concentrated by freeze-drying (P05644C) and the organic extract (P05644B) was concentrated by rotary vacuum evaporation below 45 ºC. Extracts were stored at -20 ºC and the yields of the extracts were recorded in terms of fresh plant material.

Table 7.1 Yield of extracts obtained from *T. orientalis* twigs

Extract code	Extract description	Mass of extract (g)	% Yield
P05644B	Dichloromethane/Methanol (1:1)	0.9	0.6
P05644C	Water	1.2	0.8

7.3 General Fractionation Techniques

7.3.1 Liquid/liquid partitioning

Crude extract (1 g) was dissolved in methanol-water (9:1) (100 ml), and extracted with hexane (3 x 100 ml) (Figure 6.1). The combined hexane layers were evaporated under reduced pressure to yield the hexane-soluble fraction **(A)**. The methanol from the methanol/water layer was evaporated off under reduced pressure. An additional 30 ml of water was then added to the remaining water layer, which was subsequently extracted with dichloromethane (3 x 100 ml). The combined dichloromethane layers were evaporated under reduced pressure to yield the dichloromethane-soluble fraction **(B)**. The water layer was freeze-dried to give the aqueous fraction **(C)**.

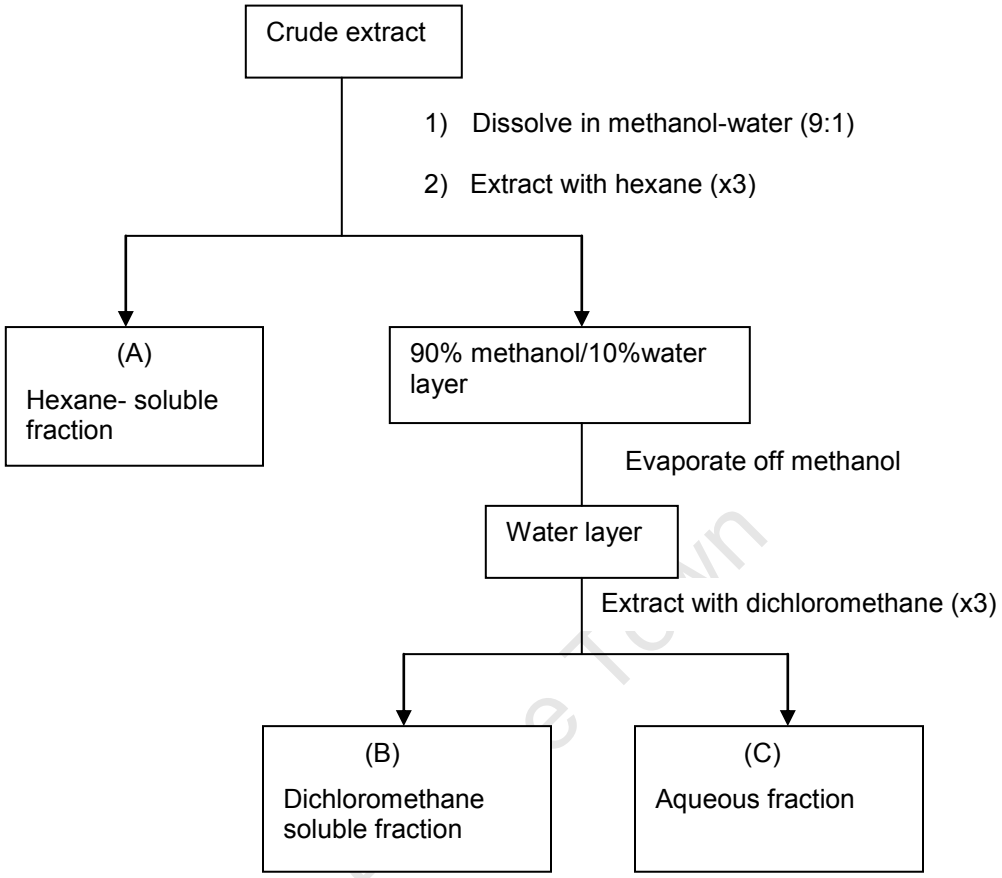

Figure 7.1 Liquid/liquid partitioning method

7.3.2 Column Chromatography

Silica gel column chromatography was conducted on various size columns, ranging from 1.5 – 6 cm in diameter, depending on the quantity of sample and the purification stage. In general, a ratio of 1:100 (sample : silica gel; w/w) was used. Silica gel 60 (0.063 - 0.2 mm) was sourced from Merck.

Column was packed with starting eluent before addition of sample. If sample was insoluble in starting eluent, it was adsorbed onto silica gel before applying to column.

Thin layer chromatography (TLC) was used to analyse and pool fractions. TLC was carried out on 0.20 mm pre-coated (SIL-25 UV_{254}) glass-backed plates. The plates were first viewed under UV, developed using a vanillin : conc. H_2SO4 (1 g : 100 ml) spray reagent and then heated.

7.4 Classical Bioassay-guided Fractionation

The fractionation process was guided by activity against the chloroquine-sensitive D10 strain of *P. falciparum* in the pLDH assay.

7.4.1 Bioassay-guided Fractionation of P05644B

697 mg of P05644B was subjected to liquid/liquid partiioning to yield:

1A (Hexane fraction); 354mg

1B (Dichloromethane fraction); 264 mg

1C (Aqueous fraction); 35 mg

Fraction **1A** was further fractionated by silica gel column chromatography using a gradient solvent of increasing polarity (5 % acetone/hexane - 30% acetone/hexane). The column was stripped with acetone. A total of sixteen pooled fractions (**2A** – **2P**) were generated.

Fraction **1B** was chromatographed on a silica gel column. Silica gel was eluted with 2% MeOH/DCM. Polarity was gradually increased by addition of MeOH in 2% increments to 10% MeOH/DCM. Column was stripped with MeOH. Sixteen pooled fractions were generated (**3A** – **3P**) (Figure 2.2).

7.4.2 Bioassay-guided Fractionation of P05644B-5B

A total of 102 kg of fresh twigs was recollected from Darnell in KwaZulu-Natal. The material was dried at 30°C and ground to yield 24 kg of material. This was extracted sequentially with de-ionized water (210 L) and DCM/MeOH (1:1) (170 L). The organic extract was concentrated down to 12.5 L and then subjected to liquid/liquid partitioning (i). The dichloromethane-soluble fraction was separated and evaporated in *vacuo* (60° C) to yield a total of 34.8 g of semi-purified extract (**4B**) (Figure 2.6).

5 – 10 g batches of extract **4B** were purified on 400 – 500 g of silica gel 60 (0.063 – 0.2mm) under vacuum pressure, using 2.5% MeOH/DCM as eluant (ii). Fractions were pooled according to their behavior on TLC (8% MeOH/DCM).

Pooled fractions were submitted for *in vitro* bioassaying against *P. falciparum* D10. Active fractions (**5D** and **5E**) were combined (8.6 g) and separated in 1 g batches on 40 g of Sephadex LH20 in methanol (iii) and fractions were pooled by TLC (8% methanol/dichloromethane) and bioassayed.

Further purification of the most active fraction (**6D**) was conducted in 200 – 300 mg batches on 10 g C-18 cartridges using a gradient eluent (10% acetonitrile/water to 100% acetonitrile increasing in 10% increments). Fractions were pooled by TLC analysis (8% MeOH/DCM).

A portion (240mg) of fraction **7D** was further separated on an Agilent semi-preparative HPLC system consisting of an auto sampler, high pressure mixing pump, column oven and DAD detector. Separation was achieved using an Eclipse XDB C-18 column and an isocratic 46% acetonitrile/water system. Four major peaks detected at 254.4 nm (Figure 7.2) were collected individually, pooled and evaporated (**8A** = 11mg, **8B** = 8mg, **8Ci** = 7mg, **8Cii** = 4mg).

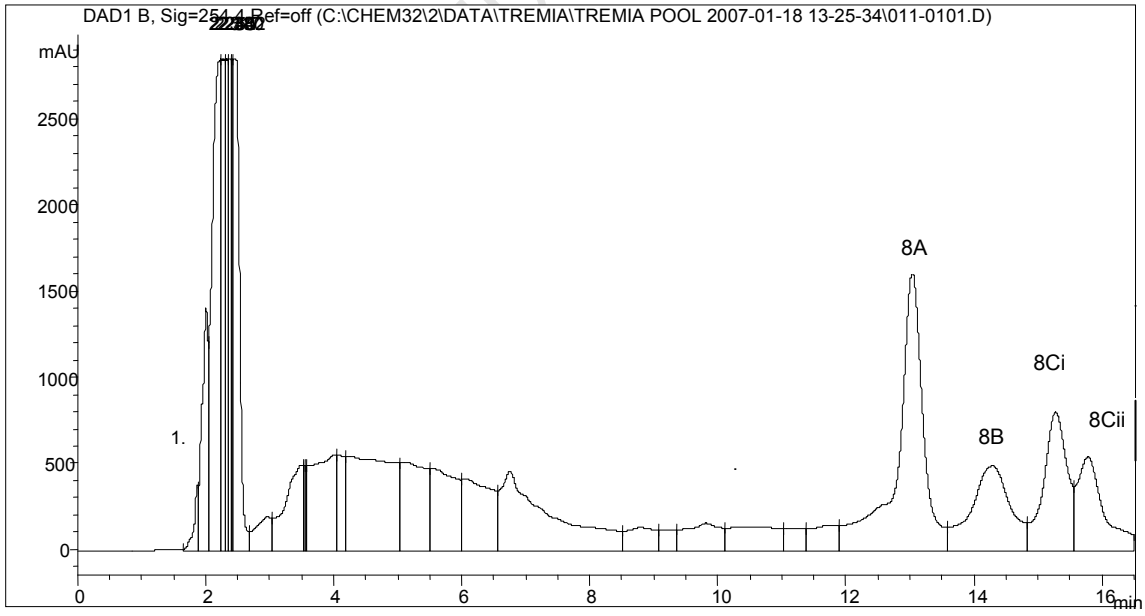

Figure 7.2 Chromatogram of semi-preparative HPLC purification

7.4.2.1 Structure of Compound 8Cii

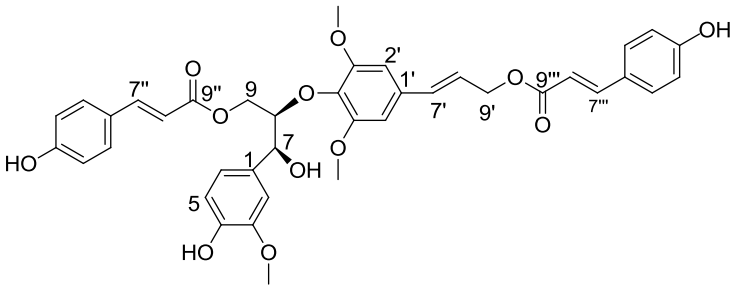

8Cii

threo-1-(4-hydroxy-3-methoxyphenyl)-2-[2,6-dimethoxy-4-{(1E)-3-(4-hydroxycinnamoyl)-1-propenyl}phenoxy]-3-(4-hydroxycinnamoyl)propan-1-ol

Common name: Dadahol A

HRESI-MS (m/z): 698.2367 (calcd for $C_{39}H_{38}O_{12}$ 698.2364)

R*f*: 0.67 (8% MeOH/DCM)

Optical rotation: $[\alpha]_D^{24}$ – 0.025°(*c* 0.1, MeOH); [lit. $[\alpha]_D^{20}$ + 20° (*c* 0.075, MeOH); (Su et al., 2002)]

1H NMR (acetone-d6), δH : 3.79 (3H, s, 3-OMe); 3.86 (6H, s, 3'-OMe; 5'-OMe); 4.02 (1H, dd, J = 4.8; 12.1 Hz, H-9b), 4.31 (1H, m, H-8), 4.44 (1H, dd, J = 3.11; 12.1 Hz, H-9a), 4.81 (2H, dd, J = 1.1; 6.2 Hz, H-9'), 4.99 (1H, d, J = 7.1 Hz, H-7), 6.25 (1H, d, J = 16.2 Hz, H-7''), 6.38 (1H, d, J = 15.9 Hz, H-7'''), 6.39 (1H, dt, J = 15.9; 6.2 Hz, H-8'), 6.68 (1H, br d, J = 15.9 Hz, H-7'), 6.73 – 6.90 (7H, m, H-5; H-6, H-2; H-3''; H-5''; H-3'''; H-5'''), 7.06 (2H, br s, H-2', H-6'), 7.37 (1H, d, J = 16.2 Hz, H8''), 7.48 (2H, d, J = 8.8 Hz, H-2''; H-6''), 7.55 (2H, d, J = 8.8 Hz, H-2'''; H-6'''), 7.64 (1H, d, J = 15.9 Hz, H-8''')

^{13}C NMR (acetone-d6), δ_C : 56.1(3-OMe, q), 56.5 (3'-OMe; 5'-OMe, q), 65.0 (C-9', t), 65.1 (C-9, t), 74.5 (C-7, d), 86.7 (C-8, d), 104.7 (C-2; C-6, d), 111.4 (C-2'; C-6', d), 115.3 (C-7''; C-7''', d), 115.7 (C-5, d), 116.7 (C-3''; C-5''; C-3''', C-5''', d), 124.4 (C-8', d), 126.7 (C-1''; C-1''', s), 131.0 (C-2''; C-6''; C-2'''; C-6''', d), 133.3 (C-4', s), 133.7 (C-1, d), 133.8 (C-1', s), 134.2 (C-7', d), 145.3 (C-8'', s), 145.7 (C-8''', d), 147.0 (C-4, s), 148.0 (C-3, s), 153.9 (C-3'; C-5', s), 160.9 (C-4''; C-4''', s), 167.1 (C-9'', s), 167.3 (C-9''', s)

7.4.2.2 Structure of Compound 8Ci

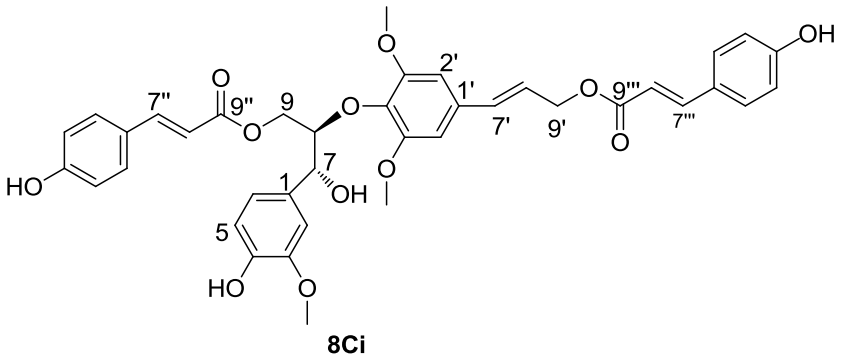

8Ci

erythro-1-(4-hydroxy-3-methoxyphenyl)-2-[2,6-dimethoxy-4-{(1E)-3-(4-hydroxycinnamoyl)-1-propenyl}phenoxy]-3-(4-hydroxycinnamoyl)propan-1-ol

Common name: Dadahol A

HRESI-MS, m/z: 698.2384 (calcd for $C_{39}H_{38}O_{12}$ 698.2364)

Rf: 0.64 (8% MeOH/DCM)

Optical rotation: $[\alpha]_D^{24}$ – 0.029°(*c* 0.1, MeOH); [lit. $[\alpha]_D^{20}$ + 20° (*c* 0.075, MeOH); (Su et al., 2002)]

^{1}H NMR (acetone-d6), δ_H : 3.85 (3H, s, 3-OMe); 3.86 (6H, s, 3'-OMe; 5'-OMe); 4.32 (1H, dd, J = 2.8; 11.8 Hz, H-9b), 4.46 (1H, dd, J = 7.6; 11.8 Hz, H-9a), 4.58 (1H, m, H-8), 4.81 (2H, dd, J = 0.9 ; J = 6.2 Hz, H-9'), 4.97 (1H, br m, H-7), 6.15 (1H, d, J = 15.9 Hz, H-8''), 6.38 (1H, d, J = 15.9, H-8'''), 6.39 (1H, dt, J = 15.9; 6.2 Hz, H-8'), 6.68 (1H, br d, J = 15.9 Hz, H-7'), 6.81 - 6.90 (7H, m, H-2, H-5, H-6, H-3''; H-5''; H-3'''; H-5'''), 7.06 (2H, br s, H-2', H-6'), 7.29 (1H, d, J = 15.9 Hz, H7''), 7.43 (2H, d, J = 8.4 Hz, H-2''; H-6''), 7.54 (2H, d, J = 8.8 Hz, H-2'''; H-6'''), 7.64 (1H, d, J = 15.9 Hz, H-7''')

^{13}C NMR (acetone-d6), δ_C : 56.2 (3-OMe, q), 56.5 (3'-OMe; 5'-OMe, q), 63.8 (C-9, t), 65.2 (C-9', t), , 73.2 (C-7, d), 84.7 (C-8, d), 104.7 (C-2; C-6, d), 110.6 (C-2', C-6', d), 115.4 (C-8'', d), 115.6 (C-8''', d), 115.7 (C-5, d), 116.7 (C-3''; C-5''; C-3''', C-5''', d), 119.7 (C-6, d), 124.3 (C-8', d), 126.7 (C-1''; C-1''', s), 131.0 (C-2''; C-6''; C-2'''; C-6''', d), 132.9 (C-1, s), 133.3 (C-1', s), 134.3 (C-7', d), 136.7 (C-4', s), 145.1 (C-7'', s), 145.7 (C-7''', d), 146.5 (C-4, s), 148.1 (C-3, s), 154.3 (C-3'; C-5', s), 160.9 (C-4''; C-4''', s), 166.0 (C-9'', s), 166.6 (C-9''', s)

7.4.2.3 Structure of Compound 8A

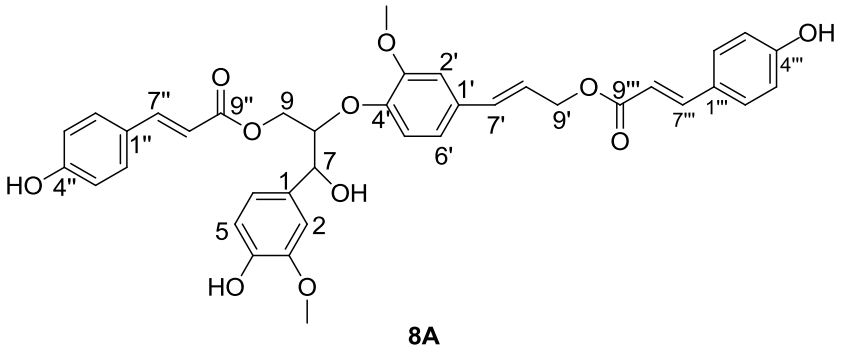

8A

threo/erythro-1-(4-hydroxy-3-methoxyphenyl)-2-[2-methoxy-4-{(1E)-3-(4-hydroxy cinnamoyl)-1-propenyl}phenoxy]-3-(4-hydroxycinnamoyl)propan-1-ol

Common name: Dadahol B

HRESI-MS (m/z): 668.2276 (calcd for $C_{38}H_{36}O_{11}$ 668.2258)

R*f*: 0.58 (8% MeOH/DCM)

Optical rotation: $[\alpha]_D^{24}$ – 0.006°(c 0.2, MeOH)

1H and 13CNMR (*cf*. Section 7.15.9.2 and 7.15.9.3)

7.5 Targeted Purification of Actives

In order to isolate sufficient quantities of compounds **8A** and **8C** for *in vivo* studies a targeted purification was undertaken. The remaining portion of fraction **7D** (790 mg) was subjected to flash silica gel chromatography using 1.5% isopropanol/chloroform and fractions containing target compounds were combined based on TLC analysis. Repetitive silica gel column chromatography using 3 – 5 % isopropanol/chloroform led to the isolation of compounds **8A** (80 mg; 0.38% w/w of dry plant material) and **8C** (50 mg; 0.25% w/w of dry plant material).

7.6 Accelerated Bioassay-guided fractionation

The dichloromethane fraction (4B; Figure 7.1) from liquid-liquid partitioning of the *T. orientalis* crude extract (P05644-5B) was fractionated into a 96-well microtiter plate.

Fractionation was conducted using an Agilent 1200 semi preparative HPLC system consisting of an auto sampler, high pressure mixing pump, column oven and DAD detector.

HPLC conditions: Sunfire™ prep C8 column (10 µm, 10 X 150 mm).

Table 7.2 Semi-preparative HPLC Gradient Table

Time	Acetonitrile	Water	Methanol
0	25	70	5
3.00	25	70	5
7.00	50	45	5
15.00	100	0	0
20.00	100	0	0
23.00	25	70	5
30.00	25	70	5

Flow rate: 5 mL/min

Injection volume: 500 µL

Sample concentration: 16.7 mg/ml in CH_3CN/MeOH

No. of injections: 6 per plate

DAD conditions: 190-700 nm

Fraction type: time fractions with 0.2 min time slices

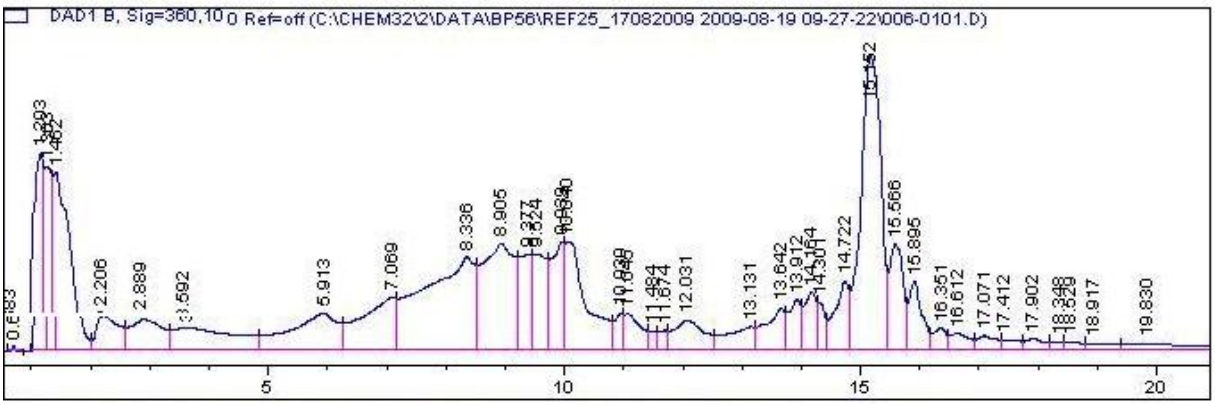

Figure 7.3 HPLC chromatogram of semi-preparative purification of *T. orientalis* extract

Four identical plates, with 85 fractions each, were generated. Plates were evaporated on a GeneVac EZ-2 Plus evaporator at 40ºC using the pre-installed “HPLC fractions” vacuum settings.

The semi-purified extract (**4B**) and one of the 96-well plates were submitted to the Swiss TPH for *in vitro* bioassaying against *T.b. rhodesiense*, *T. cruzi, P. falciparum* K1 and *Leishmania donovani* axenic amastigotes. The extract showed selectivity to the malaria parasite and the 96-well plate fractions were subsequently bioassayed against *P.falciparum* K1 at two concentrations, 4.8 and 0.8 µg/ml. IC_{50}’s were determined for those wells showing more than 50% inhibition at 0.8 µg/ml. The cytotoxicity of these fractions was also measured against an L6 (rat skeletal myoblast) cell line.

The active wells of one of the duplicate plates was analysed on a Waters Acquity SDS UPLC coupled in tandem with a 200 – 500 nm Waters Acquity PDA and a Waters SYNAPT HDMS G1. Instrument parameters were as follows:
MS Mode: ESI negative
Centroid Threshold: 1
Capillary: 2.5 kV
Sampling cone: 40.0
Extraction cone: 4.0
Source Temperature: 120 ºC
Desolvation Temperature: 400 ºC
Cone Gas Flow: 50.0 L/hr
Desolvation Gas Flow: 450 L/hr
Scan Time: 0.100 s
Start Mass: 100.0
End Mass: 1000.0
Start Time: 0.00 min
End Time: 30.00 min
Lock Mass: 554.2615 (Leucine enkephalin)

Solvent A: 0.1% Formic acid

Solvent B: Acetonitrile

Table 7.3 UPLC Gradient Table

Time/min	Flow rate	% A	% B	Curve
0.00	0.350	77	23	0
3.00	0.350	77	23	6
12.00	0.350	55	45	6
17.00	0.350	55	45	6
24.00	0.450	10	90	6
26.00	0.450	10	90	6
28.00	0.350	77	23	2
30.00	0.350	77	23	6

Sampling rate: 20 points/sec

Range: 200 - 500 nm

Resolution: 1.2 nm

Target Column Temperature: 40 ºC

Target Sample Temperature: 8.0 ºC

The bioactivity was correlated to the chemical profiles of these wells. Accurate mass and UV maxima data were used to search for known compounds in the Dictionary of Natural Products database (Chapman & Hall, 2010).

7.7 *p*LDH *In Vitro* Antiplasmodial Assay

The pLDH assay was conducted at the University of Cape Town's Division of Pharmacology (UCT Pharmacology). The chloroquine sensitive (D10) and chloroquine-resistant (K1) strains of *Plasmodium falciparum* were continuously cultured according to the methods described by Trager and Jensen (1976). The parasites were maintained at a 5% haematocrit with RPMI 1640 (Biowhittaker) medium supplemented with Albumax II (lipid rich bovine serum albumin) (GibcoBRL)

(25 g/L), hypoxanthine (44 mg/L), HEPES (N-[2-Hydroxyethyl]-piperazine-N'-[2-Ethansulphonic acid]) (Sigma-Aldrich) (6 g/L), sodium bicarbonate (Sigma-Aldrich) (2.1 g/L) and gentamycin (Sigma-Aldrich) (50 mg/L). The cultures were incubated at 37 ºC in an atmosphere of 93% N_2, 4% CO_2 and 3% O_2.

Parasite viability was measured using parasite lactate dehydrogenase (pLDH) activity (Makler *et al*., 1993). This enzymatic assay differentiates between pLDH and host LDH activity by using 3-acetylpyridine adenine dinucleotide (APAD). The pLDH uses APAD as a coenzyme in the conversion of pyruvate to lactate and reduces it to APADH. The formation of APADH can be measured by the subsequent reduction of a yellow nitroblue tetrazolium (NBT) salt to a blue formazan product, the absorbance of which can be monitored on a microplate reader.

The *in vitro* assays were performed as described by Clarkson *et al* (2003). Microtitration techniques were used to measure the activity of a large number of samples over a wide range of concentrations. The microtitre plates (Greiner) consisted of 96 wells arranged in a matrix of eight rows (A to H) and 12 coloumns (1 to 12). Rows A to H in column 1 contained unparasitised RBC (blank), column 2 served as a parasite control (parasitised RBC in the trophozoite stage, adjusted to a 2% parasitaemia and 2% haemotocrit, and no drug) and columns 3 to 12 contained parasites and varying concentrations of the drug. A solution of chloroquine diphosphate (Sigma) in Millipore water served as a positive control in all experiments. The initial concentration of chloroquine was 1000 ng/ml. All tests were performed in duplicate and no attempt was made to determine 50% inhibitory concentration (IC_{50}) values in excess of 100 µg/ml.

Samples were stored at -20 ºC prior to testing and stock solutions were made up a day before the experiment and stored at -20 ºC. Crude extracts were first dissolved in methanol or DMSO, depending on their solubility, sonicated for 10 minutes and then diluted in Millipore water to give a 2 mg/ml solution. This was further diluted in RPMI 1640 medium to give 200 µg/ml stock solutions. The highest concentration of solvent

that the parasites were exposed to was 0.5%, which was shown to have no measurable effect on parasite viability (Clarkson *et al*., 2004). Extracts were tested in nine serial twofold dilutions (final concentration range: 100 -0.2 µg/ml) in the 96-well microtitre plates. Fractions and pure compounds were dissolved in 10% methanol and were further diluted in complete medium on the day of the experiment. The starting concentration for a full dose-response was 100 µg/ml, which was diluted 2-fold in complete medium to give ten concentrations, with the lowest concentration being 0.195 µg/ml. The microtiter test plates were placed in a desiccator cabinet, flushed with a gas mixture consisting of 93% N_2, 4% CO_2 and 3% O_2, sealed and incubated at 37 ºC for 48 h.

The pLDH activity was measured using a 1.96 mM NBT (Sigma) and 0.24 mM phenazine ethosulphate (PES) (Sigma) solution in Millipore water, and the Malstat reagent containing triton (1ml/L), APAD (0.33 g/L) and TRIS buffer (3.3 g/L) in Millipore water. Malstat reagent (100 µl) and of NBT/PES (25µl) solution were added to all the wells of another 96-well microtiter plate. The test plate was removed from the desiccator after the 48 hour incubation period and the parasites were re-suspended in each well and then transferred (15 µl) with a multi-channel dispenser to the corresponding wells in the plate containing the Malstat and NBT/PES solution. This plate was placed in a 7520 Microplate Reader (Cambridge Technology), blanked on the wells in column 1 and the absorbance of the blue formazan salt was measured at λ 620 nm. Since the amount of formazan produced is proportional to parasite viability, the percentage parasite survival in each well was calculated using the formula:

$$\% \text{ Parasite Viability} = \frac{A_{\lambda 620} \text{ test well (PRBC + drug)}}{A_{\lambda 620} \text{ parasite control well (PRBC + no drug)}} \times 100$$

Dose response curves were constructed using non-linear dose-response curve fitting analyses with GraphPad Prism v.4.00 software. The concentration of the drug that

inhibits 50% of the parasites (IC_{50} values) was established from the dose response curves using GraphPad Prism.

7.8 CHO In Vitro Cytotoxicity Assay

Compounds were tested for *in vitro* cytotoxicity against a Chinese Hamster Ovarian (CHO) cell line using the 3-(4,5-dimethylthiazol-2-yl)-2,5-diphenyltetrazolium bromide (MTT) assay (Mosmann, 1983). This colorimetric assay is based on the ability of viable cells to metabolise a yellow water-soluble tetrazolium salt into a water-insoluble purple formazan product. The amount of formazan produced can be measured spectrophotometrically and is proportional to the metabolic activity and number of cells in the test plate. This assay was conducted at UCT Pharmacology. The CHO cells were cultured in Dulbecos Modified Eagles Medium (DMEM) : Hams F-12 medium (1:1) supplemented with 10% heat inactivated fetal calf serum (FCS) and gentamycin (0.04 µg/ml). The medium reagents were obtained from Highveld Biological, South Africa.

Samples were dissolved in methanol : water (1:9). Stock solutions (2 mg/ml) were prepared and were stored at -20 ºC until use. The highest concentration of methanol to which the cells were exposed to had no measurable effect on the cell viability. Emetine was used as the positive control in all cases. The initial concentration of emetine was 100 µg/ml, which was serially diluted in complete medium with 10-fold dilutions to give 6 concentrations, the lowest being 0.001 µg/ml. The same dilution technique was applied to all test samples with an initial concentration of 100 µg/ml to give 5 concentrations, with the lowest concentration being 0.01 µg/ml.

In the initial stage of the experiments, the cells were adjusted to a concentration of 10^5 / ml and 100 µl of this cell suspension were seeded in all wells except in column 1 (blank) in a 96 well culture plate (Costar). The plates were incubated at 37 ºC for 24 h in a humidified 5% CO_2-air atmosphere. After the incubation period, the medium was carefully aspirated out of the wells and 100 µl the different test substances (drug solutions) were added in quadruplicate to columns 3 through to 9. A further 100 µl of culture medium was then added to all of the wells containing cells and drugs

(columns 3 to 9), and 200 µl of medium was dispensed to the wells in column 1 (blank) and column 2 (cells and no drug). The microplate was then incubated at 37 ºC for 48 h.

After the 48 h incubation period, 25 µl of sterile MTT (5 mg/ml in PBS) was added to each well and incubation was continued for 4 h at 37 ºC. The plates were then centrifuged at 2050 rpm for 10 min and the supernatant was carefully aspirated from the wells, ensuring that the formazan crystals were not disturbed. The formazan crystals were dissolved in DMSO (100 µl) and the plate was gently shaken for 5 min on a microtitre plate shaker. The plate was blanked on the wells in column 1 and the absorbance of the crystals was measured at λ 540 nm on a Microtitre Plate Reader (Cambridge Technologies). The cell viability was calculated in each well using the formula:

$$\% \text{ Cell Viability} = \frac{A_{\lambda 540} \text{ test well (cells + drug)}}{A_{\lambda 540} \text{ cell control well (cells + no drug)}} \times 100$$

The concentration of drug that inhibits 50% of the cells (IC_{50} values) for these samples were obtained from dose-response curves, using a non-linear dose-response curve fitting analyses via GraphPad Prism v.2.01 software.

7.9 Swiss Tropical and Public Health Institute's *In Vitro* Assays

Extracts/fractions are first tested in a medium throughput screening (MTS) assay at just one standard concentration against the following protozoan parasites: *Trypanosoma brucei rhodesiense*, *T. cruzi*, *Leishmania donovani* and *Plasmodium falciparum*. All extracts/fractions found to be active in the MTS assay are subjected to the serial dilution assay against the corresponding parasite to determine an IC_{50}. At this stage a cytotoxicity assay with rat skeletal myoblasts (L-6 cells) is also be performed to obtain information on selectivity. Each assay is run in duplicate and repeated for compounds having reached the activity criteria. For each parasite a standard drug is run in parallel which acts as an internal control. If the IC_{50} for the

standard drug deviates from the established mean value by more than a factor 2x, the assay is discarded. In principle, all assays are 96-well plate based and run for 72 hours at 37 °C. The endpoint is determined in a semi-automated way by reading the plates photometrically, fluorometrically or by scintillation counting. From the signal of each well a % inhibition *vs*. the untreated control is calculated, a sigmoidal inhibition curve is drawn and an IC_{50} value is determined.

For *T.b. rhodesiense* bloodstream forms grown in MEM medium are used according to Baltz *et al*. (1985), supplemented with 15% heat-inactivated horse serum. Serial 3-fold drug dilutions are prepared, trypanosomes are added and the plate is incubated for 72 hours. Then 10 µL of Alamar blue (resazurin) is added to each well and incubation continued for another 2-4 hours. The plates are then read in a microtiter fluorometer. Data is transferred to the graphic programme Softmax Pro (Molecular Devices) which calculates the IC_{50} value.

For *T. cruzi* a parasite strain transfected with a reporter (*β*- galactosidase) gene is used. Rat skeletal myoblasts (L-6 cells) act as host cells. They are infected with trypomastigote forms from culture and 48 hours later a serial drug dilution is added. After 96 hours an enzymatic reaction is induced and the colour reaction is read photometrically at 540 nm. Data is transferred to the graphic programme Softmax Pro (Molecular Devices) which calculates the IC_{50} value.

For *Leishmania donovani* axenically grown amastigote forms are used. Serial 3-fold drug dilutions are prepared, amastigotes are added and the plate incubated for 72 hours. Then resazurin is added and the assay evaluated as described for the *T.b. rhodesiense* assay.

For *P. falciparum* a modification of the ^{3}H-hypoxanthine incorporation assay (Matile and Pink, 1990) is used. Infected human red blood cells are exposed to serial drug dilutions. After 48 hours of incubation, 0.5 µCi ^{3}H-hypoxanthine is added to each well. Cultures are incubated for a further 24 h before they are harvested onto glass-fiber

filters. The radioactivity is counted in a liquid scintillation counter. IC_{50} values are calculated from the sigmoidal inhibition curves.

Cytotoxicity is determined using rat skeletal myoblast (L-6 cells) in the Alamar blue assay as described for *T.b.rhodesiense*. A selectivity index is calculated by dividing IC_{50} values for L-6 cells/IC_{50} for *P.falciparum*. A high value (>100) indicates selective activity against the parasite.

7.10 *In Vivo* Antiplasmodial Assay

In vivo antimalarial activity was determined by a 4 day suppressive test with *P. bergei* infected mice. The assays were conducted at UCT Pharmacology. The strain of mice used for the experiment was C57 Black 6 (6-10 weeks old). There were five mice in the experimental groups and four mice in chloroquine control and negative control groups.

The mice were infected with chloroquine sensitive *Plasmodium bergei* ANKA. Mice were infected interperitoneally with 200µl of 10^6 cells/ml parasite stock. Twenty -four hours post infection, the mice were treated once a day for 4 consecutive days.

The route of administration was via subcutaneous injection. The test samples were delivered in 10% DMSO in water. Crude extracts were given at 500 mg/kg, and pure compounds at 100 mg/kg body weight. The chloroquine was delivered in water at a dose of 10mg/kg body weight. Parasitemia, body weight and survival were monitored regularly. Parasitemia was determined using Giemsa stained smears.

The activity or percentage parasitemia reduction was calculated as follows:
% Reduction = 100 – [mean parasitemia treated / mean parasitemia untreated x100]

7.11 *In Vivo* PK Evaluation

The *in vivo* PK assay was conducted at UCT Pharmacology. The compounds were administered subcutaneously at a dose of 10 mg/kg to healthy mice and blood samples were collected at relevant time intervals. Test compounds were subsequently extracted and levels were determined by LC-MS/MS.

Extraction: Spiked blank blood at a concentration of 1 µg/ml. Ten serial dilutions were prepared. 10µl of sample + 50 µl buffer (sodium carbonate, pH 10.8. 0.1M) + 250 µl ethyl acetate were vortexed, centrifuged, separated, dried, reconstituted with mobile phase and vortexed again. 5 µl of sample was injected for analysis.

LC-MS/MS: Stock solutions of the compounds (1 mg/ml in acetonitrile) were prepared. Dilutions of 1000x were made up in mobile phase.

Pump: Agilent 1200 G1312A
Column: Phenomenex, Gemini C18, 5 µm, 5 cm x 2.0 mm
Column Temperature: 30 ºC
Mobile phase: Acetonitrile: 0.1% formic acid (70:30)
Flow-rate: 300 µl/min
Sample Acquisition Duration: 1min 30sec

Table 7.4 Agilent Gradient HPLC Table

Step	Total Time(min)	Flow Rate(µl/min)	A (%)
0	0.00	300	32.0
1	1.50	300	32.0

Mass Spectrometer: Triple Quadrupole LC/MS/MS (API 3200)
Source Type: Turbo Spray
Source Temperature (at setpoint): 400.0 C
Software: Analyst 1.4.2

7.12 Nuclear Magnetic Resonance (NMR) Spectroscopy

NMR spectroscopy was carried out on a Varian 600 MHz Premium Shielded spectrometer. All the spectra were recorded at room temperature in deuteriated chloroform or acetone. The chemical shifts were all recorded in ppm relative to TMS. Proton data was acquired and analysed for all synthetic intermediates and products. Carbon and 2D NMR data were only acquired for products achieved in adequate yield and purity.

7.13 Mass Spectrometry

High resolution mass spectra were recorded on a SYNAPT G1 HDMS QTOF ESI-MS instrument, in the negative ES^+ or ES^- mode under the following conditions:

Capillary (kV): 2.5

Sampling cone: 45.0

Extraction cone: 4.0

Source Temp (ºC): 120

Desolvation Temp (ºC): 400

Scan Time (sec): 0.100

Interscan Time (sec): 0.020

Start mass: 100.00

End mass: 1000.00

7.14 Optical Rotations

Optical rotations, on selective compounds, were measured in methanol at 20ºC on a Perkin-Elmer 343 polarimeter at 589 nm (Na D-line) using a 1 cm^3 cell.

7.15 Synthesis and Analogue Generation

All synthetic intermediates and products were confirmed by ^{1}H NMR and HRESI-MS analysis. ^{13}C and 2D NMR data were only acquired and analysed for final products, recovered in sufficient yield.

7.15.1 Synthesis of Triphenylethoxycarbonylmethylphosphonium bromide

3.14 g (0.012 mol) of PPh_3 was dissolved in 6 ml of THF in a 25 ml round bottom flask attached to a reflux condenser. A solution of 2.0 g (0.012 mol) of ethyl bromoacetate in 6 ml of THF was added drop-wise to the PPh_3 solution through the top of the condenser. The mixture was stirred at room temperature for 45 min and then filtered. The white precipitate was washed with hexane and the filtrate and washings were saved and allowed to stand overnight to recover more salt (4.4g, 85% yield). This step was repeated five times to yield a total of 23.1 g of triphenylethoxycarbonylmethylphosphonium bromide (75% overall yield).

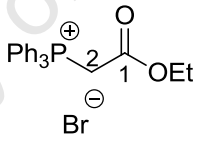

(45)
triphenylethoxycarbonylmethylphosphonium bromide

HRESI-MS (m/z): 429.0388 (calcd for $C_{22}H_{22}BrO_2P$ 429.0397)

^{1}H NMR ($CDCl_3$): δ_H 1.01 (3H, t, J = 7.1, O-$CH_2C\underline{H_3}$) 3.98 (2H, q, J = 7.1, O-$C\underline{H_2}CH_3$), 5.50 (2H, d, J = 13.8, H-2), 7.88 - 7.59 (15H, m, P-($C_6\underline{H_5}$)$_3$)

7.15.2 Preparation of triphenylethoxycarbonylmethylphosphorane

Phosphonium salt was dissolved in a minimum amount of water in 5-6 g batches; insolubles were filtered off. 2.5 M NaOH (1.2 mol equiv.) was added slowly with stirring at room temperature. Precipitate was filtered, dissolved in dichloromethane, dried over anhydrous sodium sulphate and evaporated to dryness to yield the Wittig reagent (**46**) (13.3 g, 71% yield).

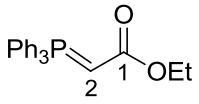

(46)
triphenylethoxycarbonylmethylphosphorane

HRESI-MS (m/z): 348.1267 (calcd for $C_{22}H_{21}O_2P$ 348.1278)

^{1}H NMR ($CDCl_3$): δ_H 1.21 (3H, t, J = 7.1 Hz, O-$CH_2\underline{CH_3}$), 4.08 (2H, q, J = 7.1 Hz, O-$C\underline{H_2}CH_3$), 6.81 (1H, s, H-2), 7.66 - 7.39 (15H, m, P-($C_6\underline{H_5}$)$_3$)

7.15.3 Wittig Reaction

2.5 g of vanillin (0.0164mol) was dissolved in 50 ml of dry dichloromethane. 6.85 g (0.0197 mol, 1.2 equiv) of triphenylethoxycarbonylmethylphosphorane **(46)** was added and the reaction was stirred at room temperature under nitrogen for 24 h. Reaction mixture was refluxed at 60° C for 90 min but with no further depletion of vanillin. Recovered 650 mg (9.3%) of *Z*- isomer and 3g (43% yield) of *E*- ethyl ferulate **(42)** after repetitive flash silica gel column chromatography, using 15% EtOAc/Hexane. Repeated process on 2-4 g batches of substrate (49% overall yield).

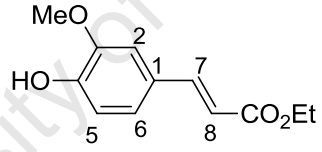

(42)
E-ethyl ferulate

HRESI-MS (m/z): 222.0830 (calcd for $C_{22}H_{21}O_2P$ 222.0796)

R*f*: 0.54 (40% EtOAc/Hexane)

^{1}H NMR ($CDCl_3$): δ_H 1.29 (3H, t, J = 7 Hz, 8-O-$CH_2\underline{CH_3}$), 3.88 (3H, s, O$\underline{CH_3}$-3), 4.21 (2H, q, J = 7 Hz, 8-O-$C\underline{H_2}CH_3$), 6.25 (1H, d, J = 15.8 Hz, H-8), 6.99 (1H, d, J = 8.2 Hz, H-5), 7.02 (1H, d, J = 2 Hz, H-2), 7.03 (1H, dd, J = 8.2, J = 2 Hz, H-6), 7.57 (1H, d, J = 15.8 Hz, H-7)

7.15.4 DIBAL Reduction of Ethyl Ferulate

11.1 g (0.05 mol) of *E*-ethyl ferulate was reduced with DIBAL (0.2 mol, 4 equiv. 36 ml) in anhydrous dichloromethane at -78°C under nitrogen. The DIBAL reaction was quenched with 500ml of saturated sodium sulphate. The mixture was filtered through

a 1 cm plug of celite and the filtrate was extracted with EtOAc (4 x 200 ml). Combined organic layers were dried over anhydrous Na_2SO_4, filtered and evaporated in *vacuo*. The residue was subjected to silica gel column chromatography using 0.5% isopropanol/dichloromethane. 3.2 g of unreacted starting material and 3.9 g (43 %) of coniferyl alcohol **(37)** was recovered.

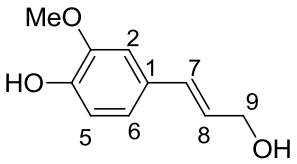

(37)
coniferyl alcohol

HRESI-MS (m/z): 180.0514 (calcd for $C_{10}H_{12}O_3$ 180.0522)

R*f*: 0.16 (1.5% MeOH/CH_2Cl_2)

^{1}H NMR (acetone-d_6): δ_H 3.72 (1H, dd, J = 5.7, J = 5.7 Hz, 9-OH), 3.87 (3H, s, 3-OCH_3), 4.19 (2H, dd, J = 5.7, J = 5.0 Hz, H-9), 6.23 (1H, dt, J = 15.8 Hz, J = 5.0, H-8), 6.50 (1H, d, J = 15.8 Hz, H-7), 6.77 (1H, d, J = 7.9 Hz, H-5), 6.86 (1H, dd, J = 7.9, J = 1.3 Hz, H-6), 7.06 (1H, d, J = 1.3 Hz, H-2), 7.57 (1H, br s, 4-OH)

7.15.5 Oxidative Coupling

90 mg (0.5 mmol) of coniferyl alcohol (**37**) and 3 mg of HRP (250 Umg^{-1}) were dissolved in dioxane-water (2/3, v/v, pH 4 – 4.5 adjusted with dil. H_3PO_4). 3% H_2O_2 was added slowly; monitoring the disappearance of the substrate on TLC. After most of the substrate reacted, 100 ml of H_2O was added to the reaction mixture, and this was then extracted with EtOAc (3 x 100 ml). EtOAc layers were combined, washed with H_2O, dried over $MgSO_4$ and then evaporated *in vacuo*. Residue was purified by silica gel column chromatography and prep TLC using 3% MeOH/DCM to yield the three major dimers, (±) pinoresinol (**39)** (6.3 mg, 7%), (±) dehydrodiconiferyl alcohol (**38)** (14.1 mg, 16%), and (±) guaiacylglycerol-8-*O*-4'-coniferyl alcohol ether (**40)** (26.5 mg, 29%).

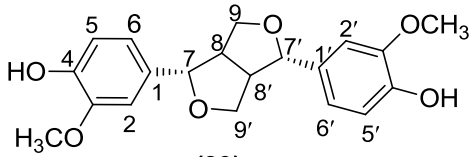

(39)

(±)-pinoresinol

HRESI-MS (m/z): 358.1416 (calcd for $C_{20}H_{22}O_6$ 358.1417)

R*f*: 0.45 (4% isopropanol/DCM)

^{1}H NMR ($CDCl_3$): δ_H 3.05 (2H, dd, J = 4.3, J = 7.2 Hz, H-8, H-8'), 3.84 (2H, dd, J = 9.1, J = 3.8 Hz, H-9b, H-9'b), 3.87 (6H, s, OC<u>H</u>$_3$-3, OC<u>H</u>$_3$-3'), 4.21 (2H, dd, J = 7.2, J = 9.1 Hz, H-9a, H-9'a), 4.70 (2H, d, J = 4.3 Hz, H-7,H-7'), 5.55 (2H, s, 4-O<u>H</u>, 4'-O<u>H</u>), 6.78 (2H, dd, J = 8.2, J = 1.9 Hz, H-6, H-6'), 6.84 (2H, d, J = 8.2 Hz, H-5, H-5'), 6.86 (2H, d, J = 1.9 Hz, H-2, H-2')

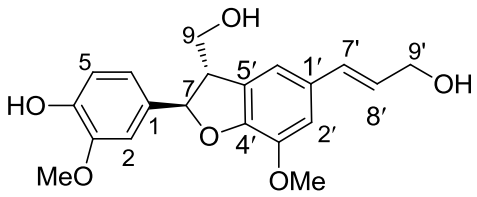

(38)

(±) dehydrodiconiferyl alcohol

HRESI-MS (m/z): 358.1452 (calcd for $C_{20}H_{22}O_6$ 358.1459)

R*f*: 0.24 (5% MeOH/DCM)

$[\alpha]_D^{24}$: + 0.099°(*c* = 0.20, MeOH) [lit: $[\alpha]_D^{20}$ + 10.9°(*c* = 2.0, Acetone); (Yuen et al., 1998)]

^{1}H NMR (acetone-d_6): δ_H 3.54 (1H, ddd, J = 6.1, J = 6.3, J = 6.4 Hz, H-8), 3.74 (1H, t, J = 6.1 Hz, 9'-O<u>H</u>), 3.83 (3H, s, 3-OC<u>H</u>$_3$), 3.87 (3H, s, 3'-OC<u>H</u>$_3$), 3.92 – 3.83 (2H, m, H-9), 4.11(1H, t, J = 5.4 Hz, 9-O<u>H</u>), 4.20 (1H, dd, J = 5.6, J = 6.1 Hz, H-9'), 5.57 (1H, d, J = 6.4 Hz, H-7), 6.25 (1H, dt, J = 15.7, J = 5.6 Hz, H-8'), 6.53 (1H, br d, J = 15.6 Hz, H-7'), 6.70 (1H, d, J = 8.1 Hz, H-5), 6.89 (1H, dd, J = 8.1, J = 1.4 Hz, H-6), 6.95 (1H, br s, H-2'), 6.99 (1H, br s, H-6'), 7.04 (1H, br d, J = 1.4 Hz, H-2), 7.57 (1H, s, 4-O<u>H</u>)

^{13}C NMR (acetone-d6): δ_C 53.9 (C-8, d), 55.4 (3-OMe, q), 55.5 (3'-OMe, q), 62.5 (C-9', t), 63.7 (C-9, t), 87.6 (C-7, d), 109.6 (C-2, d), 110.8 (C-2', d), 114.8 (C-5, d), 115.2

(C-6', d), 118.7 (C-6, d), 127.5 (C-8', d), 129.5 (C-4', s) 129.6 (C-7', d), 131.0 (C-1', s) 133.5 (C-1, s), 144.3 (C-3', s) 146.4 (C-4, s), 147.5 (C-3, s), 148.1 (C-5', s)

GGCE **(40)**: Refer to Section 17.15.8

Scale-up: 3.2 g of coniferyl alcohol was subjected to oxidative coupling in ~ 1 g batches. The substrate and 30 mg of HRP (250 Umg^{-1}) were dissolved in ~ 200 ml dioxane-water (2/3, v/v, pH 4 – 4.5 adjusted with dil. H_3PO_4). 3% H_2O_2 (~ 2ml) was added slowly; monitoring the disappearance of the substrate. 100 ml of water was added to the reaction mixture and this was then extracted with EtOAc (3 x 100 ml). EtOAc layers were combined, washed with H_2O, dried over $MgSO_4$ and then evaporated *in vacuo*. Residue was purified by silica gel column chromatography (1% MeOH/DCM to 3% MeOH/DCM), yielding the two major dimers, dehydrodiconiferyl alcohol (DHCA) **(38)** (280 mg, 9%), and (±) guaiacylglycerol-8-*O*-4'-coniferyl alcohol ether (GGCE) **(40)** (878 mg, 26%).

7.15.6 Acid Chloride Esterification of GGCE

29.6 mg (0.2 mmol) of *trans* cinnamic acid was dissolved in 5 ml of dry dichloromethane. Added 2 drops of anhydrous DMF and then 44 µl (0.5 mmol, 2.5 equiv.) of oxalyl chloride was added drop-wise at room temperature, under nitrogen. After addition the reaction mixture was refluxed at 50°C for 2.5 h. Solvent and excess oxalyl chloride was removed under vacuum pressure to yield pale yellow crystals of the acid chloride. Dissolved the acid chloride in 5 ml of dry dioxane and added to round bottom flask containing 30.0 mg (0.08 mmol) of DHCA in 0.5 ml THF. Added 13 µl of Et_3N (0.1 mmol, 1.2 equiv.) and stirred at room temperature under N_2 overnight. The reaction mixture was diluted with 10 ml EtOAc and washed with 5% $NaHCO_3$ and brine. The solution was dried over $MgSO_4$, the solvent was evaporated under reduced pressure and residue was chromatographed on silica gel using 70% EtOAc/hexane to yield 4.3 mg (8.4%) of the *erythro* diester **(53)**, and 11 mg (27.1%) of the monoester, **(54)**.

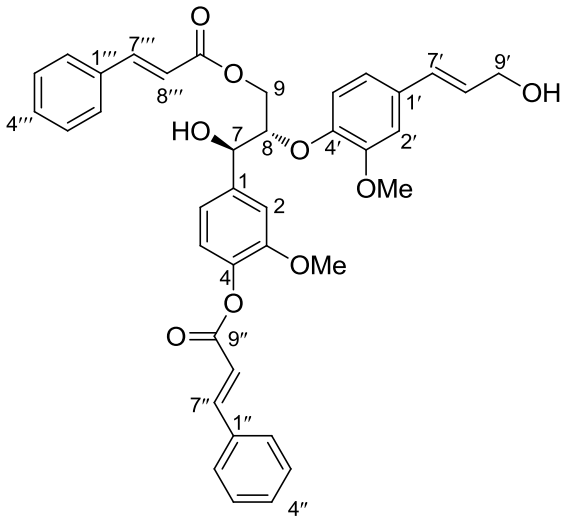

(53)
erythro 4,9-dicinnamoyl guaiacylglycerol-8-O-4'-coniferyl alcohol ether

HRESI-MS (m/z): 636.2527 (calcd for $C_{38}H_{36}O_9$ 636.2675)

R*f*: 0.32 (50% EtOAc/Hexane)

^{1}H NMR of *erythro* form (acetone-d_6): δ_H 3.83 (3H, s, 3-OC<u>H</u>$_3$), 3.85 (3H, s, 3'-OC<u>H</u>$_3$), 4.21 (2H, br d, J = 5.4 Hz, H-9'), 4.51 (2H, m, H-9), 4.75 (1H, br m, H-8), 4.85 (1H, br d, J = 3.5 Hz, 7-O<u>H</u>), 5.12 (1H, br dd, J= 3.5, J = 4.7 Hz, H-7), 6.30 (1H, dt, J = 16.1, J = 5.4 Hz, H-8'), 6.45 (1H, d, J = 15.8 Hz, H-8'''), 6.53 (1H, d, J = 16.1 Hz, H-7'), 6.77 (1H, d, J = 15.8 Hz, H-8''), 6.92 (1H, br d, J = 8.2 Hz, H-6), 6.92 (1H, d, J = 8.2 Hz, H-6), 7.01 (1H, d, J = 8.2 Hz, H-5'), 7.08 (1H, s, H-2'), 7.10 (1H, d, J = 8.2 Hz, H-5), 7.13 (1H, br d, J = 8.2 Hz, H-6'), 7.34 (1H, br s, H-2), 7.43 (3H, m, H-3''', H-4''', H-5'''), 7.49 (3H, m, H-3'', H-4'', H-5''), 7.49 (1H, d, J = 15.8 Hz, H-7'''), 7.62 (1H, br m, H-2''', H-6'''), 7.78 (1H, br m, H-2'', H-6''), 7.84 (1H, d, J = 15.8 Hz, H-7'')

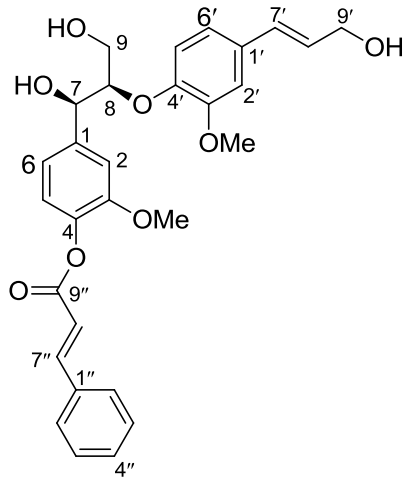

(54)

threo 4-cinnamoyl guaiacylglycerol-8-*O*-4'-coniferyl alcohol ether

HRESI-MS (m/z): 506.2815 (calcd for $C_{38}H_{36}O_9$ 506.2802)

R*f*: 0.08 (50% EtOAc/Hexane)

^{1}H NMR of *threo* form (acetone-d_6): δ_H 3.56 (1H, dd, J = 11.7, J = 5.9 Hz, H-9b), 3.76 (1H, m, H-9a), 3.81 (3H, s, 3-OC$\underline{H_3}$), 3.90 (3H, s, 3'-OC$\underline{H_3}$), 4.21 (2H, br d, J = 5.1 Hz, H-9'), 4.29 (1H, br, m, H-8), 5.02 (1H, br d, J = 5.9 Hz, H-7), 6.30 (1H, br dt, J = 16.1, J = 5.1 Hz, H-8'), 6.41 (1H, d, J = 16.1 Hz, H-7'), 6.77 (1H, d, J = 16.1 Hz, H-8''), 6.89 (1H, br d, J = 8.1 Hz, H-6), 6.93 (1H, J = 8.1 Hz, H-5'), 7.06 – 7.11 (3H, m, H-2', H-5, H-6'), 7.30 (1H,br s, H-2), 7.48 (3H, m, H-3'', H-4'', H-5''), 7.78 (2H, br m, d, H-2'', H-6''), 7.85 (1H, d, J = 16.1 Hz, H-7'')

7.15.7 CDI Coupling (GGCE with Cinnamic Acid)

31.4 mg (0.21 mmol, 2 equiv.) of *trans* cinnamic acid was dissolved in 2 ml of anhydrous dichloromethane. 34.5 mg (0.21 mmol) of CDI was added and the mixture was stirred at room temperature for 4h under nitrogen. 40 mg (0.106 mmol) of GGCE in 2 ml of THF was added and the reaction mixture was stirred at room temperature for 48h, and then refluxed at 75°C for 6h with a catalytic amount of DMAP and Na_2CO_3. The reaction did not go to completion but was eventually cooled, diluted with EtOAc, washed quickly with cold 0.05N HCl and then brine. Organic layer was dried over $MgSO_4$ and evaporated to dryness. Residue was purified over sílica gel using

20% EtOAc/hexane to yield 0.9 mg (1.3%) and 0.5 mg (0.7%) of the 9,9'-cinnamyl di-esters, **(56)** and **(57)**; and 0.5 mg (0.9%) of the *threo* 4,9,9'-cinnamyl tri-ester, **(55)**.

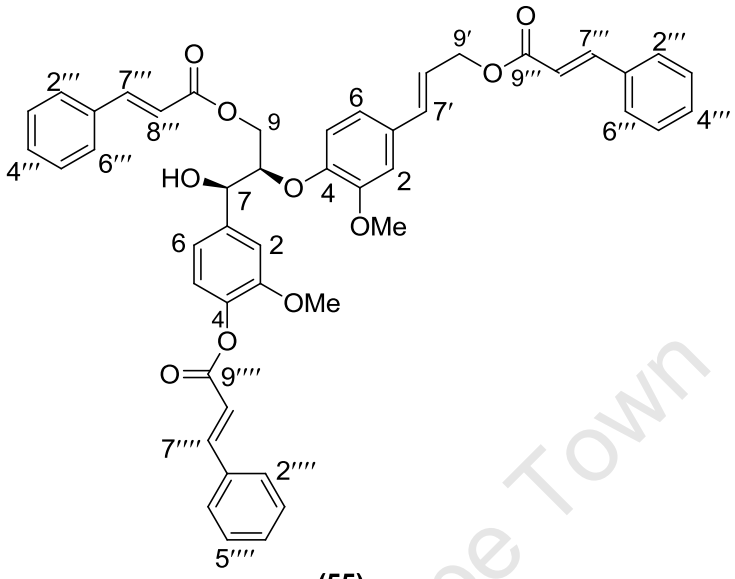

(55)

threo 4,9,9′-tricinnamoyl guaiacylglycerol-8-O-4'-coniferyl alcohol ether

HRESI-MS (m/z): 766.3065 (calcd for $C_{47}H_{42}O_{10}$ 766.3034)

R*f*: 0.47 (40% EtOAc/Hexane)

^{1}H NMR (acetone-d_6): δ_H 3.83 (3H, s, 3-OC$\underline{H_3}$), 3.88 (3H, s, 3'-OC$\underline{H_3}$), 4.24 (1H, dd, J = 6.5, J = 12.0 Hz, H-9b), 4.50 (1H, br dd, J = 12 Hz, H-9a), 4.77 (1H,br m, H-8), 4.83 (2H, br d, J = 6.5 Hz, H-9'), 5.12 (1H, br d, J = 4.1 Hz, H-7), 6.35 (1H, dt, J = 15.9, J = 6.5 Hz, H-8'), 6.48 (1H, d, J = 15.9 Hz, H-8''), 6.60 (1H, d, J = 15.9 Hz, H-7'), 6.71 (1H, d, J = 15.9 Hz, H-8'''), 6.77 (1H, d, J = 15.6 Hz, H-8''''), 7.02 (1H, d, J = 7.6 Hz, H-5), 7.11 – 7.20 (4H, m, H-6, H-6', H-5', H-2'), 7.36 (1H, br s, H-2), 7.41 – 7.52 (11H, m, H-3'', H-3''', H-3'''', H-4'', H-4''', H-4'''', H-5'', H-5''', H-5'''', H-7''), 7.64 (2H, m, H-2'', H-6''), 7.71 (2H, m, H-2''', H-6'''), 7.73 (1H, d, J = 15.9, H-7'''), 7.78 (2H, m, H-2'''', H-6''''), 7.85 (1H, d, J = 15.9 Hz, H-7'''')

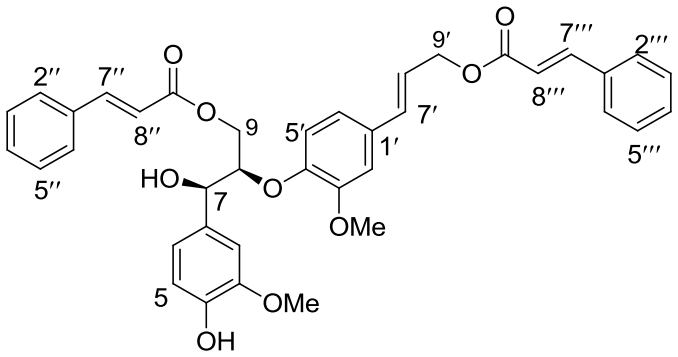

(56)

threo 9,9′-dicinnamoyl guaiacylglycerol-8-O-4'-coniferyl alcohol ether

HRESI-MS (m/z): 636.2375 (calcd for $C_{38}H_{36}O_9$ 636.2360)

R*f*: 0.38 (40% EtOAc/Hexane)

^{1}H NMR (acetone-d_6): δ_H 3.83 (3H, s, 3-OC<u>H</u>$_3$), 3.88 (3H, s, 3'-OC<u>H</u>$_3$), 4.14 (1H, dd, J = 6.5, J = 12.0 Hz, H-9b), 4.38 (1H, dd, J = 12.0, J = 4.3 Hz, H-9a), 4.58 (1H, d, J = 4.1 Hz, 7-O<u>H</u>), 4.65 (1H, br m, H-8), 4.84 (2H, br d, J = 6.5 Hz, H-9'), 4.98 (1H, br dd, J = 4.1 Hz, H-7), 6.36 (1H, dt, J = 15.8, J = 6.5 Hz, H-8'), 6.47 (1H, d, J = 15.8 Hz, H-8''), 6.60 (1H, d, J = 15.8 Hz, H-7'), 6.71 (1H, d, J = 16.4, H-8'''), 6.81 (1H, d, J = 8.5 Hz, H-5), 6.98 (1H, d, J = 7.9, H-6'), 7.01 (1H, br d, J = 8.5, H-6), 7.13 (1H, d, J = 7.9, H-5'), 7.16 (1H, s, H-2'), 7.18 (1H, br s, H-2), 7.41 – 7.49 (8H, m, H-3'', H-3''', H-5'', H-5''', H-4'', H-4''', H-7'', 4-O<u>H</u>), 7.61 (2H, br d, J = 7.1, H-2'', H-6''), 7.71 (2H, br m, J = 7.1, H-2''', H-6'''), 7.73 (1H, d, J = 16.4 Hz, H-7''')

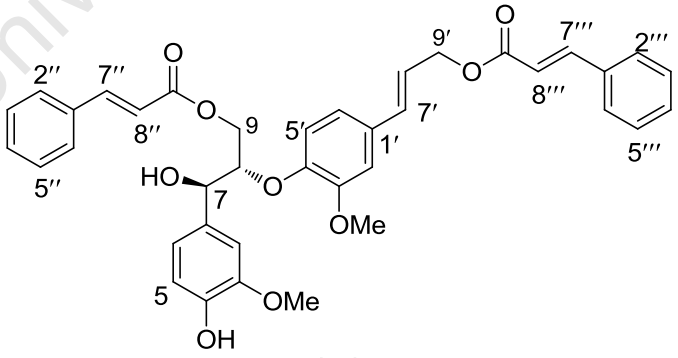

(57)

erythro 9,9′-dicinnamoyl guaiacylglycerol-8-O-4'-coniferyl alcohol ether

HRESI-MS (m/z): 636.2370 (calcd for $C_{38}H_{36}O_9$ 636.2360)

R*f*: 0.32 (40% EtOAc/Hexane)

^{1}H NMR (acetone-d_6): δ_H 3.84 (3H, s, 3-OC<u>H</u>$_3$), 3.86 (3H, s, 3'-OC<u>H</u>$_3$), 4.48 (2H, br m, H-9), 4. 61 (1H, d, J = 3.5 Hz, 7-O<u>H</u>), 4.73 (1H, br m, H-8), 4.82 (2H, br d, J = 6.5 Hz, H-9'), 5.00 (1H, br dd, J = 4.7, J = 3.5 Hz, H-7), 6.33 (1H, dt, J = 16.1, J = 6.5 Hz, H-8'), 6.42 (1H, d, J = 16.1, H-8''), 6.60 (1H, d, J = 16.4 Hz, H-7'), 6.69 (1H, d, J = 15.9 Hz, H-8'''), 6.79 (1H, d, J = 7.6 Hz, H-5), 6.96 (1H, d, J = 8.2 Hz, H-6'), 6.97 (1H, br d, J = 7.6 Hz, H-6), 7.03 (1H, d, J = 8.2 Hz, H-5'), 7.15 (1H, s, H-2'), 7.16 (1H, br s, H-2), 7.40 – 7.45 (8H, m, H-3'', H-3''', H-5'', H-5''', H-4'', H-4''', H-7'', 4-O<u>H</u>), 7.59 (2H, br m, H-2'', H-6''), 7.71 (2H, br m, H-2''', H-6'''), 7.72 (1H, d, J = 15.9 Hz, H-7''')

7.15.8 GGCE Diastereomer Separation

An anion-exchange column (35 g QAE-Sephadex A-25; Pharmacia; column dimensions 3 x 35 cm) was packed and several hundred ml of the eluent (0.06 M $K_2B_4O_7$ in EtOH-water (1:4)) was allowed to pass through the column. Mixture of *threo* and *erythro* forms of GGCE **(40)** (in 2 batches of 270 mg) was dissolved in a minimal amount of eluent and applied to the column. The eluent was collected in 2 ml fractions, which were pooled on the basis of an examination by TLC (toluene : dioxane: acetic acid (90:25:4)). The pooled fractions (volume, V ml) were extracted with EtOAc (0.75 ml + 2 x 0.25 V ml). The extracts were dried over Na_2SO_4 and solvent was removed *in vacuo*. Boric acid was removed by repeated addition and evaporation of MeOH. The pooled fractions were each purified on silica gel using 1.25% isopropanol/chloroform to yield 139.8 mg of the *threo* form **(40i)** and 80.3 mg of the *erythro* **(40ii)** form, both as amorphous gums. The ethylated *erythro* GGCE by-product **(62)** was also recovered (2.4 mg) and characterized.

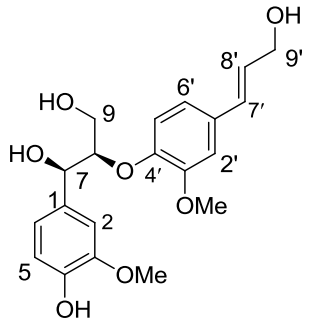

(40i)
threo guaiacylglycerol-8-*O*-4'-coniferyl alcohol ether

HRESI-MS (m/z): 376.1506 (calcd for $C_{20}H_{23}O_7$ 376.1523)

R*f*: 0.20 (5% MeOH/Me_2Cl_2)

$[\alpha]_D^{20}$: + 0.087°(*c* = 0.20, MeOH)

^{1}H NMR (acetone-d_6): δ_H 3.50 (1H, ddd, J = 6.1, J = 11.5, J = 6.1 Hz, H-9b), 3.69 (1H, ddd, J = 6.1, J = 5.4, J = 11.5 Hz, H-9b) 3.78 (1H, t, J = 6.1, 9'-OH), 3.80 (1H, t, J = 5.4, Hz, 9-OH), 3.81 (3H, s, OCH_3-3), 3.91 (3H, s, OCH_3-3'), 4.21 (3H, br m, H-9', H-8), 4.39 (1H, d, J = 3.4 Hz, 7-OH), 4.88 (1H, dd, J = 3.4, J = 6.1 Hz, H-7), 6.31 (1H, dt, J = 5.4, J = 15.8 Hz, H-8'), 6.54 (1H, d, J = 15.8 Hz, H-7'), 6.78 (1H, d, J = 8.1 Hz, H-5), 6.91 (2H, br d, J = 8.1 Hz, H-5', H-6), 7.11 (1H, d, J = 8.1 Hz, H-6'), 7.12 (1H, br s, H-2'), 7.13 (1H, br s, H-2), 7.44 (1H, s, 4-OH),

^{13}C NMR (acetone-d6), δ_C : 55.3 (3-OMe, q), 55.4 (3'-OMe, q), 61.0 (C-9, t), 62.4 (C-9', t), 73.0 (C-7, d), 87.6 (C-8, d), 110.0 (C-2', d), 110.5 (C-2, d), 114.3 (C-5, d), 118.8 (C-6, d), 119.4 (C-5', d), 119.7 (C-6', d), 128.8 (C-8', d) 130.0 (C-7', d), 132.1 (C-1', s) 132.9 (C-1, s), 146.0 (C-4, s) 147.1 (C-3, s), 148.3 (C-4', s), 150.9 (C-3', s)

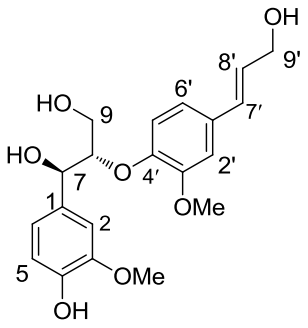

(40ii)

erythro guaiacylglycerol-8-*O*-4'-coniferyl alcohol ether

HRESI-MS (m/z): 376.1528 (calcd for $C_{20}H_{22}O_6$ 358.1523)

R*f*: 0.20 (5% MeOH/DCM)

$[\alpha]_D^{20}$: - 0.022°(*c*= 0.20, MeOH)

^{1}H NMR (acetone-d_6): δ_H 3.71 (2H,br m, H-9b, 9-OH), 3.79 (1H, ddd, J = 5.6, J = 5.7, J = 11.4 Hz, H-9b), 3.82 (3H, s, OCH_3-3), 3.86 (3H, s, OCH_3-3'), 4.20 (2H, dd, J = 5.7, J = 5.1 Hz, H-9'), 4.30 (1H, dd, J = 5.7, J = 3.8 Hz, H-8), 4.50 (1H, d, J = 5.1 Hz, 7-OH), 4.90 (1H, dd, J = 4.4, J = 5.1 Hz, H-7), 6.28 (1H, dt, J = 5.7, J = 15.7 Hz, H-8'), 6.52 (1H, d, J = 15.7 Hz, H-7'), 6.77 (1H, d, J = 7.9 Hz, H-5), 6.88 (2H, br dd, J = 8.1 Hz, H-5', H-6'), 6.92 (1H, d, J = 7.9 Hz, H-6), 7.07 (1H, br s, H-2'), 7.11 (1H, br s, H-2), 7.41 (1H, s, 4-OH),

^{13}C NMR (acetone-d6), δ_C : 55.3 (3-OMe, q), 55.4 (3'-OMe, q), 61.0 (C-9, t), 62.4 (C-9', t), 72.9 (C-7, d), 85.8 (C-8, d), 110.1 (C-2', d), 110.5 (C-2, d), 114.2 (C-5, d), 118.5 (C-6, d), 119.4 (C-5', d), 119.6 (C-6', d), 128.7 (C-8', d) 129.0 (C-7', d), 132.0 (C-1', s) 133.4 (C-1, s), 145.8 (C-4, s) 147.1 (C-3, s), 147.7 (C-4', s), 151.0 (C-3', s)

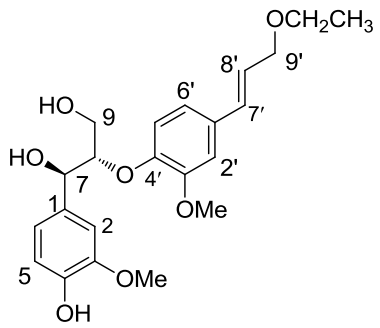

(62)

erythro 9′-ethyl guaiacylglycerol-8-*O*-4'-coniferyl alcohol ether

HRESI-MS (m/z): 404.1791 (calcd for $C_{22}H_{28}O_7$ 404.1836)

R*f*: 0.30 (5% MeOH/Me_2Cl_2)

^{1}H NMR (acetone-d_6): δ_H 1.58 (3H, t, J = 7.0 Hz, 9'-OCH$_2$C<u>H</u>$_3$), 3.50 (2H, q, J = 7.0 Hz, 9'-OC<u>H</u>$_2$CH$_3$), 3.71 (2H, br m, H-9b, 9'-O<u>H</u>), 3.84 (1H, m, H-9a), 3.82 (3H, s, 3-OC<u>H</u>$_3$), 3.86 (3H, s, 3-OC<u>H</u>$_3$), 4.06 (2H, d, J = 5.74 Hz, H-9'), 4.31 (1H, br m, H-8), 4.51 (1H, br s, 7-OH), 4.89 (1H, br m, H-7), 6.23 (1H, dt, J = 6.0, J = 16.0 Hz, H-8'), 6.53 (1H, d, 16.0 Hz, H-7'), 6.76 (1H, d, 8.0, J = 8.0 Hz, H-5), 6.88 (2H, d, J = 8.0 Hz, H-5', H-6'), 6.93 (1H, d, J = 8.0 Hz, H-6), 7.09 (1H, d, J = 1.5 Hz, H-2'), 7.11 (1H, s, H-2), 7.41 (1H, s, 4-O<u>H</u>)

^{13}C NMR (acetone-d6): δ_C 14.7 (9'-OCH$_2$<u>C</u>H$_3$, q), (55.3 (3-OMe, q), 55.4 (3'-OMe, q), 61.0 (C-9, t), 65.0 (9'-O<u>C</u>H$_2$CH$_3$, q), 70.7 (C-9', t), 72.9 (C-7, d), 85.8 (C-8, d), 110.1 (C-2', d), 110.5 (C-2, d), 114.2 (C-5, d), 118.4 (C-6, d), 119.5 (C-5', d), 119.6 (C-6', d), 125.3 (C-8', d) 131.0 (C-7', d), 131.6 (C-1', s), 133.4 (C-1, s), 145.8 (C-4, s) 147.1 (C-3, s), 147.9 (C-4', s), 151.0 (C-3', s)

7.15.9 CDI Coupling (GGCE with silylated *p*-coumaric acid)

7.15.9.1 Silylation of p-Coumaric Acid

200 mg (1.32 mmol, 1.1 equiv.) of TBS-Cl was added to a solution of *p*-coumaric acid (200 mg, 1.2 mmol) and imidazole (163 mg, 2.4 mmol, 2 equiv.) in 2 ml DMF at 0°C. The mixture was stirred at room temperature overnight, then diluted with ethyl acetate, washed with 10% $NaHCO_3$ and brine, dried over Na_2SO_4 and concentrated *in vacuo*. The residue was chromatographed on silica gel using 10% EtOAc/hexane to yield 218 mg (65%) of the white crystalline protected acid, **(66)**.

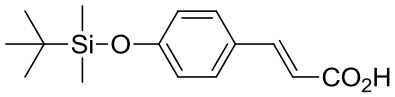

(66)
4-tertbutyl dimethyl silyl *p*-coumaric acid

^{1}H NMR (acetone-d_6): δ_H 0.25 (6H, s, 4-O-Si(C$\underline{H}_3$)$_2$), 1.00 (9H, s, 4-O-Si(C$\underline{H}_3$)$_3$), 6.38 (1H, d, J = 15.9 Hz, H-8), 6.94 (2H, d, J = 8.8 Hz, H-5, H-6), 7.60 (2H, J = 8.8 Hz, H-2, H-3), 7.63 (1H, d, J = 15.9 Hz, H-7)

7.15.9.2 CDI Coupling (*threo* GGCE)

CDI (122.5 mg, 0.76 mmol, 3 equiv.) was added to solution of 70 mg (0.25 mmol, 2.1 equiv.) of silyl protected *p*-coumaric acid **(66)** in 1 ml of anhydrous DMF and heated for 1 h at 45 ºC. Reaction mixture was cooled to room temperature before adding *threo* GGCE **(40i)** (45 mg, 0.12 mmol) in 1 ml DMF. Added catalytic amount of NaH, DMAP and Na_2CO_3; then heated to 70 ºC for 6 h. Added 1 ml of THF and 3 ml DCM and stirred at room temperature for 72 h. Diluted reaction mixture with EtOAc, washed with cold dilute (0.05N) HCL and brine. Organic layer was dried over $MgSO_4$ and evaporated to dryness. Residue was purified by sílica gel chromatography (2% MeOH/DCM), and prep TLC using 5% methanol/chloroform (x3) to yield 1.8 mg (2.2%) of *threo* Dadahol B **8Ai**, 2.3 mg (3.6%) of the 9-mono ester **(67)** and 1.4 mg (2.2 %) of the 9'-mono ester **(68)**.

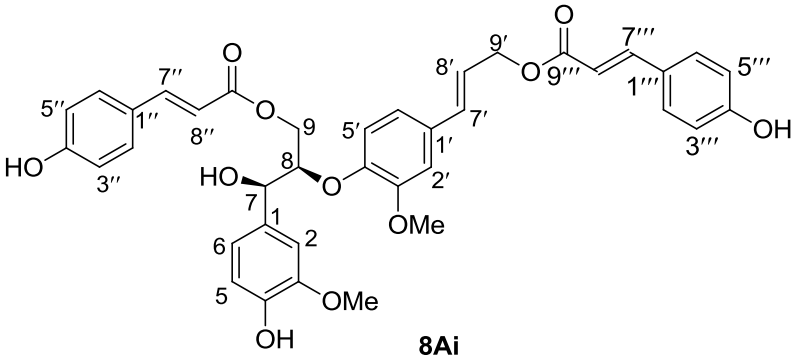

8Ai
threo Dadahol B

HRESI-MS (m/z): 668.2248 (calcd for $C_{38}H_{36}O_{11}$ 668.2258)

R*f*: 0.58 (8% MeOH/CH_2Cl_2)

^{1}H NMR (acetone-d_6): δ_H 3.83 (3H, s, 3-OC<u>H</u>$_3$), 3.88 (3H, s, 3'-OC<u>H</u>$_3$), 4.12 (1H, dd, J = 6.1, J = 11.8 Hz, H-9b), 4.35 (1H, dd, J = 11.8, J = 3.3 Hz, H-9a), 4.58 (1H,br s, 7-O<u>H</u>), 4.63 (1H, br m, H-8), 4.81 (2H, br d, J = 6.4 Hz, H-9'), 4.98 (1H, br d, J = 3.3 Hz, H-7), 6.27 (1H, d, J = 16.0 Hz, H-8''), 6.34 (1H, dt, J = 16.0, J = 6.4 Hz, H-8'), 6.40 (1H, d, J = 16.0 Hz, H-8'''), 6.69 (1H, d, J = 16.0 Hz, H-7'), 6.80 (1H, d, J = 8.0 Hz, H-5), 6.89 (4H, d, J = 8.6 Hz, H-3'', H-3''', H-5'', H-5'''), 6.97 (1H, br d, J = 8.0 Hz, H-6), 7.00 (1H, d, J = 8.3 Hz, H-6'), 7.13 (1H, d, J = 8.3 Hz, H-5'), 7.15 (1H, br s, H-2), 7.18 (1H, br s, H-2'), 7.41 (1H, d, J = 16.0 Hz, H-7''), 7.48 (2H, d, J = 8.6 Hz, H-2'', H-6''), 7.57 (2H, d, J = 8.6 Hz, H-2''', H-6'''), 7.65 (1H, d, J = 16.0 Hz, H-7''')

^{13}C NMR (acetone-d6): δ_C 55.3 (3-OMe, q), 55.4 (3'-OMe, q), 63.5 (C-9, t), 64.4 (C-9', t), 73.0 (C-7, d), 83.4 (C-8, d), 110.3 (C-2', d), 110.6 (C-2, d), 114.3 (C-8'', d), 114.5 (C-8''', d), 114.6 (C-5, d), 115.8 (C-3'', C-3''', C-5'', C-5''', d), 118.0 (C-5', d), 119.7 (C-6, d), 119.9 (C-6', d), 122.4 (C-8', d), 126.0 (C-1'', s), 126.1 (C-1''', s), 130.1 (C-2'', C-2''', C-6'', C-6''', d), 131.2 (C-1', s), 132.3 (C-1, s), 133.4 (C-7', d), 144.7 (C-7'', C-7''', d), 146.2 (C-4, s) 147.2 (C-3, s), 148.7 (C-4', s), 150.9 (C-3', s), 159.7 (C-4'', s), 159.8 (C-4''', s), 166.2 (C-9'', s), 166.3 (C-9''', s)

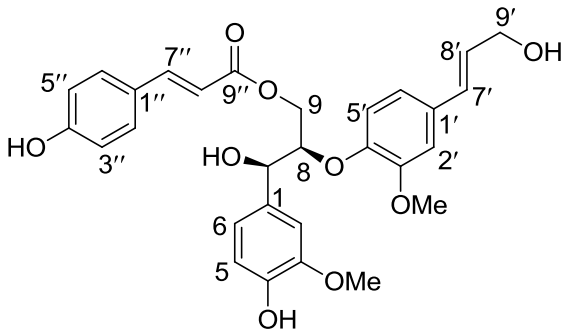

(67)

threo 9-coumaroyl guaiacylglycerol-8-*O*-4'-coniferyl alcohol ether

HRESI-MS (m/z): 522.1869 (calcd for $C_{29}H_{30}O_9$ 522.1891)

^{1}H NMR (acetone-d_6): δ_H 3.83 (3H, s, 3-OC$\underline{H_3}$), 3.88 (3H, s, 3'-OC$\underline{H_3}$), 4.10 (1H, dd, J = 6.3, J = 12.0 Hz, H-9b), 4.21 (2H, br d, H-9'), 4.36 (1H, br dd, J = 12.0 Hz, J = 3.4 Hz, H-9a), 4.58 (1H, br m, H-8), 4.97 (1H, br d, J = 3.4 Hz, H-7), 6.29 (1H, d, J = 16.0 Hz, H-8''), 6.30 (1H, dt, J = 16.0, J = 5.2 Hz, H-8'), 6.54 (1H, d, J = 16.0 Hz, H-7'), 6.80 (1H, d, J = 8.3 Hz, H-5), 6.89 (2H, d, J = 8.6 Hz, H-3'', H-5''), 6.93 (1H, br d, J = 8.6 Hz, H-6'), 6.97 (1H, d, J = 8.3 Hz, H-6), 7.01 (1H, d, J = 8.6 Hz, H-5'), 7.11 (1H, br s, H-2'), 7.15 (1H, br s, H-2), 7.43 (1H, d, J = 16.0 Hz, H-7''), 7.49 (2H, d, J = 8.6 Hz, H-2'', H-6'')

^{13}C NMR (acetone-d6): δ_C 55.3 (3-OMe, q), 55.4 (3'-OMe, q), 62.4 (C-9', t), 63.5 (C-9, t), 73.0 (C-7, d), 83.6 (C-8, d), 110.2 (C-2', d), 110.6 (C-2, d), 114.3 (C-8'', d), 114.5 (C-5, d), 115.8 (C-3'', C-5'', d), 118.3 (C-5', d), 119.3 (C-6', d), 119.7 (C-6, d), 126.0 (C-1'', s), 128.9 (C-8', d), 129.0 (C-7'', d), 130.1 (C-2'', C-6'', d), 132.2 (C-1', s), 132.3 (C-1, s), 144.7 (C-7'', d), 146.2 (C-4, s) 147.2 (C-3, s), 148.0 (C-4', s), 150.9 (C-3', s), 159.8 (C-4'', s), 166.2 (C-9'', s)

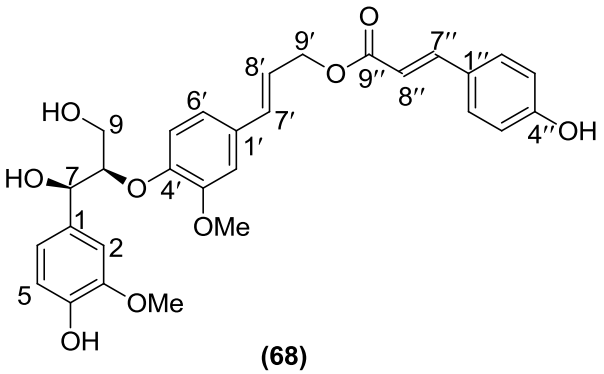

(68)

threo 9′-coumaroyl guaiacylglycerol-8-*O*-4'-coniferyl alcohol ether

HRESI-MS (m/z): 522.1894 (calcd for $C_{29}H_{30}O_9$ 522.1891)

^{1}H NMR (acetone-d_6): δ_H 3.53 (1H, br m, H-9b), 3.70 (1H, br m, H-9a), 3.82 (3H, s, 3-OC$\underline{H}_3$), 3.91 (3H, s, 3'-OC$\underline{H}_3$), 4.24 (1H, br m, H-8), 4.40 (1H, br d, 7-O$\underline{H}$), 4.81 (2H, d, J = 6.46 Hz, H-9'), 4.18 (1H, br m, H-7), 6.34 (1H, dt, J = 6.5, J = 15.8 Hz, H-8'), 6.39 (1H, d, J = 15.8 Hz, H-8''), 6.69 (1H, d, J = 15.8 Hz, H-7'), 6.77 (1H, d, J = 8.1 Hz, H-5), 6.90 (3H, d, J = 8.6 Hz, H-3'', H-5'', H-6), 6.98 (1H, br d, J = 8.6 Hz, H-6'), 7.10 (1H, br s, H-2), 7.14 (1H, d, J = 8.6 Hz, H-5'), 7.18 (1H, br s, H-2'), 7.50 (1H, br s, 4-O$\underline{H}$), 7.57 (2H, d, H-2'', H-6''), 7.65 (1H, d, J = 15.8 Hz, H-7'')

^{13}C NMR (acetone-d6): δ_C 55.3 (3-OMe, q), 55.5 (3'-OMe, q), 61.0 (C-9, t), 64.4 (C-9', t), 73.0 (C-7, d), 87.3 (C-8, d), 110.1 (C-2', d), 110.5 (C-2, d), 114.3 (C-8'', d), 114.6 (C-5, d), 115.8 (C-3'', C-5'', d), 118.4 (C-5', d), 119.6 (C-6, d), 120.0 (C-6', d), 122.4 (C-8', d), 126.1 (C-1'', s), 130.1 (C-2'', C-6'', d), 131.1 (C-1', s), 132.9 (C-1, s), 133.4 (C-7', d), 144.7 (C-7'', d), 146.0 (C-4, s) 147.1 (C-3, s), 148.9 (C-4', s), 150.9 (C-3', s), 159.8 (C-4'', s), 166.3 (C-9'', s)

7.15.9.3 CDI Coupling (*erythro* GGCE)

CDI (228.6 mg, 1.41 mmol, 3 equiv.) coupling of 130.9 mg (0.47 mmol, 2.5 equiv.) of silyl protected *p*-coumaric acid **(66)** with *erythro* GGCE **(40ii)** (70.8 mg, 0.19 mmol) was conducted as for *threo* GGCE (Section 7.15.9.2) to yield 2.0 mg (1.6%) of *erythro* Dadahol B **8Aii**, 1.4 mg (1.4%) of the 9-mono ester **(69)** and 1.4 mg (1.1 %) of the 4,9-diester **(70)**.

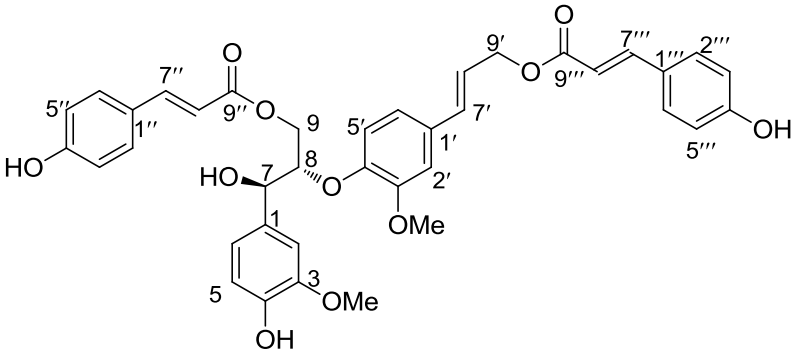

(**8Aii)**
erythro Dadahol B

HRESI-MS (m/z): 668.2234 (calcd for $C_{38}H_{36}O_{11}$ 668.2258)

R*f*: 0.58 (8% MeOH/CH_2Cl_2)

^{1}H NMR (acetone-d_6): δ_H 3.84 (3H, s, 3-OC<u>H</u>$_3$), 3.85 (3H, s, 3'-OC<u>H</u>$_3$), 4.44 (2H, m, H-9), 4.61 (1H,br s, 7-O<u>H</u>), 4.72 (1H, m, H-8), 4.80 (2H, d, J = 6.3, H-9'), 4.99 (1H, br d, J = 5.0 Hz, H-7), 6.23 (1H, d, J = 16.1 Hz, H-8''), 6.33 (1H, dt, J = 15.8, J = 6.3 Hz, H-8'), 6.40 (1H, d, J = 15.8 Hz, H-8'''), 6.68 (1H, d, J = 15.8 Hz, H-7'), 6.79 (1H, d, J = 7.6 Hz, H-5), 6.89 (4H, d, J = 8.2 Hz, H-3'', H-3''', H-5'', H-5'''), 6.95 (1H, br d, J = 7.6 Hz, H-6), 6.96 (1H, d, J = 8.2, H-6'), 7.03 (1H, d, J = 8.2 Hz, H-5'), 7.14 (1H, br s, H-2), 7.16 (1H, br s, H-2'), 7.38 (1H, d, J = 16.1 Hz, H-7''), 7.46 (2H, d, J = 8.2 Hz, H-2'', H-6''), 7.56 (2H, d, J = 8.6 Hz, H-2''', H-6'''), 7.65 (1H, d, J = 15.8 Hz, H-7''')

^{13}C NMR (acetone-d6): δ_C 55.3 (3-OMe, q), 55.4 (3'-OMe, q), 63.4 (C-9, t), 64.4 (C-9', t), 72.5 (C-7, d), 82.6 (C-8, d), 110.4 (C-2', C-2, d), 114.4 (C-5, s), 114.4 (C-8'', d), 114.6 (C-8''', d), 115.8 (C-3'', C-3''', C-5'', C-5''', d), 118.3 (C-5', d), 119.5 (C-6, d), 119.8 (C-6', d), 122.4 (C-8', d), 126.0 (C-1'', s), 126.1 (C-1''', s), 130.1 (C-2'', C-2''', C-6'', C-6''', d), 131.2 (C-1', s), 132.3 (C-1, s), 133.4 (C-7', d), 144.6 (C-7'',d) 144.7 (C-7''', d), 145.9 (C-4, s) 147.2 (C-3, s), 148.2 (C-4', s), 151.1 (C-3', s), 159.7 (C-4'', s), 159.8 (C-4''', s), 166.3 (C-9'', C-9''', s)

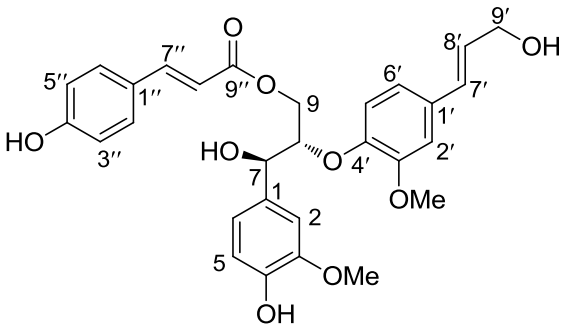

(69)

erythro 9-coumaroyl guaiacylglycerol-8-*O*-4'-coniferyl alcohol ether

HRESI-MS (m/z): 522.1887 (calcd for $C_{29}H_{30}O_9$ 522.1891)

^{1}H NMR (acetone-d_6): δ_H 3.84 (6H, s, 3-OC$\underline{H}_3$, 3'-OC$\underline{H}_3$), 4.21 (2H, br d, J = 3.9 Hz, H-9'), 4.44 (2H, H-9), 4.68 (1H, br m, H-8), 4.99 (1H, d, J = 5.1 Hz, H-7), 6.24 (1H, d, J = 15.8 Hz, H-8''), 6.29 (1H, dt, J = 15.5, J = 5.1 Hz, H-8'), 6.52 (1H, d, J = 15.8 Hz, H-7'), 6.79 (1H, d, J = 7.8 Hz, H-5), 6.87 (2H, d, J = 8.4 Hz, H-3'', H-5''), 6.90 (1H, br d, J = 8.4 Hz, H-6'), 6.94 (1H, d, J = 7.8 Hz, H-6), 7.00 (1H, d, J = 8.4 Hz, H-5'), 7.07 (1H, br s, H-2'), 7.16 (1H, br s, H-2), 7.39 (1H, d, J = 15.8 Hz, H-7''), 7.47 (2H, d, J = 8.4 Hz, H-2'', H-6'')

^{13}C NMR (acetone-d6): δ_C 55.3 (3-OMe, q), 55.4 (3'-OMe, q), 62.4 (C-9', t), 63.3 (C-9, t), 73.5 (C-7, d), 82.7 (C-8, d), 110.2 (C-2', d), 110.3 (C-2, d), 114.4 (C-8'', d), 114.8 (C-5, d), 115.8 (C-3'', C-5'', d), 118.6 (C-5', d), 119.4 (C-6', d), 119.5 (C-6, d), 126.0 (C-1'', s), 128.8 (C-8', d), 128.9 (C-7', d), 130.1 (C-2'', C-6'', d), 132.2 (C-1', s), 132.8 (C-1, s), 144.6 (C-7'', d), 145.9 (C-4, s) 147.2 (C-3, s), 147.6 (C-4', s), 151.1 (C-3', s), 159.7 (C-4'', s), 166.3 (C-9'', s)

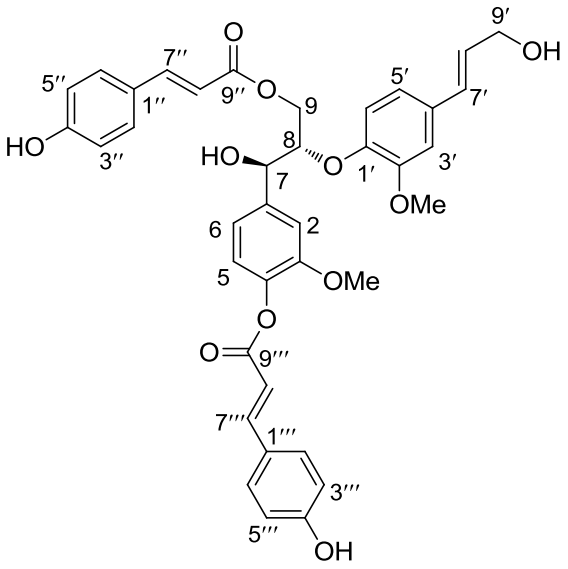

(70)

erythro 4,9-dicoumaroyl guaiacylglycerol-8-*O*-4'-coniferyl alcohol ether

HRESI-MS (m/z): 668.2252 (calcd for $C_{38}H_{36}O_{11}$ 668.2258)

^{1}H NMR (acetone-d_6): δ_H 3.85 (3H, s, 3-OC<u>H</u>$_3$, 3'-OC<u>H</u>$_3$), 4.21 (2H, d, J = 5.0 Hz, H-9'), 4.47 (2H, m, H-9), 4.62 (1H,br s, 7-O<u>H</u>), 4.69 (1H, m, H-8), 5.00 (1H, br d, H-7), 6.29 (1H, dt, J = 15.8, J = 5. Hz, H-8'), 6.42 (1H, d, J = 15.8 Hz, H-8''), 6.53 (1H, d, J = 15.8 Hz, H-7'), 6.57 (1H, d, J = 16.0 Hz, H-8'''), 6.80 (1H, d, J = 8.1 Hz, H-5), 6.93 (4H, d, H-3'', H-5'', H-6, H-6'), 7.01 (1H, d, J = 8.1 Hz, H-5'), 7.08 (1H, br s, H-2'), 7.17 (1H, br s, H-2), 7.25 (2H, d, J = 8.4 Hz, H-3''', H-5'''), H-8''), 7.46 (1H, d, J = 16.0 Hz, H-7''), 7.66 (2H, d, J = 8.4 Hz, H-2'', H-6''), 7.68 (2H, d, J = 8.4 Hz, H-2''', H-6'''), 7.82 (1H, d, J = 16.0 Hz, H-7''')

^{13}C NMR (acetone-d6): δ_C 55.3 (3-OMe, q), 55.3 (3'-OMe, q), 62.4 (C-9', t), 63.6 (C-9, t), 72.5 (C-7, d), 82.7 (C-8, d), 110.3 (C-2', C-2, d), 113.3 (C-8''', d), 114.4 (C-5, s), 115.9 (C-3'', C-5'', d), 117.9 (C-8'', d), 118.7 (C-5', d), 119.2 (C-6, d), 119.4 (C-6', d), 122.4 (C-8', d), 122.4 (C-3''', C-5''', d), 128.9 (C-8', d), 129.3 (C-2'', C-6'', d), 130.5 (C-7', d), 130.5 (C-2''', C-6''', d), 131.9 (C-1'', s), 132.3 (C-1', s), 132.8 (C-1, s), 133.2 (C-1''', s), 143.5 (C-7'', C-7‴, d), 145.9 (C-4, s) 147.2 (C-3, s), 147.5 (C-4', s) 151.2 (C-3', s), 153.7 (C-4'', s), 160.3 (C-4''', s), 165.2 (C-9'', s), 166.3 (C-9''', s)

7.15.10 Auto-oxidation Products

7.15.10.1 DHCA

DHCA **(38)** and its auto-oxidation product, balanophonin **(99)**, were separated by silica gel column chromatography using 1% MeOH/DCM.

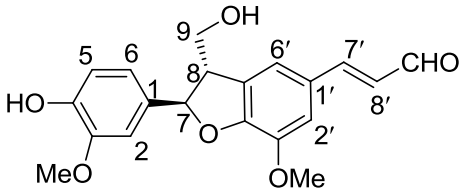

(99)

Common name: Balanophonin (Lee et al., 2007b)

HRESI-MS (m/z): 356.1269 (calcd for $C_{20}H_{20}O_6$ 356.1259)

R*f*: 0.59 (5% MeOH/DCM)

^{1}H NMR (acetone-d_6): δ_H 3.63 (1H, br m, H-8) , 3.81 – 3.88 (2H, m, H-9), 3.83 (3H, s, 3-OC$\underline{H}_3$), 3.92 (3H, s, 3'-OC$\underline{H}_3$), 4.18 (1H, br m, 9-O$\underline{H}$), 5.66 (1H, d, J = 6.5 Hz, H-7), 6.67 (1H, dd, J = 7.9, J = 15.7 Hz, H-8'), 6.83 (1H, d, J = 8.3 Hz, H-5), 6.90 (1H, dd, J = 8.3, J = 1.9 H, H-6), 7.06 (1H, br d, J = 1.9 Hz, H-2), 7.31 (1H, s, H-2'), 7.33 (1H, s, H-6′), 7.60 (1H, d, J = 15.7 Hz, H-7′), 7.64 (1H, s, 4-O$\underline{H}$), 9.65 (1H, d, J = 7.9 Hz, H-9')

^{13}C NMR (acetone-d6): δ_C 53.4 (C-8, d), 55.4 (3-OMe, q), 55.5 (3'-OMe, q), 63.4 (C-9, t), 88.5 (C-7, d), 109.7 (C-2, d), 112.6 (C-2', d), 114.9 (C-5, d), 118.8 (C-6', d; C-6, d), 126.2 (C-8', d), 128.1 (C-1', s), 130.3 (C-4', s), 132.9 (C-1, s), 144.8 (C-3', s), 146.6 (C-4, s), 146.6 (C-3, s), 151.5 (C-5', s), 153.2 (C-7', d), 190.0 (C-9', d)

7.15.10.2 GGCE

GGCE **(40)** and its auto-oxidation product **(100)** were separated by silica gel column chromatography using 5% MeOH/DCM. Typical yields were 3 – 5 %.

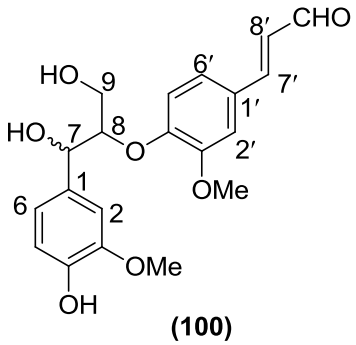

(100)
guaiacylglycerol-8-O-4'-coniferyl aldehyde ether

HRESI-MS (m/z): 374.1276 (calcd for $C_{20}H_{22}O_7$ 374.1366)

R*f*: 0.50 (5% MeOH/DCM)

^{1}H NMR of *threo* diastereomer (600 MHz, acetone-d_6): δ 3.58 (1H, br m, H-9b), 3.76 (1H, br m, H-9a), 3.82 (3H, s, 3-OC<u>H</u>$_3$), 3.94 (3H, s, 3'-OC<u>H</u>$_3$), 4.49 (1H, br m, H-8), 4.56 (1H, d, J = 3.5 Hz, 7-O<u>H</u>), 4.92 (1H, br m, H-7), 6.68 (dd, J = 7.8, J = 15.8 Hz, H-8'), 6.77 (1H, d, J = 7.9 Hz, H-5), 6.92 (1H, br d, J = 7.9 Hz, H-6), 7.10 (1H, d, J = 8.4 Hz, H-5'), 7.12 (1H, br s, H-2), 7.20 (1H, br d, J = 8.4 Hz, H-6'), 7.40 (1H, br s, H-2'), 7.58 (1H, d, J = 15.8 Hz, H-7'), 9.66 (1H, d, J = 7.8 Hz, H-9')

^{13}C NMR (acetone-d6): δ_C 55.6 (3-OMe, q; 3'-OMe, q), 61.1 (C-9, t), 72.8 (C-7, d), 86.2 (C-8, d), 110.5 (C-2, d), 112.8 (C-2', d), 114.3 (C-5, d), 116.5 (C-5', d), 119.6 (C-6, d), 123.2 (C-6', d), 127.0 (C-8', d), 129.1 (C-1', s), 132.9 (C-1, s), 146.0 (C-4, s), 147.2 (C-3, s), 150.6 (C-4', s), 151.8 (C-3', s), 152.6 (C-7', d), 193.0 (C-9', d)

7.15.11 Alternative Preparation of DHCA

7.15.11.1 Alternative Preparation via Ethyl Ferulate

2 x 5 g batches of ferulic acid **(101)** were boiled in EtOH (30 cm^3) containing H_2SO_4 (1.2 cm^3) for 4 h. The orange solution was concentrated to a gum, dissolved in ethyl acetate and extracted with H_2O. After drying ($MgSO_4$) and concentrating *in vacuo*, the combined organic fractions were chromatographed on a silica gel column using 10% ethyl acetate/hexane to give a total yield of 4.1 g (36 %) of ethyl ferulate **(42)**. DIBAL reduction of ethyl ferulate **(42)** to coniferyl alcohol **(37)** was as reported before (Section 7.15.4). Silver (I) oxide (773 mg, 3.33 mmol) was added to a solution of coniferyl alcohol **(37)** (400 mg, 2.22 mmol) in anhydrous DCM (12 ml). After stirring at room temperature for ~ 24 h, the reaction mixture was filtered through a bed of celite,

and evaporated to dryness *in vacuo*. Column chromatography (1% MeOH/chloroform as eluent) afforded DHCA **(38)** as a beige solid (90 mg, 23%).

7.15.11.2 Dimerisation of Coniferyl Alcohol in DMF

Coniferyl alcohol **(37)** (150 mg, 0.83 mmol) was treated with silver (I) oxide (290 mg, 1.25 mmol) in anhydrous DMF (2 ml) as in Section 7.15.11.1 to yield 2.5 mg of aldehyde **(103)** (1.6%), 12.6 mg of methylated GGCE analogue **(102)** (7.8%), 12 mg of DHCA (38) (8%) and 2 mg (1.4 %) of oxidation product **(99)**.

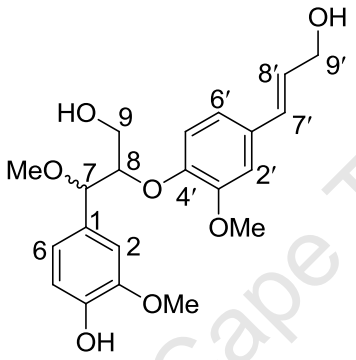

(102)

7-methoxy guaiacylglycerol-8-*O*-4'-coniferyl alcohol ether

HRESI-MS (m/z): 390.1643 (calcd for $C_{21}H_{26}O_7$ 390.1679)

R*f*: 0.37 (5% MeOH/DCM)

^{1}H NMR of *threo* diastereomer (acetone-d_6): δ_H 3.22 (3H, s, 7-OCH_3), 3.41 (1H, br m, H-9b), 3.56 (1H, br m, H-9a), 3.81 (3H, s, 3-OC$\underline{H_3}$), 3.87 (3H, s, 3'-OC$\underline{H_3}$), 4.20 (2H, br d, J = 5.1 Hz, H-9'), 4.34 (1H, br m, H-8), 4.42 (1H, br m, H-7), 6.27 (1H, dt, J = 5.1, J = 15.8 Hz, H-8'), 6.51 (1H, d, J = 15.8 Hz, H-7'), 6.79 – 6.89 (4H, m, H-5, H-6, H-5', H-6'), 7.02 (1H, s, H-2), 7.05 (1H, s, , H-2'), 7.52 (1H, br s, 4-O$\underline{H}$)

^{13}C NMR (acetone-d6): δ_C 55.4 (3-OMe, q; 3'-OMe, q), 56.0 (7-Ome, q), 60.8 (C-9, t), 62.4 (C-9', t), 82.5 (C-7, d), 84.5 (C-8, d), 110.1 (C-2', d), 111.3 (C-2, d), 114.3 (C-5, d), 117.8 (C-6', d), 119.3 (C-6, d), 121.0 (C-8, d), 128.5 (C-7', d), 130.0 (C-1', s), 131.5 (C-1, s), 146.3 (C-3, s), 147.3 (C-4, s), 147.8 (C-4', s), 150.7 (C-3', s)

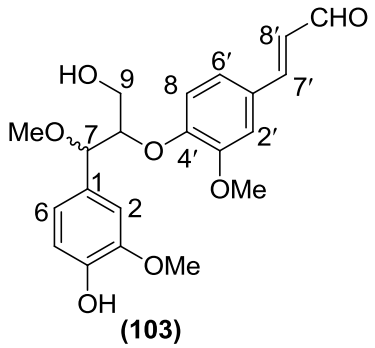

(103)

HRESI-MS (m/z): 388.1343 (calcd for $C_{38}H_{36}O_{11}$ 356.1675)

R*f*: 0.82 (5% MeOH/DCM)

^{1}H NMR of *threo* diastereomer (acetone-d_6): δ_H 3.22 (3H, s, 7-OC$\underline{H}_3$), 3.52 (1H, br m, H-9b), 3.65 (1H, br m, H-9a), 3.82 (3H, s, 3-OC$\underline{H}_3$), 3.93 (3H, s, 3'-OC$\underline{H}_3$), 4.44 (1H, d, J = 8 Hz, H-7), 4.57 (1H, br m, H-8), 6.67 (1H, dt, J = 7.9, J = 15.9 Hz, H-8'), 6.77 (1H, d, J = 7.9 Hz, H-5), 6.87 (1H, dd, J = 7.9 Hz, J = 1.5 Hz, H-6), 7.04 (1H, d, J = 8.2 Hz, H-5'), 7.07 (1H, d, J = 1.5 Hz, H-2), 7.17 (1H, d, J = 8.2 Hz, H-6'), 7.31 (1H, s, H-2'), 7.55 (1H, d, J = 15.9 Hz, H-7'), 9.65 (1H, d, J = 7.9 Hz, H-9')

7.15.12 *p*-Nitrobenzoyl Esterification of DHCA

30mg (0.083 mmol) of DHCA was dissolved in 1 ml of dry THF. 23 mg (0.125 mmol, 1.5 equiv.) of *p*-nitrobenzoyl chloride and 1 mg of DMAP was added. 14 µl (0.1 mmol, 1.2 equiv.) of Et_3N was added and the reaction mixture was stirred at room temperature overnight. The reaction was quenched by addition of 10 ml EtOAc which was then washed with 0.05 N HCl and water, dried over $MgSO_4$ and evaporated under vacuum pressure. The residue was chromatographed over silica gel using 10% ethyl acetate/hexane. 9.7mg (29%) of the triester **(104)** and 3.4 mg (8.3%) of the diester **(105)** was recovered.

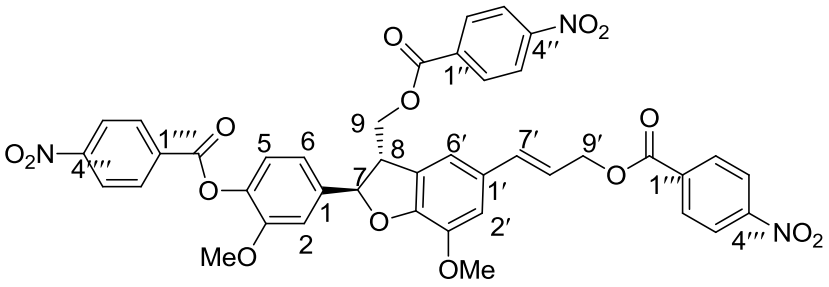

(104)
4,9,9′-tri-*p*-nitrobenzoyl dehydrodiconiferyl alcohol

HRESI-MS (m/z): 805.2045 (calcd for $C_{41}H_{31}N_3O_{15}$ 805.2011)

R*f*: 0.6 (50% ethyl acetate/hexane)

^{1}H NMR (acetone-d_6): δ_H 3.65 (3H, s, 3-OC<u>H</u>$_3$), 3.79 (3H, s, 3'-OC<u>H</u>$_3$), 3.99 (1H, br ddd, J = 6.5, J = 7.6, J = 11.2 Hz, H-8), 4.61 (1H, dd, J = 5.3, J = 11.2 Hz, H-9b), 4.78 (1H, dd, J = 6.5, J = 5.3 Hz, H-9a), 4.89 (2H, dd, J = 6.5, J = 1.2 Hz, H-9'), 5.72 (1H, d, J = 7.6 Hz, H-7), 6.30 (1H, dt, J = 15.9, J = 7.0 Hz, H-8'), 6.70 (1H, d, J = 15.9 Hz, H-7'), 7.01 (1H, br s, H-2'), 7.06 (1H, d, J = 8.2 Hz, H-5), 7.07 (1H, s, H-6'), 7.19 (1H, dd, J = 8.2 Hz, H-6), 7.24 (1H, s, H-2), 8.01 – 8.33 (8H, 12 x dd, J = 8.8, J = 1.8 Hz, H-2"", H-6"", H-2"', H-6"', H-2", H-6", H-3"", H-5"", H-3", H-5", H-3"', H-5"')

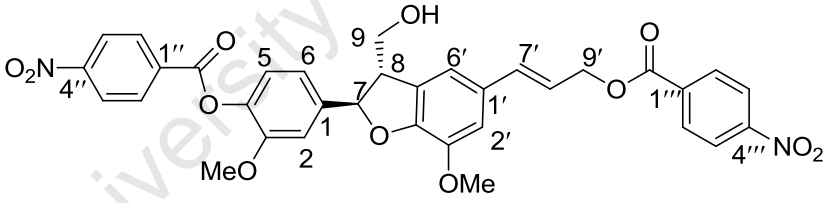

(105)
4,9′-di-*p*-nitrobenzoyl dehydrodiconiferyl alcohol

HRESI-MS (m/z): 656.1905 (calcd for $C_{34}H_{28}N_2O_{12}$ 656.1859)

R*f*: 0.25 (50% ethyl acetate/hexane)

^{1}H NMR (acetone-d_6): δ_H 3.49 (1H, br ddd, J = 6.5, J = 5.9, J = 12.9 Hz, H-8), 3.67 (3H, s, 3-OC<u>H</u>$_3$), 3.78 (3H, s, 3'-OC<u>H</u>$_3$), 3. 76 (1H, m, H-9b), 3.84 (1H, dd, J = 5.3, J = 12.9, H-9b), 4.12 (1H, t, J = 5.3 Hz, 9'-OH), 4.90 (2H, dd, J = 6.8, J = 5.3 Hz, H-9'), 5.62 (1H, d, J = 5.9 Hz, H-7), 6.27 (1H, dt, J = 15.8, J = 6.8 Hz, H-8'), 6.68 (1H, d, J = 15.8, H-7'), 6.96 (3H, m, H-2', H-6', H-6), 7.14 (1H, d, J = 8.2 Hz, H-5), 7.15 (1H, s, H-

2), 8.17 – 8.32, 8 x dd, J = 8.8, J = 1.8 Hz, H-3'', H-5'', H-3''', H-5''', H-2''', H-6''', H-2'', H-6'')

7.15.13 Acid Chloride Esterification of DHCA

15.4 mg (0.104 mmol) of cinnamic acid **(51)** was dissolved in 5 ml of dry dichloromethane. 2 drops of anhydrous DMF were added and then 18 µl (0.208 mmol, 2 equiv.) of oxalyl chloride was added drop-wise at room temperature, under nitrogen. After addition the reaction mixture was refluxed at 50°C for 2h. Solvent and excess oxalyl chloride was removed under vacuum pressure to yield pale yellow crystals of the cinnamoyl chloride **(52)** (17.3 mg, 100%, 1.1 equiv.). The acid chloride was dissolved in 5 ml of dry dichloromethane and added to round bottom flask containing 33.8 mg (0.094 mmol) of DHCA **(38)**. Added a few drops of Et_3N and stirred at room temperature under N_2. Reaction was monitored on TLC and eventually refluxed at 50°C for 1h to force to completion. The reaction was then quenched with water and the organic layer was washed with 0.1M HCl and saturated $NaHCO_3$. The solution was dried over $MgSO_4$, the solvent was evaporated under reduced pressure and residue was chromatographed on silica gel using 2% MeOH/$CHCl_3$ to yield 34 mg (74%) of the ester **(108)**.

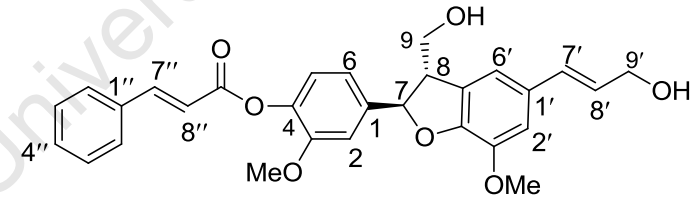

(108)
4-cinnamoyl dehydrodiconiferyl alcohol

HRESI-MS (m/z): 488.1834 (calcd for $C_{29}H_{28}O_7$ 488.1836)

R*f*: 0.35 (5% MeOH/Me_2Cl_2)

^{1}H NMR (acetone-d_6): δ_H 3.58 (1H, br ddd, J = 6.5, J = 5.3, J = 5.9 Hz, H-8), 3.82 (3H, s, 3-OC$\underline{H}_3$), 3.84 – 3.88 (1H, br m, H-9b), 3.88 (3H, s, 3'-OC$\underline{H}_3$), 3.96 (1H, br dd, J = 5.3, J = 10.6 Hz, H-9a), 4.20 (2H, br d, J = 5.3 Hz, H-9'), 5.71 (1H, d, J = 6.5 Hz, H-7), 6.26 (1H, dt, J = 16.1, J = 5.3 Hz, H-8'), 6.54 (1H, d, J = 16.1 Hz, H-7'), 6.78 (1H, d, J = 15.8 Hz, H-8''), 6.97 (1H, s, H-2'), 6.98 (1H, s, H-6'), 7.05 (1H, br d, J = 8.2

Hz, H-6), 7.13 (1H, d, J = 8.2 Hz, H-5), 7.23 (1H, br s, H-2), 7.48 (3H, br m, H-3", H-4", H-5"), 7.78 (2H, br m, H-2", H-6"), 7.85 (1H, d, J = 15.8 Hz, H-7")

7.15.14 Silyl Protection of DHCA

18 mg (0.12 mmol, 1.1eq) of *tert*-butyldimethylsilyl chloride, 14.4 mg of imidazole (0.21 mmol, 2 equiv.) and 0.6mg (0.005 mmol, 0.05 equiv.) of DMAP were added to a flask containing 38 mg (0.106 mmol) of DHCA **(38)** in 2 ml of THF at 0 ºC. The reaction mixture was stirred at room temperature overnight, then diluted with ethyl acetate, washed with 10% $NaHCO_3$ and brine, dried over Na_2SO_4 and concentrated *in vacuo*. The residue was chromatographed on silica gel using 1% MeOH/DCM and 1.8 mg (5%) of **(109)** and 23 mg (46%) of **(110)** were recovered.

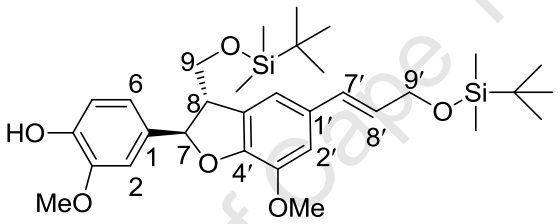

(109)

9,9′-di-*tert*-butyldimethylsilyl dehydrodiconiferyl alcohol

HRESI-MS (m/z): 586.3152 (calcd for $C_{32}H_{50}O_6Si_2$ 586.3342)

R*f*: 0.88 (3% MeOH/DCM)

^{1}H NMR (acetone-d_6): δ_H 0.03 (12H, s, 9'-*O*-Si(C$\underline{H}_3$)$_2$, 9-*O*-Si(C$\underline{H}_3$)$_2$), 0.83 (9H, s, 9-O-Si-C(C$\underline{H}_3$)$_3$), 0.86 (9H, s, 9'-O-Si-C(C$\underline{H}_3$)$_3$), 3.49 (1H, br ddd, J = 7.0, J = 5.9, J = 10.0 Hz, H-8), 3.75 (3H, s, 3-OC$\underline{H}_3$), 3.79 (3H, s, 3'-OC$\underline{H}_3$), 3.82 (1H, br dd, J = 7.0, J = 10.0 Hz, H-9b), 3.91 (1H, dd, J = 5.9, J = 10.0 Hz, H-9a), 4.26 (1H, dd, J = 1.8, J = 5.3, H-9'), 5.44 (1H, d, J = 5.9 Hz, H-7), 6.13 (1H, dt, J = 15.9, J = 5.3 Hz, H-8'), 6.48 (1H, br d, J = 15.9 Hz, H-7'), 6.74 (1H, d, J = 7.9 Hz, H-5), 6.80 (1H, dd, J = 7.9, J = 1.8 Hz, H-6), 6.90 (1H, br s, H-2'), 6.93 (1H, d, J = 1.8 Hz, H-2), 6.94 (1H, br s, H-6'), 7.52 (1H, s, 4-O$\underline{H}$)

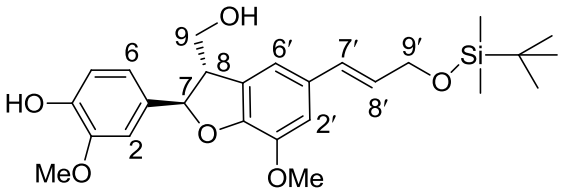

(110)

9′-*tert*-butyldimethylsilyl dehydrodiconiferyl alcohol

HRESI-MS (m/z): 472.2296 (calcd for $C_{26}H_{36}O_6Si$ 472.2265)

R*f*: 0.22 (3% MeOH/DCM)

^{1}H NMR (acetone-d_6): δ_H 0.08 (6H, s, 9'-O-Si(C<u>H</u>$_3$)$_2$), 0.91 (9H, s, 9'-O-Si-C(C<u>H</u>$_3$)$_3$), 3.52 (1H, m, H-8), 3.75 (3H, s, 3-OC<u>H</u>$_3$), 3.79 (3H, s, 3'-OC<u>H</u>$_3$), 3.91 – 3.80 (2H, m, H-9), 4.32 (2H, dd, J = 1.2, J = 5.0 Hz, H-9'), 5.55 (1H, d, J = 6.5 Hz, H-7), 6.19 (1H, dt, J = 15.9, J = 5.0 Hz, H-8'), 6.53 (1H, br d, J = 15.9 Hz, H-7'), 6.79 (1H, d, J = 8.2 Hz, H-5), 6.86 (1H, dd, J = 8.2, J = 1.8 Hz, H-6), 6.94 (1H, br s, H-2'), 6.97 (1H, s, H-6'), 7.02 (1H, d, J = 1.8 Hz, H-2), 7.56 (1H, s, 4-O<u>H</u>)

7.15.15 Trityl Protection of DHCA

16.4 mg (0.06 mmol, 1.1 equiv.) of trityl chloride, 11.7 µl (0.08 mmol, 1.5 equiv.) of triethylamine and 0.3 mg (0.003 mmol, 0.05 equiv.) of DMAP were added to a flask containing 20 mg (0.056 mmol) of DHCA **(38)** in 2 ml of dichloromethane at 0 ºC. The reaction mixture was allowed to reach room temperature stirring for at least 2 h, then was diluted with dichloromethane, washed with 10% $NaHCO_3$ and brine, dried over Na_2SO_4 and concentrated *in vacuo*. The residue was chromatographed on silica gel using 1% MeOH/CH_2Cl_2 and 18.4 mg (55%) of the trityl ether **(111)** was recovered.

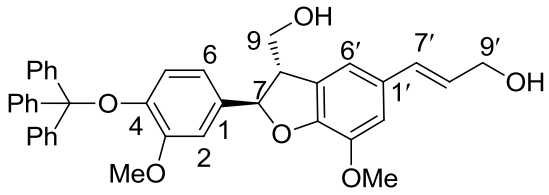

(111)

4-trityl dehydrodiconiferyl alcohol

^{1}H NMR (acetone-d_6): δ_H 3.39 (1H, m, H-8), 3.57 (3H, s, 3-OC<u>H</u>$_3$), 3.71 – 3.80 (2H, m, H-9), 3.84 (3H, s, 3'-OC<u>H</u>$_3$), 4.19 (2H, dd, J = 1.2, J = 5.3 Hz, H-9'), 5.48 (1H, d, J = 6.5 Hz, H-7), 6.23 (1H, dt, J = 15.9, J = 5.3 Hz, H-8'), 6.51 (1H, br d, J = 15.9 Hz, H-7'), 6.58 (1H, dd, J = 8.2, J = 1.8 Hz, H-6), 6.62 (1H, d, J = 8.2 Hz, H-5), 6.85 (1H, d, J

= 1.8 Hz, H-2), 6.92 (1H, s, H-2'), 6.94 (1H, d, H-2), 7.23 (3H, m, *para* Ph-H), 7.28 (6H, m, *meta* Ph-H), 7.48 (6H, *ortho* Ph-H)

7.15.16 DCC Coupling between DHCA and *p*-Coumaric Acid

16.5 mg (0.05 mmol) of DHCA **(38)** and 25.6 mg (0.09 mmol 2 equiv.) silyl protected p-coumaric acid (66) were dissolved in 2 ml 1:1 dichloromethane/THF. The solution was cooled to 0 ºC. 20.9 mg (0.1 mmol, 2.1 equiv.) of DCC and 1.2 mg (0.01 mmol) of DMAP were added in portions to the solution, which was allowed to stirr at 0 ºC for 30 min before warming to room temperature. The suspension as filtered through celite and the solvent removed *in vacuo*. Residue was purified on silica gel (0.5 % MeOH/dichloromethane eluent) to yield 3.6 mg (9%) of 9-monoester **(113)** and 2.1 mg (7.5%) of 4-monoester **(114)**. Ester **(113)** was deprotected with 2.5 equiv. TBAF to yield the 9-coumaroyl ester **(132)** (*cf.* Section 7.15.19.4 for structural data)

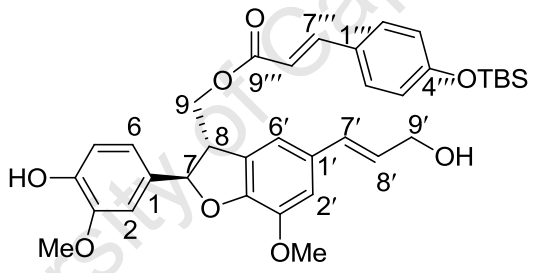

(113)

R*f*: 0.46 (3% MeOH/DCM)

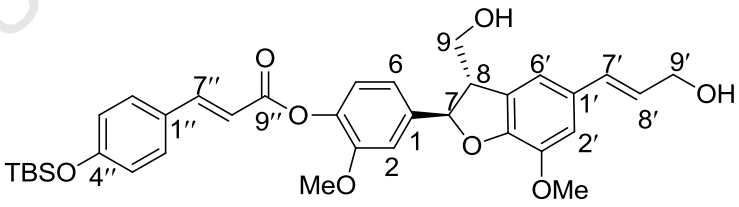

(114)

R*f*: 0.21 (3% MeOH/DCM)

7.15.17 CDI Coupling between DHCA and Cinnamic Acid

41.4 mg (0.28 mmol, 2 equiv.) of cinnamic acid **(51)** was dissolved in 2 ml of anhydrous dichloromethane. 45.4 mg of CDI (0.28 mmol) was added and the mixture

was stirred at room temperature for 4h at room temperature under nitrogen. 50 mg (0.14 mmol) of DHCA **(38)** in 2 ml of THF was added and the reaction mixture was stirred at room temperature for 48h, and then refluxed at 75°C for 7h with a catalytic amount of DMAP and Na_2CO_3. The reaction did not go to completion but was cooled, diluted with EtOAc, washed quickly with cold 0.05N HCl and then brine. Organic layer was dried over $MgSO_4$ and evaporated to dryness. Residue was purified over sílica gel using 40% EtOAc/hexane to yield 1.3mg (1.9%) of the 4,9,9'-tricinnamoyl analogue **(115),** 2.1mg (2.4%) 9,9'-cinnamoyl di-esters **(116)**, 1.1 mg (1.3%) of the 4,9'- diester **(117)**, 2.1mg (3.1%) of the 9-monoester and 3.2 mg (4.7%) of the 9'-cinnamoyl mono-ester **(118)**.

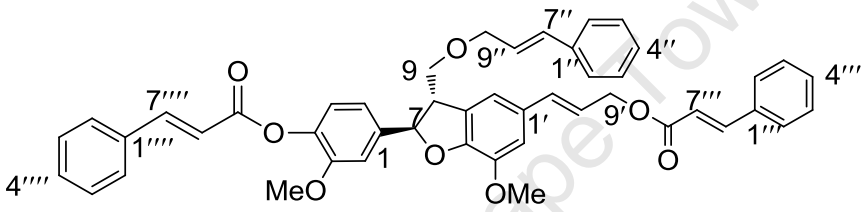

(115)

4,9,9′-tricinnamoyl dehydrodiconiferyl alcohol

HRESI-MS (m/z): 748.3487 (calcd for $C_{47}H_{40}O_9$ 748.3356)

R*f*: 0.58 (40% ethyl acetate/hexane)

^{1}H NMR (acetone-d_6): δ_H 3.81 (3H, s, 3-OC$\underline{H}_3$), 3.93 (3H, s, 3'-OC$\underline{H}_3$), 4.21 (1H, br m, H-8), 4.54 (1H, dd, J = 7.6, J = 11.2 Hz, H-9b), 4.66 (1H, dd, J = 5.3, J = 11.2 Hz, H-9b), 4.83 (2H, d, J = 6.4 Hz, H-9'), 5.76 (1H, d, J = 7.1 Hz, H-7), 6.35 (1H, dt, J = 15.9, J = 6.4 Hz, H-8'), 6.59 (1H, d, J = 15.9 Hz, H-7'), 6.59 (1H, d, J = 15.8, H-8''), 6.74 (1H, d, J = 16.4 Hz, H-8'''), 6.78 (1H, d, J = 15.8 Hz, H-8''''), 7.11 (2H, br m, H-5, H-2'), 7.16 (2H, br m, H-6, H-6'), 7.28 (1H, s, H-2), 7.44 (6H, br m, H-3'', H-4'', H-5'', H-3'''', H-4'''', H-5''''), 7.48 (3H, br m, H-3''', H-4''', H-5'''), 7.67 (1H, d, J = 15.8, H-7''), 7.69 (4H, br m, H-2'', H-6'', H-2'''', H-6''''), 7.72 (1H, br d, J = 15.8 Hz, H-7''''), 7.78 (2H, br m, H-2''', H-6'''), 7.85 (1H, d, J = 156.4 Hz, H-7''')

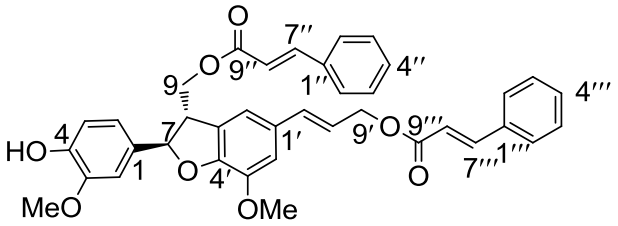

(116)

9,9′-dicinnamoyl dehydrodiconiferyl alcohol

HRESI-MS (m/z): 618.2768 (calcd for $C_{38}H_{34}O_8$ 618.2847)

R*f*: 0.40 (40% ethyl acetate/hexane)

^{1}H NMR (acetone-d_6): δ_H 3.82 (3H, s, 3-OC$\underline{H}_3$), 3.87 - 3.92 (1H, m, H-8), 3.90 (3H, s, 3'-OC$\underline{H}_3$), 4.50 (1H, dd, J = 7.0, J = 11.2 Hz, H-9b), 4.61 (1H, dd, J = 5.3, J = 11.2 Hz, H-9a), 4.82 (2H, d, J = 6.5 Hz, H-9'), 5.61 (1H, d, J = 7.1 Hz, H-7), 6.34 (1H, dt, J = 15.9, J = 6.5 Hz, H-8'), 6.53 (1H, d, J = 15.8 Hz, H-8''), 6.58 (1H, d, J = 15.8 Hz, H-8'''), 6.73 (1H, br d, J = 15.9 Hz, H-7'), 6.84 (1H, d, J = 7.6 Hz, H-5), 6.94 (1H, br d, J = 7.6 Hz, H-6), 7.09 (2H, br s, H-2', H-6'), 7.14 (1H, s, H-2), 7.44 (6H, br m, H-3'', H-4'', H-5'', H-3''', H-4''', H-5'''), 7.62 (1H, d, J = 15.8 Hz, H-7''), 7.66 (2H, br m, H-2'', H-3''), 7.69 (2H, br m, H-2''', H-6'''), 7.72 (1H, d, J = 15.8 Hz, H-7''')

^{13}C NMR (acetone-d6): δ_C 50.4 (C-8, d), 55.4 (3-OMe, q), 55.5 (3'-OMe, q), 64.8 (C-9', t), 65.3 (C-9, t), 88.4 (C-7, d), 109.7 (C-2', d), 111.4 (C-6', d), 114.9 (C-5, d), 115.5 (C-2, d), 117.7 (C-8'', d), 118.1 (C-8''', d), 119.1 (C-6, d), 121.3 (C-8', d), 128.2 (C-7'', d, C-7''', d), 128.9 (C-3'', C-5'', C-3''', C-5''', d), 130.3 (C-7', d), 130.4 (C-4', s), 130.5 (C-4'', s), 132.5 (C-4''', s), 134.1 (C-1, s, C-1', s), 134.4 (C-1'', s), 134.5 (C-1''', s), 144.5 (C-3', s), 144.9 (C-2'', C-6'', C-2''', C-6''', d), 147.6 (C-4, s), 148.6 (C-3, s), 150.6 (C-5', s), 165.9 (C-9'', s, C-9''', s)

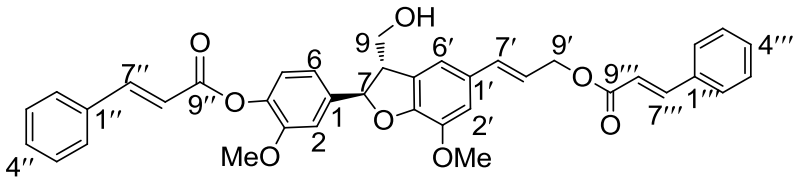

(117)

4,9′-dicinnamoyl dehydrodiconiferyl alcohol

HRESI-MS (m/z): 618.2469 (calcd for $C_{38}H_{34}O_8$ 618.2509)

R*f*: 0.21 (40% ethyl acetate/hexane)

^{1}H NMR (acetone-d_6): δ_H 3.61 (1H, br m, H-8), 3.82 (1H, s, 3-OC$\underline{H}_3$), 3.90 (3H, s, 3'-OC$\underline{H}_3$), 3.84 – 4.02 (2H, m, H-9), 4.83 (1H, d, J = 6.2 Hz, H-9'), 5.73 (1H, d, J = 5.9 Hz, H-7), 6.31 (1H, dt, J = 15.8, J = 6.2 Hz, H-8'), 6.60 (1H, d, J = 15.8 Hz, H-8''), 6.72 (1H, d, J = 15.8 Hz, H-7'), 6.78 (1H, d, J = 16.4, H-8'''), 7.08 (3H, br m, H-5, H-6', H-2'), 7.13 (1H, d, J = 8.2 Hz, H-6), 7.23 (1H, s, H-2), 7.44 (3H, br m, H-3'', H-4'', H-5''), 7.48 (3H, br m, H-3''', H-4''', H-5'''), 7.71 (2H, br m, H-2'', H-6''), 7.72 (1H, br d, J = 15.8 Hz, H-7''), 7.78 (2H, br m, H-2''', H-6'''), 7.85 (1H, d, J = 16.4 Hz, H-7''')

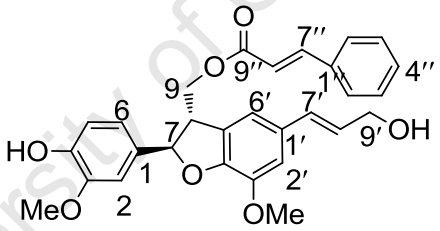

(118)

9-cinnamoyl dehydrodiconiferyl alcohol

HRESI-MS (m/z): 488.1784 (calcd for $C_{29}H_{28}O_7$ 488.1836)

R*f*: 0.07 (40% ethyl acetate/hexane)

^{1}H NMR (acetone-d_6): δ_H 3.82 (3H, s, 3-OC$\underline{H}_3$), 3.85 (1H, br m, H-8), 3.88 (3H, s, 3'-OC$\underline{H}_3$), 4.20 (2H, br d, J = 5.3 Hz, H-9'), 4.49 (1H, dd, J = 11.2, J = 7.6 Hz, H-9b), 4.61 (1H, dd, J = 11.2, J = 5.3 Hz, H-9a), 5.59 (1H, d, J = 7.0 Hz, H-7), 6.28 (1H, dt, J = 15.9, J = 5.3 Hz, H-8'), 6.56 (2H, d, J = 15.9 Hz, H-7', H-8''), 6.84 (1H, d, J = 8.2 Hz, H-5), 6.95 (1H, br d, J = 8.2 Hz, H-6), 7.01 (1H, br s, H-2'), 7.05 (1H, br s, H-6'), 7.09 (1H, s, H-2), 7.44 (3H, br m, H-3'', H-4'', H-5''), 7.62 (1H, d, J = 15.9 Hz, H-7''), 7.66 (2H, br m, H-2'', H-6'')

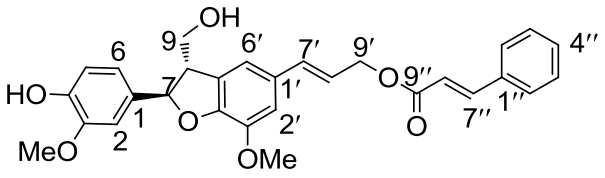

(119)

9′-cinnamoyl dehydrodiconiferyl alcohol

HRESI-MS (m/z): 488.1789 (calcd for $C_{29}H_{28}O_7$ 488.1836)

R*f*: 0.10 (40% ethyl acetate/hexane)

^{1}H NMR (acetone-d_6): δ_H 3.56 (1H, br m, H-8), 3.82 (3H, s, 3-OC$\underline{H}_3$), 3.88 (3H, s, 3'-OC$\underline{H}_3$), 3.89 – 3.94 (1H, m, H-9b), 4.22 (1H, br m, H-9a), 4.83 (2H, d, J = 6.5 Hz, H-9'), 5.58 (1H, d, J = 6.5 Hz, H-7), 6.30 (1H, dt, J = 15.9, J = 6.5 Hz, H-8'), 6.59 (1H, d, J = 15.9 Hz, H-8''), 6.71 (1H, br d, J = 15.9 Hz, H-7'), 6.81 (1H, d, J = 8.2 Hz, H-5), 6.89 (1H, br d, J = 8.2 Hz, H-6), 7.04 (2H, br s, H-2', H-6'), 7.06 (1H, s, H-2), 7.44 (3H, br m, H-3', H-4'', H-5''), 7.59 (1H, s, 4-O$\underline{H}$), 7.70 (2H, br m, H-2'', H-6''), 7.77 (1H, d, J = 15.9 Hz, H-7'')

^{13}C NMR (acetone-d6): δ_C 53.8 (C-8, d), 55.4 (3-OMe, q), 55.5 (3'-OMe, q), 63.7 (C-9, t), 64.9 (C-9', t), 87.8 (C-7, d), 109.6 (C-2', d), 111.1 (C-6', d), 114.8 (C-5, d), 115.7 (C-2, d), 118.1 (C-6, d), 118.7 (C-8'', d), 120.8 (C-7', d), 128.2 (C-7'', d, C-8', d), 128.9 (C-3'', C-5'', C-3''', C-5''', d), 130.3 (C-4', d), 131.1 (C-4'', s), 134.4 (C-1, s, C-1', s), 134.5 (C-1'', s), 134.5 (C-1''', s), 144.3 (C-3', s), 144.5 (C-2'', C-6'', d), 146.5 (C-4, s), 147.8 (C-3, s), 149.6 (C-5', s), 165.9 (C-9'', s)

7.15.18 CDI Coupling between DHCA and Caffeic Acid

CDI (160.5 mg, 0.99 mmol, 3 equiv.) coupling between 132.7 mg (0.33 mmol) of silyl protected *p*-caffeic acid **(120)** and DHCA **(38)** (45 mg, 0.13 mmol) was conducted as in Section 7.15.17 to yield 2.1 mg (1.6%) of inseparable mixture (~ 2:1 ratio) of 9'- and 9-caffeoyl esters **(121)**.

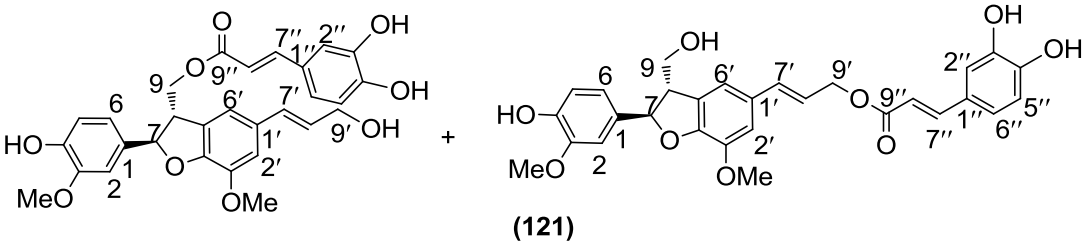

(121)

Mixture of 9-caffeoyl dehydrodiconiferyl alcohol and 9′-caffeoyl dehydrodiconiferyl alcohol

HRESI-MS (m/z): 520.1725 (calcd for $C_{29}H_{28}O_9$ 520.1734)

^{1}H NMR (acetone-d_6) of 9'-ester: δ_H 3.52 (1H, br m, H-8), 3.78 (3H, s, 3-OC$\underline{H}_3$), 3.79 – 3.87 (2H, m, H-9), 3.84 (3H, s, 3'-OC$\underline{H}_3$), 4.75 (2H, d, J = 6.3 Hz, H-9'), 5.54 (1H, d, J = 5.7 Hz, H-7), 6.20 (1H, d, J = 15.5 Hz, H-8''), 6.24 (1H, dt, J = 16.0, J = 6.3 Hz, H-8'), 6.65 (1H, d, J = 16.0 Hz, H-7'), 6.77 (1H, d, J = 8.2 Hz, H-5, H-5''), 6.81 – 7.09 (6 H, m, H-2, H-6, H-2', H-6', H-6'', H-2''), 7.53 (1H, d, J = 15.5 Hz, H-7'')

7.15.19 Alternative Route to DHCA Esterification via Ethyl Ferulate Dimer

7.15.19.1 Dimerisation of Ethyl Ferulate

Silver(i) oxide (3.75 g, 16.2 mmol) was added to a solution of ethyl ferulate (2.4 g, 10.8 mmol, 1.5 equiv.) in anhydrous dichloromethane (20 ml). After stirring at room temperature for 4 h, the reaction mixture was filtered through celite and evaporated to dryness. The residue was chromatographed on silica gel using 25% ethyl acetae/hexane to yield 293 mg (12.3%) of the dimer **(124)**. Repeated dimerisation reaction three times.

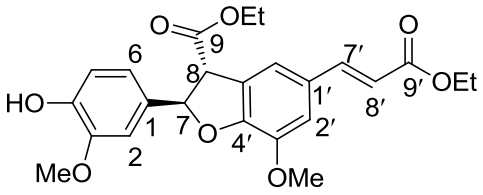

(124)

dehydrodiethyl ferulate

HRESI-MS (m/z): 442.1627 (calcd for $C_{24}H_{26}O_8$ 442.1628)

R*f*: 0.56 (45% ethyl acetate/hexane)

^{1}H NMR (acetone-d_6): δ_H 1.28 (3H, t, J = 7.1 Hz, 9-OCH$_2$C$\underline{H}_3$), 1.31 (3H, t, J = 7.1 Hz, 9'-OCH$_2$C$\underline{H}_3$), 3.84 (3H, s, 3-OC$\underline{H}_3$), 3.93 (3H, s, 3'-OC$\underline{H}_3$), 4.20 (1H, q, J = 7.1 Hz, 9-

OC$\underline{H}_2$CH$_3$), 4.27 (1H, br q, J = 7.1 Hz, 9'-OC$\underline{H}_2$CH$_3$), 4.44 (1H, d, J = 7.9 Hz, H-8), 6.04 (1H, d, J = 7.9 Hz, H-7), 6.42 (1H, d, J = 15.8 Hz, H-8'), 6.85 (1H, d, J = 8.2 Hz, H-5), 6.92 (1H, dd, J = 8.2, J = 1.5 Hz, H-6), 7.10 (1H, d, J = 1.5 Hz, H-2), 7.29 (1H, br s, H-6'), 7.34 (1H, br s, H-2'), 7.63 (1H, d, J = 15.8 Hz, H-7'), 7.73 (1H, s, 4-O$\underline{H}$)

^{13}C NMR (acetone-d6): δ_C 13.60 (9-OCH$_2\underline{C}$H$_3$, q), 13.75 (9'-OCH$_2\underline{C}$H$_3$, q), 55.2 (C-8, d), 55.4 (3-OMe, q), 55.6 (3'-OMe, q), 59.7 (9-O$\underline{C}$H$_2$CH$_3$, t), 61.3 (9'-O$\underline{C}$H$_2$CH$_3$, t), 87.5 (C-7, d), 109.8 (C-2, d), 112.4 (C-2', d), 114.9 (C-5, d), 115.8 (C-8', d), 118.0 (C-6', d), 119.3 (C-6, d), 126.5 (C-4', s), 128.6 (C-1', s) 131.2 (C-1, s), 144.3 (C-7', d), 144.9 (C-3', s), 147.1 (C-4, s), 147.7 (C-3, s), 150.1 (C-5', s), 166.4 (C-9, s), 170.2 (C-9', s)

7.15.19.2 Silyl Protection of Ethyl Ferulate Dimer

391.8 mg (2.6 mmol, 1.5 equiv.) of *tert*-butyldimethylsilyl chloride, 294 mg (4.3 mmol, 2.5 equiv.) of imidazole and 11 mg (0.09 mmol) of DMAP were added to a flask containing 764 mg (1.73 mmol) of dimer **(124)** in 10 ml of dichloromethane at 0 °C. The reaction mixture was stirred at room temperature overnight, then diluted with ethyl acetate, washed with 10% $NaHCO_3$ and brine, dried over Na_2SO_4 and concentrated *in vacuo*. The residue was chromatographed on silica gel using 30% EtOAc/hexane and 910 mg (95%) of silyl protected dimer **(125)** was recovered.

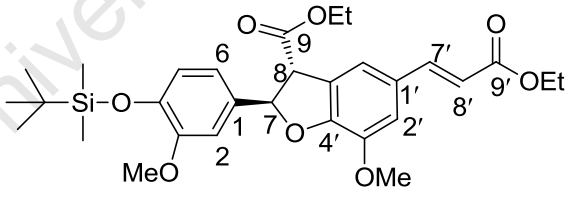

(125)

4-*O*-*tert*-butyldimethylsilyl dehydrodiethyl ferulate

HRESI-MS (m/z): 556.2497 (calcd for $C_{30}H_{40}O_8Si$ 556.2493)

R*f*: 0.86 (45% ethyl acetate/hexane)

^{1}H NMR (acetone-d$_6$): δ_H 0.00 (6H, s, 4-*O*-Si(C$\underline{H}_3$)$_2$), 0.84 (9H, s, 4-*O*-Si-C(C$\underline{H}_3$)$_3$), 1.12 (3H, t, J = 7.1 Hz, 9-OCH$_2$C$\underline{H}_3$), 1.15 (3H, t, J = 7.1 Hz, 9'-OCH$_2$C$\underline{H}_3$), 3.83 (3H, s, 3-OC$\underline{H}_3$), 3.94 (3H, s, 3'-OC$\underline{H}_3$), 4.19 (1H, q, J = 7.1 Hz, 9-OC$\underline{H}_2$CH$_3$), 4.28 (1H, br q, J = 7.1 Hz, 9'-OC$\underline{H}_2$CH$_3$), 4.44 (1H, d, J = 8.0 Hz, H-8), 6.07 (1H, d, J = 8.0 Hz, H-

7), 6.42 (1H, br d, J = 16.2 Hz, H-8'), 6.90 (1H, d, J = 8.2 Hz, H-5), 6.93 (1H,br d, J = 8.2 Hz, H-6), 7.12 (1H, br s, H-2), 7.30 (1H, br s, H-6'), 7.35 (1H, br s, H-2'), 7.63 (1H, d, J = 16.2 Hz, H-7')

7.15.19.3 DIBAL reduction of Silyl Protected Ethyl Ferulate Dimer

562 mg (1.0 mmol) of silyl dimer **(125)** dissolved in 20 ml anhydrous dichloromethane and 1 ml (6 mmol, 6 equiv.) of DIBAL-H in 5 ml of dichloromethane was added gradually to the reaction mixture at -78°C under nitrogen. The DIBAL reaction was quenched with 100ml of saturated sodium sulphate. The mixture was filtered through a 1cm plug of celite and the filtrate was extracted with EtOAc (4 x 100ml). Combined organic layers were dried over anhydrous Na_2SO_4, filtered and evaporated in *vacuo*. This reaction was repeated on 910 mg (1.67 mmol) of silyl dimer **(125)** and 1 ml (6 mmol, 3.6 equiv.) of DIBAL-H. The combined reaction residues were subjected to silica gel column chromatography using 1.2% MeOH/DCM. A total of 96 mg (8%) of desired product **(126)** was recovered and 160 mg of by-product **(133)** (13%) was recovered, a port. 25 mg of by-product **(133)** was treated with 30 µl of TBAF in THF to yield 2.4 mg (13%) of the enol ether **(134)**.

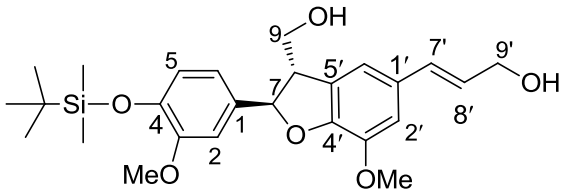

(126)

4-*O*-*tert*-butyldimethylsilyl dehydrodiconiferyl alcohol

^{1}H NMR (acetone-d_6): δ_H 0.15 (6H, s, 4-*O*-Si(C<u>H</u>$_3$)$_2$), 0.99 (9H, s, 4-*O*-Si-C(C<u>H</u>$_3$)$_3$), 3.54 (1H, m, H-8), 3.74 (2H, t, J = 5.3 Hz, 9'-O<u>H</u>), 3.81 (3H, s, 3-OC<u>H</u>$_3$), 3.82 – 3.92 (2H, m, H-9), 3.87 (3H, s, 3'-OC<u>H</u>$_3$), 4.13 (1H, t, J = 5.0 Hz, 9-O<u>H</u>), 4.20 (1H, br dd, J = 5.3, J = 5.6 Hz, H-9'), 5.60 (1H, d, J = 5.9 Hz, H-7), 6.24 (1H, dt, J = 15.9, J = 5.6 Hz, H-8'), 6.53 (1H, br d, J = 15.9 Hz, H-7'), 6.85 (1H, d, J = 8.2 Hz, H-5), 6.89 (1H, br d, J = 8.2 Hz, H-6), 6.95 (1H, br s, H-2'), 6.98 (1H, br s, H-6'), 7.06 (1H, br s, H-2)

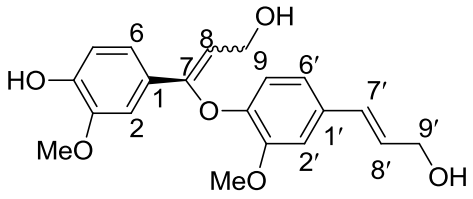

(134)

HRESI-MS (m/z): 358.1396 (calcd for $C_{20}H_{22}O_6$ 358.1417)

^{1}H NMR (acetone-d_6): δ_H 3.65 (3H, s, 3-OC$\underline{H}_3$), 3.81 (1H, t, J = 5.5 Hz, 9'-O$\underline{H}$), 3.88 (3H, s, 3'-OC$\underline{H}_3$), 4.11 (2H, br d, J = 5.5 Hz, H-9), 4.17 (2H, dd, J = 5.6, J = 5.5 Hz, H-9'), 4.22 (1H, t, J = 5.5 Hz, 9-O$\underline{H}$), 6.18 (1H, br m, H-8), 6.27 (1H, dt, J = 15.7, J = 5.5 Hz, H-8'), 6.50 (1H, br d, J = 15.7 Hz, H-7'), 6.68 (1H, d, J = 8.2 Hz, H-5), 6.83 (1H, br d, J = 7.5 Hz, H-6'), 6.87 (1H, d, J = 8.2 Hz, H-5'), 6.95 (1H, br s, H-6'), 7.12 (1H, br s, H-2'), 7.27 (1H, br s, H-2), 7.57 (1H, s, 4-O$\underline{H}$)

^{13}C NMR (acetone-d6): δ_C 54.9 (3-OMe, q), 55.3 (3'-OMe, q), 61.1 (C-9, t), 62.3 (C-9', t), 110.2 (C-2', d), 111.7 (C-6, d), 113.3 (C-8, d),114.6 (C-5, d), 115.7 (C-6', d), 119.1 (C-5', d), 122.1 (C-8', d), 126.7 (C-1', s) 122.1 (C-7', d), 132.4 (C-1, s) 144.5 (C-4', s), 145.7 (C-4, s) 147.0 (C-3', s), 150.0 (C-3, s), 150.2 (C-7, s)

7.15.19.4 *p*-Coumaroyl Esterification of DHCA

89 mg (0.30 mmol) of silyl protected *p*- coumaric acid **(66)** was dissolved in 2 ml of dry dichloromethane. 2 drops of anhydrous DMF were added and then 60 µl (0.38 mmol) of oxalyl chloride was added drop-wise at room temperature, under nitrogen. After addition the reaction mixture was refluxed at 50°C for 2h. Solvent and excess oxalyl chloride was removed under vacuum pressure to yield the acid chloride, which was dissolved in 3 ml of dry dichloromethane and added to round bottom flask containing 70 mg (0.15 mmol) of silyl protected DHCA **(126)**. 25 µl of Et_3N and a catalytic amount of DMAP were added and the reaction mixture which was stirred at room temperature under N_2. Reaction was monitored on TLC and then quenched with water and the organic layer was washed with 0.1M HCl and saturated $NaHCO_3$. The solution was dried over $MgSO_4$, the solvent was evaporated under reduced pressure and residue was chromatographed on silica gel using 30% ethyl acetate hexane to yield the three silyl esters, which were each subsequently deprotected with TBAF (3 –

4 equiv.) to yield 13.2 mg (14%) of the 9,9'-dicoumaroyl **(130)**, 6.0 mg (8%) of the 9'-coumaroyl **(131)** and 1.2 mg (1.6%) of the 9-coumaroyl **(132)** DHCA analogues.

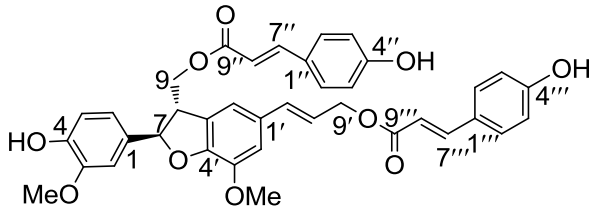

(130)
9,9′-dicoumaroyl dehydrodiconiferyl alcohol

HRESI-MS (m/z): 650.2584 (calcd for $C_{38}H_{34}O_{10}$ 650.2153)

R*f*: 0.44 (45% ethyl acetate/hexane)

^{1}H NMR (acetone-d_6): δ_H 3.81 (3H, s, 3-OC<u>H</u>$_3$), 3.85 - 3.92 (1H, m, H-8), 3.90 (3H, s, 3'-OC<u>H</u>$_3$), 4.46 (1H, dd, J = 7.6, J = 10.5 Hz, H-9b), 4.59 (1H, dd, J = 5.2, J = 10.5 Hz, H-9a), 4.80 (2H, d, J = 6.7 Hz, H-9'), 5.60 (1H, d, J = 7.6 Hz, H-7), 6.32 (1H, dt, J = 15.9, J = 6.7 Hz, H-8'), 6.34 (1H, d, J = 16.2 Hz, H-8''), 6.38 (1H, d, J = 15.7 Hz, H-8'''), 6.71 (1H, br d, J = 15.6 Hz, H-7'), 6.84 (1H, d, J = 8.6 Hz, H-5), 6.90 (4H, d, J = 8.6 Hz, H-3'', H-5'', H-3''', H-5'''), 6.94 (1H, br d, H-6), 7.08 (2H, br s, H-2', H-6'), 7.12 (1H, br s, H-2), 7.53 (2H, br d, J = 8.6 Hz, H-2'', H-6''), 7.55 (1H, d, J = 16.2 Hz, H-7''), 7.56 (2H, br d, J = 8.6 Hz, H-2''', H-6'''), 7.64 (1H, d, J = 15.7 Hz, H-7'''), 8.01 (1H, s, 4-O<u>H</u>)

^{13}C NMR (acetone-d6): δ_C 50.5 (C-8, d), 55.4 (3-OMe, q), 55.5 (3'-OMe, q), 64.5 (C-9', t), 65.0 (C-9, t), 88.4 (C-7, d), 109.8 (C-2', d), 111.3 (C-6', d), 114.2 (C-8'', d), 114.6 (C-8''', d), 114.9 (C-5, d), 115.5 (C-2, d), 115.8 (C-3'', C-5'', C-3''', C-5''', d), 119.1 (C-6, d), 121.5 (C-8', d), 126.0 (C-1'', s), 126.12 (C-1''', s), 128.4 (C-1', d), 130.1 (C-2'', C-6'', d), 130.2 (C-2''', C-6''', d), 130.6 (C-4', s), 132.5 (C-4''', s), 134.1 (C-1, s), 133.9 (C-7', d), 144.5 (C-3', s), 144.6 (C-7'', d), 145.0 (C-7''', d), 146.7 (C-3, s), 147.6 (C-4, s), 148.6 (C-5', s), 159.7 (C-4'', s), 159.8 (C-4'''), 166.3 (C-9'', s), 166.4 (C-9''', s)

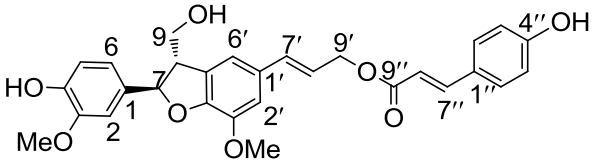

(131)

9′-coumaroyl dehydrodiconiferyl alcohol

HRESI-MS (m/z): 504.1788 (calcd for $C_{29}H_{28}O_8$ 504.1785)

R*f*: 0.23 (45% ethyl acetate/hexane)

^{1}H NMR (acetone-d_6): δ_H 3.56 (1H, br m, H-8), 3.82 (3H, s, 3-OC$\underline{H}_3$), 3.85 – 3.89 (2H, m, H-9), 3.86 (3H, s, 3'-OC$\underline{H}_3$), 4.12 (1H, br s, 9-O$\underline{H}$), 4.80 (2H, d, J = 6.5 Hz, H-9'), 5.58 (1H, d, J = 6.5 Hz, H-7), 6.29 (1H, dt, J = 15.3, J = 6.5 Hz, H-8'), 6.39 (1H, d, J = 15.7 Hz, H-8''), 6.69 (1H, br d, J = 15.3 Hz, H-7'), 6.81 (1H, d, J = 8.1 Hz, H-5), 6.88 (1H, dd, J = 8.2, J = 1.6 Hz, H-6), 6.89 (2H, d, J = 8.1 Hz, H-3'', H-5''), 7.03 (1H, br s, H-2'), 7.04 (1H, d, J = 1.6 Hz, H-2), 7.05 (1H, br s, H-6',), 7.56 (2H, d, J = 8.1 Hz, H-2'', H-6''), 7.65 (1H, d, J = 15.7 Hz, H-7'')

^{13}C NMR (acetone-d6): δ_C 53.8 (C-8, d), 55.4 (3-OMe, q), 55.5 (3'-OMe, q), 63.7 (C-9, t), 64.6 (C-9', t), 87.8 (C-7, d), 109.6 (C-2', d), 111.1 (C-6', d), 114.7 (C-8'', d), 114.9 (C-5, d), 115.6 (C-2, d), 115.8 (C-3'', C-5'', d), 118.8 (C-6, d), 121.1 (C-8', d), 126.2 (C-1''), 129.8 (C-1', s), 130.2 (C-2'', C-6'', d), 133.5 (C-1, s), 134.2 (C-7', d), 144.4 (C-3', s), 144.6 (C-7'', d), 146.5 (C-3, s), 147.6 (C-4, s), 148.8 (C-5', s), 159.7 (C-4'', s), 166.4 (C-9'', s)

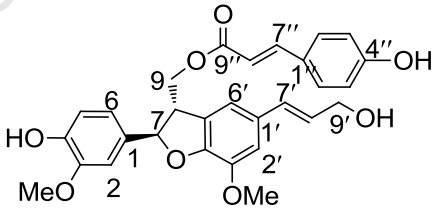

(132)

9-coumaroyl dehydrodiconiferyl alcohol

HRESI-MS (m/z): 504.1800 (calcd for $C_{29}H_{28}O_8$ 504.1785)

R*f*: 0.14 (45% ethyl acetate/hexane)

^{1}H NMR (acetone-d_6): δ_H 3.82 (3H, s, 3-OC$\underline{H}_3$), 3.85 - 3.92 (1H, m, H-8), 3.89 (3H, s, 3'-OC$\underline{H}_3$), 4.20 (2H, br m, H-9'), 4.46 (1H, br m, H-9b), 4.57 (1H, dd, J = 11.2, J = 5.3 Hz, H-9a), 5.58 (1H, d, J = 7.4 Hz, H-7), 6.32 (1H, dt, J = 15.9, J = 6.7 Hz, H-8'), 6.36 (1H, d, J = 16.1 Hz, H-8''), 6.55 (1H, br d, J = 16.1 Hz, H-7'), 6.84 (1H, d, J = 7.9 Hz,

H-5), 6.90 (2H, d, J = 8.6 Hz, H-3'', H-5''), 6.94 (1H, br d, H-6), 7.00 (1H, br s, H-2'), 7.05 (1H, br s, H-6'), 7.09 (1H, br s, H-2), 7.54 (2H, br d, J = 8.6 Hz, H-2'', H-6''), 7.61 (1H, d, J = 16.1 Hz, H-7'')

7.15.19.5 Piperonylic Esterification of DHCA

18.8 mg (0.11 mmol) of piperonylic acid was dissolved in 1 ml of dry dichloromethane. 1 drop of anhydrous DMF and 15 µl of oxalyl chloride were added. After addition the reaction mixture was refluxed at 50°C for 2h. Solvent and excess oxalyl chloride was removed under vacuum pressure to yield the acid chloride, which was dissolved in 2 ml of dry dichloromethane and added to round bottom flask containing 26 mg (0.06 mmol) of silyl protected DHCA **(126)**. 20 µl of Et_3N and a catalytic amount of DMAP were added and the reaction mixture which was stirred at room temperature under N_2. Reaction was monitored on TLC and then quenched with water and the organic layer was washed with 0.1M HCl and saturated $NaHCO_3$. The solution was dried over $MgSO_4$, the solvent was evaporated under reduced pressure and residue was chromatographed on silica gel using 20% ethyl acetate/hexane to yield the two silyl esters, which were each subsequently deprotected with TBAF (3 – 4 equiv.) to give 2.1 mg (5%) of the 9,9'-dipiperonylic **(135)** and 1.8 mg (3.7%) of the 4,9,9'-tripiperonylic **(136)** ester analogues.

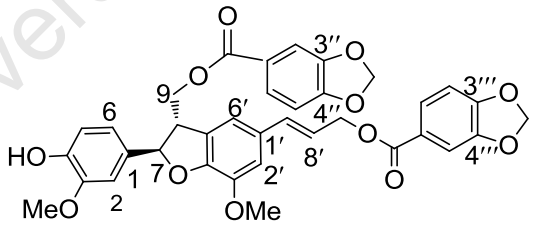

(135)

HRESI-MS (m/z): 654.2103 (calcd for $C_{36}H_{30}O_{12}$ 654.2106)

^{1}H NMR (acetone-d_6): δ_H 3.79 (3H, s, 3-OC$\underline{H}_3$), 3.89 (3H, s, 3'-OC$\underline{H}_3$), 3.96 (1H, m, H-8), 4.56 (1H, dd, J = 7.6, J = 11.1 Hz, H-9b), 4.70 (1H, dd, J = 5.5, J = 11.1 Hz, H-9a), 4.91 (2H, d, J = 5.9 Hz, H-9'), 5.66 (1H, d, J = 6.9 Hz, H-7), 6.11 (3''-O-C$\underline{H}_2$-O-4''), 6.13 (3'''-O-C$\underline{H}_2$-O-4'''), 6.36 (1H, dt, J = 15.9, J = 5.9 Hz, H-8'), 6.75 (1H, d, J = 15.9 Hz, H-7'), 6.83 (1H, d, J = 8.6 Hz, H-5), 6.93 (3H, m, H-5'', H-5''', H-6), 7.08 (1H, br s, H-2), 7.09 (1H, br s, H-6'), 7.15 (1H, br s, H-2'), 7.33 (1H, d, J = 1.4 Hz, H-2''), 7.44

(1H, d, J = 1.4 Hz, H-2'''), 7.55 (1H, dd, J = 8.3, J = 1.4 Hz, H-6''), 7.64 (1H, s, 4-O<u>H</u>), 7.67 (1H, dd, J = 8.3, J = 1.4 Hz, H-6''')

^{13}C NMR (acetone-d6): δ_C 50.4 (C-8, d), 55.3 (3-OMe, q), 55.5 (3'-OMe, q), 65.3 (C-9', t), 65.8 (C-9, t), 88.6 (C-7, d), 102.1 ([3''-O-<u>C</u>H$_2$-O-4''], t), 102.2 ([3'''-O-<u>C</u>H$_2$-O-4'''], t), 107.9 (C-5'', C-5''', d), 108.8 (C-2'', C-2''', d), 109.8 (C-2', d), 111.5 (C-6', d), 114.9 (C-5, d), 115.5 (C-2, d), 119.1 (C-6, d), 121.2 (C-8', d), 123.9 (C-1'', s), 124.3 (C-1''', s), 125.1 (C-6'', d), 125.2 (C-6''', d), 128.3 (C-4, s), 130.5 (C-1', d), 132.5 (C-1), 134.1 (C-7', d), 144.5 (C-3', s), 146.8 (C-3, s), 147.6 (C-4, s), 148.0 (C-4'', C-4'''), 148.7 (C-5', s), 151.8 (C-3'', s), 151.9 (C-3'''), 165.0 (C-9'', C-9''', s)

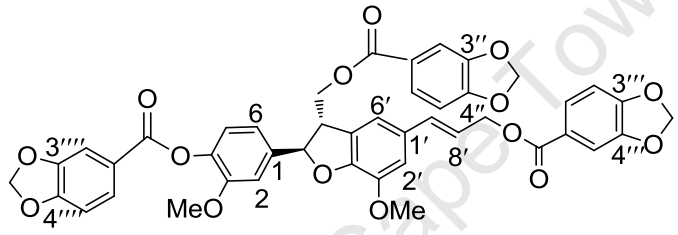

(136)

HRESI-MS (m/z): 802.1790 (calcd for $C_{44}H_{34}O_{15}$ 802.1812)

^{1}H NMR (acetone-d$_6$): δ_H 3.76 (3H, s, 3-OC<u>H</u>$_3$), 3.92 (3H, s, 3'-OC<u>H</u>$_3$), 4.01 (1H, m, H-8), 4.61 (1H, dd, J = 8.3, J = 11.1 Hz, H-9b), 4.75 (1H, dd, J = 5.5, J = 11.1 Hz, H-9a), 4.91 (2H, d, J = 6.9 Hz, H-9'), 5.81 (1H, d, J = 6.9 Hz, H-7), 6.12 (3''-O-C<u>H</u>$_2$-O-4''), 6.13 (3'''-O-C<u>H</u>$_2$-O-4'''), 6.17 (3''''-O-C<u>H</u>$_2$-O-4''''), 6.38 (1H, dt, J = 15.2, J = 6.9 Hz, H-8'), 6.76 (1H, d, J = 15.2 Hz, H-7'), 6.94 (2H, d, J = 8.3 Hz, H-5'', H-5'''), 7.02 (1H, d, J = 8.3 Hz, H-5''''), 7.11 (1H, d, J = 6.9 Hz, H-5), 7.12 (1H, br s, H-6'), 7.17 (1H, br s, H-2), 7.20 (1H, d, J = 6.9 Hz), 7.28 (1H, br s, H-2'), 7.38 (1H, br s, H-2''), 7.44 (1H, br s, H-2'''), 7.54 (1H, br s, H-2''''), 7.56 (1H, br d, J = 8.3 Hz, H-6''), 7.67 (1H, br d, J = 8.3 Hz, H-6'''), 7.80 (1H, br d, J = 8.3 Hz, H-6'''')

7.15.20 DHCA and GGCE Ring Substitution

7.15.20.1 Monolignol synthesis

4.9 g (0.027 mol) of syringaldehyde was dissolved in 100 ml of dry dichloromethane. 11.3 g (0.0325 mol,1.2 equiv.) of triphenylcarbethoxymethylphosphorane **(46)** was added and the reaction was stirred at room temperature under nitrogen for 48 h. The

reaction residue was purified by silica gel column chromatography, using 12% EtOAc/Hexane. Recovered 3.7 g (0.015 mol, 54% overall yield) of *E*- isomer, ethyl sinapate, which was reduced with DIBAL (0.06 mol, 4 equiv. 10.5 ml) in dichloromethane at -78°C under nitrogen. The reaction was worked up as previously and the residue was subjected to silica gel column chromatography using 1.5% isopropanol/dichloromethane. Recovered 1.2 g of unreacted starting material and 1.3 g (43 %) of sinapyl alcohol **(151)**.

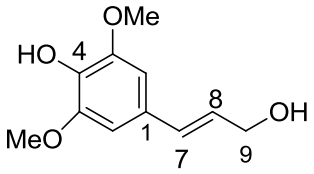

(151)
Sinapyl alcohol

HRESI-MS (m/z): 210.0871 (calcd for $C_{11}H_{14}O_4$ 210.0893)

R*f*: 0.32 (2% methanol/dichloromethane)

^{1}H NMR (acetone-d_6): δ_H 3.84 (6H, s, 3-OC<u>H</u>$_3$, 5-OC<u>H</u>$_3$), 4.19 (2H, d, J = 5.0 Hz, H-9), 6.25 (1H, dt, J = 15.9, J = 5.0 Hz, H-8), 6.48 (1H, d, J = 15.9 Hz, H-7), 6.73 (2H, s, H-2, H-6)

Similarly, the following monolignols were prepared:

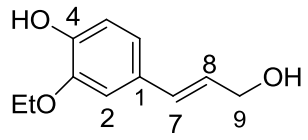

(137)

HRESI-MS (m/z): 194.0875 (calcd for $C_{11}H_{14}O_3$ 194.0866)

R*f*: 0.45 (6% methanol/dichloromethane)

^{1}H NMR (acetone-d_6): δ_H 1.38 (3H, t, J = 7.0 Hz, 3-*O*-CH$_2$C<u>H</u>$_3$), 3.71 (1H, t, J = 5.5 Hz, 9-O<u>H</u>), 4.12 (2H, q, J = 7.0 Hz, 3-*O*-C<u>H</u>$_2$CH$_3$), 4.19 (2H, dd, J = 5.3, J = 5.5 Hz, H-9), 6.22 (1H, dt, J = 16.0, J = 5.5 Hz, H-8), 6.49 (1H, d, J = 16.0 Hz, H-7), 6.77 (1H, d, J = 8.2 Hz, H-5), 6.86 (1H, dd, J = 8.2, J = 1.5 Hz, H-6), 7.04 (1H, d J = 1.5 Hz, H-2)

^{13}C NMR (acetone-d6): δ_C 14.2 (3-*O*-$CH_2\underline{C}H_3$), 62.5 (C-9, t), 64.1 (3-*O*-$\underline{C}H_2CH_3$, t), 110.2 (C-2, d), 114.9 (C-5, d), 119.7 (C-6, d), 127.2 (C-8, d), 129.4 (C-1, s), 129.5 (C-7, d), 146.5 (C-3, s), 146.7 (C-4, s)

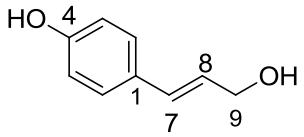

(138)

HRESI-MS (m/z): 150.0349 (calcd for $C_9H_{10}O_2$ 150.0270)

R*f*: 0.40 (8% methanol/dichloromethane)

^{1}H NMR (acetone-d_6): δ_H 3.71 (1H, t, J = 5.3 Hz, 9-O$\underline{H}$), 4.19 (2H, dd, J = 5.3, J = 5.9 Hz, H-9), 6.20 (1H, dt, J = 15.9, J = 5.9 Hz, H-8), 6.50 (1H, d, J = 15.9 Hz, H-7), 6.80 (2H, d, J = 8.5 Hz, H-3, H-5), 7.27 (2H, d, J = 8.5 Hz, H-2, H-6)

^{13}C NMR (acetone-d6): δ_C 62.5 (C-9, t), 115.3 (C-3, C-5, d), 127.0 (C-8, d), 127.5 (C-2, C-6, d), 128.9 (C-1, s), 129.2 (C-7, d), 156.9 (C-4, s)

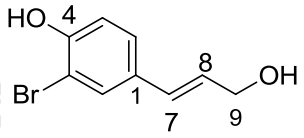

(139)

HRESI-MS (m/z): 229.9775 (calcd for $C_9H_9BrO_2$ 229.9763)

R*f*: 0.49 (6% methanol/dichloromethane)

^{1}H NMR (acetone-d_6): δ_H 4.20 (2H, br d, J = 5.3 Hz, H-9), 6.27 (1H, dt, J = 15.9, J = 5.3 Hz, H-8), 6.50 (1H, d, J = 15.9 Hz, H-7), 6.96 (1H, d, J = 8.5 Hz, H-5), 7.28 (1H, dd, J = 8.5, J = 1.8 Hz, H-6), 7.57 (1H, d, J = 1.8 Hz, H-2)

^{13}C NMR (acetone-d6): δ_C 62.3 (C-9, t), 109.7 (C-3, s), 116.4 (C-5, d), 126.6 (C-6, d), 127.5 (C-7, d), 129.0 (C-8, d), 130.6 (C-2, d), 131.0 (C-1, s), 153.2 (C-4, s)

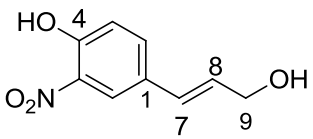

(140)

HRESI-MS (m/z): 195.0513 (calcd for $C_9H_8NO_4$ 195.0532)

R*f*: 0.54 (5% methanol/dichloromethane)

^{1}H NMR (acetone-d_6): δ_H 4.25 (2H, br d, J = 5.2 Hz, H-9), 6.45 (1H, dt, J = 15.8, J = 5.2 Hz, H-8), 6.65 (1H, d, J = 15.8 Hz, H-7), 7.17 (1H, d, J = 8.8 Hz, H-5), 7.83 (1H, dd, J = 8.8, J = 1.9 Hz, H-6), 8.08 (1H, d, J = 1.9 Hz, H-2)

^{13}C NMR (acetone-d6): δ_C 62.0 (C-9, t), 120.1 (C-5, d), 122.1 (C-2, d), 126.53 (C-7, d), 130.3 (C-1, s), 131.4 (C-8, d), 134.6 (C-6, d), 137.7 (C-3, s), 153.6 (C-4, s)

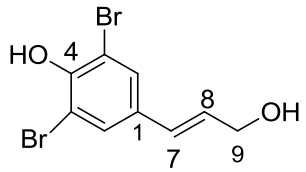

(149)

HRESI-MS (m/z): 307.8869 (calcd for $C_9H_8BrO_2$ 307.8853)

R*f*: 0.50 (6% methanol/dichloromethane)

^{1}H NMR (acetone-d_6): δ_H 4.22 (2H, d, J = 4.9 Hz, H-9), 6.37 (1H, dt, J = 4.9, J = 15.8 Hz, H-8), 6.50 (1H, d, J = 15.8 Hz, H-7), 7.61 (2H, s, H-2, H-6)

^{13}C NMR (acetone-d6): δ_C 62.3 (C-9, t), 109.7 (C-3, s), 116.4 (C-5, d), 126.6 (C-6, d), 127.5 (C-7, d), 129.0 (C-8, d), 130.6 (C-2, d), 131.0 (C-1, s), 153.2 (C-4, s), 8.01 (1H, s, 4-O<u>H</u>)

7.15.20.2 Oxidative Coupling of Coniferyl Alcohol Analogues

Oxidative coupling of each monolignol was conducted as for coniferyl alcohol (Section 7.15.5) in dioxane-water 92/3, v/v, pH 4 – 4.5 adjusted with dil. H_3PO_4) with HRP (120 U/10ml) and 0.5 – 1.5 equiv. H_2O_2 as the oxidant.

i) Oxidative coupling of 345 mg (1.78 mmol) of monolignol **(137)** yielded 162 mg (47%) of *β*-5 dimer **(141)** and 44 mg (12%) of the *β*-*O*-4 dimer **(145)**.

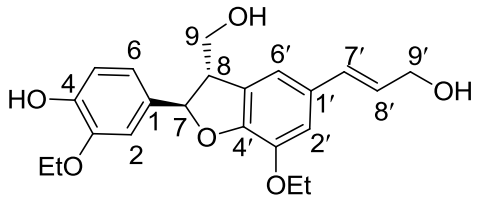

(141)

HRESI-MS (m/z): 386.1783 (calcd for $C_{22}H_{26}O_6$ 386.1772)

R*f*: 0.17 (6% methanol/dichloromethane)

^{1}H NMR (acetone-d_6): δ_H 1.35 (6H, t, J = 7.2 Hz, 3-*O*-$CH_2C\underline{H}_3$, 3'-*O*-$CH_2C\underline{H}_3$), 3.53 (1H, m, H-8), 3.74 (1H, t, J = 5.6 Hz, 9'-O<u>H</u>), 3.82 (1H, br m, H-9b), 3.88 (1H, m, H-9a), 4.08 (2H, q, J = 7.2 Hz, 3-*O*-$C\underline{H}_2CH_3$), 4.16 (2H, q, J = 7.2 Hz, 3'-*O*-$C\underline{H}_2CH_3$), 4.20 (2H, br dd, J = 5.6, J = 5.7 Hz, H-9'), 5.55 (1H, d, J = 6.2 Hz, H-7), 6.23 (1H, dt, J = 15.7, J = 5.7 Hz, H-8'), 6.51 (1H, br d, J = 15.7 Hz, H-7'), 6.81 (1H, d, J = 8.3 Hz, H-5), 6.88 (1H, br d, J = 8.3 Hz, H-6), 6.93 (1H, br s, H-2'), 6.98 (1H, br s, H-6'), 7.02 (1H, br s, H-2), 7.57 (1H, s, 4-O<u>H</u>)

^{13}C NMR (acetone-d6): δ_C 14.2 (3-*O*-$CH_2\underline{C}H_3$, q), 14.4 (3'-*O*-$CH_2\underline{C}H_3$, q), 53.9 (C-8, d), 62.5 (C-9', t), 63.8 (C-9, t), 64.2 (3-*O*-$\underline{C}H_2CH_3$, t), 64.3 (3'-*O*-$\underline{C}H_2CH_3$, t), 87.6 (C-7, d), 110.6 (C-2, d), 112.4 (C-2', d), 114.8 (C-5, d), 115.2 (C-6', d), 118.7 (C-6, d), 127.4 (C-8', d), 129.6 (C-7', d), 129.7 (C-4', s), 131.0 (C-1', s) 133.5 (C-1, s), 143.4 (C-3', s), 146.5 (C-4, s), 146.6 (C-3, s), 148.3 (C-5', s)

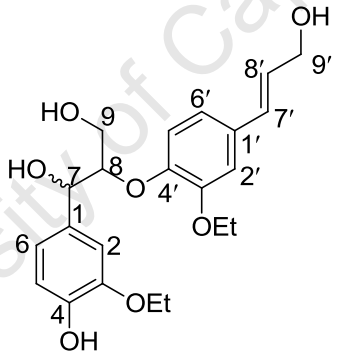

(145)

HRESI-MS (m/z): 404.1830 (calcd for $C_{22}H_{28}O_7$ 404.1836)

R*f*: 0.15 (6% methanol/dichloromethane)

^{1}H NMR (acetone-d_6) of *erythro* diastereomer: δ_H 1.35 (3H, t, J = 7.2 Hz, 3-*O*-$CH_2C\underline{H}_3$), 1.41 (3H, t, J= 7.2 Hz, 3'-*O*-$CH_2C\underline{H}_3$), 3.81 (2H, m, H-9), 4.06 (2H, q, J = 7.2 Hz, 3-*O*-$C\underline{H}_2CH_3$), 4.09 (2H, q, J = 7.2 Hz, 3'-*O*-$C\underline{H}_2CH_3$), 4.21 (2H, br d, J = 5.2 Hz, H-9'), 4.24 (1H, m, H-8), 4.51 (1H, d, J = 4.1 Hz, 7-O<u>H</u>), 4.87 (1H, dd, J = 4.8, J = 4.1 Hz, H-7), 6.29 (1H, dt, J = 15.5, J = 5.2 Hz, H-8'), 6.51 (1H, br d, J = 15.5 Hz, H-7'), 6.78 (1H, d, J = 8.3 Hz, H-5), 6.87 (1H, dd, J = 8.3, J = 2.0 Hz, H-6), 6.91 (1H, br d, J = 8.3 Hz, H-6'), 6.93 (2H, br s, H-2, H-2'), 7.16 (1H, d, J = 8.3 Hz, H-5'), 7.41 (1H, s, 4-O<u>H</u>)

^{13}C NMR (acetone-d6): δ_C 14.2 (3-*O*-$CH_2\underline{C}H_3$, q), 14.3 (3'-*O*-$CH_2\underline{C}H_3$, q), 61.0 (C-9, t), 62.4 (C-9', t), 64.2 (3-*O*-$\underline{C}H_2CH_3$, t), 64.3 (3'-*O*-$\underline{C}H_2CH_3$, t), 73.0 (C-7, d), 86.6 (C-8, d), 111.6 (C-2, C-2', d), 114.3 (C-6, d), 119.4 (C-6', d), 119.6 (C-5', d), 119.8 (C-5, d), 128.9 (C-8', d), 129.0 (C-7', d), 132.4 (C-1', s), 133.3 (C-1, s), 146.0 (C-3', s), 146.2 (C-3, s), 148.4 (C-4, s), 150.5 (C-4', s)

ii) Oxidative coupling of 82.4 mg (0.55 mmol) of monolignol **(138)** yielded 15.2 mg (19%) of the *β*-5 dimer **(142)** and 7.7 mg (9%) of the *β*-*O*-4 dimer **(146)**.

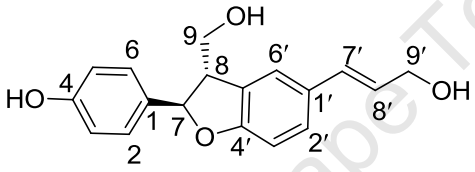

(142)

HRESI-MS (m/z): 298.1257 (calcd for $C_{18}H_{18}O_4$ 298.1248)

R*f*: 0.23 (8% methanol/dichloromethane)

^{1}H NMR (acetone-d_6): δ_H 3.49 (1H, m, H-8), 3.74 (1H, br s, 9'-O$\underline{H}$), 3.83 (1H, br m, H-9b), 3.88 (1H, br m, H-9a), 4.1(1H, br s, 9-O$\underline{H}$), 4.20 (2H, br m, H-9'), 5.56 (1H, d, J = 6.2 Hz, H-7), 6.23 (1H, dt, J = 15.8, J = 5.8 Hz, H-8'), 6.54 (1H, br d, J = 15.8 Hz, H-7'), 6.75 (1H, d, J = 8.2 Hz, H-3'), 6.83 (2H, d, J = 8.4 Hz, H-5, H-3), 7.22 (1H, dd, J = 8.2, J = 1.6 Hz, H-2'), 7.24 (1H, d, J = 8.4 Hz, H-2, H-6), 7.40 (1H, s, H-6')

^{13}C NMR (acetone-d6): δ_C 53.6 (C-8, d), 62.6 (C-9', t), 63.9 (C-9, t), 87.2 (C-7, d), 108.8 (C-3', d), 115.2 (C-5, C-3, d), 122.6 (C-6', d), 127.2 (C-2', C-2, C-6, d), 127.3 (C-8', d), 128.6 (C-4', s), 129.4 (C-7', d), 130.2 (C-1', s), 133.2 (C-1, s), 157.2 (C-4, s), 159.7 (C-5', s)

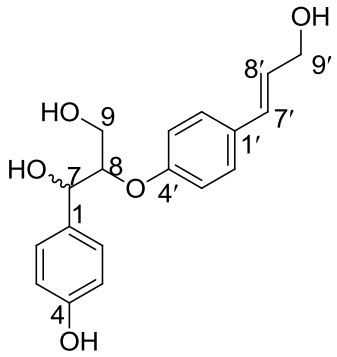

(146)

HRESI-MS (m/z): 316.1293 (calcd for $C_{18}H_{20}O_5$ 316.1354)

R*f*: 0.10 (8% methanol/dichloromethane)

^{1}H NMR (acetone-d_6) of the *erythro* diastereomer: δ_H 3.76 (2H, br m, H-9), 4.20 (2H, br d, J = 5.5 Hz, H-9'), 4.44 (1H, m. H-8), 4.95 (1H, br m, H-7), 6.25 (1H, dt, J = 16.0, J = 5.5 Hz, H-8'), 6.53 (1H, br d, J = 16.0 Hz, H-7'), 6.78 (2H, d, J = 8.8 Hz, H-3, H-5), 6.97 (2H, d, J = 8.8 Hz, H-5', H-3'), 7.29 (4H, m, H-2, H-2', H-6, H-6')

^{13}C NMR (acetone-d6): δ_C 60.8 (C-9, t), 62.5 (C-9', t), 72.4 (C-7, d), 83.6 (C-8, d), 114.6 (C-3, C-5, d), 116.4 (C-5', C-3', d), 127.2 (C-6, C-2, C-6', C-2', d), 128.0 (C-8', d), 128.9 (C-7', d), 130.2 (C-1', s), 133.7 (C-1, s), 156.7 (C-4, s), 158.8 (C-4', s)

iii) Oxidative coupling of 462 mg (2.02 mmol) of monolignol **(139)** yielded 67 mg (15%) of the *β*-5 dimer **(143)** and 88.7 mg (19%) of the *β*-*O*-4 dimer **(147)**.

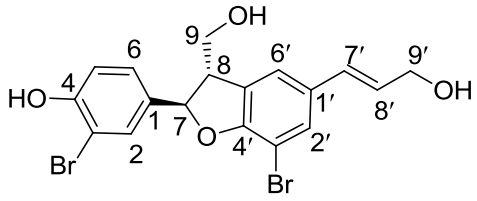

(143)

HRESI-MS (m/z): 456.9420 (calcd for $C_{18}H_{16}Br_2O_4$ 456.9516)

R*f*: 0.28 (6% methanol/dichloromethane)

^{1}H NMR (acetone-d_6): δ_H 3.64 (1H, m, H-8), 3.88 (1H, dd, J = 7.6 Hz, 11.4 Hz, H-9b), 3.94 (1H, dd, J = 6.3, 11.4 Hz, H-9a), 4.21 (2H, d, J = 4.4 Hz, H-9'), 5.69 (1H, d, J = 6.3 Hz, H-7), 6.30 (1H, dt, J = 15.8, J = 4.4 Hz, H-8'), 6.53 (1H, br d, J = 15.7 Hz, H-

7'), 7.02 (1H, d, J = 8.8 Hz, H-5), 7.27 (1H, dd, J = 8.8, J = 2.5 Hz, H-6), 7.40 (2H, br d, J = 8.8 Hz, H-2', H-6'), 7.58 (1H, br s, H-2)

^{13}C NMR (acetone-d6): δ_C 54.4 (C-8, d), 62.2 (C-9', t), 63.5 (C-9, t), 86.7 (C-7, d), 101.7 (C-3', s), 109.5 (C-3, s), 116.5 (C-5, d), 121.8 (C-2', d), 126.4 (C-7', d), 127.7 (C-8', d), 129.2 (C-6, d), 129.7 (C-6', d), 129.9 (C-4', s), 130.5 (C-2, d), 132.5 (C-1', s), 134.4 (C-1, s), 153.9 (C-4, s), 156.2 (C-5', s)

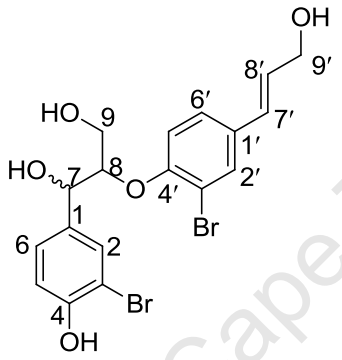

(147)

HRESI-MS (m/z): 474.9497 (calcd for $C_{18}H_{18}Br_2O_5$ 474.9418)

R*f*: 0.20 (6% methanol/dichloromethane)

^{1}H NMR (acetone-d_6) of the *erythro* diastereomer: δ_H 3.83 (2H, br m, H-9), 4.20 (2H, br d, J = 4.7 Hz, H-9'), 4.56 (1H, br m, H-8), 5.01 (1H, d, J = 4.8 Hz, H-7), 6.29 (1H, dt, J = 15.5, J = 4.7 Hz, H-8'), 6.51 (1H, br d, J = 15.5 Hz, H-7'), 6.95 (1H, d, J = 8.1 Hz, H-5), 7.17 (1H, d, J = 8.8, H-5'), 7.32 (2H, m, H-6, H-6'), 7.60 (1H, br s, H-2'), 7.70 (1H, br s, H-2)

^{13}C NMR (acetone-d6): δ_C 60.9 (C-9, t), 62.2 (C-9', t), 71.7 (C-7, d), 83.6 (C-8, d), 109.0 (C-3, s), 112.6 (C-3', s), 115.6 (C-5, d), 126.3 (C-7', d), 127.2 (C-6, d), 127.7 (C-8', d), 129.7 (C-5', d), 130.6 (C-2, d), 131.6 (C-2', d), 132.1 (C-6', d), 134.4 (C-1', s), 134.6 (C-1, s), 153.2 (C-4', s), 154.7 (C-4, s)

iv) Oxidative coupling of 333 mg (1.7 mmol) of monolignol **(140)** yielded 4.3 mg (1.3%) of the *β*-5 dimer **(144)**, 4.5 mg (1.3%) of the *threo* form of the β-O-4 dimer **(148i)** and 24.4 mg (7.1%) of the *erythro* β-O-4 dimer **(148ii)**.

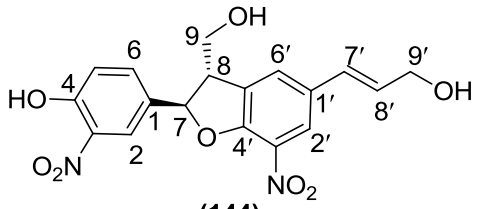

(144)

HRESI-MS (m/z): 388.0890 (calcd for $C_{18}H_{16}N_2O_8$ 388.0907)

R*f*: 0.28 (5% methanol/dichloromethane)

^{1}H NMR (acetone-d_6): δ_H 3.75 (1H, m, H-8), 4.00 (1H, dd, J = 6.6 Hz, 10.4 Hz, H-9b), 3.94 (1H, dd, J = 5.1, 10.4 Hz, H-9a), 4.26 (2H, d, J = 4.4 Hz, H-9'), 6.02 (1H, d, J = 5.9 Hz, H-7), 6.45 (1H, dt, J = 15.9, J = 4.4 Hz, H-8'), 6.67 (1H, br d, J = 15.9 Hz, H-7'), 7.26 (1H, d, J = 8.8 Hz, H-5), 7.83 (2H, br m, H-6, H-2'), 7.95 (1H, br s, H-6'), 8.24 (1H, br s, H-2)

^{13}C NMR (acetone-d6): δ_C 52.5 (C-8, d), 62.0 (C-9', t), 63.2 (C-9, t), 88.5 (C-7, d), 120.5 (C-5, d), 121.8 (C-2, d), 122.5 (C-2', d), 126.7 (C-7', d), 128.2 (C-6', d), 131.2 (C-8', d), 131.5 (C-4', s), 129.9 (C-4', s), 132.5 (C-1, s), 133.2 (C-3, s), 133.5 (C-3', s), 134.0 (C-1', s), 134.9 (C-6, d), 153.4 (C-5', s), 154.3 (C-4, s)

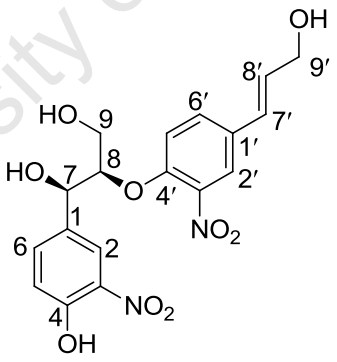

(148i)

HRESI-MS (m/z): 406.1013 (calcd for $C_{18}H_{18}N_2O_9$ 406.1013)

R*f*: 0.22 (5% methanol/dichloromethane)

^{1}H NMR (acetone-d_6) of the *threo* diastereomer: δ_H 3.67 (1H, dd, J = 5.9, 11.8 Hz, H-9b), 3.87 (1H, m, H-9a), 4.23 (2H, br d, J = 4.8 Hz, H-9'), 4.78 (1H, br m, H-8), 4.94 (1H, d, J = 4.3 Hz, H-7), 6.42 (1H, dt, J = 16.1, J = 4.8 Hz, H-8'), 6.60 (1H, br d, J = 16.1 Hz, H-7'), 7.16 (1H, d, J = 8.8 Hz, H-5), 7.42 (1H, d, J = 8.8 Hz, H-5'), 7.61 (1H,

dd, J = 8.8, J = 1.6 Hz, H-6'), 7.79 (1H, br s, H-2'), 7.82 (1H, dd, J = 8.8, J = 1.6 Hz, H-6), 8.24 (1H, br d, J = 1.6 Hz, H-2)

^{13}C NMR (acetone-d6): δ_C 60.9 (C-9, t), 62.0 (C-9', t), 71.5 (C-7, d), 85.3 (C-8, d), 117.3 (C-5', d), 119.5 (C-5, d), 122.1 (C-2', d), 123.2 (C-2, d), 126.3 (C-7', d), 131.0 (C-6', d), 131.4 (C-8', d), 133.8 (C-1, s), 136.0 (C-6, d), 141.0 (C-1', s), 150.9 (C-4, C-4', s), 153.8 (C-3, C-3', s)

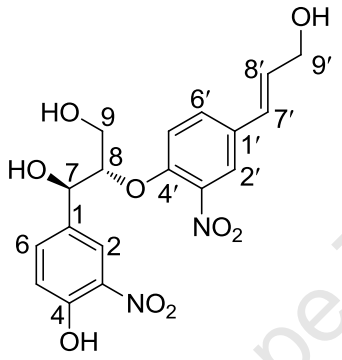

(148ii)

HRESI-MS (m/z): 406.1002 (calcd for $C_{18}H_{18}N_2O_9$ 406.1013)

R*f*: 0.15 (5% methanol/dichloromethane)

^{1}H NMR (acetone-d_6) of the *threo* diastereomer: δ_H 3.88 (1H, dd, J = 5.7, 11.5 Hz, H-9b), 3.93 (1H, dd, J = 3.8 , J = 11.5 Hz, H-9a), 4.22 (2H, br d, J = 4.2 Hz, H-9'), 4.77 (1H, br m, H-8), 5.07 (1H, d, J = 6.1 Hz, H-7), 6.40 (1H, dt, J = 16.0, J = 4.2 Hz, H-8'), 6.58 (1H, br d, J = 16.0 Hz, H-7'), 7.11 (1H, d, J = 8.8 Hz, H-5), 7.39 (1H, d, J = 8.8 Hz, H-5'), 7.58 (1H, dd, J = 8.8, J = 1.5 Hz, H-6'), 7.74 (1H, d, J = 1.5 Hz, H-2'), 7.78 (1H, dd, J = 8.8, J = 2.2 Hz, H-6), 8.19 (1H, br d, J = 2.2 Hz, H-2)

^{13}C NMR (acetone-d6): δ_C 60.9 (C-9, t), 62.0 (C-9', t), 71.2 (C-7, d), 84.2 (C-8, d), 116.9 (C-5', d), 119.3 (C-5, d), 122.0 (C-2', d), 123.5 (C-2, d), 126.2 (C-7', d), 130.9 (C-6', d), 131.3 (C-8', d), 134.1 (C-1, s), 136.3 (C-6, d), 140.9 (C-1', s), 150.4 (C-4, C-4', s), 153.8 (C-3, C-3', s)

v) Oxidative coupling of 374 mg (1.22 mmol) of monolignol **(149)** yielded 246 mg (64%) of the *threo β-O*-4 dimer **(150i)** and 32 mg (8%) of the *erythro β-O*-4 dimer **(150ii)**.

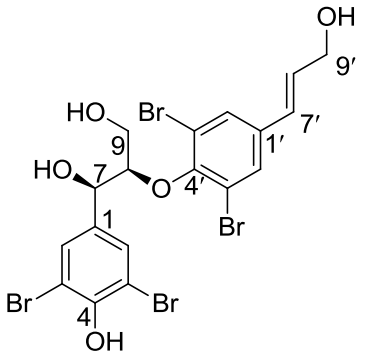

(150i)

HRESI-MS (m/z): 631.7663 (calcd for $C_{18}H_{16}Br_4O_5$ 631.7584)

R*f*: 0.29 (6% methanol/dichloromethane)

^{1}H NMR (acetone-d_6) of the *threo* diastereomer: δ_H 3.87 (1H, dd, J = 4.2, J = 12.0 Hz, H-9b), 3.93 (1H, dd, J = 5.4, J = 12.0 Hz, H-9a), 4.24 (2H, br d, J = 4.2 Hz, H-9'), 4.81 (1H, br ddd, J = 4.2, J = 5.4, J = 5.4 Hz, H-8), 5.12 (1H, d, J = 5.4 Hz, H-7), 6.44 (1H, dt, J = 15.9, J = 4.2 Hz, H-8'), 6.53 (1H, br d, J = 15.9 Hz, H-7'), 7.61 (2H, s, H-2', H-6'), 7.67 (2H, s, H-2, H-6), 7.70 (1H, s, 4-O<u>H</u>)

^{13}C NMR (acetone-d6): δ_C 60.9 (C-9, t), 61.9 (C-9', t), 72.3 (C-7, d), 85.9 (C-8, d), 110.1 (C-3, C-5, s), 118.0 (C-3', C-5', d), 125.4 (C-7', d), 130.4 (C-2', C-6', d), 131.0 (C-2, C-6, d), 132.8 (C-8', d), 135.9 (C-1', s), 136.3 (C-1, s), 149.8 (C-4, s), 150.7 (C-4', s)

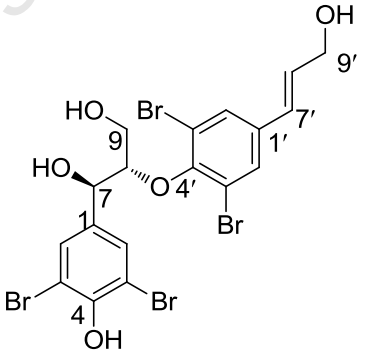

(150ii)

HRESI-MS (m/z): 631.7505 (calcd for $C_{18}H_{16}Br_4O_5$ 631.7584)

R*f*: 0.23 (6% methanol/dichloromethane)

^{1}H NMR (acetone-d_6) of the *erythro* diastereomer: δ_H 3.87 (2H, m, H-9), 4.23 (1H, br d, J = 4.6 Hz, H-9'), 4.80 (1H, br m, H-8), 5.13 (1H, br m, H-7), 6.43 (1H, dt, J = 15.9,

J = 4.6 Hz, H-8'), 6.52 (1H, br d, J = 15.9 Hz, H-7'), 7.61 (2H, s, H-2', H-6'), 7.69 (2H, s, H-2, H-6)

^{13}C NMR (acetone-d6): δ_C 60.8 (C-9, t), 61.9 (C-9', t), 72.1 (C-7, d), 85.7 (C-8, d), 110.2 (C-3, C-5, s), 117.2 (C-3', C-5', d), 125.5 (C-7', d), 130.4 (C-2', C-6', d), 131.0 (C-2, C-6, d), 132.8 (C-8', d), 135.9 (C-1', C-1, s), 150.7 (C-4, C-4', s)

vi) Oxidative coupling of 366.5 mg (1.75 mmol) of the dimethoxy-substituted monolignol (**151**) yielded 222 mg (61%) of the *β-β* coupling product, syringaresinol **(152)**.

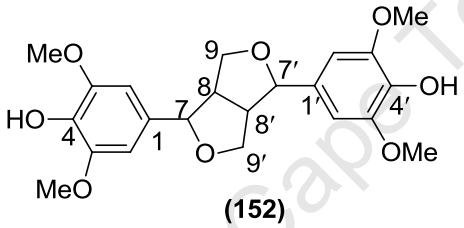

(152)
syringaresinol

HRESI-MS (m/z): 418.1627 (calcd for $C_{22}H_{26}O_8$ 418.1628)

R*f*: 0.50 (6% methanol/dichloromethane)

^{1}H NMR ($CDCl_3$): δ_H 3.10 (2H, br d, J = 1.8 Hz, H-8, H-8'), 3.82 (12H, s, 3-OC$\underline{H}_3$, 3'-OC$\underline{H}_3$, 5-OC$\underline{H}_3$, 5'-OC$\underline{H}_3$), 3.84 (H, m, H-9b, H-9'b), 4.23 (2H, dd, J = 6.8, J = 1.8 Hz, H-9a,H-9'a), 4.67 (2H, d, J = 3.6 Hz, H-7,H-7'), 6.69 (4H, br s, H-2, H-2', H-6,H-6')

^{13}C NMR (acetone-d6): δ_C 54.4 (C-8, C-8', d), 55.7 (3-OMe, 3'-OMe, 5-OMe, 5'-Ome, q), 71.5 (C-9, C-9', t), 85.9 (C-7, C-7', d), 103.6 (C-2, C-6, C-2', C-6', d), 132.3 (C-1, C-1', s), 135.3 (C-4, C-4', s), 147.8 (C-3, C-3', C-5, C-5', s)

7.15.21 Oxidative Cross-coupling

59 mg (0.28 mmol, 0.5 equiv.) of sinapyl alcohol (152) and ~ 1 ml of 3% H_2O_2 were added slowly to 100mg (0.56 mmol) of coniferyl alcohol, dissolved in ~ 60 ml dioxane-water (2/3, v/v, pH 4 – 4.5 adjusted with dil. H_3PO_4) containing 6 mg of HRP (250 Umg^{-1}). TLC was used to monitor the disappearance of the substrates. 40 ml of water was added to the reaction mixture and this was then extracted with

EtOAc (3 x 50 ml). EtOAc layers were combined, washed with H_2O, dried over $MgSO_4$ and then evaporated *in vacuo*. Residue was purified by silica gel column chromatography and prep TLC using 0.5 – 1.5% MeOH/DCM to yield 10.6 mg (18%) of syringaresinol **(152)**, 13.4 mg (12%) of the *β*-5 cross-coupled benzofuran analogue **(153)**, 11.3 mg (11%) of DHCA **(38)**, 7.6 mg (7.2%) of GGCE **(40)** and 15 mg (13%) of an inseparable mixture of the *β*-*O*-4 cross coupled products **(154)**.

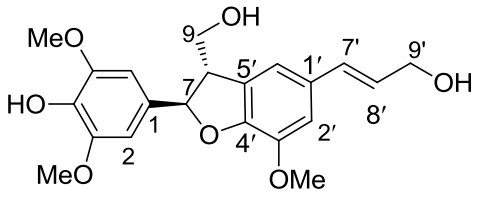

(153)
5-methoxy dehydrodiconiferyl alcohol

HRESI-MS (m/z): 388.1530 (calcd for $C_{21}H_{24}O_7$ 388.1523)

R*f*: 0.12 (5% methanol/dichloromethane)

^{1}H NMR (acetone-d_6): δ_H 3.55 (1H, br ddd, J = 6.5, J = 7.1, J = 5.3, H-8), 3.73 (1H, t, J = 5.3 Hz, 9'-O<u>H</u>), 3.80 (6H, s, 3-OC<u>H</u>$_3$, 5-OC<u>H</u>$_3$), 3.82 – 3.94 (2H, m, H-9), 3.87 (3H, s, 3'-OC<u>H</u>$_3$), 4.11 (1H, t, J = 5. Hz, 9-O<u>H</u>), 4.20 (2H, br dd, J = 5.3, J = 5.9 Hz, H-9'), 5.55 (1H, d, J = 7.0, H-7), 6.25 (1H, dt, J = 15.9, J = 5.3 Hz, H-8'), 6.53 (1H, , J = 15.9 Hz, H-7'), 6.75 (2H, br s, H-2, H-6), 6.95 (1H, br s, H-2'), 6.98 (1H, br s, H-6'), 7.21 (1H, s, 4-O<u>H</u>)

^{13}C NMR (acetone-d6): δ_C 53.9 (C-8, d), 55.5 (3-OMe, 5-OMe, q), 55.8 (3'-OMe, q), 62.5 (C-9', t), 63.6 (C-9, t), 87.9 (C-7, d), 103.7 (C-2, C-6, d), 110.9 (C-2', d), 115.2 (C-6', d), 127.5 (C-8', d), 129.5 (C-4', s) 129.6 (C-7', d), 131.1 (C-1', s) 132.4 (C-1, s), 135.8 (C-4, s) 144.3 (C-3', s), 147.9 (C-3, C-5, s), 148.1 (C-5', s)

REFERENCES

Agrawal, P.K., Thakur, R.S., 1985. ^{13}C NMR Spectroscopy of lignan and neolignan derivatives. Magnetic Resonance in Chemistry. 23, 389-418.

Akinyemi, K.O., Mendie, U.E., Smith, S.T., Oyefolu, A.O., Coker, A.O., 2005. Screening of some medicinal plants used in south-west Nigerian traditional medicine for anti-Salmonella typhi activity. Journal of Herbal Pharmacotherapy. 5, 45-60.

Akiyama, T., Matsumoto, Y., Okuyama, T., Meshitsuka, G., 2003. Ratio of *erythro* and *threo* forms of *β-O*-4 structures in tension wood lignin. Phytochemistry. 64, 1157-1162.

Alam, M.S., Katayama, T., Suzuki, T., Sultana, D., Sultana, S., Hossain, M.D., 2008. Enzymatic formation of guaiacylglycerol 8-*O*-4'-(coniferyl alcohol) ether from coniferyl alcohol with enzyme preparations of *Eucommia ulmoides*. Journal of Crop Science and Technology. 11, 45-50.

Apers, S., Vlietinck, A., Pieters, L., 2003. Lignans and neolignans as lead compounds. Phytochemistry Reviews. 2, 201-217.

Appendino, G., Minassi, A., Daddario, N., Bianchi, F., Tron, G.C., 2002. Chemoselective esterification of phenolic acids and alcohols. Organic Letters. 4, 3839-3841.

Bakunov, S.A., Bakunova, S.M., Wenzler, T., Barszcz, T., Werbovetz, K.A., Brun, R., Tidwell, R.R., 2008. Synthesis and antiprotozoal activity of cationic 2-phenylbenzofurans. Journal of Medicinal Chemistry. 51, 6927-6944.

Ballini, R., Bigi, F., Carloni, S., Maggi, R., Sartori, G., 1997. Solvent free tetrahydropyranylation of phenols and alcohols over zeolites HSZ as reusable catalysts. Tetrahedron Letters. 38, 4169-4172.

Baltz, T., Baltz, D., Giroud, C., Crockett, J., 1985. Cultivation in a semi-defined medium of animal infective forms of *Trypanosoma brucei*, *T. equiperdum*, *T. evansi*, *T. rhodesiense* and *T. gambiense*. The EMBO Journal. 4, 1273.

Barata, L.E.S., Santos, L.S., Ferri, P.H., Phillipson, J.D., Paine, A., Croft, S.L., 2000. Anti-leishmanial activity of neolignans from *Virola* species and synthetic analogues. Phytochemistry. 55, 589-595.

Barbera, R., Trovato, A., Rapisarda, A., Ragusa, S., 1992. Analgesic and antiinflammatory activity in acute and chronic conditions of *Trema guineense* (Schum. et Thonn.) *Ficalho* and *Trema micrantha* Blume extracts in rodents. Phytotherapy Research. 6, 146-148.

Bastos, J.K., Albuquerque, S., Silva, M.L.A., 1999. Evaluation of the trypanocidal activity of lignans isolated from the leaves of *Zanthoxylum naranjillo*. Planta Medica. 65, 541-544.

Benet, L.Z., 1984. Pharmacokinetics: Basic principles and its use as a tool in drug metabolism. in: Mitchell, J.R., Horning, M.G. (Eds.), Drug Metabolism and Drug Toxicity, Raven Press, New York, pp. 199.

Berndtsson, I., Lundquist, K., 1977. On the Synthesis of Lignin Model compounds of the Arylglycerol-B-aryl Ether Type. Acta Chemica Scandinavica. B31, 725-726.

Binns, A.N., Chen, R.H., Wood, H.N., Lynn, D.G., 1987. Cell division promoting activity of naturally occurring dehydrodiconiferyl glucosides: do cell wall components control cell division? Proceedings of the National Academy of Sciences. 84, 980-984.

Bloland, P.B., 2001. Drug resistance in malaria. World Health Organization, Geneva.

Bode, M.L., Kaye, P.T., George, R., 1994. Indolizine studies. Part 3. Synthesis and dynamic NMR analysis of indolizine-2-carboxamides. Journal of the Chemical Society, Perkin Transactions 1. 3023-3027.

Boudet, A.M., Grima-Pettenati, J., 1996. Lignin genetic engineering. Molecular Breeding. 2, 25-39.

Bray, P.G., Martin, R.E., Tilley, L., Ward, S.A., Kirk, K., Fidock, D.A., 2005. Defining the role of PfCRT in *Plasmodium falciparum* chloroquine resistance. Molecular Microbiology. 56, 323-333.

Butler, M.S., 2004. The Role of Natural Product Chemistry in Drug Discovery. Journal of Natural Products. 67, 2141-2153.

Cabral, M.M.O., Azambuja, P., Gottlieb, O.R., Garcia, E.S., 1999. Neolignans inhibit Trypanosoma cruzi infection of its triatomine insect vector, *Rhodnius prolixus*. Parasitology Research. 85, 184-187.

Cabral, M.M.O., Barbosa-Filho, J.M., Maia, G.L.A., Chaves, M.C.O., Braga, M.V., De Souza, W., Soares, R.O.A., 2010. Neolignans from plants in northeastern Brazil (Lauraceae) with activity against *Trypanosoma cruzi*. Experimental Parasitology. 124, 319-324.

Campbell, M.M., Sederoff, R.R., 1996. Variation in Lignin Content and Composition (Mechanisms of Control and Implications for the Genetic Improvement of Plants). Plant Physiology. 110, 3.

Canel, C., Moraes, R.M., Dayan, F.E., Ferreira, D., 2000. Podophyllotoxin. Phytochemistry. 54, 115-120.

Caniato, R., Puricelli, L., 2003. Review: natural antimalarial agents (1995-2001). Critical Reviews in Plant Sciences. 22, 79-105.

Chapman & Hall, 2010. Dictionary of Natural Products on DVD. CRC Press, *v* 19.1, June 2010.

Charlton, J.L., 1998. Antiviral activity of lignans. Journal of Natural Products. 61, 1447-1451.

Chauhan, A.K., Dobhal, M.P., Joshi, B.C., 1988. A review of medicinal plants showing anticonvulsant activity. Journal of Ethnopharmacology. 22, 11-23.

Cherigo, L., Polanco, V., Ortega-Barria, E., Heller, M.V., Capson, T.L., Rios, L.C., 2005. Antitrypanosomal activity of a novel norlignan purified from *Nectandra lineata*. Natural Product Research. 19, 373-377.

Chioccara, F., Poli, S., Rindone, B., Pilati, T., Brunow, G., Pietikainen, P., Setala, H., 1993. Regio-and diastereo-selective synthesis of dimeric lignans using oxidative coupling. Acta Chemica Scandinavica. 47, 610-610.

Chowdhury, A.A., Islam, M.S., 2004. Antimicrobial activity of *Trema orientalis*. Pharmaceutical Journal. 3, 201.

Clarkson, C., Campbell, W.E., Smith, P., 2003. *In vitro* antiplasmodial activity of abietane and totarane diterpenes isolated from *Harpagophytum procumbens* (Devil's claw). Planta Medica. 69, 720-724.

Clarkson, C., Maharaj, V.J., Crouch, N.R., Grace, O.M., Pillay, P., Matsabisa, M.G., Bhagwandin, N., Smith, P.J., Folb, P.I., 2004. *In vitro* antiplasmodial activity of medicinal plants native to or naturalised in South Africa. Journal of Ethnopharmacology. 92, 177-191.

Craigo, J., Callahan, M., Huang, R.C.C., DeLucia, A.L., 2000. Inhibition of human papillomavirus type 16 gene expression by nordihydroguaiaretic acid plant lignan derivatives. Antiviral Research. 47, 19-28.

Croasmun, W.R., Carlson, R.M.K., 1987. Two Dimensional NMR Spectroscopy: Applications for Chemists and Biochemists. VCH Publishers, New York.

da Silva Filho, A.A., Albuquerque, S., e Silva, M.L.A., Eberlin, M.N., Tomazela, D.M., Bastos, J.K., 2004. Tetrahydrofuran Lignans from *Nectandra megapotamica* with Trypanocidal Activity. Journal of Natural Products. 67, 42-45.

Davin, L.B., Wang, H.B., Crowell, A.L., Bedgar, D.L., Martin, D.M., Sarkanen, S., Lewis, N.G., 1997. Stereoselective bimolecular phenoxy radical coupling by an auxiliary (dirigent) protein without an active center. Science. 275, 362-366.

de Andrade-Neto, V.F., da Silva, T., Lopes, L.M.X., do Rosario, V.E., de Pilla Varotti, F., Krettli, A.U., 2007. Antiplasmodial activity of aryltetralone lignans from *Holostylis reniformis*. Antimicrobial Agents and Chemotherapy. 51, 2346-2350.

Department of Health, South Africa, 2008. Malaria: Seasonal data. 2010.

Department of Health, South Africa, 2003. National Heath Report: Malaria cases in South Africa. 2010.

Desjardins, R.E., Canfield, C.J., Haynes, J.D., Chulay, J.D., 1979. Quantitative assessment of antimalarial activity in vitro by a semiautomated microdilution technique. Antimicrobial Agents and Chemotherapy. 16, 710.

Dijoux-Franca, M.G., Tchamo, D.N., Cherel, B., Cussac, M., Tsamo, E., Mariotte, A.M., 2001. New Dihydrophenanthrene and Phenyldihydroisocoumarin Constituents of *Trema orientalis*. Journal of Natural Products. 64, 832-835.

Dimo, T., Ngueguim, F.T., Kamtchouing, P., Dongo, E., Tan, P.V., 2006. Glucose lowering efficacy of the aqueous stem bark extract of *Trema orientalis* (Linn) Blume in normal and streptozotocin diabetic rats. Pharmazie. 61, 233-236.

Dixon, R.A., Paiva, N.L., 1995. Stress-induced phenylpropanoid metabolism. The Plant Cell. 7, 1085.

Dondorp, A.M., Nosten, F., Yi, P., Das, D., Phyo, A.P., Tarning, J., Lwin, K.M., Ariey, F., Hanpithakpong, W., Lee, S.J., 2009. Artemisinin resistance in *Plasmodium falciparum* malaria. New England Journal of Medicine. 361, 455.

Durbeej, B., Eriksson, L.A., 2003a. Formation of β-O-4 lignin models: A theoretical study. Holzforschung. 57, 466-478.

Durbeej, B., Eriksson, L.A., 2003b. A Density Functional Theory Study of Coniferyl Alcohol Intermonomeric Cross Linkages in Lignin - Three-Dimensional Structures, Stabilities and the Thermodynamic Control Hypothesis. Holzforschung. 57, 150-164.

Elder, T., Ede, R.M., 1995. Coupling of coniferyl alcohol in the formation of dilignols: A molecular orbital study. Proceedings of 8th International Symposium on Wood and Pulping Chemistry. 1, 115-122.

Elder, T.J., Worley, S.D., 1984. The application of molecular orbital calculations to wood chemistry. The dehydrogenation of coniferyl alcohol. Wood Science and Technology. 18, 307-315.

Fidock, D.A., 2010. Priming the antimalarial pipeline. Nature. 465, 297-298.

Freudenberg, K., 1965. Lignin: Its Constitution and Formation from *p*-Hydroxycinnamyl Alcohols. Science. 148, 595-600.

Fura, A., Shu, Y.Z., Zhu, M., Hanson, R.L., Roongta, V., Humphreys, W.G., 2004. Discovering drugs through biological transformation: role of pharmacologically active metabolites in drug discovery. Journal of Medicinal Chemistry. 47, 4339-4351.

Gamo, F.J., Sanz, L.M., Vidal, J., De Cozar, C., Alvarez, E., Lavandera, J.L., Vanderwall, D.E., Green, D.V.S., Kumar, V., Hasan, S., Brown, J.R., Peishoff, C.E., Cardon, L.R., Garcia-Bustos, J.F., 2010. Thousands of chemical starting points for antimalarial lead identification. Nature. 465, 305-310.

Ganem, B., 1978. From glucose to aromatics: recent developments in natural products of the shikimic acid pathway. Tetrahedron. 34, 3353-3383.

Gellerstedt, G., Lundquist, K., Wallis, A.F.A., Zhang, L., 1995. Revised structures for neolignans from *Arum italicum*. Phytochemistry. 40, 263-265.

Gertsch, J., Tobler, R.T., Brun, R., Sticher, O., Heilmann, J., 2003. Antifungal, Antiprotozoal, Cytotoxic and Piscicidal Properties of Justicidin B and a New Arylnaphthalide Lignan from *Phyllanthus piscotorum*. Planta Medica. 69, 420-424.

Gessler, M.C., Nkunya, M.H.H., Mwasumbi, L.B., Heinrich, M., Tanner, M., 1994. Screening Tanzanian medicinal plants for antimalarial activity. Acta Tropica. 56, 65-77.

Guiguemde, W.A., Shelat, A.A., Bouck, D., Duffy, S., Crowther, G.J., Davis, P.H., Smithson, D.C., Connelly, M., Clark, J., Zhu, F., 2010. Chemical genetics of *Plasmodium falciparum*. Nature. 465, 311-315.

Hagiwara, H., Morohashi, K., Suzuki, T., Ando, M., Yamamoto, I., Kato, M., 1998. Solid State Acetylation with Acetylimidazole: Selective Protection of Primary Alcohols and Phenols. Synthetic Communications. 28, 2001-2006.

Hahm, J., Lee, I., Kang, W., Kim, S., Ahn, Y., 2005. Cytotoxicity of neolignans identified in *Saururus chinensis* towards human cancer cell lines. Planta Medica. 71, 464.

Haslam, E., 1974. The shikimate pathway, . John Wiley & Sons, New York.

Haworth, R.D., 1942. The chemistry of the lignan group of natural products. Journal of the American Chemical Society. 1942, 448-456.

He, Z.D., Ma, C.Y., Tan, G.T., Sydara, K., Tamez, P., Southavong, B., Bouamanivong, S., Soejarto, D.D., Pezzuto, J.M., Fong, H.H.S., 2006. Rourinoside and rouremin, antimalarial constituents from *Rourea minor*. Phytochemistry. 67, 1378-1384.

Houlihan, F., Bouchard, F., Frechet, J.M.J., Willson, C.G., 1985. Phase transfer catalysis in the tert-butyloxycarbonylation of alcohols, phenols, enols, and thiols with di-tert-butyl dicarbonate. Canadian Journal of Chemistry. 63, 153-162.

Houtman, C.J., 1999. What factors control dimerization of coniferyl alcohol? Holzforschung. 53, 585-589.

Hu, K., Jeong, J.H., 2006. A convenient synthesis of an anti-helicobacter pylori agent, dehydrodiconiferyl alcohol. Archives of Pharmacal Research. 29, 563-565.

Hughes, D., Reamer, R., Bergan, J., Grabowski, E., 1988. A mechanistic study of the Mitsunobu esterification reaction. Journal of the American Chemical Society. 110, 6487-6491.

Hutchings, A., 1996. Zulu Medicinal plants, . University of Natal Press, Pinetown.

Hwu, J.R., Tseng, W.N., Gnabre, J., Giza, P., Huang, R.C.C., 1998. Antiviral activities of methylated nordihydroguaiaretic acids. 1. Synthesis, structure identification, and inhibition of tat-regulated HIV transactivation. Journal of Medicinal Chemistry. 41, 2994-3000.

Ibrahim, W., Lundquist, K., 1994. Synthesis of erythro and threo Forms of Lignin Models of the Arylglycerol ß-Guaiacyl Ether Type. Acta Chemica Scandinavica. 48, 149-151.

International Society for Infectious Diseases, 2010. ProMed mail, January 9, 2010.

Jenkins, M.D., 1987. Madagascar: An environmental profile. IUCN Conservation Monitoring Centre, Gland.

Jensen, J.F., Kvist, L.P., Christensen, S.B., 2002. An Antiplasmodial Lignan from *Euterpe precatoria*. Journal of Natural Products. 65, 1915-1917.

Jensen, S., Hansen, J., Boll, P.M., 1993. Lignans and neolignans from *Piperaceae*. Phytochemistry. 33, 523-530.

Jones, M.K., Good, M.F., 2006. Malaria parasites up close. Nature Medicine. 200, 6.

Kanaani, J., Ginsburg, H., 1992. Effects of cinnamic acid derivatives on in vitro growth of *Plasmodium falciparum* and on the permeability of the membrane of malaria-infected erythrocytes. Antimicrobial Agents and Chemotherapy. 36, 1102-1108.

Karlsson, O., Lundquist, K., Stomberg, R., 1990. Studies on Hydrobenzoins: Preparation, Crystal Structure and Stability of Borate Complexes. Acta Chemica Scandinavica. 44, 617-624.

Kashiwada, Y., Nishizawa, M., Yamagishi, T., Tanaka, T., Nonaka, G., Cosentino, L.M., Snider, J.V., Lee, K.H., 1995. Anti-AIDS agents, 18. Sodium and potassium salts of caffeic acid tetramers from *Arnebia euchroma* as anti-HIV agents. Journal of Natural Products. 58, 392-400.

Kaur, K., Jain, M., Kaur, T., Jain, R., 2009. Antimalarials from nature. Bioorganic & Medicinal Chemistry. 17, 3229-3256.

Kirby, G.C., 1996. Medicinal plants and the control of parasites. Transactions of the Royal Society of Tropical Medicine and Hygiene. 90, 605-609.

Klayman, D.L., 1985. Qinghaosu (artemisinin): an antimalarial drug from China. Science. 228, 1049.

Kong, Z.L., Tzeng, S.C., Liu, Y.C., 2005. Cytotoxic neolignans: an SAR study. Bioorganic & Medicinal Chemistry Letters. 15, 163-166.

Konuklugil, B., 1994. Lignans with Anticancer Activity. Journal of Faculty of Pharmacy Ankara. 23, 1-2.

Kotler, S., 2003. Building a better mosquito. Accessed 2010 http://www.thepowerhour.com/news/better_mosquito.htm.

Kraft, C., Jenett-Siems, K., Köhler, I., Tofern-Reblin, B., Siems, K., Bienzle, U., Eich, E., 2002. Antiplasmodial activity of sesquilignans and sesquineolignans from *Bonamia spectabilis*. Phytochemistry. 60, 167-173.

Kristersson, P., Lundquist, K., Strand, A., 1980. Derivatization and analysis of low molecular weight lignin acidolysis products. Wood Science and Technology. 14, 297-300.

Kuo, W.-., Huang, Y.-., Wang, S.-., Ni, C.-., Shien, B.-., Chen, C.-., 2007. Chemical constituents of *Trema orientalis*. Journal of Chinese Medicine. 18, 27-36.

Lee, D.Y., Song, M.C., Yoo, K.H., Bang, M.H., Chung, I.S., Kim, S.H., Kim, D.K., Kwon, B.M., Jeong, T.S., Park, M.H., 2007a. Lignans from the fruits of *Cornus kousa Burg*. and their cytotoxic effects on human cancer cell lines. Archives of Pharmacal Research. 30, 402-407.

Lee, D.Y., Song, M.C., Yoo, K.H., Bang, M.H., Chung, I.S., Kim, S.H., Kim, D.K., Kwon, B.M., Jeong, T.S., Park, M.H., 2007b. Lignans from the fruits of *Cornus kousa* Burg. and their cytotoxic effects on human cancer cell lines. Archives of Pharmacal Research. 30, 402-407.

Lee, M.R., 2002. Plants against malaria, part 2: *Artemisia annua* (Qinghaosu or the sweet wormwood). The Journal of the Royal College of Physicians of Edinburgh. 32, 300-305.

Lewis, N.G., Davin, L.B., 1994. Evolution of Lignan and Neolignan Biochemical Pathways, Isopentenoids and Other Natural Products, American Chemical Society, Washington, pp. 202-246.

Lopes, N.P., Chicaro, P., Kato, M.J., Albuquerque, S., Yoshida, M., 1998. Flavonoids and lignans from *Virola surinamensis* twigs and their *in vitro* activity against *Trypanosoma cruzi*. Planta Medica. 64, 667-669.

Luize, P.S., Ueda-Nakamura, T., Filho, B.P.D., Cortez, D.A.G., Nakamura, C.V., 2006. Activity of neolignans isolated from *Piper regnellii* (MIQ.) C. DC. var. pallescens (C. DC.) Yunck against *Trypanosoma cruzi*. Biological & Pharmaceutical Bulletin. 29, 2126-2130.

Lynn, D.G., Chen, R.H., Manning, K.S., Wood, H.N., 1987. The structural characterization of endogenous factors from Vinca rosea crown gall tumors that promote cell division of tobacco cells. Proceedings of the National Academy of Sciences. 84, 615-619.

Makler, M.T., Ries, J.M., Williams, J.A., Bancroft, J.E., Piper, R.C., Gibbins, B.L., Hinrichs, D.J., 1993. Parasite lactate dehydrogenase as an assay for *Plasmodium falciparum* drug sensitivity. The American Journal of Tropical Medicine and Hygiene. 48, 739-741.

Malan, C., Notten, A., 2005. *Trema orientalis*. Accessed 2010 http://www.plantzafrica.com/planttuv/tremorient.htm

Martins, R.C.C., Lago, J.H.G., Albuquerque, S., Kato, M.J., 2003. Trypanocidal tetrahydrofuran lignans from inflorescences of *Piper solmsianum*. Phytochemistry. 64, 667-670.

Matile, H., Pink, J.R.L., 1990. *Plasmodium falciparum* malaria parasite cultures and their use in immunology. Immunological methods. 4, 221-234.

Miert, S.V., Dyck, S.V., Schmidt, T.J., Brun, R., Vlietinck, A., Lemiere, G., Pieters, L., 2005. Antileishmanial activity, cytotoxicity and QSAR analysis of synthetic dihydrobenzofuran lignans and related benzofurans. Bioorganic & Medicinal Chemistry. 13, 661-669.

Mosmann, T., 1983. Rapid colorimetric assay for cellular growth and survival: Application to proliferation and cytotoxicity assays. Journal of Immunological methods. 65, 55-63.

Moss, G.P., 2000. Nomenclature of lignans and neolignans. Pure and Applied Chemistry. 72, 1493-1523.

Muñoz, V., Sauvain, M., Bourdy, G., Callapa, J., Bergeron, S., Rojas, I., Bravo, J.A., Balderrama, L., Ortiz, B., Gimenez, A., Deharo, E., 2000. A search for natural

bioactive compounds in Bolivia through a multidisciplinary approach: Part I. Evaluation of the antimalarial activity of plants used by the Chacobo Indians. Journal of Ethnopharmacology. 69, 127-137.

Na-Bangchang, K., Karbwang, J., 2009. Current status of malaria chemotherapy and the role of pharmacology in antimalarial drug research and development. Fundamental & Clinical Pharmacology. 23, 387-409.

Nahmany, M., Melman, A., 2004. Chemoselectivity in reactions of esterification. Organic and Biomolecular Chemistry 2, 1563-1572.

Newman, D.J., Cragg, G.M., 2007. Natural Products as Sources of New Drugs over the Last 25 Years. Journal of Natural Products 70, 461-477.

Newton, P., White, N., 1999. Malaria: new developments in treatment and prevention. Annual Review of Medicine. 50, 179-192.

N'Gouemo, P., Pambou-Tchivounda, H., Baldy-Moulinier, M., Koudogbo, B., N'Guemby-Bina, C., 1994. Some pharmacological effects of an ethanolic extract of *Trema guineensis* on the central nervous system in rodents. Planta Medica. 60, 305-307.

Nocito, I., Castelli, M.V., Zacchino, S.A., Serra, E., 2007. Activity of 8. O. 4′-neolignans against *Trypanosoma cruzi*. Parasitology Research. 101, 1453-1457.

Noedl, H., Wongsrichanalai, C., Wernsdorfer, W.H., 2003. Malaria drug-sensitivity testing: new assays, new perspectives. Trends in Parasitology. 19, 175-181.

Nundkumar, N., Ojewale, J.A.O., 2002. Studies on the antiplasmodial properties of some South African medicinal plants used as antimalarial remedies in Zulu folk medicine. Methods and Findings in Experimental and Clinical Pharmacology. 24, 397-401.

Ogunkoya, L., Olubajo, O.O., Sondha, D.S., 1977. A new triterpenoid alcohol from *Trema orientalis*. Phytochemistry. 16, 1606-1608.

Ogunkoya, L., Olubajo, O.O., Sondha, D.S., 1973. Simiarenone from *Trema orientalis*. Phytochemistry. 12, 732-733.

Ogunkoya, L., Olubajo, O.O., Sondha, D.S., 1972a. Derivatives of long chain hydrocarbon from *Trema orientalis*. Phytochemistry. 11, 2361-2361.

Ogunkoya, L., Olubajo, O.O., Sondha, D.S., 1972b. Triterpenoid alcohols from *Trema orientalis*. Phytochemistry. 11, 3093-3094.

Oketch-Rabah, H.A., Dossaji, S.F., Christensen, S.B., Frydenvang, K., Lemmich, E., Cornett, C., Olsen, C.E., Chen, M., Kharazmi, A., Theander, T., 1997. Antiprotozoal compounds from *Asparagus africanus*. Journal of Natural Products. 60, 1017-1022.

Pathak, A.K., Pathak, V., Seitz, L.E., Tiwari, K.N., Akhtar, M.S., Reynolds, R.C., 2001. A facile method for deprotection of trityl ethers using column chromatography. Tetrahedron Letters. 42, 7755-7757.

Paula, V.F., Barbosa, L.C.A., Howarth, O.W., Demuner, A.J., Cass, Q.B., Viera, I.J.C., 1995. Lignans from *Ochroma lagopus*. Tetrahedron. 51, 12453-12462

Persson, K.E.M., Lee, C.T., Marsh, K., Beeson, J.G., 2006. Development and optimization of high-throughput methods to measure *Plasmodium falciparum*-specific growth inhibitory antibodies. Journal of Clinical Microbiology. 44, 1665-1673.

Pillay, P., Maharaj, V.J., Smith, P.J., 2008. Investigating South African plants as a source of new antimalarial drugs. Journal of Ethnopharmacology. 119, 438-454.

Pink, R., Hudson, A., Mouriès, M.A., Bendig, M., 2005. Opportunities and challenges in antiparasitic drug discovery. Nature Reviews Drug Discovery. 4, 727-740.

Potterat, O., Hamburger, M., 2006. Natural products in drug discovery - Concepts and approaches for tracking bioactivity. Current Organic Chemistry. 10, 899-920.

Prozesky, E.A., Meyer, J.J.M., Louw, A.I., 2001. *In vitro* antiplasmodial activity and cytotoxicity of ethnobotanically selected South African plants. Journal of Ethnopharmacology. 76, 239-245.

Quideau, S., Ralph, J., 1992. Facile large-scale synthesis of coniferyl, sinapyl, and p-coumaryl alcohol. Journal of Agricultural and Food Chemistry. 40, 1108-1110.

Rakotondramanana, D.L.A., Delomenède, M., Baltas, M., Duran, H., Bedos-Belval, F., Rasoanaivo, P., Negre-Salvayre, A., Gornitzka, H., 2007. Synthesis of ferulic ester dimers, functionalisation and biological evaluation as potential antiatherogenic and antiplasmodial agents. Bioorganic & Medicinal Chemistry. 15, 6018-6026.

Ralph, J., Lundquist, K., Brunow, G., Lu, F., Kim, H., Schatz, P.F., Marita, J.M., Hatfield, R.D., Ralph, S.A., Christensen, J.H., 2004. Lignins: Natural polymers from oxidative coupling of 4-hydroxyphenyl-propanoids. Phytochemistry Reviews. 3, 29-60.

Ramachandran, R., 2002. Resistance to anti-malarial drugs. Accessed 2010. http://www.frontlineonnet.com/fl1913/19130870.htm

Rasoanaivo, P., Petitjean, A., Ratsimamanga-Urverg, S., Rakoto-Ratsimamanga, A., 1992. Medicinal plants used to treat malaria in Madagascar. Journal of Ethnopharmacology. 37, 117-127.

Ridley, R.G., 2002. Medical need, scientific opportunity and the drive for antimalarial drugs. Nature. 415, 686-693.

Robert, A., Benoit-Vical, F., Dechy-Cabaret, O., Meunier, B., 2001. From classical antimalarial drugs to new compounds based on the mechanism of action of artemisinin. Pure and Applied Chemistry. 73, 1173-1188.

Roll Back America, 2010. Malaria endemic countries. 2010, .

Russell, W.R., Forrester, A.R., Chesson, A., Burkitt, M.J., 1996. Oxidative coupling during lignin polymerization is determined by unpaired electron delocalization within parent phenylpropanoid radicals. Archives of Biochemistry and Biophysics. 332, 357-366.

Ryu, K., Dordick, J.S., 1992. How do organic solvents affect peroxidase structure and function? Biochemistry. 31, 2588-2598.

Ryu, K., Dordick, J.S., 1989. Free energy relationships of substrate and solvent hydrophobicities on enzymic catalysis in organic media. Journal of the American Chemical Society. 111, 8026-8027.

Saklani, A., Kutty, S.K., 2008. Plant-derived compounds in clinical trials. Drug Discovery Today. 13, 161-171.

Saleem, M., Kim, H.J., Ali, M.S., Lee, Y.S., 2005. An update on bioactive plant lignans. Natural Product Reports. 22, 696-716.

Saliba, K.J., Folb, P.I., Smith, P.J., 1998. Role for the *Plasmodium falciparum* digestive vacuole in chloroquine resistance. Biochemical Pharmacology. 56, 313-320.

Sanders, J.K.M., Hunter, B.K., 1987. Modern NMR spectroscopy. A guide for chemists. . Oxford University Press, Oxford.

Schulze, D.L.C., Makgato, E.M., Coetzer, T.L., Louw, A.I., van Rensberg, C.E.J., Visser, L., 1997. Development and application of a modified flow cytometric procedure for rapid in vitro quantification of malaria parasitaemea. South African Journal of Science. 93, 156-158.

Schwikkard, S., Heerden, F.R., 2002. Antimalarial activity of plant metabolites. Natural Product Reports. 19, 675-692.

Seca, A.M.L., Silva, A.M.S., Silvestre, A.J.D., Caveleiro, J.A.S., Domingues, F.M.J., Pascoal-Neto, C., 2001. Phenolic constituents from the core of Kenaf (*Hibiscus cannabinus*). Phytochemistry. 56, 759-767.

Sefkow, M., Kaatz, H., 1999. Selective protection of either the phenol or the hydroxy group in hydroxyalkyl phenols. Tetrahedron Letters. 40, 6561-6562.

Setälä, H., 2008. Regio-and stereoselectivity of oxidative coupling reactions of phenols. Academic Dissertation, Department of Chemistry, Faculty of Science, University of Helsinki. 21-58.

Shigematsu, M., Kobayashi, T., Taguchi, H., Tanahashi, M., 2006. Transition state leading to B-O' quinone methide intermediate of p-coumaryl alcohol analysed by semi-empirical molecular orbital calculation. Journal of Wood Science. 52, 128-133.

Shu, Y.Z., Li, W., Leet, J.E., Alberts, J., Arora, V.K., Yeola, S., Philip, T., Qian-Cutrone, J., Zhao, N., Santone, K., 2002. Biogram enabled evaluation of active metabolites: an exploratory approach for detecting and characterizing active/toxic drug metabolites. Drug Metabolism Reviews. 34, 75.

Sidhu, A.B.S., Verdier-Pinard, D., Fidock, D.A., 2002. Chloroquine resistance in Plasmodium falciparum malaria parasites conferred by pfcrt mutations. Science. 298, 210-213.

Strickland, G.T., Hunter, K.W., 1982. The Pathophysiology of Human Malaria. Praeger, Westport.

Stüwe, H.T., Bruhn, G., König, W.A., Hausen, B.M., 1989. The synthesis of caffeic acid esters, a new group of naturally occurring contact allergens. Naturwissenschaften. 76, 426-427.

Su, B.N., Cuendet, M., Hawthorne, M.E., Kardono, L.B.S., Riswan, S., Fong, H.H.S., Mehta, R.G., Pezzuto, J.M., Kinghorn, A.D., 2002. Constituents of the bark and twigs

of *Artocarpus dadah* with cyclooxygenase inhibitory activity. Journal of Natural Products. 65, 163-169.

Syrjanen, K., Brunow, G., 1998. Oxidative cross coupling of *p*-hydroxycinnamic alcohols with dimeric arylglycerol [small beta]-aryl ether lignin model compounds. The effect of oxidation potentials. Journal of the Chemical Society, Perkin Transactions 1. 3425-3430.

Syrjänen, K., Brunow, G., 2001. Regioselectivity in oxidative cross-coupling of phenols. Application to the synthesis of dimeric neolignans. Tetrahedron. 57, 365-370.

Takara, K., Kinjyo, A., Matsui, D., Wada, K., Nakasone, Y., Yogi, S., 2000. Antioxidative phenolic compounds from non-sugar fraction in Kokuto, non-centrifugal cane sugar. Nippon Nogeikagaku Kaishi. 74, 885-890.

Targett, G.A.T., 1991. Malaria: Waiting for the Vaccine, in: London School of Hygiene and Tropical Medicine (Ed.), John Wiley & Sons, Chichester, pp. 13.

Taubes, G., 2000. Malaria Parasite Outwits the Immune System. Science. 290, 435-435.

Tchamo, D.N., Cartier, G., Dijoux-Franca, M.G., Tsamo, E., Mariotte, A.M., 2001. Xanthones and other constituents of *Trema orientalis*. Pharmaceutical Biology. 39, 202-205.

Terashima, N., Atalla, R.H., 1995. Formation and structure of lignified plant cell wall-factors controlling lignin structure during its formation. Proceedings of the 8th International Symposium on Wood and Pulping Chemistry. 1, 69-76.

Tillekeratne, L.M.V., Sherette, A., Grossman, P., Hupe, L., Hupe, D., Hudson, R.A., 2001. Simplified catechin-gallate inhibitors of HIV-1 reverse transcriptase. Bioorganic & Medicinal Chemistry Letters. 11, 2763-2767.

Trager, W., Jensen, J.B., 1976. Human malaria parasites in continuous culture. Science. 193, 673.

Umezawa, T., 2003. Diversity in lignan biosynthesis. Phytochemistry Reviews. 2, 371-390.

University of Pretoria Botanical Garden, 2006. *Trema orientalis*. 2010

van der Leij, M., Oosterink, H.J., Hall, R.H., Reinhoudt, D.N., 1981. A novel synthesis of 2'-hydroxy-1', 3'-xylyl crown ethers. Tetrahedron. 37, 3661-3666.

Van Wyk, B.E., Van Oudtshoorn, B., Gericke, N., 2000. Medicinal Plants of South Africa, . Briza Publications, Pretoria.

Vedejs, E., Peterson, M.J., 1994. Stereochemistry and mechanism in the Wittig reaction. Topics in Stereochemistry. 21, 1-157.

von Unge, S., Lundquist, K., Stomberg, R., 1988. Synthesis of Lignin Model Compounds of the Arylglycerol *β*-Syringyl Ether Type. Acta Chemica Scandinavica. B42, 469-474.

Vroman, J.A., Alvim-Gaston, M., Avery, M.A., 1999. Current progress in the chemistry, medicinal chemistry and drug design of artemisinin based antimalarials. Current Pharmaceutical Design. 5, 101.

Ward, R.S., 1999. Lignans, neolignans and related compounds. Natural Product Reports. 16, 75-96.

Watt, J.M., Breyer-Brandwijk, M.G., 1962. The Medicinal and Poisonous plants of Southern and Eastern Africa, . E & S Livingstone, London.

Weinert, E.E., Dondi, R., Colloredo-Melz, S., Frankenfield, K.N., Mitchell, C.H., Freccero, M., Rokita, S.E., 2006. Substituents on quinone methides strongly

modulate formation and stability of their nucleophilic adducts. Journal of the American Chemical Society. 128, 11940-11947.

Whetten, R., Sederoff, R., 1995. Lignin biosynthesis. The Plant Cell. 7, 1001.

Whiting, D.A., 1985. Ligans and neolignans. Natural Product Reports. 2, 191-211.

Wikipedia, 2010. Trema. Accessed 2010. http://en.wikipedia.org/wiki/Trema

Wipf, P., 2005. Handbook of Reagents for Organic Synthesis: Reagents for high-throughput solid-phase and solution-phase organic synthesis. John Wiley & Sons Inc.

World Agroforestry Centre, 2010. Species Information: *Trema orientalis*. http://www.worldagroforestrycentre.org/Sea/Products/AFDbases/AF/asp/SpeciesInfo.asp?SpID=1654

World Health Organisation, 2010. Malaria. Fact Sheet no. 94. Accessed 2010. http://www.who.int/mediacentre/factsheets/fs094/en/index.html

World Health Organisation, 2009. World Malaria Report 2009. Accessed 2010. http://www.who.int/malaria/world_malaria_report_2009/en/index.html

World Health Organisation, 1995. Traditional Practitioners as Primary Health Care Workers. Accessed 2010. http://apps.who.int/medicinedocs/en/d/Jh2941e/

Yuen, M.S.M., Xue, F., Mak, T.C.W., Wong, H.N.C., 1998. On the absolute structure of optically active neolignans containing a dihydrobenzo [b] furan skeleton. Tetrahedron. 54, 12429-12444.

Zhang, H.J., Tamez, P.A., Hoang, V.D., Tan, G.T., Van Hung, N., Le Thi Xuan, , Le Mai H., Cuong, N.M., Do T.T., , Soejarto, D.D., 2001. Antimalarial Compounds from *Rhaphidophora decursiva*. Journal of Natural Products. 64, 772-777.

Zhang, J., Krugliak, M., Ginsburg, H., 1999. The fate of ferriprotorphyrin IX in malaria infected erythrocytes in conjunction with the mode of action of antimalarial drugs. Molecular and Biochemical Parasitology. 99, 129-141.

Zhong, Y., Xian, L., 2003. NMR Methods for determining the configuration of 8-*O*-4'neolignans. Chinese Journal of Magnetic Resonance. 3, 16.

Zishiri, V.K., Joshi, M.C., Hunter, R., Chibale, K., Smith, P.J., Summers, R.L., Martin, R.E., Egan, T.J., 2011. Quinoline Antimalarials containing a dibemethin group are active against chloroquine resistant *P. falciparum* and inhibit chloroquine transport via the *Plasmodium falciparum* Chloroquine-Resistance Transporter (PfCRT). Journal of Medicinal Chemistry. 54, 6956-6968.

APPENDIX I

Figure A1 BPI and UV chromatograms of semi-purified extract P05644-4B

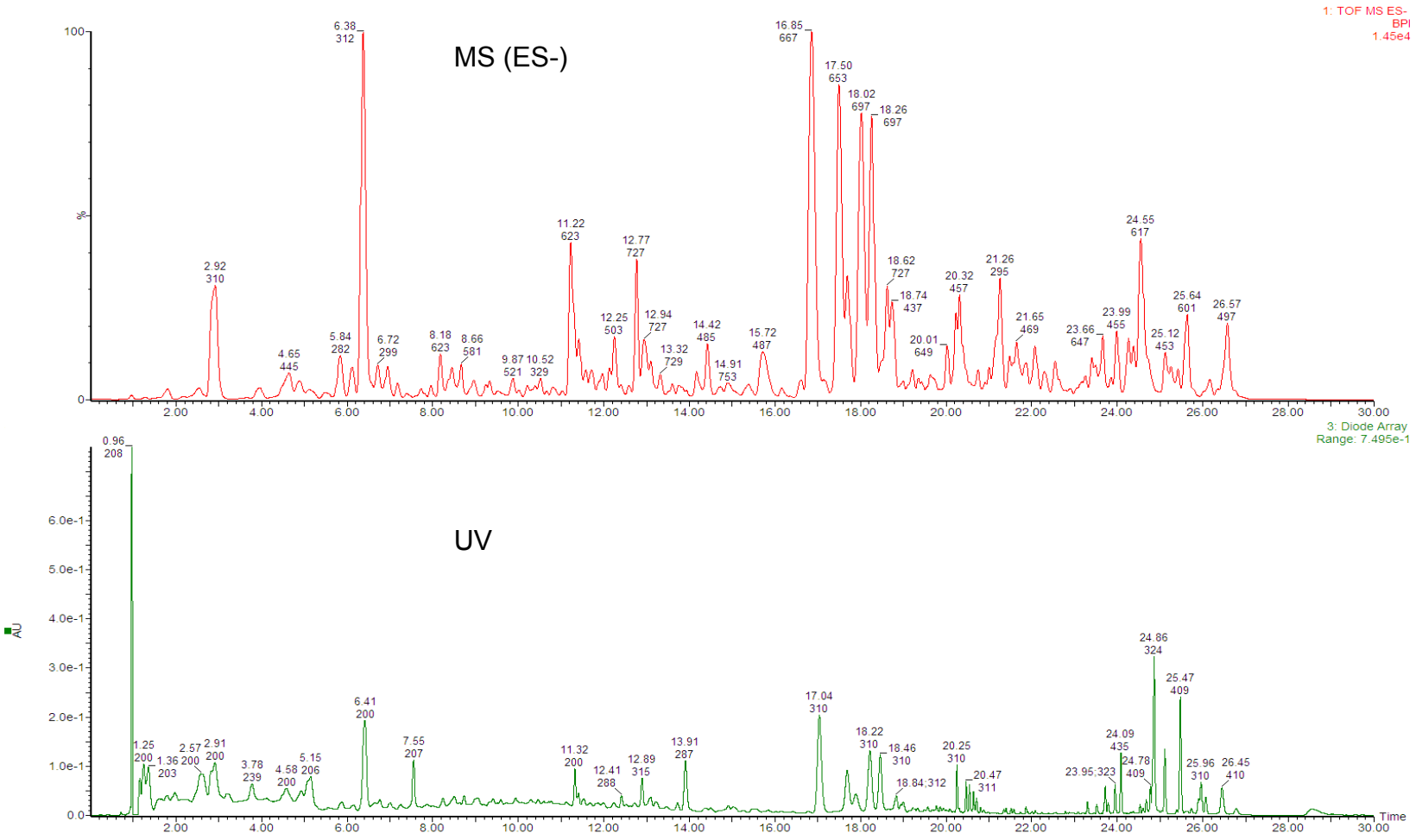

APPENDIX I I

Raw data of in vivo evaluation of extract P0544-4B

Table A1 The parasitemia percentages from three mice/per group , on given number of days after infection with *Plasmodium berghei*

Days	Control			Chloroquine			P05644-4B		
	A1	A2	A2	A1	A2	A3	A1	A2	A3
0	0	0	0	0	0	0	0	0	0
3	5.2	5.5	5.3	1.54	0.91	0.60	0.93	0.92	1.55
4	13.7			0.94	0.8	0.78	5.5	8.9	10.9
5	25.2			0.57	0.2	0.89	14.1	28.1	31.1
6	28.4			0.71	0.46	0.97	16.4	26.8	35.1
7				1.6	0.46	0.55	22.3	36.4	43.4
9				1.65	1.4	0.62	19.2	24.7	26.7
10				2.6	3.13	0.67	17.3	28	19.6
13				4.7	4.8	0.8	48.5	18.9	17.6
15							60	49.3	

Table A2 The average parasitimia percentages in each group, on a given number of days after infection with Plasmodium berghei

No of days post infection	Average Control	Average Chloroquine	Average P05644-4B
0	0	0	0
3	5.3	1.02	1.15
4	13.7	0.84	8.4
5	25.2	0.55	24.4
6	28.4	0.71	26.1
7		0.87	23.5
9		0.89	21.6

No of days post infection	Average Control	Average Chloroquine	Average P05644-4B
10		2.13	28.3
13		3.43	47.3
15		5.66	

Table A3 Weight loss over time post infection

No of days	Control	CQ	PO5644-4B
1	23.4	29.9	24.96
4	24.7	29.3	24.82
5	24.1	29.4	23.24
6	23.1	29.2	22.4
7	22.3	29.2	20.9
8		29.7	20.44
9		29	20
10		28.7	20.09
11		28.73	19.56

APPENDIX I I I

Table A4 Swiss TPH Bioassay data for 96 well plate fractions of *T.orientalis* extract

	Activity *vs P. falciparum* K1					Cytotoxicity	Selectivity
Well	Conc1 (ug/ml)	% Growth Inhibition (Conc1)	Conc2 (ug/ml)	% Growth Inhibition (Conc2)	K1 IC50 (ug/ml)	L6 IC50 (ug/ml)	SI
a1	4.8	99.8	0.8	98.4	0.459	5.19	11.3
a2	4.8	99.4	0.8	85.8	0.544	7.8	14.3
a3	4.8	98.3	0.8	80.0	0.877	17.8	20.3
a4	4.8	90.5	0.8	55.1	2.44	>20	
a5	4.8	29.5	0.8	16.4			
a6	4.8	1.2	0.8	45.3			
a7	4.8	33.3	0.8	5.4			
a8	4.8	38.0	0.8	19.3			
a9	4.8	33.5	0.8	0.0			
a10	4.8	44.5	0.8	10.6			
a11	4.8	50.1	0.8	6.7			
a12	4.8	71.4	0.8	0.0			
b1	4.8	45.3	0.8	18.7			
b2	4.8	48.2	0.8	22.9			
b3	4.8	44.1	0.8	4.0			
b4	4.8	47.5	0.8	17.7			
b5	4.8	52.1	0.8	26.0			
b6	4.8	54.8	0.8	22.3			
b7	4.8	71.4	0.8	23.1			
b8	4.8	39.5	0.8	15.1			
b9	4.8	43.4	0.8	0.0			
b10	4.8	77.8	0.8	36.9			
b11	4.8	53.8	0.8	18.1			
b12	4.8	52.1	0.8	0.0			
c1	4.8	68.4	0.8	23.8			
c2	4.8	63.4	0.8	26.8			
c3	4.8	72.8	0.8	28.6			
c4	4.8	84.2	0.8	35.8			
c5	4.8	90.5	0.8	39.5			
c6	4.8	96.2	0.8	55.8	2.01	19.1	9.5
c7	4.8	97.4	0.8	55.1	1.68	>20	
c8	4.8	97.4	0.8	68.6	>10	>20	
c9	4.8	98.8	0.8	62.8	0.983	14.1	14.3
c10	4.8	99.4	0.8	76.6	0.507	7.2	14.2
c11	4.8	99.8	0.8	94.9	0.729	9.3	12.8

	Activity *vs P. falciparum* K1					Cytotoxicity	Selectivity
Well	Conc1 (ug/ml)	% Growth Inhibition (Conc1)	Conc2 (ug/ml)	% Growth Inhibition (Conc2)	K1 IC50 (ug/ml)	L6 IC50 (ug/ml)	SI
c12	4.8	100.0	0.8	92.8	0.771	11.4	14.8
d1	4.8	99.3	0.8	79.3	0.945	12.4	13.1
d2	4.8	100.0	0.8	92.2	0.601	5.56	9.3
d3	4.8	100.0	0.8	96.6	0.501	5.8	11.6
d4	4.8	100.0	0.8	97.4	0.403	4.83	12.0
d5	4.8	100.0	0.8	98.6	0.502	3.2	6.4
d6	4.8	100.0	0.8	98.6	0.324	3.32	10.2
d7	4.8	100.0	0.8	98.0	0.374	9.1	24.3
d8	4.8	100.0	0.8	98.4	1.54	>20	
d9	4.8	100.0	0.8	98.2	0.296	10.7	36.1
d10	4.8	100.0	0.8	98.5	0.381	8.9	23.4
d11	4.8	100.0	0.8	99.6	0.286	9.1	31.8
d12	4.8	100.0	0.8	98.4	0.652	13.7	21.0
e1	4.8	99.7	0.8	94.4	0.521	14.8	28.4
e2	4.8	99.6	0.8	70.9	1.13	>20	
e3	4.8	98.2	0.8	57.6	0.647	6.4	9.9
e4	4.8	98.1	0.8	52.2	1.88	>20	
e5	4.8	96.1	0.8	45.0			
e6	4.8	91.8	0.8	49.7	1.93	>20	
e7	4.8	73.6	0.8	24.0			
e8	4.8	73.1	0.8	18.3			
e9	4.8	66.6	0.8	22.0			
e10	4.8	64.2	0.8	22.8			
e11	4.8	70.7	0.8	15.3			
e12	4.8	55.6	0.8	44.0			
f1	4.8	63.9	0.8	26.7			
f2	4.8	66.5	0.8	15.0			
f3	4.8	68.4	0.8	20.6			
f4	4.8	78.8	0.8	32.0			
f5	4.8	68.9	0.8	23.2			
f6	4.8	66.9	0.8	28.7			
f7	4.8	78.5	0.8	18.2			
f8	4.8	77.4	0.8	13.3			
f9	4.8	78.6	0.8	13.5			
f10	4.8	83.5	0.8	25.8			
f11	4.8	78.5	0.8	29.3			
f12	4.8	67.6	0.8	6.9			
g1	4.8	83.2	0.8	30.8			

	Activity *vs P. falciparum* K1					Cytotoxicity	Selectivity
Well	Conc1 (ug/ml)	% Growth Inhibition (Conc1)	Conc2 (ug/ml)	% Growth Inhibition (Conc2)	K1 IC50 (ug/ml)	L6 IC50 (ug/ml)	SI
g2	4.8	83.0	0.8	37.3			
g3	4.8	95.4	0.8	25.6			
g4	4.8	73.4	0.8	16.3			
g5	4.8	73.3	0.8	40.0			
g6	4.8	92.1	0.8	42.2			
g7	4.8	100.0	0.8	69.6	0.256	8.5	33.2
g8	4.8	97.3	0.8	41.9			
g9	4.8	86.1	0.8	11.8			
g10	4.8	91.5	0.8	41.9			
g11	4.8	73.0	0.8	25.3			
g12	4.8	69.1	0.8	13.7			
h1	4.8	39.1	0.8	20.4			
h2	4.8	64.1	0.8	15.0			
h3		95.7		25.1			
Chloro-quine					0.085		
Podo-phyllo-toxin						0.004	

APPENDIX IV

Figure A2 BPI and UV chromatograms of representative wells from each active region

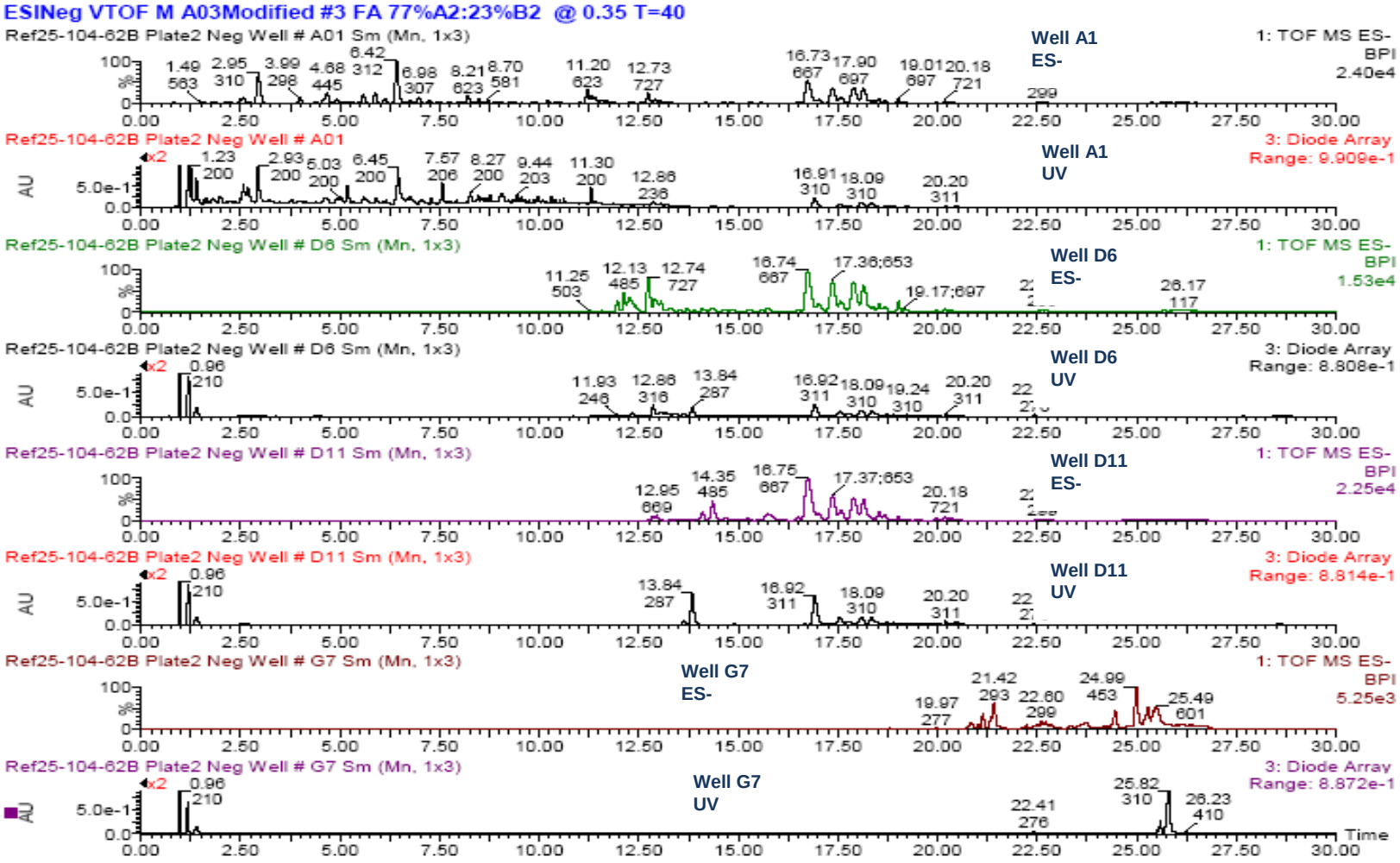

APPENDIX V

Figure A2 ES- BPI chromatograms of representative active wells

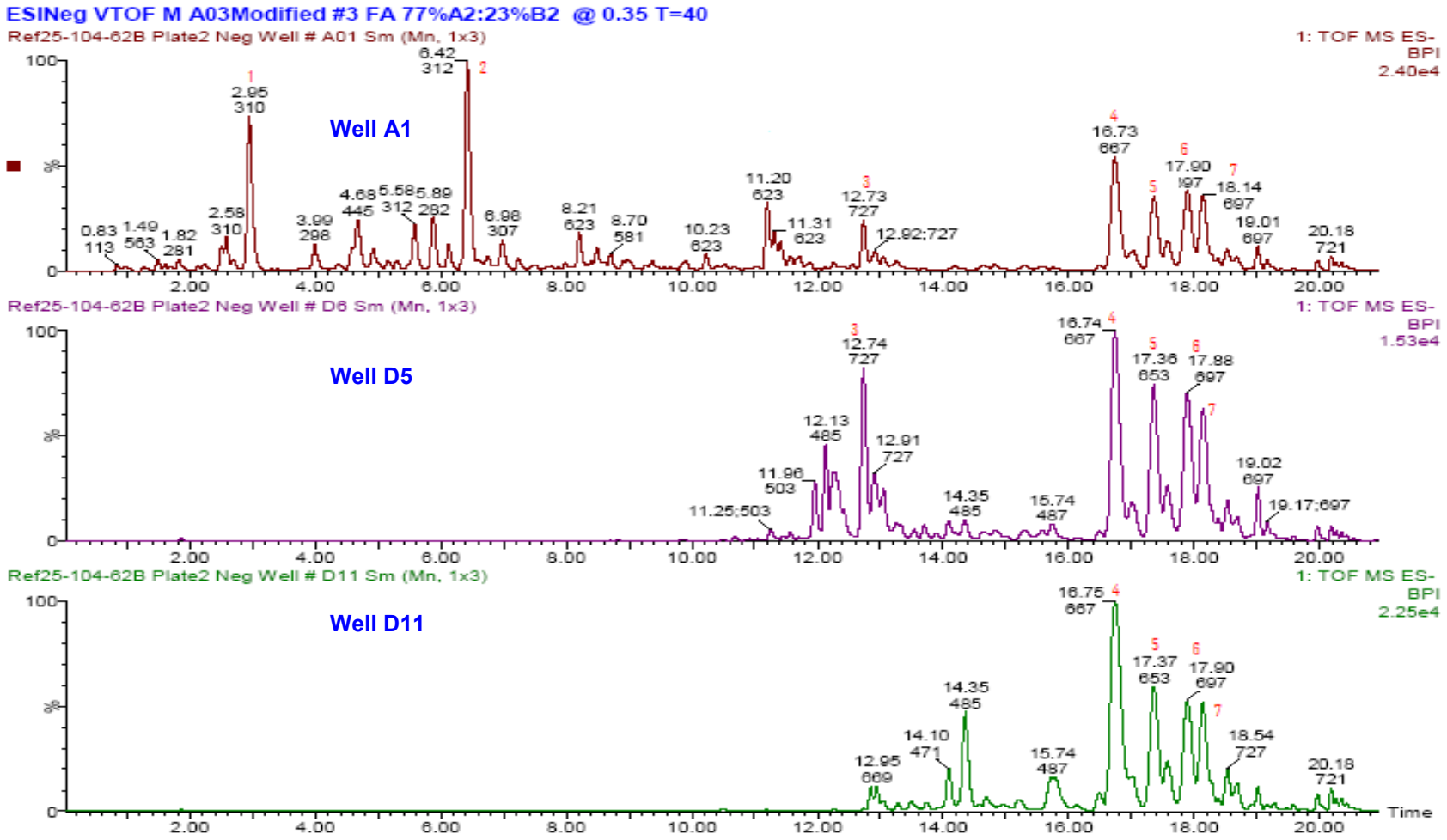

Table A5 Summary of spectroscopic data, DNP search criteria and results for major compounds in active fractions

Peak No.	Rt (min)	Present in Wells	M - H	Accurate mass	UV max	DNP Search parameters		No. of hits in DNP	Possible structure/s
						Accurate mass	UV Max		
1	2.93	A1	328.1166	329.12454	220, 318	329.12 - 329.14	215-225; 315-322	1	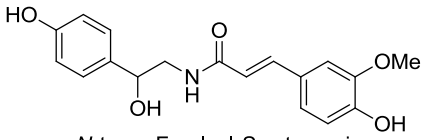 *N*-trans-Feruloyl-*S*-octopamine Accurate mass: 329.126324
2	6.42	A1	312.1201	313.12804	219, 318	313.12 – 313.14	215-225; 315-322	2	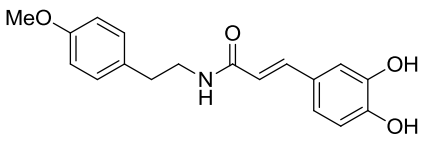 *N*-trans-Caffeoyl-*O*-methyltyramine Accurate mass: 313.131409 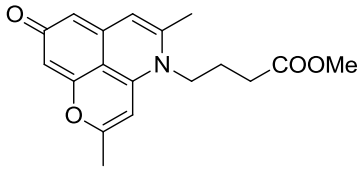 Cassiarine B Accurate mass: 313.131409

Peak No.	Rt (min)	Present in Wells	M - H	Accurate mass	UV max	DNP Search parameters		No. of hits in DNP	Possible structure/s
						Accurate mass	UV Max		
3	12.73	A1, D4, D6, D7	727.2421	728.25004	220, 317	728.24 – 728.26	218-230; 315-322	0	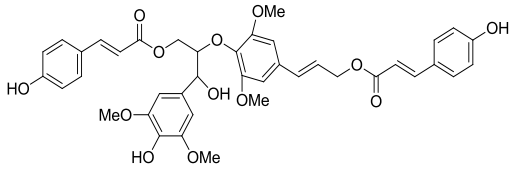 Exact Mass: 728.25
4	16.74	A1, D4, D6, D7, D9, D10, D11	667.2184	668.22634	222, 310	668.22 – 668.24	218-225; 300-320	1	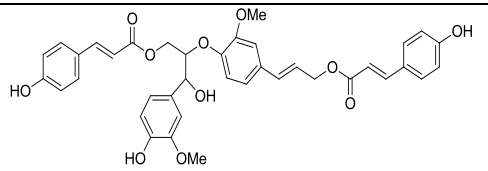 Dadahol B Accurate mass: 668.225765
5	17.38	A1, D4, D6, D7, D9, D10, D11	653.2396	654.24754	227, 311	654.23 – 654.26	218-230; 315-322	0	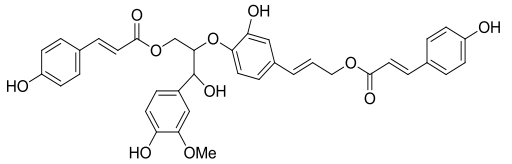 Exact Mass: 654.21
6	17.89	A1, D4, D6, D7, D9, D10, D11	697.2315	698.23944	222, 310	698.22 – 698.24	218-225; 300-320	1	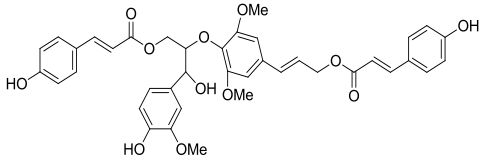 Dadahol A Accurate mass: 698.23633

Peak No.	Rt (min)	Present in Wells	M - H	Accurate mass	UV max	DNP Search parameters		No. of hits in DNP	Possible structure/s
						Accurate mass	UV Max		
7	18.16	A1, D4, D6, D7, D9, D10, D11	697.2305	698.23844	223, 310	698.22 – 698.24	218-225; 300-320	1	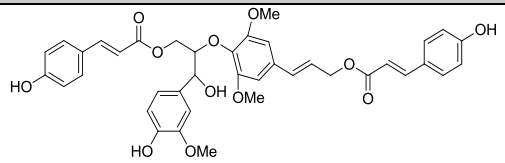 Dadahol A Accurate mass: 698.23633

APPENDIX VI

^{1}H NMR spectra (with selected resonances labelled) of Dadahol B and its two diastereomers

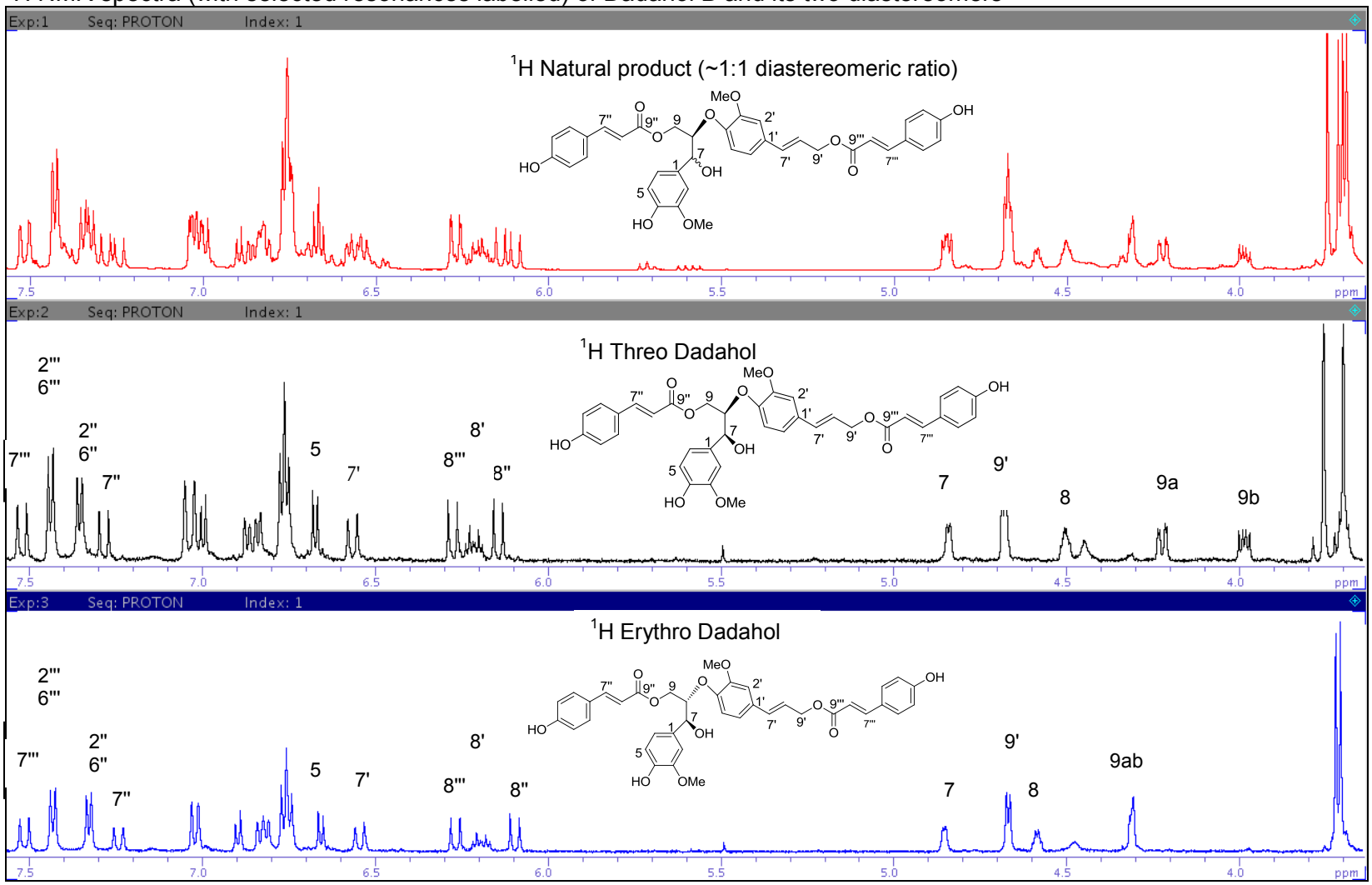

APPENDIX VII

Raw data of in vivo evaluation of extract P0544-4B

Weight and % Parasitemia of individual mice measured on days 4 and 6 post infection (PI) of *in vivo* study:

Table A6 Chloroquine group

No of days PI	Measure-ment	M1(g) / %	M2(g) / %	M3(g) / %	M4(g) / %	Average (g) / %
0	Weight	26.11	21.72	19.60	25.22	23.16
4	Weight	26.04	21.8	19.68	25.25	23.19
	Parasitemia	3.88	3.83	3.14	4.10	3.7
6	Weight	26.19	21.04	19.36	24.65	22.81
	Parasitemia	8.57	6.2	2.86	2.8	5.1
8	Weight	27.18	21.22	25.54	19.83	23.44

Table A7 Negative control group

No of days PI	Measure-ment	M1(g) / %)	M2 (g / %	M3(g) / %	M4(g) / %	Average (g) / %
0	Weight	24.32	19.64	27.25	21.98	23.30
4	Weight	22.22	18.05	25.08	19.6	21.23
	Parasitemia	11.49	10.24	11.83	5	8.78
6	Weight	20.26	16.77	22.27	17.98	19.32
	Parasitemia	25.65	29.67	23.84	23.19	25.59
8	Weight	19.66	15.24	20.16		18.35

Table A8 Dadahol A group

No of days PI	Measure-ment	M1(g) / %	M2 (g) / %	M3(g) / %	M4(g) / %	M5(g) / %	Average (g) / %
0	0	25.02	23.77	20.63	24.69	22.02	23.23
4	Weight	23.35	21.37	18.92	24.20	19.45	21.52
	Parasite mia	4.4	3.3	3.2	0.8	4.5	3.85
6	Weight	20.79	19.98	16.86	24.16	17.70	19.90
	Parasite mia	24.1	22.68	20.3	0.75	27.1	23.55
8	Weight	19.30	19.34	*	16.5*	*	18.38

Table A9 Dadahol B group

No of days PI	Measure-ment	M1(g) / %	M2 (g) / %	M3(g) / %	M4(g) / %	M5(g) / %	Average (g) / %
	0	17.09	22.94	24.34	24.14	25.86	22.90
4	Weight	16.12	20.86	22.90	23.68	23.5	21.41
	Parasite mia	6.0	3.3	6.0	6.1	3.5	5.0
6	Weight	13.88	19.15	20.05	20.20	21.15	18.89
	Parasite mia	16.7	19	17.6	16.5		17.5
	8	13.6*	18.10	*	19.2	*	16.97

* = Dead or sacrificed on that day